University of Nottingham
Faculty of Medicine and Health Sciences
School of Medicine
Division of Cancer Genetics & Stem Cell
Cancer Biology Unit

Heterochromatin Protein HP1BP3 Modulates Haematopoiesis and Leukemogenesis

Amany Ibrahim A. Almars

(B.Sc., M.Sc.)

Under supervision of

Dr Abdolrahman S. Nateri

Dr Claire Seedhouse

Thesis submitted to the University of Nottingham for the degree of

Doctor of Philosophy

March 2021

Declaration

I declare that the research studies presented in this thesis are my own work in Cancer Genetics & Stem Cell Group, supervised by Dr. Abdolrahman S. Nateri at the School of Medicine, Faculty of Medicine and Health Sciences, University of Nottingham, UK, except where otherwise stated in the text. I hereby acknowledge that this thesis has not been submitted for any other university or application purposes.

Amany Ibrahim Almars

Student ID No: 428149

Date: 31/03/2021

Abstract

Acute myeloid leukaemia (AML) is a heterogeneous malignancy characterized by uncontrolled proliferation of undifferentiated hematopoietic stem/progenitor cells. AML is one of the most comprehensively studied malignancies. Although genetic mutations, particularly chromosomal abnormalities and mutations in known oncogenes, have an integral impact in the development of the disease, increasing evidence suggest the important roles of epigenetic dysregulation on the pathogenesis of AML. Unlike genetic abnormalities, epigenetic alterations are reversible; thus, they can be potential therapeutic targets using specific inhibitors.

The dynamic architecture of chromatin is vital for proper epigenetic response in various cellular events and is maintained by the concerted action of numerous histone and non-histone proteins. Histones undergo different covalent post-translational modifications (PTMs) that take place on the histone tails. Histone PTMs impact the dynamic of the nucleosome, the fundamental unit of chromatin, through wrapping/unwrapping, assembly/disassembly to modulate the chromatin architecture, i.e. conversion from heterochromatin “inactive chromatin” to euchromatin “active chromatin”. PTMs control the interactions between the DNA and the core histones, therefore, the dynamic conversion from heterochromatin to euchromatin influence DNA accessibility, and ultimately regulates cellular processes.

Heterochromatin Protein 1 Binding Protein 3 (HP1BP3) was identified in Dr Nateri's laboratory as a downstream target of the E3 ubiquitin ligase FBXW7 for degradation. HP1BP3 evolutionarily and structurally belongs to the linker histone H1 family. Moreover, HP1BP3 modulates the entry/exit of nucleosomal DNA by binding to Heterochromatin Protein 1 α (HP1α) and maintains the chromatin integrity during the G1–S phase transition.

However, the roles and mechanism of HP1BP3 action in stem cells and cancers, including haematopoiesis and AML, is largely unknown. Hence in this thesis, we investigated the major role(s) of HP1BP3 underlying the epigenetic reprogramming mechanisms in murine haematopoiesis and AML.

Herein, in brief we demonstrate that:

- HP1BP3 is required for HSC and leukemic self-renewal *in vitro*, and its reduction (knockdown and knockouts) promotes the myeloid progenitor cells differentiation and apoptosis of AML cells.
- HP1BP3 plays a significant role in hypoxic AML cells *in vitro* by possibly targeting hypoxia-inducible factors (HIFs).
- Accumulation of HP1BP3 was positively correlated with the downregulation of H3K9me3 "heterochromatin marker" and upregulation of H3K9ac "euchromatin marker" while loss of HP1BP3 induced H3K9me3 levels and decreased H3K9ac.
- HP1BP3 regulates several key genes and miRNAs involved in proliferation, the cell cycle, proto-oncogenes, tumour suppressor genes and chromatin modifiers identified via sRNA-seq and mRNA-seq transcriptomic analysis and qRT-PCR assays.

Together, our findings reveal a crucial role of HP1BP3 in leukemogenesis, while a further clinical study could identify HP1BP3, an attractive therapeutic target for leukaemia.

Acknowledgements

I would like to acknowledge my supervisor, Dr Abdolrahman Shams Nateri, for his constructive supervision and continuous support throughout my PhD studies. His generous guidance enlightened me over the last few years in the lab at the University of Nottingham.

My deepest thanks to my beloved family for their constant care and support. My sincerest gratitude to my sister Eman and brothers (Mahmoud and Musab) and my friends in Saudi Arabia (Dr Shahad Kattan and Dr Sameera Shahin) for being in my life and giving me the hope and strength to finish my study and return home with proud.

A big thank you to my lab mates in our Cancer Genetics and Stem Cells group (Miss Aieda Sedaie-Bonab, Dr Hossein Kashfi and Mr. Nickolas Jinks) and in Tumour and Vascular Biology group (Dr Mussarat Wahid, Dr Nahlah Ghouth, Dr Naseeb Malhi and Dr Teresa Raposo) who encouraged me to embrace and overcome all challenges, thanks for your friendship and support. This achievement would not have been possible without you, I love you all and I could not be more appreciative.

I also would like to thank the Ministry of Higher Education of Saudi Arabia, the Saudi Cultural Bureau in London, and King Abdul-Aziz University in Jeddah for generously funding my PhD scholarship at the University of Nottingham.

Finally, this work is dedicated to the ones who gave me life, who will be always in my heart, my thoughts and my prayers. For my parents may their kind souls rest in peace.

List of figures

Figure 1-1: Normal haematopoiesis and AML…… 3

Figure 1-2: Molecular classes associated with specific gene rearrangements in patients with AML……9

Figure 1-3: Organization of DNA in chromatin within the cell……..13

Figure 1-4: Nucleosome core particle structure……..15

Figure 0-5: Histone tails posttranslational modifications…… ……...18

Figure 1-6: Histone acetylation and deacetylation…… ……21

Figure 1-7: Schematic representation of HP1α protein and heterochromatin structure……...27

Figure 1-8: The schematic human metaphase chromosome-associated proteins…28

Figure 1-9: GeneMANIA analysis of HP1BP3 showing novel nuclear proteins interactions……..32

Figure 1-10: STRING analysis of HP1BP3 showing nodes proteins interactions....33

Figure 1-11: Schematic diagram of the cell cycle……..….36

Figure 1-12: Scheme of the domain organization of human HP1BP3 protein…...41

Figure 2-1: Schematic representation of developing a Hp1bp3-conditional knockout mouse model (Hp1bp3fl/fl)…….45

Figure 2-2: Dissection and isolation of mouse bone marrow…….51

Figure 2-3: Schematic representation of the major step of Tri-Reagent RNA extraction…….66

Figure 3-1: HP1BP3 as a potential prognostic marker in patients with AML……79

Figure 3-2: Differential expression of HP1BP3 in different AML cell lines……..80

Figure 3-3: mRNA expression of HP1BP3 and HP1α in AML cell lines……..84

Figure 3-4: Fluorescence nuclear foci co-localization and expression patterns of HP1BP3 and HP1α in AML cell lines……85

Figure 3-5: The pLVX-eGFP-HP1BP3"L", pLVX-eGFP-HP1BP3"S" and pLVX-eGFP plasmid maps and validation analysis by restriction enzyme digestion…...87

Figure 3-6: Expression of GFP-HP1BP3 protein in MOLM13 stable cell lines…88

Figure 3-7: Schematic presentation of inserted HP1BP3-shRNA into pGIPZ plasmid and validation analysis by restriction enzyme digestion……..……..90

Figure 3-8: shRNA-mediated knockdown of HP1BP3 in AML cell lines…….91

Figure 3-9: Ectopic expression of HP1PB3 decreases the expression of H3K9me3 while increases H3K9ac expression……94

Figure 3-10: Loss of HP1BP3 induced the expression of H3K9me3 in AML cell lines…….95

Figure 3-11: Expression of HP1BP3 changes AML cells proliferation…….97

Figure 3-12: Overexpression of HP1BP3 induced MOLM13 cell cycle progression…… …… ..100

Figure 3-13: HP1BP3 inhibition induced G0/G1 phase arrest in MV4-11 cells…102

Figure 3-14: Representative images of CFUs formed by AML cell lines……. ..104

Figure 3-15: Ectopic expression of HP1BP3 increases the size of CFUs in MOLM13 cells……..… .106

Figure 3-16: HP1BP3 downregulation reduces the number and the size of CFUs in MV4-11 cells……..……108

Figure 3-17: Overview of the RNA-seq data analysis in TF1a AML cells…… ...111

Figure 3-18: Visualization of DEGs between TF1a and TF1aKD cells identified by RNA-seq analysis……..113

Figure 3-19: Expression patterns of twenty genes selected DEGs of TF1aKD cells by RNA-Seq……..114

Figure 4-1: miRNA biogenesis…… …….121

Figure 4-2: HP1BP3-mediated regulation of miRNAs might be linked to HSCs and LSCs……..125

Figure 4-3: HP1BP3-knockdown reduces the number of (CD34+/CD38-) and (CD34+/CD38+) fractions in AML cell lines…… ……...128

Figure 4-4: HP1BP3 downregulation alters the expression of miRNAs in TF1a AML cells…… ……...130

Figure 4-5: Sequence length distribution in TF1a and TF1KD cells…… …..……132

Figure 4-6: TPM distribution in TF1a cells…… …….……..133

Figure 4-7: Analysis of differentially expressed miRNAs between TF1aKD and TF1a cells……..135

Figure 4-8: Expression patterns and qRT-PCR validation analysis of miRNAs differentially expressed in TF1aKD cells by sRNA-Seq…… …… …...138

Figure 4-9: Predicted novel miRNAs structures and sequence in TF1a cells……140

Figure 4-10: HP1BP3 inhibition doesn't change the expression of microprocessors. …… …..141

Figure 5-1: Cross-talk between LSCs and their niche…… …...148

Figure 5-2: Expression of HP1BP3 is induced in hypoxia in MO91 AML cells…152

Figure 5-3: HP1BP3 is induced in AML cells in response to hypoxia (Hx)…….154

Figure 5-4: HP1BP3-knockdown reduced the expression of hypoxia-related genes in AML cells……..155

Figure 5-5: knockdown of HP1BP3 decreased the expression level of Hypoxia-inducible factor 1-α in AML cells…….156

Figure 5-6: knockdown of HP1BP3 increased the expression level of FBXW7 in AML cell lines…….……..158

Figure 5-7: *HP1BP3*-knockdown reduced the proliferation in AML cells treated with Nx and Hx…….…….160

Figure 5-8: knockdown of *HP1BP3* changes the expression of some chromatin modifiers in AML cell lines……..……..162

Figure 6-1: Generation of *Hp1bp3*$^{fl/fl}$ homozygous mouse model……..……176

Figure 6-2: Cre-recombinase lentivirus generation and validation…….…..…..179

Figure 6-3: Control lentivirus production and validation…….…….180

Figure 6-4: Schematic demonstration of murine Lin- HSCs isolation and in-vitro knock-out of Hp1bp3……..…182

Figure 6-5 Efficient Cre-LV mediated *Hp1bp3 in-vitro* knock-out in mouse Lin$^-$ HSCs……..…183

Figure 6-6: Loss of *Hp1bp3* induced the expression of H3K9me3 in the Lin$^-$ HSCs…….185

Figure 6-7: Deletion of *Hp1bp3* leads to early haematopoiesis imbalance…..…..187

Figure 3-8: *Hp1bp3* inactivation reduced HSCs but increased the main myeloid multipotent progenitor MPP3……190

Figure 6-9: Knockout of Hp1bp3 impaired HSCs and increased cells differentiation……192

Figure 7-1: Schematic presentation of HP1BP3 role in AML……..……209

List of tables

Table 1-1: Cell surface markers for the diagnosis of AML……..6

Table 1-2: Cytogenetic risk groups in AML…….7

Table 2-1: Genetic features of leukemic cell lines used in the study……...44

Table 2-2: DNA plasmids used in the study. ……..…..44

Table 2-3: List of antibodies used in this project for flow cytometry analysis…...45

Table 2-4: List of primary and secondary antibodies used for western blot (WB) and immunofluorescence (IF) analyses……..46

Table 2-5: List of the primers used for AML cell lines qRT-PCR…….……..…48

Table 2-6: List of the primers used for mouse qRT-PCR…….…….…...49

Table 2-7: List of the primers used for mouse genotyping……...49

Table 2-8: Solution components (ml) for SDS/PAGE electrophoresis gels…...…..60

Table 3-1: quality of RNA sequencing for TF1a AML cells……..……110

Table 4-1: Differentially expressed miRNAs in TF1aKD cells and their function in AML……..……136

Abbreviations

AML	Acute Myeloid Leukaemia
BM	Bone Marrow
BSA	Bovine Serum Albumin
C- Terminus	Carboxyl Terminus
CD	Chromodomain
CSD	Chromo Shadow Domain
CIN	Chromosomal Instability
CTD	C-Terminal Domain
DAPI	4',6-Diamidino-2-Phenylindole
DMEM	Dulbecco Modified Eagle Medium
DMSO	Dimethyl Sulfoxide
DNA	Deoxyribonucleic Acid
EDTA	Ethylenediaminetetraacetic Acid
EtBr	Ethidium-Bromide
FACS	Fluorescence-Activated Cell Sorting
FBS	Fetal Bovine Serum
FBXW7	F-Box and WD Repeat Domain–Containing 7
FLT-3	Fms-like tyrosine kinase 3
GD	Globular Domain
GFP	Green Fluorescent Protein
H3K9ac	Acetylated Lysine 9 Residue of Histone 3
H3K9me3	Trimethylated Lysine 9 Residue of Histone H3
HAT	Histone Acetyltransferase
HDAC	Histone Deacetylase
HDM	Histone Demethylase
HIF1	Hypoxia Inducible Factor1
HMT	Histone Methyltransferase
HP1BP3	Heterochromatin Protein–Binding Protein 3
HP1BP3-S	Short Isoform of HP1BP3
HP1α	Heterochromatin Protein 1α

HREs	Hypoxia Response Elements
HSC	Hematopoietic Stem Cell
Hx	Hypoxia
IF	Immunofluorescent
LB	Luria Broth
LSC	Leukemic Stem Cell
MCS	Multiple Cloning Site
miRNA	MicroRNA
MNase	Micrococcal Nuclease
mRNA	Messenger RNA
MSI	Microsatellite Instability
NLS	Nuclear Localisation Signal
NSD1	Nuclear Receptor Binding SET domain protein
NTD	N-Terminal Domain
N-Terminus	Amino Terminus
PBS	Phosphate Buffered Saline
PCR	Polymerase Chain Reactions
PFA	Paraformaldehyde.
PI	Propidium Iodide
PTM	Post-Translational Modification
PVDF	Polyvinylidene Difluoride
RNA	Ribonucleic Acid
SCF-Complex	Skp1/Cullin1/F-Box
SDS	Sodium Dodecyl Sulphate
SDS-PAGE	Sodium Dodecyl Sulfate Polyacrylamide Gel Electrophoresis
shRNA	Small Hairpin RNA
STDEV	Standard Deviation
SUV39H1/2	Suppressor of Variegation 3-9 Homolog 1/2
TBS-T	Tris-Buffered Saline-Tween 20
TET2	Tet Methylcytosine Dioxygenase 2
Tm	Melting Temperature
TMA	Tissue Microarray
UVIdoc	Ultraviolet Transilluminator Unit

VEGFA	Vascular Endothelial Growth Factor A
WB	Western Blot

Table of contents

Declaration.....i
Abstract.....ii
Acknowledgements v
List of figures vi
List of tables ix
Abbreviations x
Table of contents I
CHAPTER 1.....1
General Introduction.....1
1.1 Haematopoiesis and the development of Leukaemia 2
1.2 Diagnose of AML.....5
1.2.1 Morphology 5
1.2.2 Immunophenotyping.....5
1.2.3 Karyotyping.....6
1.2.4 Fluorescence *in situ* Hybridization (FISH).....6
1.3 Pathogenesis of AML 6
1.3.1 Cytogenetics and genetics 6
1.3.2 The role of miRNAs in AML 11
1.3.3 The role of epigenetics in AML 13
.....18
1.4 Heterochromatin Protein (HP1).....25
1.5 Heterochromatin Protein 1 Binding Protein 3 (HP1BP3) 27
1.5.1 HP1BP3 structure and localization.....29
1.5.2 HP1BP3 protein-interactions.....31

1.5.3 Functions of HP1BP3 33

1.6 Rational and objectives 40

CHAPTER 2 44

General Materials & Methods 44

2.1 Material 45

2.1.1 Animal work 45

2.1.2 Cell lines 46

2.1.3 DNA Plasmids 47

2.1.4 Antibodies 47

2.1.5 Oligonucleotides 50

2.2 METHODS 52

2.2.1 Isolation of mouse bones and bone marrow cells 52

2.2.2 Lineage^{neg} HSCs isolation 53

2.2.3 GENERAL CELL CULTURE TECHNIQUES 55

2.2.4 Lentivirus system 57

2.2.5 FUNCTIONAL ASSAYS 59

2.2.6 PROTEIN EXPRESSION ASSAYS 61

2.2.7 Giemsa staining 65

2.2.8 DNA AND RNA ISOLATION AND ANALYSIS 65

2.2.9 STATISTICAL ANALYSIS 72

CHAPTER 3 74

Mechanisms, biological and clinical significance of HP1BP3 alteration in AML 74

3.1 Brief introduction 75

3.2 Results 77

3.2.1 *HP1BP3* as a potential prognostic marker in AML.....77

3.2.2 Differential expression of HP1BP3 and epigenetic markers associated with transcriptional activity among AML cell lines.....80

3.2.3 Generation of AML cells stably over-expressing HP1BP3 long and short isoforms.....85

3.2.4 Generation of AML cells over-expressing HP1BP3-shRNA..88

3.2.5 Chromatin marker expression profiling of stable AML cell lines overexpressing HP1BP3 and of Lin^- HSCs and AML cells lacking HP1BP3 91

3.2.6 Overexpression/knockdown of *HP1BP3* alters the proliferation of AML cells.....95

3.2.7 Cell cycle progression in AML cells is highly regulated by the expression of HP1BP3.....97

3.2.8 Influence of HP1BP3 expression on the clonogenic potential in AML cell lines using colony-forming unit (CFU) assay 102

3.2.9 RNA sequencing analysis to identify differential gene expression in *HP1BP3* knockdown cells.....108

3.3 Discussion.....114

CHAPTER 4.....118

HP1BP3 induction of AML activity, possibly mediated through miRNA regulation.....118

4.1 Brief introduction 119

4.2 RESULTS.....123

4.2.1 HP1BP3 may play a key role in AML-miRNA regulation ...123

4.2.2 Knockdown of HP1BP3 decreases the number of $CD34^{+}/CD38^{-}$ and $CD34^{+}/CD38^{+}$ cell populations in AML cell lines.....125

4.2.3 Inhibition of HP1BP3 expression changes the expression level of miRNAs in the TF1a AML cell line.....128

4.2.4 sRNA sequencing analysis to identify differential miRNA expression in $TF1a^{KD}$ AML cells.....129

4.2.5 *HP1BP3* downregulation does not change the expression of Drosha 139

4.3 Discussion.....141

CHAPTER 5.....145

Hypoxia-induced HP1BP3 modulates AML cells survival.....145

5.1 Brief introduction.....146

5.2 RESULTS.....150

5.2.1 HP1BP3 expression is induced in hypoxia.....150

5.2.2 HP1BP3 could be involved in the regulation of genes associated with hypoxia.....152

5.2.3 Knockdown of *HP1BP3* induced the expression of *FBXW7* in AML cell lines.....155

5.2.4 Loss of HP1BP3 reduces the growth rate of AML cell lines 158

5.2.5 HP1BP3 can mediate chromatin modification by regulating different chromatin modifiers.....160

5.3 Discussion.....163

CHAPTER 6.....168

In vivo loss-of-function analyses of *Hp1bp3* and *Hp1bp3* knockout mouse haematopoietic stem cells.....168

6.1 Brief introduction.....169

6.2 RESULTS: 172

6.2.1 Generation of the homozygous floxed *Hp1bp3* allele (*Hp1bp3*$^{fl/fl}$) mouse 172

6.2.2 Optimization of a lentivirus Cre-mediated DNA recombination system for *in vitro* knockout of murine *Hp1bp3* in lineage-negative (Lin$^-$) HSCs 176

6.2.3 Deletion of *Hp1bP3* induced H3K9me3 in murine Lin$^-$ HSCs .183

6.2.4 Loss of *Hp1bp3* induces early differentiation in murine Lin$^-$ HSCs 184

6.2.5 *Hp1bp3* knockout impaired HSCs while inducing MMP3 population, a subset known of its myeloid potential 187

6.2.6 Hp1bp3 depletion leads to differentiation towards mature cell lineages in murine Lin$^-$ HSCs 192

6.3 Discussion 195

CHAPTER 7 199

General Discussion 199

7.1 Overview 200

7.1.1 HP1BP3-knockdown/ knockouts promotes the myeloid progenitor cells differentiation and apoptosis of AML cells 200

7.1.2 HP1BP3 modulates the chromatin state at the H3K9 residue in HSC and AML cells 202

7.1.3 HP1BP3 regulates gene and miRNA expression in AML 207

7.2 Experimental limitations and perspectives 210

Appendix 213

References 214

CHAPTER 1

General Introduction

1.1 **Haematopoiesis and the development of Leukaemia**

The regulation of transcription factors, growth factors and epigenetic modifiers are involved in the highly controlled multistage haematopoiesis process, the normal transition of hematopoietic stem cells (HSCs) and their progenitors in the bone marrow (BM) to terminally differentiated blood cells (Zon, 2008). Throughout embryogenesis, sequential processes including complex structural sites contribute to the production of HSCs. At birth, mature hematopoietic stem cells transfer to BM, the ultimate place which is suitable for HSCs maintenance and colonisation (Birbrair and Frenette, 2016). HSCs have the ability to self-renewal and to differentiate to all blood lineages. The balance between HSC self-renewal and differentiation maintains haematopoiesis homeostasis. Symmetrical division of HSCs can produce two identical cells, however asymmetrical division forms two different cells with different potential (Birbrair and Frenette, 2016) (Figure 1-1). HSCs are heterogenous, they can be subdivided into two groups according to their multipotency and regeneration capacities: long-term (LT-HSCs) cells and short-term (ST-HSCs) (Ulirsch et al., 2019). LT-HSCs have self-renewal capacity and relatively quiescent (non-dividing). The self-renewal process is essential and requires at least one daughter cell to maintain the stem cell pool at the BM (Figure 1-1) (Wang et al., 2017). However, ST-HSCs have limited self-renewal capacity with multipotent progenitors (MPPs) (Ulirsch et al., 2019). MPPs can be further divided into lineage-committed progenitors known as common myeloid progenitors (CMPs) and common lymphoid progenitors (CLPs) (Ulirsch et al., 2019).

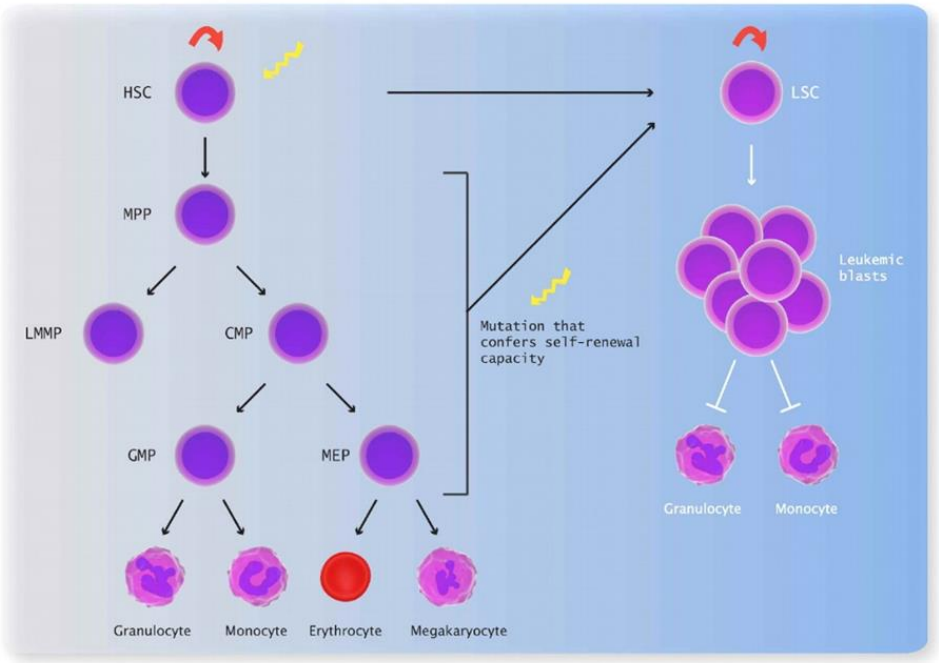


Figure 1-1: Normal haematopoiesis and AML. HSCs differentiate into normal mature blood cells such as granulocyte, monocyte, erythrocyte and megakaryocyte during myelopoiesis. Accumulation of mutations in HSCs or more committed progenitors can block differentiation and lead to formation of leukemic stem cells (LSCs) and non-functional leukemic blasts [Adapted from (Horton and Huntly 2012)].

In leukaemia, the processes guiding HSC self-renewal, differentiation and progenitor cell development are disordered (Figure 1-1) (Wang et al., 2017). HSCs that acquire errors in their genome or epigenome can be transformed into leukemic cells, which are characterized by genomic instability (chromosomal translocation, inversions, deletions), molecular aberration (mutations associated with gain-of-function or loss-of-function, amplifications, insertions) or epigenetic modifications (alteration in epigenetic modifiers, hypomethylation of oncogenes, hypermethylation of tumour-suppressor genes). The acquisition of one or more of these abnormalities in HSCs leads to the accumulation of non-functioning

immature malignant cells (i.e. leukemic blasts) (Lane et al., 2009, Wang et al., 2017).

A hallmark of all cancers is the ability for unlimited proliferation (Hanahan and Weinberg, 2011), which is also an important characteristic of normal stem cells. Given this common feature, it has been suggested that leukemic blasts might be initiated by transforming lesions that occur in HSC (Jordan, 2007). Alternatively, leukaemia can also arise from more lineage-committed progenitors (Riether et al., 2015). The ratio of the affected hematopoietic lineages divides acute leukaemia from chronic leukaemia. The leukemic blasts can be affected in their development of the myeloid or lymphoid lineage of the hematopoietic process distinguishing myeloid from lymphoid leukaemia's (Lockwood, 2015). Acute Myeloid Leukaemia (AML) which is the focus of this study is a heterogeneous malignancy that is characterized by uncontrolled proliferation and failure in the stem cell compartment differentiation. This causes accumulation of non-functional cells called myeloblasts (Estey and Döhner, 2006).

In the UK, around 3,200 new AML cases have been reported in 2017; 1,800 (56.25%) in males and 1,400 (43.75%) in females (Cancer Research UK). AML is the most frequent malignant myeloid disease in adults where the prevalence is 1.8 cases per 100,000 people in the <65 years' age group and 17.9 cases per 100,000 people in >65 years' age group (Jemal et al., 2010). In the UK, around 42% of all new cases of AML are in individuals >75 years old (Cancer Research UK).

Here, I will; firstly present a brief overview of AML and its pathogenesis, then highlight the role of epigenetic alterations in AML including the chromatin structure and mechanism(s) of function and finally introduce the heterochromatin protein 1 binding protein 3 (HP1BP3), its critical role(s) in gene regulation, chromatin and epigenetics in cell and cancer biology.

1.2 **Diagnose of AML**

In 2003, a panel of working groups who recognized clinical and research expertise in AML reported recommendations for routine diagnostic procedures for cases with suspected AML (Döhner et al., 2010). The panel recommended procedures based on studies that were carried out in United States and Europe (Döhner et al., 2010).

1.2.1 Morphology

Aspiration from blood and bone marrow (BM) is part of the routine diagnostic procedure for patients with suspected AML (Vardiman et al., 2009). The smears are morphologically investigated using histological stains such as Giemsa stain. It is suggested that at least 200 leukocytes on peripheral blood samples and 500 cells on BM be counted (Vardiman et al., 2009).

1.2.2 Immunophenotyping

Expression of cell-surface and cytoplasmic markers for the diagnosis of AML is recommended using flow cytometry to determine the involvement of the lineages in newly diagnosed patients (Table 1-1) (Bene et al., 1995, Döhner et al., 2010). This procedure is required to determine the minimal lineage differentiation, however, it should not replace the morphological assessment (Döhner et al., 2010).

Table 1-1: Cell surface markers for the diagnosis of AML.

Expression of markers for diagnoses	
Precursor stage	CD34, CD38, CD117, CD133, HLA-DR
Granulocytic markers	CD13, CD15, CD16, CD33, CD65
Monocytic markers	CD11c, CD14, CD64, lysozyme, CD4, CD11b, CD36
Megakaryocytic markers	CD41, CD61, CD42
Erythroid marker	CD235a

1.2.3 Karyotyping

Conventional cytogenetics evaluation is a compulsory part in the diagnostic assessment of cases with suspected AML. A minimum of 20 karyotyping of metaphase cells examined from BM is a mandatory to determine the diagnosis of a normal cytogenetic analysis, and chromosomal abnormalities.

1.2.4 Fluorescence *in situ* Hybridization (FISH)

Molecular cytogenetic such as FISH analysis is an optional practice to identify gene rearrangements, gene fusions, gene deletion or chromosomal translocation (Fröhling et al., 2002, Lugthart et al., 2008).

1.3 Pathogenesis of AML

1.3.1 Cytogenetics and genetics

To date, more than 200 chromosomal abnormalities such as chromosomal translocations, inversion or deletions, as well as extensive array of non-random karyotype anomalies and chromosomal lesions affecting proteins including cell surface receptors, intracellular signalling proteins and transcription factors, have been associated with the malignant development

in AML (Mrozek et al., 2004, Nimer 2008, Renneville et al., 2008). The prognosis and predict disease outcome are strongly linked to cytogenetics of AML through karyotype abnormalities with respect to induction therapy response, relapse risk and survival (Grimwade et al., 2010). Chromosomal abnormalities have been recognized in AML in about 50% of adults at diagnosis (Mrózek et al., 2001). Patients are positioned in one of three cytogenetic risk groups summarised in Table 1-2 (Grimwade et al., 2010).

Table 1-2: Cytogenetic risk groups in AML (Grimwade, Hills et al. 2010).

Risk category	Cytogenetics and genetic features
Favourable risk	t(8;21)(q22;q22), -t(15;17)(q22;q21), and inv(16)(p13q22)/t(16;16)(p13;q22), irrespective of the presence of additional cytogenetic changes.
Intermediate-risk	Normal karyotype and entities not classified as favourable or adverse
Adverse risk	t(10;11)(p11 13;q23), -abn(3q) (excluding t(3;5)(q25;q34)), t(6;11)(q27;q23), inv(3)(q21q26)/t(3;3)(q21;q26), add(5q)/del(5q), -5, -7, add(7q)/del(7q), -17, abn(17p) and other t(11q23) (excluding t(9;11)(p21 22;q23) and t(11;19)(q23;p13)), t(9;22)(q34;q11) -Lack favourable and adverse aberrations but with complex karyotype (i.e., 4 or more unrelated cytogenetic abnormalities)

t. translocation, inv: inversion, abn: abnormalities, del: deletion.

The molecular pathogenesis of AML may arise from an array of genetic lesions that disrupt normal cell transformation (Steffen et al., 2005). In the last two decades, nucleotide-level mutations that are undetectable by normal cytogenetics have been identified in a growing list of genes (Figure 1-2), a wide range of gene mutations have been discovered in AML (Steffen et al., 2005). These genetic alterations include dysregulation of cell expansion in the form of the lack of normal growth signals, unlimited self-renewal in a stem cell-like manner, escape from apoptosis, differentiation inhibition, cell

cycle checkpoint aberrations, alteration of genomic stability and leukemic cell dissemination (Steffen et al., 2005).

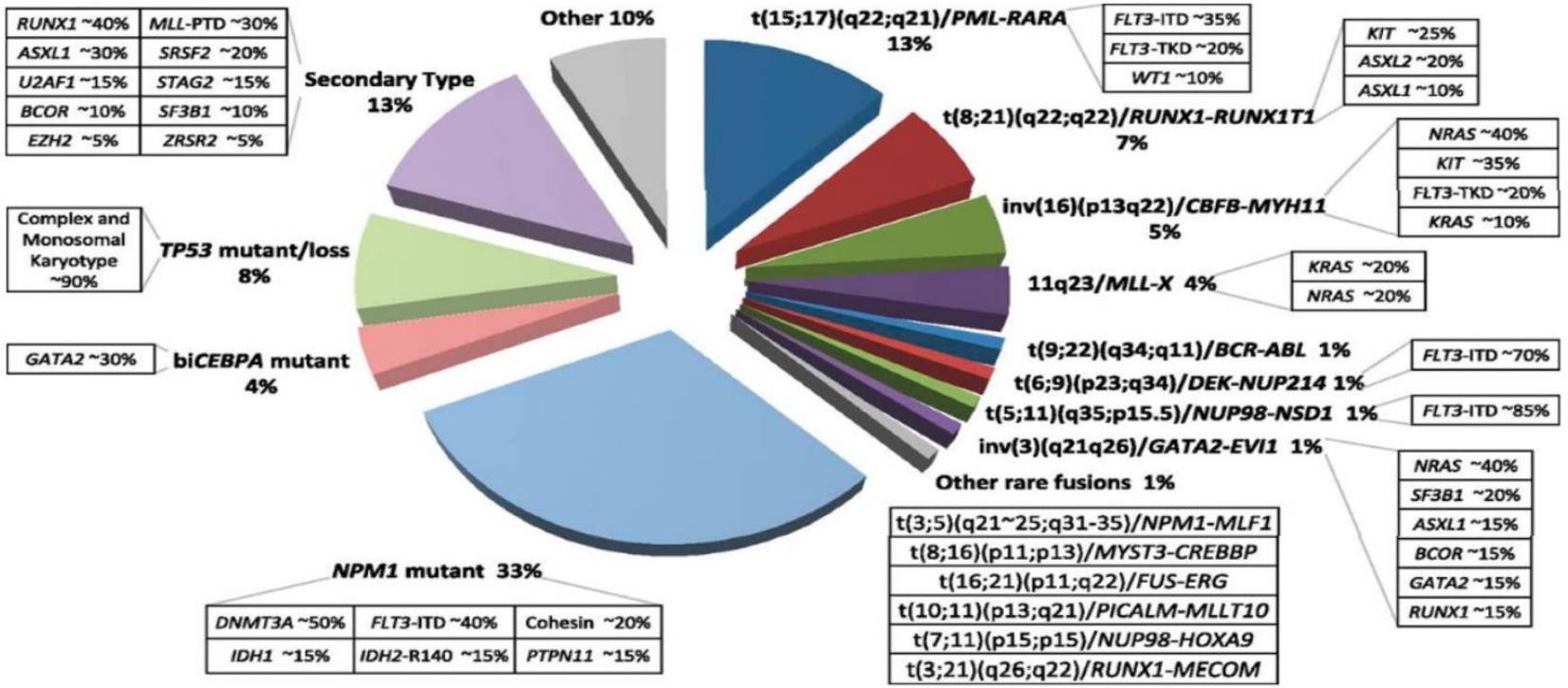


Figure 1-2: Molecular classes associated with specific gene rearrangements in patients with AML (Dohner et al., 2017).

Inappropriate Proliferation: mutations in the Fms-like tyrosine kinase 3 (FLT3) receptor are one of the most common alterations in patients with AML. The FLT3 receptor plays an important role in normal haematopoiesis progression in addition to leukemogenesis. Expression of FLT3 was reported in all stem cell progenitors and almost all patients with AML, and its activation triggers a sequence of phosphorylation-driven protein recruitment events that leads to the alteration of the transcription and stimulation of cell cycle progression (Licht and Sternberg 2005, DeAngelo et al., 2005). Other mutations affecting proliferation signalling pathways include the activation of c-KIT tyrosine kinase (Wakita et al., 2011), JAK2 kinase (Kaushansky, 2005) and RAS family (Ward et al., 2012).

Differentiation blockade: In AML, point mutations in myeloid transcription factors can affect normal myeloid differentiation, such as mutations in CCAAT/enhancer binding protein α (C/EBPα) (Song et al., 2015). HOX genes control the balance between HSC proliferation/differentiation; therefore, they have an essential role in haematopoiesis progression and regulation. Therefore, the deregulation of HOX genes is a dominant transformation process in leukemic cells (De Braekeleer et al., 2014).

Escape from programmed cell death (PCD): PCD, or apoptosis, is one of the most important terminal mechanisms in cells, and the ability to evade it is critical for malignant development (Klein, 2004). p53 protein is the main regulator of the apoptotic signalling pathways as well as cell cycle integrity (Petitjean et al., 2007), and its mutation is frequently identified in patients with AML (Kindle et al., 2005). They have been reported in 7% of 500 cases with *de novo* AML and 58.8% of cases with complex karyotype (Hou et al.,

2015). Moreover, p53 mutations are related to adverse effects to chemotherapy in patients with AML (Licht and Sternberg, 2005).

Self-renewal: Primary AML cells are committed to self-renewal rather than differentiation. Additionally, AML LSCs are not functionally homogenous and comprise heterogeneous self-renewal potential (Hope et al., 2004). Elevated expression of wingless-type (Wnt)/β-catenin in cells from patients with AML are associated with increased self-renewal capacity, as well as poor prognosis in those patients (Ysebaert et al., 2006). Analysis of genome-wide expression of HSC and AML LSC profiles has revealed that Wnt–β-catenin is a crucial pathway disrupted in AML LSCs (Chen et al., 2009). Nucleophosmin (NPM) is mutated in almost one-third of AML, while the expression of cytoplasmic NPM is restricted to AML (Falini et al., 2005, Liso et al., 2008), Moreover, its expression maintains the stem cell phenotype in these cells (Alcalay et al., 2005).

1.3.2 The role of miRNAs in AML

miRNAs regulate several biological processes such as development, differentiation and haematopoiesis by regulating expression of target genes. In haematopoiesis, miRNAs regulate both myeloid and lymphoid lineages (Garzon and Croce, 2008). miR-181 was one of the first miRNAs differentially expressed identified in different hematopoietic lineages. Overexpression of miR-181 stimulated the differentiation of HSCs into B-lineage cells (Chen and Lodish, 2005). Moreover, miR-328 promotes the master myeloid differentiation regulator C/EBPα and stimulates myeloid differentiation (Eiring et al., 2010). In contrast to miR-328, miR-124a

inhibits the myeloid differentiation by inhibiting C/EBPα expression (Hackanson et al., 2008). Downregulation of miR-15a and miR-16-1 due to genetic mutations in patients with chronic lymphocytic leukaemia (CLL) was the first discovery that linked miRNAs dysregulation with cancer (Calin et al., 2002). Knockout of miR-15a and miR-16-1 led to CLL development in mice (Klein et al., 2010). miRNAs are strongly dysregulated in haematological malignancies including AML (Peng and Croce, 2016).

It is well-established in AML that miRNAs can act as either onco-miRNAs or tumour suppressors by regulating several cellular mechanisms including proliferation, survival, epigenetic changes and drug response. Moreover, miRNA genome-wide analysis in patients with AML underlined the significance of miRNAs in the disease progression (Dixon-McIver East et al., 2008, Li et al., 2008, De Leeuw et al., 2016) as well as leukemic stem cell (LSC) quiescence, self-renewal and chemotherapy response (Lechman et al., 2016). Alteration in miRNAs levels promotes AML leukemogenesis by altering the expression of the downstream target genes. For example, miR-9 impairs myeloid differentiation (Nowek et al., 2016) and promotes leukemic blast proliferation by inhibiting Hairy and Enhancer of Split 1 (*Hes1*) expression (Tian et al., 2016). Other studies have demonstrated that miR-193a contributes to AML development by activating *PTEN/PI3K* signalling pathway (Li et al., 2013). Downregulation of miR-328 was associated with poor clinical outcome in patients with AML and could be used as a prognostic biomarker (Liu et al., 2015). Moreover, miR-135a has a tumour suppressive activity regulating HOXA10 expression in AML (Xu and Wen, 2018).

1.3.3 The role of epigenetics in AML

In early studies, AML was predominantly determined as a cytogenetic/genetic pathological process that deregulates signalling pathways and cellular differentiation. However, recent evidence from *de novo* AML identified that over 40% of patients do not have mutations in the signalling genes (Cancer Genome Atlas Research Network, 2013). Moreover, around 50% of AML cases harbour normal karyotypes (Mrózek et al., 2001) and only 20% of patients with AML have mutations in myeloid-associated transcription factors (Cancer Genome Atlas Research Network, 2013, Mehdipour et al., 2015). These findings are unable to completely explain the severe block in myeloid cell differentiation and the rapid expansion of leukemic blasts, which are the main characteristics of AML. However, recently, whole-exome and whole-genome sequencing analysis of 200 cases of *de novo* AML has revealed that over 70% of the samples had mutations in either the DNA methylation-related genes or the chromatin modifiers (Cancer Genome Atlas Research Network, 2013), suggesting that epigenetic modifications play an essential role in the development of most, if not all, AMLs.

The term ‘epigenetics’ refers to the stably heritable phenotype subsequent from modifications in a chromosome and that do not result from changes in the DNA structure (Jaenisch and Bird, 2003). However, it is well established that disturbances in epigenetic regulation underlie changes in every stage of gene regulation, such as DNA methylation, histone post-translational modifications (PTMs), nucleosome positioning, chromatin looping and short non-coding RNA (miRNA) (Jaenisch and Bird, 2003). The association of

gene mutations and epigenetic alterations involves signalling pathways and creates a fertile environment for the development of impaired blasts and the further promotion and progression of the malignant process. In order to elucidate the background of epigenetic alterations in haematological malignancies and myeloid leukemogenesis, it is essential to understand the normal structure of chromatin and its construction of its physiological mechanisms.

1.3.3.1 Chromatin structure

Chromatin is a compacted form of DNA and proteins in the interphase nucleus. Whereas chromosomes represent condensed form of chromatin in metaphase during mitosis, which ensure equal and proper segregation of the genetic materials into daughter cells (Laufer and Singh, 2015). High-order chromatin organisation governs the transcriptional process through a series of diverse posttranslational modifications taking place at the amino-terminal tails of chromatin proteins or to the DNA itself (Jenuwein and Allis, 2001, Rice and Allis 2001, Laufer and Singh, 2015). A set of nuclear proteins (histone and non-histone) are involved in the chromatin organisation which has an important role in the construction of the condensed form. This condensation process stabilizes and compacts the 2-m long linear DNA into

a nanofiber form to package it in the nucleus of the human cell (Dillon and Festenstein, 2002) (Figure1-3).

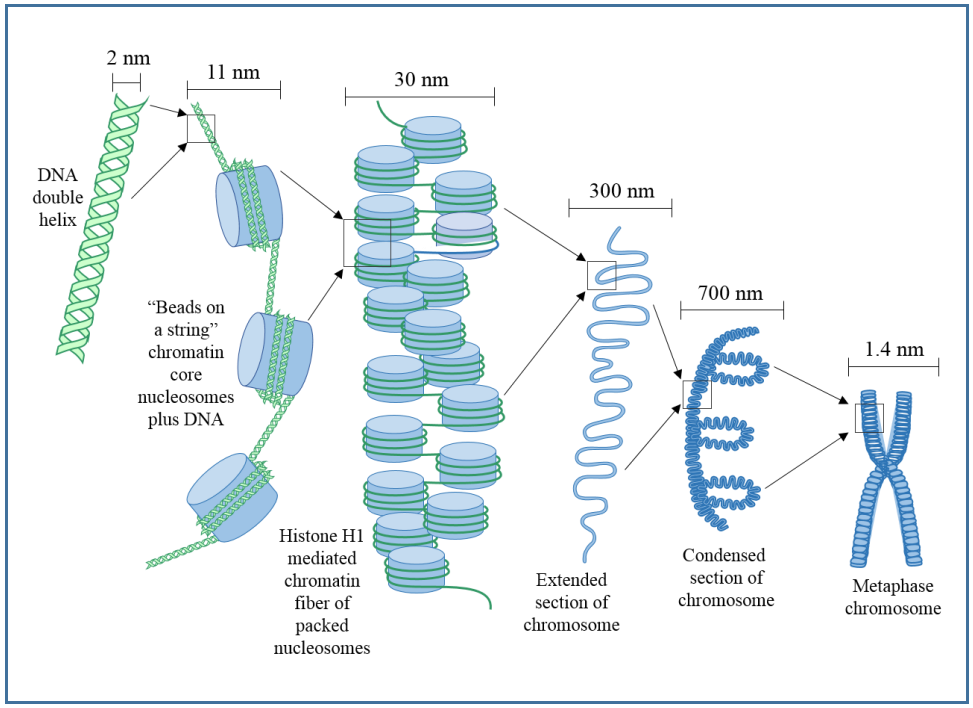


Figure 1-3: Organization of DNA in chromatin within the cell. Typically, the double helix DNA is wrapped around a histone octamer, creating nucleosomes that appear as beads on a string. These beads of nucleosome elements are then folded to form fibres of 30 nm in diameter and further coiled into higher-order structures which known as chromosomes. The total condensation of DNA in a chromosome form is more than 10,000-fold. [Modified from (Hübner, Eckersley-Maslin et al. 2013)].

Moreover, the collaboration of DNA-packaging proteins and associated covalent modifications impacts on the structure of chromatin template, thus leading to the inherited changes in transcriptional states which underlie the "on" or "off" states of the dynamic chromatin polymer (Maison and Almouzni, 2004). The altered pattern of gene expression enable cancer cells to obtain their hallmark characteristics (Fouad and Aanei, 2017). However, the genomic instability plays an essential role in allowing cells to acquire

genetic changes that promote oncogenesis (Charames and Bapat, 2003). Chromatin plays a significant role in both maintaining genome stability as well as regulating gene expression (Abbas et al., 2013). Cancer genome studies indicated number of gene mutations encode chromatin modifiers such that have implication in the pathogenesis of both solid tumours and haematological malignancies (Morgan and Shilatifard, 2015).

1.3.3.2 Chromatin states

Historically, the microscopic observation of the chromatin in interphase revealed two distinct domains, heterochromatin and euchromatin, which reflect different aspects of chromatin behavior including regulation of gene expression, activating or silencing the transcription according to the signals imposing upon it (Maison and Almouzni, 2004). Degree of chromatin condensation is determined by participation of a diverse array of posttranslational modifications (PTMs), which occur on the N-terminal charged tails of core histones. Additionally, chromatin architecture can be altered by the action of ATP-dependent remodelling proteins (Piatti et al., 2011). Hence, the formation of compacted chromatin architecture as well as the storage and regulation of genetic information are governed by covalent modifications which also known as “histone code”. Despite the fact that every single cell carries the same genetic code, the gene expression pattern

varies from one cell to another, which is believed to be influenced by histone modifications (Schäfer and Jung, 2005).

1.3.3.3 Histone types

Histones are proteins playing the role of building blocks by compacting the DNA chain and folding it into a high-order chromatin structure. The nucleosome is composed of core histones, or an octamer, around which 146 base pairs of a DNA sequence are wrapped in two superhelical turns (Figure 1-4) (Luger et al., 1997). Nucleosomes are the fundamental building blocks of chromatin, where histone protein forms the heart of this complex (Strahl and Allis, 2000). There are five histone isotypes: H2A, H2B, H3, H4 and H1. The nucleosome octamer is composed of a H3–H4 tetramer and two H2A–H2B dimers (Arents and Moudrianakis, 1993), while H1 is termed and functions as the internucleosome linker histone. The assembly of H1 and the nucleosome is known as the chromatosome, considered a basic repeat unit of chromatin fibres (Hayashihara et al., 2010). The H1 globular domain (GD) interacts with linker DNA at the entry/exit site of nucleosomal DNA, creating higher levels of chromatin condensed structure (Maresca et al., 2005,

Soshnev et al., 2016); therefore, H1 might play an important role in mitotic chromosome compaction and segregation.

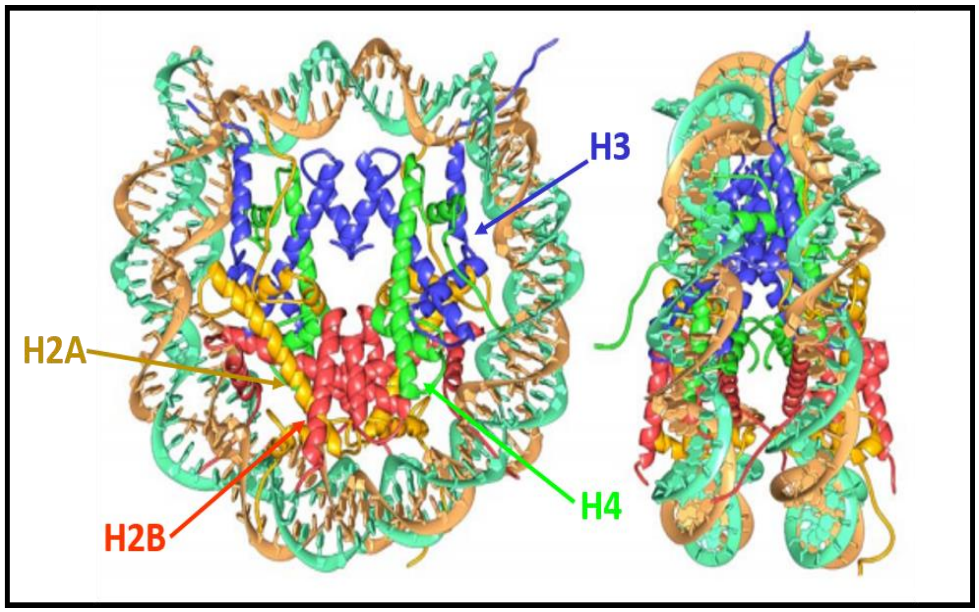


Figure 1-4: Nucleosome core particle structure. Ribbons represent histone proteins (yellow H2A, red H2B, blue H3 and green H4). Brown and turquoise superhelix represent DNA [Modified from (Luger et al., 1997)].

1.3.3.4 Histone post-translational modifications (PTMs)

Histone post-translational modifications are covalent modifications that take place on the histone N-terminal tails such as; acetylation, methylation, phosphorylation and ubiquitination (Figure 1-). Histone proteins share the same primary structure, but undergo different covalent modifications, which influence gene expression (Kouzarides, 2007, Soshnev et al., 2016).

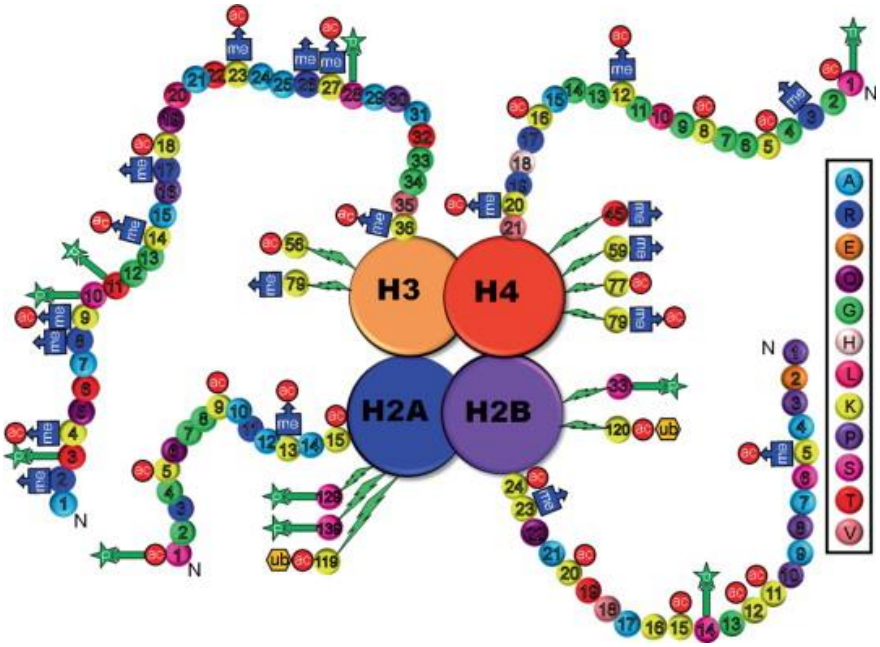


Figure 1-5: Histone tails posttranslational modifications. Histone core consists of two common parts: histone fold and histone tails. Histone tails are flexible, protruding from the nucleosome and can be covalently modified. They are consisting of amino acid which are numbered according to their positions at the N-terminals. [Adapted from (Jayani et al., 2010)].

PTMs act as transcriptional controllers that balance the transposition between the active euchromatin and the inactive heterochromatin. In addition to modifying the condensation of the local chromatin landscape, epigenetic alterations can function as signals to recruit other regulatory factors including transcription factors to influence gene expression and also have great impact on all DNA-templated processes such replication, genome packaging, maintenance of genome stability and chromatin segregation (Schäfer and Jung, 2005, Vaiopoulos et al., 2014).

The involvement of a range of enzymes catalysing PTMs is crucial for initiating the function of the PTM regulatory machinery. Deregulation of enzymatic interactions or expression can alter the flow of normal physiological processes and induce incorrect transcription patterns by

silencing or down-regulating tumour suppressor expression or enhancing oncogene expression (Vaiopoulos et al., 2014).

1.3.3.5 DNA modification

DNA methylation is a hereditary epigenetic change that includes covalent addition of a methyl group to the C-5 position of the cytosine residue of DNA. Cytosine methylation (5-methyl cytosine [5mC]) in CpG dinucleotide sites is generally related to heterochromatin construction and transcriptional repression catalyses by a group of enzymes terms, DNA methyltransferases (DNMTs) (Jin et al., 2011). Oppositely, the unmethylated CpG dinucleotides, recognized as CpG islands, are related to euchromatin and usually present in the promoters of actively transcribed genes. CpG methylation removal involves sequential oxidation events which convert 5-hydroxymethylcytosine (5hmC), 5-formylcytosine (5fC) and 5-carboxylcytosine (5caC) that catalysed by Ten-eleven translocation (TET) enzyme. 5caC, can be deleted by thymine DNA glycosylase (TDG)-dependent DNA repair (Wu and Zhang, 2017).

1.3.3.6 Chromatin modifications and gene expression

Histone tail PTMs can serve as a suppressive or activating signal depending on the site of the histone tail being modified, type and number of chemical groups (Dong and Weng, 2013). Histone tail acetylation is an important epigenetic regulation that involves the addition of acetyl group to histones and is usually characteristic of transcriptionally active, non-compact ‘euchromatin’ (Grunstein et al., 1995) (Figure 1-6).

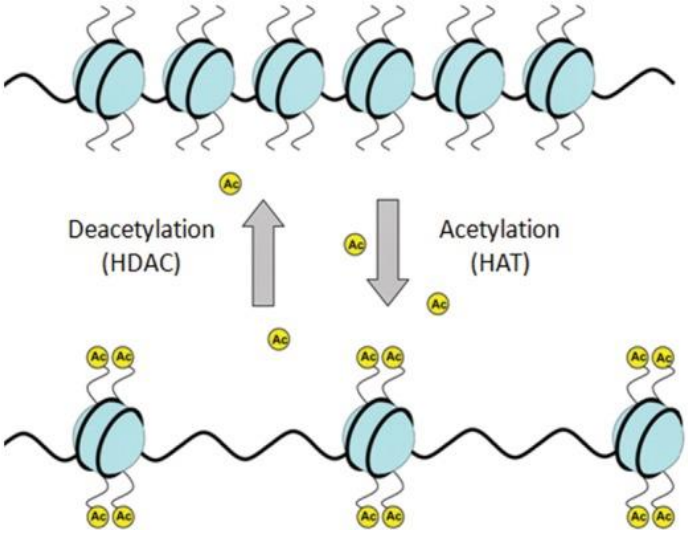


Figure 1-6: Histone acetylation and deacetylation. Histone tail acetylation involves the addition of the acetyl group (Ac) by histone acetyltransferase (HATs), leading to the formation of euchromatin and initiation of gene transcription. Histone deacetylases (HDACs) remove the Ac group from the histone tails, which results in the formation of heterochromatin [Adapted from (Baghaban Eslaminejad et al., 2013)].

Histone acetylation is tightly regulated by the activity of two enzyme groups: histone acetyltransferases (HATs) and histone deacetylases (HDACs) (Kuo and Allis, 1998, Dawson and Kouzarides, 2012, Gargalionis et al., 2012, Vaiopoulos et al., 2014). HATs, such as PCAF, GCN5 and HAT1, promote histone acetylation and hence transcriptional activation (Hebbes et al., 1988, Kuo and Allis, 1998) (Figure 1-6). Regions of active DNA are marked with H3 and/or H4 acetylation (van Engeland et al., 2011, Vaiopoulos et al., 2014). HDACs have antagonistic properties to HATs, stimulating the removal of acetyl groups from the lysine residues of histone tails, leading to chromatin condensation and the repression of gene transcription by enabling interaction between DNA and histones (Davie and Spencer, 1999). This chromatin state is termed heterochromatin. Typically, HATs and HDACs regularly add and

remove acetyl groups to and from the N-terminal of histone lysine residues (Kuo and Allis, 1998, Vaiopoulos et al., 2014). HAT and HDAC functions are well-described and their role in tumorigenesis has been largely studied (Marks, 2010).

In patients with AML, for example, have a significant deficiency in histone acetylation in comparison with people without leukaemia, which would suggest excessive deacetylation, which might be due to excessive deacetylase activity, deficient acetyltransferase activity, or a combination of both (Xiao et al., 2010). Moreover, Chromatin immunoprecipitation (ChIP) followed by microarray hybridization (ChIP–ChiP) analysis for a large cohort of AML cases has identified that histone deacetylase 1 (HDAC1) dyslocalization is a frequent attribute in AML and several HDAC-binding proteins alter the promoters of genes associated with signal transduction, regulation of gene transcription and haematopoiesis (Tickenbrock et al., 2011).

Unlike histone tail acetylation, histone tail methylation can be activating or repressive (Bannister et al., 2002). Similar to other histone tail modifications, methylation is reversible and is tightly regulated by the activities of two groups of antagonistic enzymes: histone methyltransferases (HMTases) and histone demethylases (HDMs) (Bannister and Kouzarides, 2005). HMTases and HDMs catalyse the addition and removal of methyl groups to and from specific histone lysine or arginine residues, respectively (Vaiopoulos et al., 2014). Histone H3 undergoes methylation at several lysine sites, such as K4, K9, K27, K36 and K79; in addition, a lysine residue can be unmethylated (me0), monomethylated (me1), dimethylated (me2) or trimethylated (me3) (Fischle et al., 2005). H4 is also methylated mostly at K20 and less commonly

at K79 and K59 (Wang et al., 2001). Trimethylation of H3K4, H3K36 and H3K79 are linked with transcriptional activation; however, trimethylated H3K9, H4K20 and H3K27 are linked with transcriptional suppression (Bártová-Krejčí et al., 2008, Benard, Goossens-Beumer et al., 2014, Vaiopoulos et al., 2014, García-Giménez, 2015). Upregulation of H3K9 methylation, which leads to gene silencing, has been reported in various types of cancer (Pogribny et al., 2007, Park et al., 2008), and an elevated level of H3K9me3 in patients with gastric carcinoma has been associated with poor prognosis (Park et al., 2008). However, deregulation of these two histone markers (H3K9ac/H3K9me3) in cancer cells is not essentially related to bad prognosis. H3K9me3 deregulation in patients with AML that arises as a reduction in H3K9me3 levels in the core promoter regions is related to improved prognosis (Müller-Tidow-Klein et al., 2010).

1.3.3.7 Chromatin modifiers mutated in AML

Complex developmental mechanism such as haematopoiesis requires a sequence of accurate as well as controlled changes in the origin of the cell to sustain blood homeostasis (Jagannathan-Bogdan and Zon, 2013). Epigenetic processes regulate gene expression to ensure the accurate transition from HSC to terminally differentiated blood progenitors (Rice et al., 2007).

Numerous chromatin-modifying enzymes are mutated in haematological malignancies, here I will discuss some of the most important somatic mutations in chromatin modifiers that have been reported in AML and how these modifiers cause aberrant cell differentiation and alter self-renewal and proliferation (Rice et al., 2007, Sharma and Gurudutta, 2016).

Methylation of cytosine residue has an important role in HSC self-renewal, moreover myeloid commitment (Tadokoro et al., 2007, Bröske et al., 2009). Methylation profiling of mouse multipotent progenitor cells has identified methylation of promoters for transcription factors during cellular differentiation to common myeloid or lymphoid progenitors (Ji et al., 2010). The main enzymes that catalyse cytosine methylation are members of two DNAMTs families known as DNMT1 and DNMT3. Conditional deletion of Dnmt1 in HSCs and progenitor cells showed that Dnmt1 plays a crucial role in early stages of haematopoiesis and its absence led to decreased self-renewal capacity in HSC (Trowbridge et al., 2009). The DNMT3 family is required for *de novo* methylation, and includes 2 active enzymes, DNMT3a and DNMT3b. Mutations impairing the of DNMT3a catalytic function have been reported in approximately one third of patients with AML (Ley et al., 2010).

The conversion of 5-mc to 5hmC by the TET protein family is believed to be an important stage during DNA demethylation path. knock out of *Tet2* in mice causes elevated HSC self-renewal and alters cell differentiation potential (Li et al., 2011). Mutations of *TET2* found in 7–23% of AML (Chou et al., 2011) and usually related to reduced 5hmC levels and both DNA hyper-methylation and hypo-methylation (Figueroa et al., 2010).

Isocitrate dehydrogenase (IDH) controls the transformation of isocitrate to a-ketoglutarate (a-KG). IDH1/2 mutations alter its enzymatic function, leading to the reduction of α-ketoglutarate to d-2-hydroxyglutarate. Expression of IDH1/2 mutants that are found in 15–33% of AML inhibits

TET2-induced 5hmC leading to induced in global DNA hyper methylation and reduce DNA demethylation (Figueroa et al., 2010, Rakheja et al., 2012).

Enhancer of Zeste Homologue 2 (EZH2) is a histone methyltransferase that catalyses the di- and trimethylation of K27 of histone H3 (H3K27), which is a mark of heterochromatin. EZH2 plays a vital role in SC development including HSC, its mutation is infrequent in most acute leukaemia (1–2% of AML cases) but it was reported in 16–19% of T-cell acute lymphoblastic leukaemia (T-ALL) (Lund et al., 2014).

The Nuclear SET Domain (NSD1) is also a histone methyltransferase that regulates gene expression through methylating K36 of histone H3 (H3K36). It is involve in leukaemia via its fusion with the NUP98, causing NUP98-NSD1-fusion protein which is related to poor prognosis in AML cases (Wagatsuma et al., 2016).

Additional sex comb-like 1 (*ASXL1*) gene mutations have been reported in different kinds of myeloid malignant diseases. Analysis of ASXL1 in 882 AML cases revealed mutations in 46 cases (5.3%) (Pratcorona et al., 2012).

1.4 **Heterochromatin Protein (HP1)**

Proper condensation and segregation of chromosomes during mitosis are provided by accurate packaging of the DNA in nucleosomes (Eissenberg and Elgin, 2000). The compacted form of chromatin is maintained by the collaboration of nucleosomes with non-histone proteins. HP1 is one of the non-histone proteins that directly interact with heterochromatin regions (Chevillard-Reik et al., 1993, Mateescu et al., 2008). HP1 is a highly conserved small protein molecule (15–35 KDa) of the chromatin protein

family that was initially identified in *Drosophila melanogaster* (James et al., 1989, Vermaak et al., 2005).

HP1 subtypes have been reported in different organisms, from yeast (Swi6, Chp2 and Chp1) to humans (HP1α, HP1β, and HP1γ) (Zeng et al., 2010). In mammals, all three HP1 subtypes have the same amino acid sequences and structure but have different functions and localization. Both HP1α and HP1β interact with more compacted chromatin areas (heterochromatin), for example centromeres and telomeres, and are associated with gene silencing (Zeng et al., 2010). However, HP1γ can interact with both heterochromatin and euchromatin regions and can serve as a marker of transcription activation (Fanti et al., 2003). Therefore, their function may vary according to their localization.

The structure of HP1 subtypes consists of two highly conserved domains from yeast to humans (Zeng et al., 2010). The chromodomain (CD) at the N-terminal and a chromoshadow domain (CSD) at the C-terminal are connected by a variable-length hinge region (Figure 1-7) (Lomberk et al., 2006). The CD directly interacts with H3K9me3, which known as a heterochromatin marker, while the CSD interacts with other different proteins (Muchardt et al., 2002).

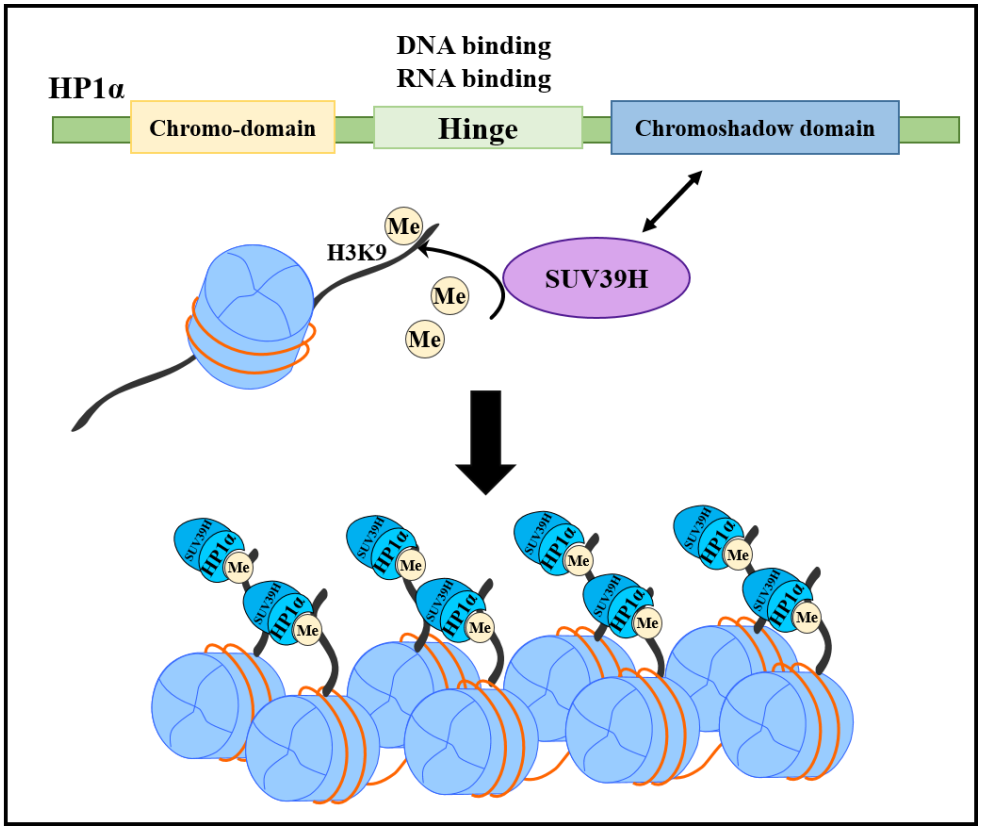


Figure 1-7: Schematic representation of HP1α protein and heterochromatin structure. The CD of HP1α interacts with H3K9me3 promoting heterochromatin formation. While the CSD binds to SUV39h which methylates H3K9. [Modified from (Muchardt et al., 2002)].

1.5 Heterochromatin Protein 1 Binding Protein 3 (HP1BP3)

Heterochromatin protein 1 binding protein 3 (HP1BP3, also known as HP1BP47) is a novel chromatin binding protein that directly binds to HP1α protein (Hayashihara et al., 2010). HP1BP3 was discovered as a result of salt stripping of isolated and purified human metaphase chromosomes from HeLa S3 cells (Figure 1-8) (Hayashihara et al., 2010).

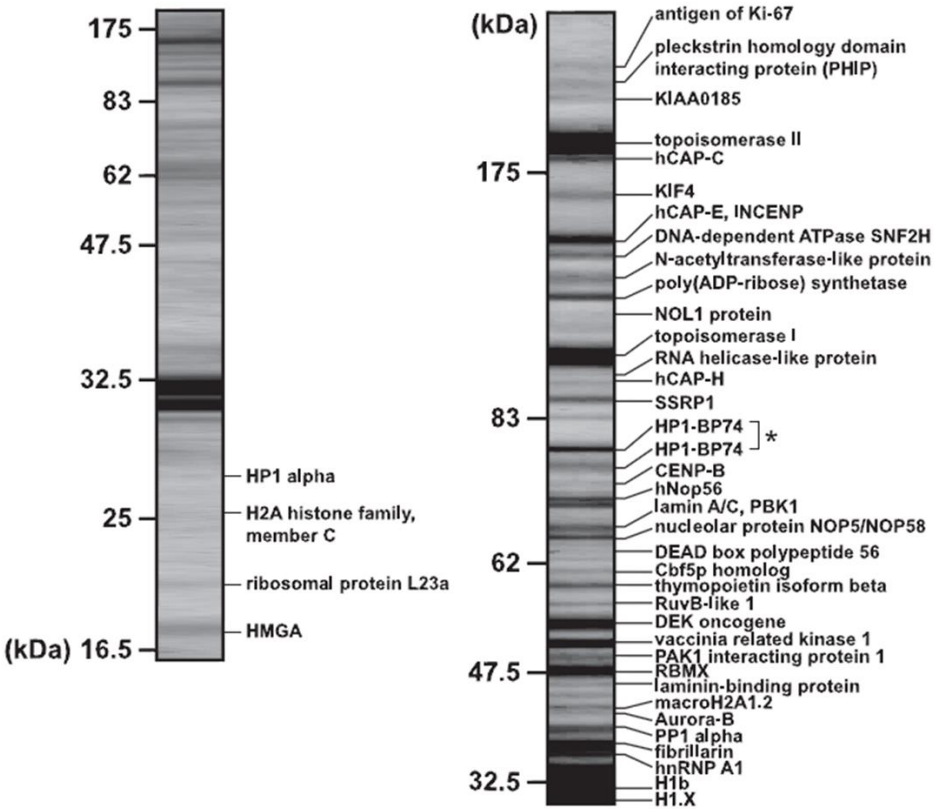


Figure 1-8: The schematic human metaphase chromosome-associated proteins. Proteins were dissociated and identified using salt striping (0.4 NaCL) and analyzed with mass spectrometry. HP1BP3 (HP1BP74) demonstrated in two separate bands. [Adapted from (Hayashihara et al., 2010)].

Human *HP1BP3* was mapped to chromosome 1p36.12 and consists of 13 exons, while the murine *Hp1bp3* gene is located on chromosome 4 D3; 4 and comprises 12 exons. HP1BP3 is a highly conserved protein in mammals, with 93% similarity between humans and murines (Garfinkel et al., 2015). As a result of alternative splicing at the 5′ terminal, the gene encodes two transcripts in both humans and mice, which translate eventually to HP1BP3a (long isoform) and HP1BP3b (short isoform). Consequently, the splice variant of the short isoform lacks the first two exons and as a result it lacks the first 38 amino acids located at the N-terminal (Hayashihara et al., 2010, Garfinkel et al., 2015). HP1BP3 is ubiquitously expressed in all tissue types

in both humans and mice. The long and short HP1BP3 consist of 553 and 402 amino acids in humans, respectively, and 500 and 462 amino acids in mice (Garfinkel et al., 2015).

1.5.1 HP1BP3 structure and localization

HP1BP3 is a novel nuclear protein containing different domains involved in diverse interactions (Hayashihara et al., 2010, Garfinkel et al., 2015). Recently, Garfinkel et al. reported that HP1BP3 is evolutionary and structurally related to the linker histone H1 family, the most abundant nucleosome-binding proteins (Garfinkel et al., 2015). H1 is important for proper chromatin architecture and chromosome segregation (Maresca et al., 2005), regulation of gene expression (Fan et al., 2005), mammalian development (Fan et al., 2003) and stem cell differentiation (Zhang et al., 2012, Pan and Fan, 2016). Like H1 subtypes, HP1BP3 contains different domains; the middle part of HP1BP3 (K97–K274) contains a GD (M153–T237) that has a sequence identical to the linker histone H1 and associates with linker DNA at the entry/exit site of nucleosomal DNA (Hayashihara et al., 2010). Further structural studies have reported that the middle region of HP1BP3 is comprised of three consecutive GDs, termed GD1, GD2 and GD3, with high sequence similarity with the GDs of H1 variants. The N-terminal residue (NTD) contains the first 157 amino acids and contains a glutamine-rich unstructured domain, while the C-terminal residue (CTD) is hydrophobic and 34% positively charged (Garfinkel et al., 2015).

Similar to H1 subtypes, both the NTD and CTD are required for the chromatin binding properties of HP1BP3, which are dependent on the cell

cycle and PTMs (Garfinkel et al., 2015). Experimental analysis has revealed that deletion of the basic C-terminal tail dramatically diminished the interaction of HP1BP3 with chromatin (Garfinkel et al., 2015). furthermore, deletion of the N-terminal extension reduced the affinity of HP1BP3 for chromatin (Garfinkel et al., 2015). Therefore, these data suggest that a triple globular region along with the CTD and NTD exert a cooperative function towards the proper chromatin binding of HP1BP3 (Garfinkel et al., 2015).

Apart from its similarity with H1 family members, HP1BP3 has its own structural characteristics. HP1BP3 interacts with HP1α CSD through a novel PxVxL-binding motif at proline 255–leucine 259 (Hayashihara et al., 2010), which is close to the second HP1BP3 GD (Garfinkel et al., 2015). Using site-directed mutagenesis from valine (V257) to glutamic acid substitution led to complete abolishment of HP1BP3 interaction with heterochromatic regions, strongly suggesting HP1α-dependent heterochromatin enrichment of HP1BP3 (Garfinkel et al., 2015). HP1BP3 showed strong colocalisation with both HP1α and H3K9me3 (heterochromatin markers), whereas there was significantly reduction in the colocalisation between HP1BP3 and HP1γ (euchromatin marker), supported that HP1α-dependent HP1BP3 involvement in heterochromatin (Garfinkel et al., 2015).

Recent findings showed that the HP1BP3 nuclear expression pattern is predominant in all investigated cell lines and tissues and its distribution varies between cell type (Garfinkel et al., 2015). The highest expression was shown in the brain compared to other observed tissues, while germ cells are null for HP1BP3 expression.

1.5.2 HP1BP3 protein-interactions

In this project, we used publicly accessible bioinformatics databases to find novel HP1BP3 interactions, pathways, co-expression and co-localization: First, GeneMANIA (GeneMANIA.org) provides information on gene function for a single or multiple gene set (Franz et al., 2018). Second, STRING (Search Tool for the Retrieval of Interacting Genes/Proteins, String-DB.org), a biomolecular network for known and predicted protein–protein interactions or interactions by other molecules and scores each prospective interaction based on experimental or curated evidence (Szklarczyk-Gable et al., 2021).

GeneMANIA analysis of *HP1BP3* identified several novel interactions with linker histone H1 clusters and nucleosome assembly proteins (GeneMANIA.org). data were extracted and analysed using the GeneMANIA node network for co-expression, physical interactions and shared protein domains (Figure 1-9). HP1BP3 interacts and co-expresses with nine different histone clusters 1: Ha-e, t, HfO, HfOO and Hfx; RNA binding proteins: LIN28A and TARBP2 and other kinases and nuclear proteins (Figure 1-9). However, it shares a protein domain with only the H1 family and RIOK2 (serine/threonine protein kinase 2). This database was last updated for HP1BP3 on 13 March 2017.

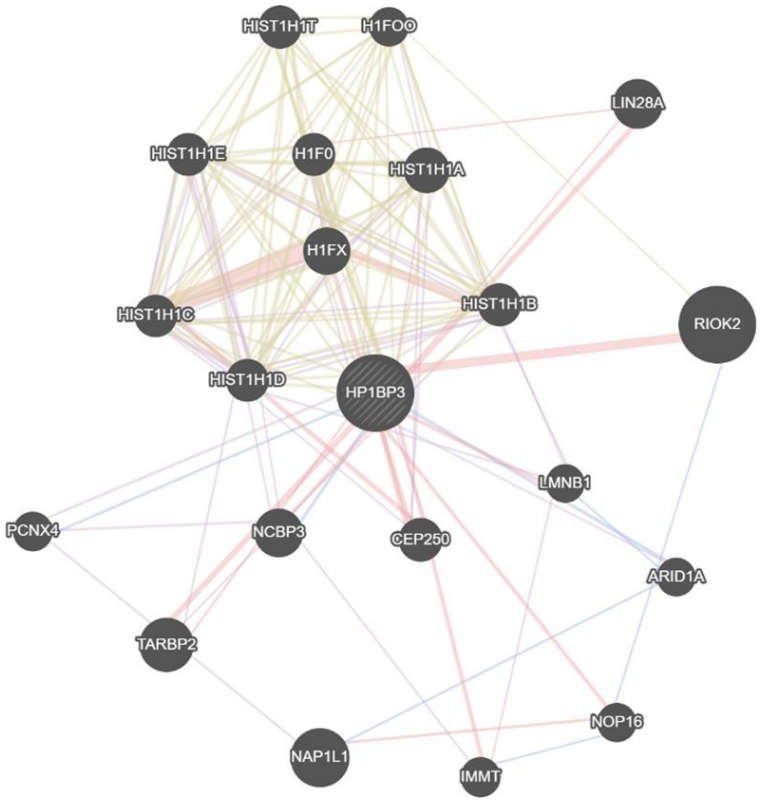


Figure 1-9: GeneMANIA analysis of HP1BP3 showing novel nuclear proteins interactions. Data indicates mainly histone clusters 1, RNA binding and nuclear proteins interact with HP1BP3. Coloured lines: pink; physical interactions, purple; co-expression, blue; co-localization and green; shared protein domain.

STRING analysis of *HP1BP3* identified a novel interaction with the histone-specific demethylase KDM1A (lysine-specific histone demethylase 1A) which demethylates both H3K4 and H3K9 (Ismail et al., 2018). Other interactions included the core histone H2A variants, the pre-rRNA processing protein FTSJ3, kinases and other proteins with lower confidence scores (Figure 1-10). Analysis was carried out using online STRING platforms (STRING-DB.org) for the highest confidence interaction (0.7–0.9) for the 10 closest direct or indirect interaction nodes.

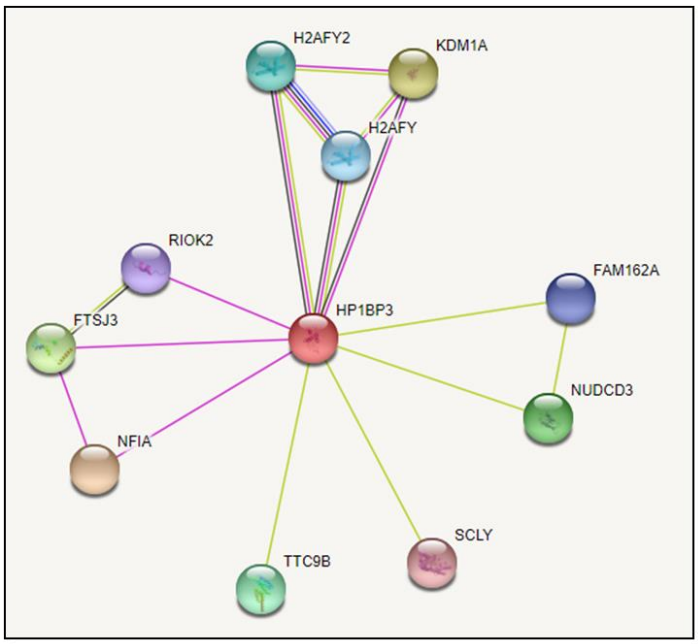


Figure 1-10: STRING analysis of HP1BP3 showing 10 nodes proteins interactions. Coloured node: pink; experimentally analysed, navy; gene co-occurrence, green; gene neighbourhood.

1.5.3 Functions of HP1BP3

HP1BP3 was initially discovered as a novel heterochromatin binding protein (Hayashihara et al., 2010), therefore several attempts have been carried out to explore its role in the chromatin architecture and cellular biology (Dutta et al., 2014, Dutta et al., 2014, Garfinkel et al., 2015, Garfinkel, Melamed-Book et al., 2015, Garfinkel-Arad et al., 2016, Hadac et al., 2016, Liu et al., 2016, Neuner, Garfinkel et al., 2016).

Chromatin compaction and gene expression: Intriguingly, most available reports about HP1BP3 suggest that it is a nuclear protein (Dutta et al., 2014, Garfinkel et al., 2015, Liu et al., 2016). Moreover, two reports showed strong evidence that HP1BP3 localises in the nuclei but not in the nucleoli during interphase or the chromosomes in the mitosis (Hayashihara et al., 2010,

Garfinkel et al., 2015), such expression pattern was also reported in high-order chromatin structure associated proteins (Cherukuri et al., 2008). However, Shi et al., recently showed that HP1BP3 localises at the telomere regions by binding to death domain-associated protein (DAXX) in the alternative lengthening of telomeres (ALT) tumour cells (Shi et al., 2020). DAXX forms a complex by binding to alpha-thalassemia X-linked syndrome protein (ATRX) and together they function as chaperon telomeres (Hoelper Huang et al., 2017) and maintain telomer stability (He-Kim et al., 2015, Tang, Li et al., 2015). Dutta et al has reported that HP1BP3 depletion led to chromatin unfolding in HEK293T cells (Dutta et al., 2014). Suggesting a novel regulatory function of HP1BP3 in maintaining heterochromatin integrity and higher-order chromatin structure. Furthermore, HP1BP3-null HEK293T cells demonstrated considerable reduction in chromatin compaction compared with control cells and showed more susceptibility to micrococcal nuclease (MNase) digestion. This finding suggests the possible mechanism of HP1BP3 in chromatin remodelling through euchromatin-heterochromatin conversion and thus regulation of gene transcription in Dutta's et al. model (Dutta et al., 2014). Additionally, HP1BP3 depletion reduced the telomere chromatin compaction in ALT cells (Shi et al., 2020). However, Garfinkel et al., showed that HP1BP3 inhibition does not affect the global chromatin structure in HeLa cells (Garfinkel et al., 2015). Despite the contradictory findings, two groups reported that HP1BP3 inhibition influenced the expression of many genes in their models (Dutta et al., 2014, Garfinkel et al., 2015). Microarray showed that the loss of HP1BP3 altered the expression of 384 genes in HeLa cells: 271 genes were upregulated and

113 were downregulated (Garfinkel et al., 2015). Another proteomic methodology revealed that 384 proteins were differentially expressed (176 up- regulated and 208 down-regulated) in HP1BP3-null HEK293T cells compared to the control cells (Dutta et al., 2014).

Cell cycle regulation: A chromatin proteomic approach, revealed a dynamic association of HP1BP3 through the different stages of cell cycle progression (Dutta et al., 2014). In all eukaryotic, the cell cycle consists of two major phases: interphase (DNA replication in the nucleus) and mitosis (nucleus division and separation of the two daughter cells) (Figure 1-11). Usually, human cells spend most of their time i.e. around 95% of the time at the interphase. Interphase, the stage between two consecutive mitoses consists of three stages; the first gap phase (G1) followed by the synthesis phase (S) and eventually the second gap phase (G2) (Cooper, 2000, Ma-Kanakousaki et al., 2014).

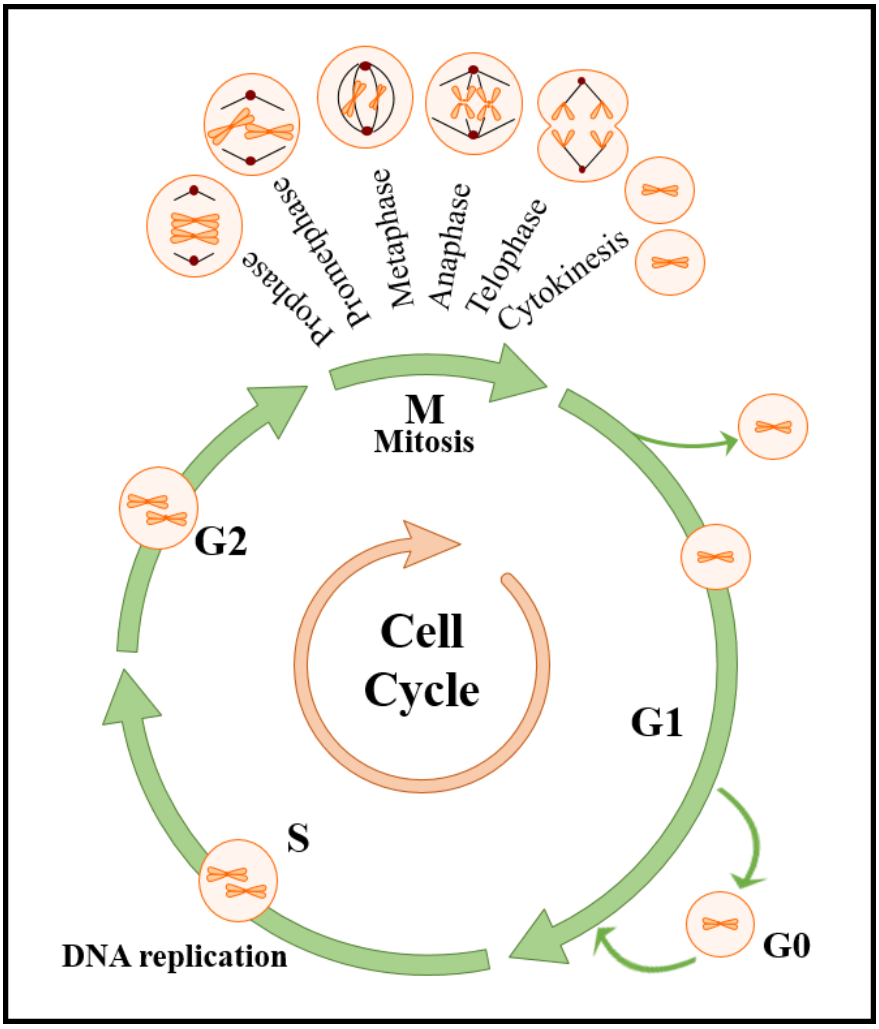


Figure 1-11: Schematic diagram of the cell cycle. The cell cycle is divided into two stages: interphase and mitosis. Interphase is subdivided into G1, S and G2 phase and mitosis is further divided into prophase, prometaphase, metaphase, anaphase, telophase and cytokinesis. At the end of each mitosis, cells either re-enter the cycle or exit the cycle and enter the G0-phase 'quiescent state'. [Modified from (Cooper, 2000)]

Furthermore, HP1BP3 expression was abundance during the transition from G1 to S phase, indicating its regulatory role of cell cycle progression and ultimately cell proliferation (Dutta et al., 2014). The precise G1–S transition plays a crucial role in regulating cell proliferative potential (Nielsen et al., 1999, Bertoli et al., 2013, Wang et al., 2014, Liu et al., 2016). Regulation of cell cycle and the duration of each phases is essential, and dysregulation of any phase can impact the cell proliferation leading to cancer development.

During cell cycle progression, chromatin condensation and de-condensation are essential for the correct procession of basic cellular events (Ma et al., 2014). The chromatin integrity can be maintained by chromatin–protein interaction that regulates cellular functions during interphase (Hayakawa et al., 2003, Alexandrow and Hamlin, 2005, Probst and Almouzni, 2008, Park et al., 2011, Bhaskara et al., 2013, Ma et al., 2014, Park et al., 2014). There are two constantly interchanging chromatin in interphase: euchromatin and heterochromatin. Euchromatin allows transcription factors access to DNA in the nucleosomes, which is required for normal cell function. While heterochromatin contains genes that are differentially expressed through development and/or differentiation. Hence, a highly dynamic state of chromatin is important for proper DNA replication and the transfer of genetic and epigenetic material to progeny cells (Richards and Elgin, 2002, Bannister and Kouzarides, 2011). Dysregulation of chromatin-associated proteins could alter the cell cycle and subsequently the expression of numerous cellular function–associated proteins, consequently promoting carcinogenesis (Czvitkovich et al., 2001, Di Paola et al., 2012, Ramadoss et al., 2012, Kogure et al., 2013, Stypula-Cyrus et al., 2013, Ji et al., 2015, Petti et al., 2015). As HP1BP3 contributes to chromatin dynamics, it might act as a critical driving force behind tumour initiation and/or progression via cell cycle deregulation and therefore lead to uncontrolled cell proliferation, the hallmark of cancer.

Growth and viability: Conventional HP1BP3 knockout led to partial post-natal lethality in mice and growth retardation (Garfinkel et al., 2015,

Garfinkel et al., 2015), indicating the physiological role of HP1BP3 in growth and viability and highlighting the influence of HP1BP3 in G1–S transition regulation and cell proliferation.

Low oxygen availability (Hypoxia, Hx): Dutta et al., reported that the expression of HP1BP3 is increased in response to low oxygen availability (Hx) altering epigenetic modifications and gene expression in A431 cells (Dutta et al., 2014). Tumour microenvironment, is one of the main factors of oncogenesis that promotes tumour initiation, progression and resistance to radio/chemotherapy (Ghattass et al., 2013). The loss of HP1BP3 in a hypoxic environment was investigated in both *in vitro* and *in vivo* (Dutta et al., 2014). Using tumour xenografts, HP1BP3-null A431 cells were injected subcutaneously in six mice, the tumour engraftment was reported in 3 mice compared within all six mice in the control group injected with mock-null A431 cells (Dutta et al., 2014). These data indicate that the hypoxia induced-HP1BP3 promoted cancer cell survivability and therefore enhanced cancer progression. (Dutta et al., 2014).

Drug response: HP1BP3 is involved in chemotherapy resistance of 5-fluorouracil (5-FU) (Hadac et al., 2016). HP1BP3 was highly expressed in 5-FU–resistant colon tumours compared to 5-FU–sensitive tumours (Hadac et al., 2016). Moreover, Casado et al., identified HP1BP3 as one of the phosphopeptides correlated with resistance to MEK-inhibitors in AML cell lines using phosphoproteomic analysis (Casado et al., 2013). Indicating that

HP1BP3 is associated in the tumour resistance to chemotherapy/radiotherapy.

Novel biomarker in leukaemia: A large scale proteomic analysis identified 1,360 proteins differentially expressed in chronic lymphocytic leukaemia (CLL)-derived lymphocytes compared to normal white blood cells. Among those proteins, HP1BP3 was identified as a novel biomarkerthat can impact diagnosis, treatment and prognosis (Admoni-Elisha et al., 2016).

miRNA biogenesis and expression: In 2016, Liu et al reported that HP1BP3 is a chromatin retention factor involved in microRNA (miRNA) biogenesis (Liu Liang et al., 2016). miRNAs are short conserved ~22 nucleotides (nt) of single-stranded non-coding RNA regulating various cellular processes (He and Hannon, 2004). miRNA biosynthesis occurs in a stepwise manner and is typically catalysed by two RNase III enzymes: Drosha in the nucleus and Dicer in the cytoplasm (He and Hannon, 2004). Depletion of HP1BP3, altered the expression of 74 miRNAs in human cells (Liu et al., 2016). It reduced the expression of mature miRNAs relative to primary miRNAs (pri-miRNAs) (Liu et al., 2016), suggesting HP1BP3 involvement in miRNA processing in human cells. A combination of co-immunoprecipitation (co-IP) and immunoprecipitation sequencing (ChIP-seq) revealed the HP1BP3 co-localise with Drosha at 42 highly transcribed miRNA loci. Moreover the ChIP-seq analysis showed that HP1BP3 binds to the actively transcribed miRNA loci, which is similar to the microprocessor Drosha (Liu et al., 2016).

All of the discussed findings suggest the important role of HP1BP3 in cancer progression and its potential implementation as a novel biomarker and therapeutic target in human cancer; however, its function and mechanisms of action in AML have not been addressed.

1.6 **Rational and objectives**

Epigenetics can be defined as "outside conventional genetics" which describes the inherited alteration in gene expression that are not encoded by the DNA itself. Chromatin post-translational modifications and DNA methylation have been identified as significant permissive and suppressive factors in regulating the genome expression via gene transcription. Therefore, the regulation of epigenetic events including DNA methylation, histone modification, and nucleosome remodelling is crucial for the biological process. The epigenetic regulatory machinery, which operates through association with a wide-range of histone and non-histone proteins and modifier enzymes, must be tightly controlled. Epigenetic alterations may cause cancer via incorrect transcription patterns by silencing or down-regulating tumour suppressor expression or enhancing oncogene expression.

A yeast 2-hybrid reverse Ras Recruitment System (rRRS), identifying proteins interacting with Fbxw7 in a GSK-3β phosphorylation-dependent manner, have identified HP1BP3 as a downstream target of FBXW7 for degradation using mouse cDNA library was carried out as previously described in Dr Nateri's laboratory (Li N, et al., 2019). The RRS uses the yeast strain cdc25–2, deficient in Ras activity and cannot grow at 36-37 °C. In this study, cdc25–2 cells stably transformed with pMET3- GSK-3β. The

activated form of GSK-3β, under the control of the methionine-regulated MET3 promoter, induces phosphorylation of encoded myristoylated proteins through the pMyr-cDNA library. FBXW7-associated proteins can only rescue the growth of cdc25–2 cells if they interact with RasV12-FBXW7ΔF. Yeast colonies showing a galactose-dependent and efficient growth in the absence of methionine, and therefore the GSK-3β-phosphorylation-dependent interactors were isolated and further analysed through plasmid rescuing and sequencing. Apart from above few published articles, very little is known about HP1BP3, including its regulatory machinery, function and its roles in cancer cells.

HP1BP3 is a nuclear protein with different domains involved in distinct DNA-protein and protein–protein interactions (Figure 1-12). HP1BP3 consists of linker histone 1 and histone 5 domains (H1.5) that binds to HP1α and interacts with nucleosomal DNA at the entry/exit site (Hayashihara et al., 2010) and therefore, is involved in chromatin structure and function. Moreover, it has different important sites including; ATM/ATR phosphorylation SQ/TQ sites, GSK-3β (T/SXXXS/TP) phosphorylation sites, three H15 (linker histone H1/H5 globular) domains, a HP1α binding motif, a lysine-rich domain at the C-terminal and several nuclear localisation signals (NLS) (Figure 1-12).

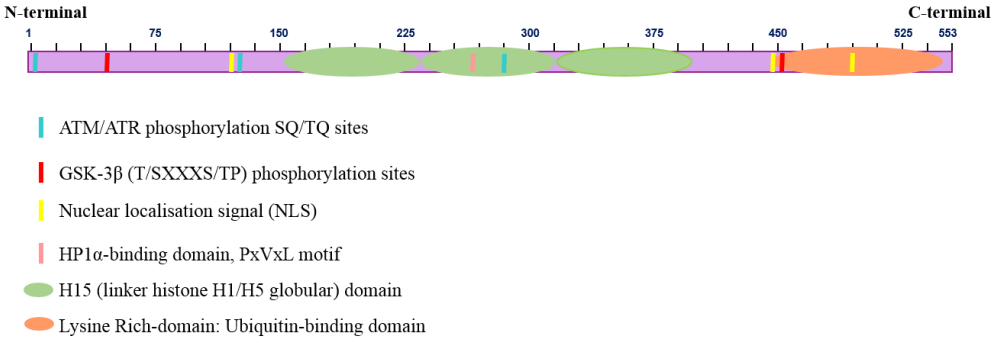


Figure 1-12: Scheme of the domain organization of human HP1BP3 protein. Long-HP1BP3 isoform consists of 553 amino acids and short-HP1BP3 isoform consists of 442 amino acids. Numbers refer to amino acid positions.

Previous work in our group also indicated that HP1BP3 degradation by FBXW7 regulates mouse HSC cell cycle progression and the transcriptional signature associated with HSC self-renewal and pre-leukemic phenotype.

HP1BP3 binds directly to the chromoshadow domain (CSD) of HP1α where SUV39h also binds to the same domain to methylate H3K9 promoting the heterochromatin formation at this site. Modulation of heterochromatin-euchromatin through HP1α is important in normal homeostasis and cancer. We, therefore, investigated whether the expression of HP1BP3 disrupts HP1α-SUV39h binding and modulate heterochromatin-euchromatin conversion which can influence major cellular mechanisms using gain-and-loss of function analysis. Thereby, to explore the regulatory role of HP1BP3 in chromatin remodelling and its implication in haematopoiesis and leukemogenesis the aims and objectives of the present study were as follow:

HP1BP3 and haematopoiesis:

- HSC fate *in vitro* determination derived from the bone marrow of an *Hp1bp3* conditional knockout mouse model.

HP1BP3 and AML:

- Investigating the expression pattern of HP1BP3 in AML using AML cell lines via western blot and immunofluorescence (IF).
- Investigating the HP1BP3/ HP1α co-localisation using IF.
- Stemness activity and clonogenic potential using Colony Forming Unit (CFU) assay.
- Examining the effect of HP1BP3 expression on the growth and proliferation.
- Characterising the cell cycle function of HP1BP3 in AML cell lines that stably over-expressing/lacking HP1BP3.
- Identifying genes differentially expressed using transcriptomic analysis
- Investigating the role of HP1BP3 in AML cells in hypoxia
- Investigating the role of HP1BP3 in regulating miRNAs expression using small RNA sequencing analysis (sRNA-seq).

CHAPTER 2

General Materials & Methods

2.1 Material

2.1.1 Animal work

2.1.1.1 Mouse strain

The *Hp1bp3*$^{fl/fl}$ mouse model was generated with the assistance of MRC-Harwell institute. In brief, the Tm1a allele was originally designed to be a knockout by splicing the cDNA to a LacZ cassette. The cassette was then inserted upstream of exon 8 to create a null allele of *hp1bp3* (Figure 2-1). The Tm1c allele was produced by deletion of LacZ reporter and neomycin selection cassette using a site-specific Flp recombinase that recognises FRT sites (Figure 2-1). Exon 8 of *hp1bp3* in Tm1c mouse is flanked by loxP sites, which allow a tissue-specific cre- deleter to create a tissue-specific knockout of the gene. Mice then were shipped to the biomedical service unit (BSU) at the University of Nottingham as heterozygous and were maintained in a pathogen-free transgenic unit. Thus, we started by crossing, breeding and genotyping of the heterozygous mice until we got the homozygous mice. Offspring were genotyped regularly and upon any experiments.

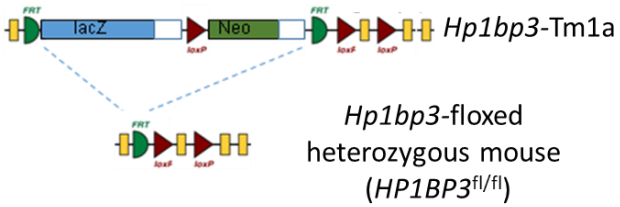


Figure 2-1: Schematic representation of developing a *Hp1bp3*-conditional knockout mouse model (*Hp1bp3*$^{fl/fl}$).

2.1.2 Cell lines

The human myeloid leukaemia cell lines MOLM-13, M0-7e, and OCI-AML3 were obtained from the German Collection of Microorganisms and Cell Cultures (DSMZ, Braunschweig, Germany). U937, HL-60, and KG-1a cell lines were purchased from the European Collection of Animal Cell Cultures (Salisbury, UK). The MV4-11 M0-91 and TF1a cell lines were from the American Tissue Culture Collection (Manassas, VA, USA). Some of genetic characterization of these cell lines is summarized in (Table 2-1). Cell lines were routinely tested and approved mycoplasma-free in the laboratory.

Table 2-1: Genetic features of leukemic cell lines used in the study.

Cell line	P53	FLT3*	NPM*
M091	Mutated	WT	WT
U937	Mutated	WT	WT
MO72	WT	WT	WT
MOLM-13	WT	Mutated	WT
OCI-AML3	WT	WT	Mutated
KG1a	Mutated	WT	WT
MV4-11	WT	Mutated	WT
TF1a	WT	WT	WT
HL60	Mutated	WT	WT

*FLT3; Fms Related Tyrosine Kinase 3, *NPM; Nucleophosmin

2.1.3 DNA Plasmids

DNA plasmids used in this project are listed in the following table.

Table 2-2: DNA plasmids used in the study.

Plasmid	Supplier	Backbone vector	Bacterial selection
pLVX-eGFP	Dr Nateri's lab	pLVX-Puro	Ampicillin
pLVX-eGFP-HP1BP3 "long"	Dr Nateri's lab	pLVX-eGFP	Ampicillin
pLVX-eGFP-HP1BP3 "short"	Dr Nateri's lab	pLVX-eGFP	Ampicillin
Ad-h-HP1BP3-shRNA	Vector Biolab	pLVX-eGFP	Ampicillin
pLVX-Cre	Dr. Dominic Bonnet	pLV	Ampicillin
pMD.G2	Dr. Dominic Bonnet	-	Ampicillin
pCMV.R8.74	Dr. Dominic Bonnet	-	Ampicillin

2.1.4 Antibodies

The antibodies used in flow cytometry, western blotting (WB) and immunofluorescent (IF) analysis are listed in the following tables.

Table 2-3: List of antibodies used in this project for flow cytometry analysis.

Primary Antibody	Supplier	Cat Number	Clone	Dilution factor
APC anti-human CD38	BioLegend	303509	HIT2	1:100
PE anti-human CD34	BioLegend	343605	561	1:100

Pacific Blue™ anti-mouse Lineage Cocktail with Isotype Ctrl	BioLegend	133305	17A2/RB6-8C5/RA3-6B2/Ter-119/M1/70	1:100
Brilliant Violet 605™ anti-mouseCD117 (c-kit)	BioLegend	135120	ACK2	1:100
Brilliant Violet 785™ anti-mouse Ly-6A/E (Sca-1)	BioLegend	108139	D7	1:100
PE/Cy7 anti-mouse CD34	BioLegend	119326	MEC14.7	1:100
PerCP/Cyanine5.5 anti-mouse CD48	BioLegend	103422	HM48-1	1:100
PE anti-mouse CD135	BioLegend	135306	A2F10	1:100
APC anti-mouse CD150 (SLAM)	BioLegend	115910	TC15-12F12.2	1:100
APC Mouse IgG1, κ isotype Ctrl	BioLegend	400119	MOPC-21	1:100
APC Rat IgG2a, κ Isotype Ctrl	BioLegend	400512	RTK2758	1:100
Brilliant Violet 785™ Rat IgG2a, κ Isotype Ctrl	BioLegend	400546	MOPC-173	1:100
PE Mouse IgG2a, κ isotype Ctrl	BioLegend	400211	RTK2758	1:100
PE Rat IgG2a, κ Isotype Ctrl	BioLegend	400508	RTK2758	1:100
PE/Cy7 Rat IgG2a, κ Isotype Ctrl	BioLegend	400522	HM48-1	1:100

PerCP/Cyanine5.5 Armenian Hamster IgG Isotype Ctrl	BioLegend	400932	HTK888	1:100

Table 2-4: List of primary and secondary antibodies used for western blot (WB) and immunofluorescence (IF) analyses.

Primary Antibody	Supplier	Cat Number	Source	Dilution Factor	
				WB	IF
HP1BP3	Sigma-Aldrich	HPA028215	Rabbit	1:1000	1:100
HP1α	Millipore	05-689	Rabbit	1:1000	1:100
H3K9me3	Millipore	07-442	Rabbit	1:1000	N/A
H3K9ac	Sigma-Aldrich	H0913	Rabbit	1:1000	N/A
Drosha	Abcam		Rabbit	1:1000	N/A
H3	GeneTex	GTX122148	Rabbit	1:1000	N/A
β-actin	Abcam	Ab6276	Rabbit	1:10,000	N/A
GFP	Santa-Cruz	Sc-9996	Mouse	1:1000	N/A
Secondary Antibody	**Supplier**	**Cat Number**	**Source**	**Dilution Factor**	
				WB	**IF**
Alexa Fluor® 594 anti-mouse	Life Technologies	A-21155	Goat	N/A	1:500
Alexa Fluor® 488 anti-rabbit	Life Technologies	A-21206	Donkey	N/A	1:500

IRDye anti-rabbit	LI-COR	926-68073	Donkey	1:15000	N/A
IRDye anti-mouse	LI-COR	926-68072	Donkey	1:15000	N/A

2.1.5 Oligonucleotides

The oligonucleotides/primers used in for quantitative real-time polymerase chain reaction (qRT-PCR) were designed using primer design tool: Primer3 (Version 4.1.0, available at *http://frodo.wi.mit.edu/primer3/*). The oligonucleotide specificity was checked by blasting the designed sequence to the NCBI Primer-BLAST tool for both human and mouse transcripts databases (*http://www.ncbi.nlm.nih.gov/tools/primer-blast/*). Primers used for genotyping were designed and provided by Harwell institute. Upon primers reconstitution, all vials were spun down, then they were resuspended in DNase/RNase-free water (Sigma-Aldrich, 4502) to a final concentration of 100 µM stock solution and stored at −20°C. All primers were purchased from Sigma-Aldrich.

Table 2-5: List of the primers used for AML cell lines qRT-PCR.

Gene	Sequence (5'--------3')
HP1BP	TCCATCCTAAGGCACTCCCA GGAGGAGTTTCCCGGGTAGA
IDH2	TGAACTGCCAGATAATACGGG CTGACAGCCCCCACCTC
DNMT3A	ATAGATCCCGGTGTTGAGCC ACCCAGCGCAGAAGCAG
TET2	TGTGGTGGCTGCTTCTGTAG AAGCCAGGCTAAACAGTTGG
EZH2	CCCTTCTCAGATTTCTTCCCA GGACTCAGAAGGCAGTGGAG
SUV39H1	ACACGTCCTCCACGTAGTCC

	CAAGAACAGCTTCGTCATGG
NSD1	CAACTTCATACTTCAGTGGCG TTTCGGATGATCCAGATTCC
HP1α *CBX5*	ACTGTCAGCTGTCCGCTTG GGCCTCACCATACAGGAACA
HIF1α	GATAGCAAGACTTTCCTCAGTCG TGGCTCATATCCCATCAATTC
VEGFA	GCAGCTTGAGTTAAACGAACG GGTTCCCGAAACCCTGAG
CA9	CTTGGAAGAAATCGCTGAGG TGGAAGTAGCGGCTGAAGTC
β-ACTIN	GCGCGGCTACAGCTTCA CTTAATGTCACGCACGATTTCC

Table 2-6: List of the primers used for mouse qRT-PCR

Gene	Sequence (5'--------3')
HP1BP	TCCATCCTAAGGCACTCCCA GGAGGAGTTTCCCGGGTAGA
IDH2	TGAACTGCCAGATAATACGGG CTGACAGCCCCCACCTC
DNMT3A	ATAGATCCCGGTGTTGAGCC ACCCAGCGCAGAAGCAG
TET2	TGTGGTGGCTGCTTCTGTAG AAGCCAGGCTAAACAGTTGG
EZH2	CCCTTCTCAGATTTCTTCCCA GGACTCAGAAGGCAGTGGAG
SUV39H1	ACACGTCCTCCACGTAGTCC CAAGAACAGCTTCGTCATGG
NSD1	CAACTTCATACTTCAGTGGCG TTTCGGATGATCCAGATTCC
HP1α *(CBX5)*	ACTGTCAGCTGTCCGCTTG GGCCTCACCATACAGGAACA
β-ACTIN	GCGCGGCTACAGCTTCA CTTAATGTCACGCACGATTTCC

Table 2-7: List of the primers used for mouse genotyping

Gene	Sequence (5'--------3')
Hp1bp3	GAAAGGTGAGTCTGTCCCCG CCCTTCTGCAACACAGCATC

2.2 METHODS

2.2.1 Isolation of mouse bones and bone marrow cells

Hp1bp3$^{fl/f}$ mice were euthanised using CO_2 followed by cervical dislocation for death confirmation and they were then sprayed with 70% (v/v) ethanol. Bone and bone marrow isolation was achieved by following an optimised protocol provided and previously used by Dr Dominique Bonnet at Crick institute (Zhu et al., 2010). The euthanised mouse was placed on its back on the dissecting bored. Mouse skin was removed by cutting and peeling down the legs from the inguinal region; muscles then were carefully removed from femurs and tibias, allowing bones to be totally exposed (Figure 2-2 A, B). The femurs and tibias bones were then separated carefully by cutting above the joints making sure not to break the top of the bones (Figure 2-2 C). After that, the bones were splashed with 70% (v/v) ethanol and rubbed gently with lint-free wipes to remove any extra fat or tissues (Figure 2-2 C).

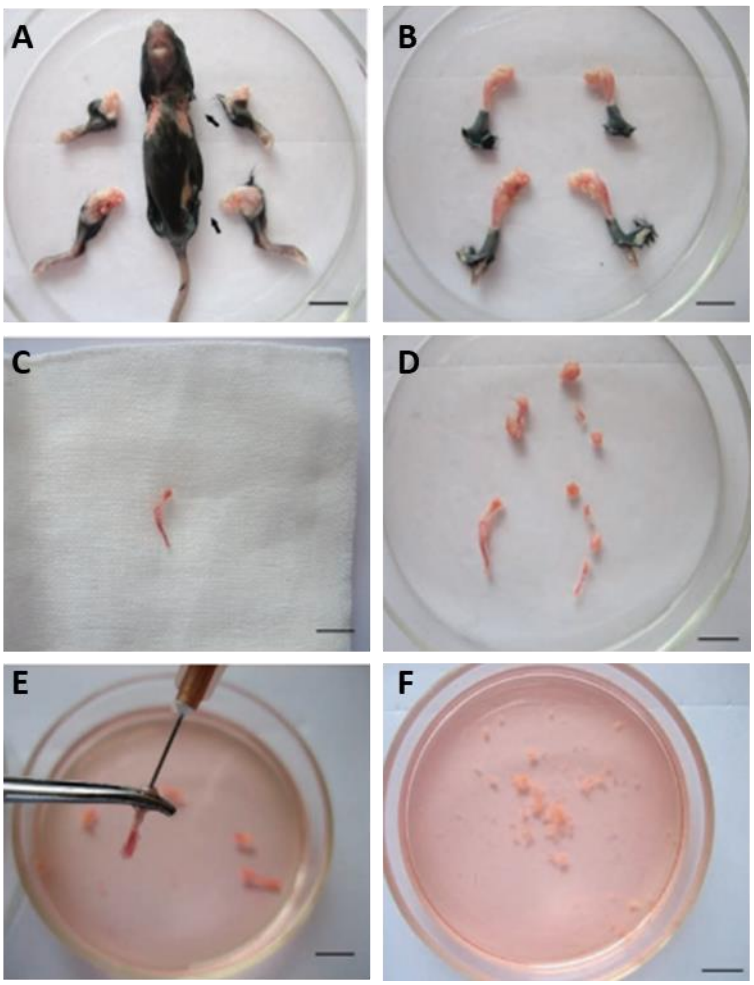


Figure 2-2: Dissection and isolation of mouse bone marrow. Representative images for mouse bone and bone marrow isolation. **(A)** The euthanised mouse was sprayed with 70% ethanol. **(B)** The skin was pulled down from femurs and tibias and cut. **(C)** The bones were cleaned with sterile gauze. **(D)**The bones were collected in a 10cm dish. **(E-F)** The bone marrow cavity was flushed to isolate the bone marrow. Adapted from (Zhu et al., 2010).

2.2.2 Lineage^{neg} HSCs isolation

2.2.2.1 Preparation of BM single cell suspension

Following isolation of mouse compact bones, BM cells were processed to produce single cell suspension. Briefly, the compact bones were transferred to a class II safety cabinet for further processing of the cells. Bone marrow

cells from both femurs and tibias were flushed with MACS rinsing solution (Miltenyi Biotech, 130-091-222) using a 26G needle (BD microneedle, 305110) (Figure 2-1 E, F). Once all marrow was collected, the cells were disaggregated by gently pipetting them several times and passing them through a 30um nylon mesh pre-separation filter (Miltenyi Biotech, 130-041-407). The cells were then centrifuged at 300xg at 4°C for 10 minutes for further labelling and MACS separation.

2.2.2.2 Magnetic labelling of Lin$^-$ HSC fraction

Separation of *Hp1bp3*$^{fl/f}$ mouse Lin$^-$ HSCs was accomplished using mouse lineage Cell Depletion Kit (Miltenyi Biotech, 130-090-858) following manufacturer procedure. In brief, the Lin$^-$ cells were isolated by depleting mature hematopoietic cells, such as T cells, B cells, monocytes/ macrophages, granulocytes and erythrocytes and their committed precursors from bone marrow. For this depletion, cells were magnetically labelled with a cocktail of biotinylated antibodies against a panel of so called "lineage" antigens (CD5, CD45R (B220), CD11b, Anti-Gr-1 (Ly6G/C), 7-4, and Ter-119 antibodies) and Anti-Biotin MicroBeads. This labelling procedure leaves lineage negative cells untouched, thus allowing further separation of Lin$^-$ cells according to the expression of markers such as CD117 or Sca-1. Subsequently, the magnetically labelled Lin$^+$ cells were depleted by retaining on an MS or LS MACS column, depending on the total BM cells, in the magnetic field separated. The unlabelled fraction of cells containing the Lin$^-$ HSCs was collected as an eluate. The purity of the enriched lineage negative cells was evaluated by fluorescence microscopy after staining an aliquot of the cell fraction with Anti-Biotin-APC (Miltenyi Biotech, 130-090-856).

2.2.2.3 Expansion of Lin$^-$ HSCs

Expansion of Lin$^-$ HSCs in culture was done by using STEMSPAN medium (stem cell technology, 09650) supplemented with a cytokine cocktail containing Stem Cell Factor (SCF), IL-6 and IL-3 (Sigma Aldrich, S9915, SRP3330 and SRP3208) which are reported to maintain HSCs in culture and enhance their expansion (Peters et al., 1996). Cells were plated in 24-well plate with a seeding density of $2.5X10^5$ cells/well for up to 3 weeks in culture. Mouse total BM was usually pooled from 6-8 mice for each experiment as the total number of Lin$^-$ HSCs was always low. Cells were then grown in a humidified, 37°C, 5% CO_2 incubator, carefully checked daily and re-fed every 2-3 days with a fresh STEMSPAN medium containing cytokines and split into two wells.

2.2.3 GENERAL CELL CULTURE TECHNIQUES

2.2.3.1 Thawing, maintaining, sub-culturing and freezing cells

Cell lines were thawed and recovered from liquid nitrogen at a low passage and cultured in T75 flasks (Costar, CLS3375). Cells were first defrosted at 37°C for 1 min and transferred to 10 ml of pre-warmed complete medium. Then, cells were centrifuged at 500g for 5 mins, and the cell pellets were resuspended in 15 ml of fresh medium. MO91, U937, MOLM13, OCI-AML3, MV4-11, TF-1a and HL60 were cultured in complete medium composed of RPMI1640 medium (Sigma Aldrich, R0883) supplemented with 10% fetal bovine serum (FBS, Sigma Aldrich, F7524), 2 mM L-

glutamine (Thermo Fisher Scientific, 25030-024), and 1% penicillin/streptomycin (100 units/ml, Invitrogen, 15140-122). The M-07e and KG-1a cell lines were cultured as above but supplemented with 20% FCS and 10 ng/mL granulocyte macrophage colony-stimulating factor (GM-CSF, Millipore, GF004). Cells were then grown in a humidified, 37°C, 5% CO_2 incubator, and assays were set up using cells in the log phase of growth.

Cells were maintained by feeding them regularly every 3 to 4 days until they reach confluency. This was done by directly adding fresh medium to the cells, and expanding them, or discarding a portion of the cells and diluting the remaining cells to a seeding density appropriate for the cell line.

Cell number was estimated by the Neubauer haemocytometer (Marienfeld-Superior, Germany) using Trypan blue (Sigma Aldrich, T8154) for staining the non-viable cells. To facilitate the counting procedure the cells were diluted in a fresh medium (2X dilution) and 10 µl of the last cells dilution were stained with Trypan blue. After that, 10µl of the cell/Trypan blue mixture were loaded on the counting chamber and living cells were counted within four different squares of the chamber. Finally, to calculate the final number of cells per ml, the average count number was multiplied by the applied dilution factors (4X).

In order to freeze the cells, they were centrifuged for 5 mins at 400g and the pellet was resuspended in 1 ml of freezing medium (10% dimethyl sulfoxide (DMSO, Sigma Aldrich, D4540) and 90% FBS). The cells were kept overnight at -80°C and then transferred to liquid nitrogen for long term storage.

2.2.4 Lentivirus system

2.2.4.1 Lentivirus production

Lentiviruses were produced following an established and optimised protocol from our lab (Dr. Nateri's lab) which involved co-transfecting human HEK-293T cells with plasmids constructs including the backbone vector as well as packaging plasmids using Lipofectamine 2000 (Invitrogen, 11668027) as transfecting reagent. For this, around $5x10^6$ human HEK 293T cells were seeded in virus production medium [DMEM high glucose (sigma, D5796) supplemented with 10% FBS and 2 mM L-glutamine] in three T75 flasks (Costar, CLS3375). Cells were transfected when they reached 70-80% confluency. On the day of the transfection, medium was changed and replaced with Opti-MEM I reduced serum medium (Invitrogen, 31985-047) and plasmids (Table 2-2). Transfection mixture was then mixed well and distributed to the pre-seeded HEK293T cells in the T75 flasks and incubated overnight in CO_2 incubator.

2.2.4.2 Collection of lentivirus medium

Around 16 hours after transfection, supernatants were discarded and replaced with 10ml of lentivirus production medium. Cells were incubated for 24 hrs and supernatants were collected daily for 4 days. Lentivirus supernatants were filtered, stored at 4°C and were eventually pooled together.

2.2.4.3 Infectivity of lentivirus supernatant

The infectivity of the collected lentivirus supernatant was tested daily prior to pooling samples and titration of the viral particles. Briefly, around $5x10^4$ HEK 293T cells were seeded in a 6-well plate in a completed medium [RPMI supplemented with 1% L-glutamine and 10% FBS] and incubated with 100 ul of un-concentrated lentivirus supernatant. The cells were incubated overnight with lentivirus supernatants that was collected at 48 hrs, 72 hrs and 96 hrs post-transfection followed by changing and replacing the medium and incubating the cells for 24 hrs. The expression of GFP was examined using fluorescence microscope.

2.2.4.4 Lentivirus purification and concentration

Lentivirus high-titer is required for efficient transduction of some cells that require high Multiplicity of Infection (MOI) such as AML cells and HSCs (Millington et al., 2009, Abbasalipour et al., 2019). To achieve a high titration of lentivirus, an optimized method for preparations was used (Jiang et al., 2015) as follow. Lentivirus was first centrifuged at 1000g for 10 mins to remove cell debris. The viral supernatant was then passed through 0.45um filter (Corning) for further removal of any fragments. After that, 40 ml of the purified lentivirus supernatant was transferred to 50 ml falcon and mixed with 10 ml of sterile lentivirus concentration solution [10% sucrose, 50mM Tris HCl pH7.4, 100mM NaCl, 0.5mM EDTA] and centrifuged at 10.000xg for 4 hrs at 4°C. After centrifugation, the supernatant was removed, tubes placed upside down for 3 mins, 200uL sterile PBS was added to reconstitute virus particles overnight at 4°C. Lentivirus was finally pooled together, mixed, aliquoted and stored at -80°C.

2.2.4.5 Lentivirus transduction

Lentivirus transduction was used to generate stable gene overexpression/knockdown of AML cell lines or knockout murine HSCs. To achieve this, AML cells were seeded in 24-well plates and transduced with pLVX-HP1BP3 lentivirus (generated in our laboratory), HP1BP3 shRNA-GFP lentivirus) or scrambled shRNA-GFP lentivirus (Applied Biological Materials Inc., LVP015-G). HP1BP3$^{fl/fl}$ HSCs were seeded in 48-well plate and transduced with lentivirus GFP-Cre (gifted from Dr. Dominique Bonnet, Crick institute) Table 2-2. After cells reached 60-70% confluency, 50 µl of viral particles (with a titer of 10^7 IU/ml) and 8 µg/ml polybrene (Sigma Aldrich, H9268) were added to the cells. After 48 hrs incubation, infected cells were either selected with 2-2.5 µg/ml puromycin (Sigma Aldrich, P8833) or sorted by flow cytometry. Cells were then amplified and processed for validation assays.

2.2.5 FUNCTIONAL ASSAYS

2.2.5.1 Propidium Iodide (PI) Staining and Cell Cycle Analysis

Propidium iodide (PI) is a red-fluorescent stain that binds to both DNA and RNA, thus, it can be used for DNA content in cell cycle analysis using flow cytometry as described (Almars et al., 2019). To assess the biological effect of HP1BP3 protein on the cell proliferation, about 10^5 cells were transferred into FACS tubes (Falcon, 352054). Cells were washed twice with 1 ml of PBS and were fixed by adding 1 ml of ice-cold 70% ethanol (Sigma Aldrich,

E7023) in a drop-wise manner, while gently vortexing. Samples were incubated for 30 mins at 4°C. Consequently, the cells were washed twice with PBS after discarding the ethanol by centrifugation. Finally, cells were incubated for 30 mins in the dark with 500 µl PI (Sigma Aldrich, 4864) (50 µg/ml) and 100 µg/ml RNase A (Sigma Aldrich, 6513) to eliminate the RNA. DNA content was measured by FC500 flow cytometer (Beckman Coulter) and data were analysed by Weasel 3.2.1 software.

2.2.5.2 Colony Formation Units (CFU) assay

Colony forming units was performed to examine the ability of a single cell to proliferate and grow into a colony consisting of 50 or more cells. For this, 1000 cells were seeded in triplicate into 24 well plate in semi-solid matrix (MethoCult™, StemCell Technologies, 04236) and incubated for 14 days according to manufacturer protocol. The colonies were monitored microscopically on regular basis, and finally, they were identified, counted and images were captured using a phase-contrast microscope (Almars et al., 2019).

2.2.5.3 Surface phenotyping using flow cytometry

Staining for surface markers followed by flow cytometry was mainly done to examine the role of HP1BP3 on mouse Lin^- HSC differentiation or to sort the leukemic stem cells as well as the leukemic progenitors in AML cell lines. For this, Lin^- HSCs were stained with a panel of markers expressed in HSCs and the progenitor cells listed in (Table 2-3) or CD34, CD38 for AML cells. Cells were washed twice with FACS buffer (0.5% BSA in PBS) by centrifugation at 500g for 5 mins. Cells were first stained with Zombie NIR™

dye (BioLegend, 423106) and incubated for 15 mins in RT to assess live vs. dead cells. They were then washed, resuspended in 100 µl FACS buffer and stained with primary fluorochrome conjugated antibodies or isotypes control (Table 2-3) and incubated in 4°C for 20 mins in the dark. Cells were washed 3 times with FACS buffer before analysis on Astrios Cell Sorter flow cytometer.

2.2.6 PROTEIN EXPRESSION ASSAYS

2.2.6.1 Protein extraction and quantification

In order to extract the protein, about 6×10^6 cells were washed twice with ice-cold PBS and lysed with 1 ml lysis buffer (50mM Tris PH 6.8, 150mM NaCl, 1% Triton X-100, 0. 1% SDS, 10mM EDTA, 0.5% Na-Deoxycholic Acid and ddH2O to the desired volume). The samples were incubated at 4°C for 20-30 mins while shaking. Followed by centrifugation at 10,000g at 4°C for 15 mins, the cell lysates were then transferred into new pre-cooled tubes and stored at –20 °C.

To quantify the protein in the samples, a Bradford Assay was performed. In brief, a series of five protein standards (50, 100, 150, 200, 250 µg/ml) was prepared from a stock solution of 2 mg/ml BSA. Similarly, each experimental sample was diluted 1:50. Next, 20 µl of distilled water (blank), BSA standards and diluted experimental samples were loaded in triplicate into a 96-well plate. Then, 200 µl of 5x diluted Bradford reagent (Sigma Aldrich, B-6916) was added to each well and the absorbance was read at 620 nm of wavelength by spectrophotometer (Bio-Rad). The standard curve and the

protein concentration were calculated by Microsoft Office Excel software. The samples were directly used for Western blotting analysis or stored at -80°C.

2.2.6.2 SDS-PAGE and Western blotting (WB) analysis

Sodium dodecyl sulphate-poly acrylamide gel electrophoresis (SDS-PAGE) separates proteins according to their molecular weight. SDS-PAGE consists of two parts: stacking: upper part and the resolving (bottom part). Both stacking and resolving gel were made according to the instructions (Table 2-8). The resolving gel percentage was selected based on the size of the tested protein.

Table 2-8: Solution components (ml) for SDS/PAGE electrophoresis gels

	Resolving gel (10 ml)				Stacking gel (5ml)
	10%	12%	15%		5%
H2O	4.0	3.3	2.3	H2O	3.4
30% acrylamide mix	3.3	4.0	5.0	30% acrylamide mix	0.83
1.5 Tris (pH 8.8)	2.5	2.5	2.5	1.5 Tris (pH 6.8)	0.63
10% SDS	0.1	0.1	0.1	10% SDS	0.05
10% ammonium persulfate	0.1	0.1	0.1	10% ammonium persulfate	0.05
TEMED	0.004	0.004	0.004	TEMED	0.005

The protein lysate was mixed with 5x loading buffer (250 mM Tris-HCl pH 6.8, 10% SDS, 50% glycerol, 5% β-Mercaptoethanol and 0.05% bromophenol blue) and denatured for 5 mins at 95°C. To determine the apparent molecular mass of the proteins, the Precision Plus 40 Protein™ Dual Colour Standards ladder (Bio-Rad, P7711S) was loaded alongside with the experimental samples. The upper and the lower compartments of electrophoretic unit (Mini-PROTEAN® Tetra Vertical Electrophoresis Cell,

Bio-Rad, 1658004) were filled with the running buffer (25 mM Tris-HCl pH 8.3, 192 mM glycine and 0.1% SDS) and the gel was run for approximately 2 hrs at 90 volts (V).

Proteins separated across the gel were transferred to a hydrophobic polyvinylidene difluoride membrane (PVDF, GE Healthcare, RPN303F) using a semi-dry transfer system (Bio-Rad) at 14 V for 30 mins. Prior to the transfer, PVDF membrane was activated by using absolute methanol for 30 second and then was washed with distilled water. The transfer sandwich was composed of filter papers, gel, membrane and filter papers. The filter papers were incubated in the transfer buffer (25 mM Tris HCl, 192 mM glycine and 20% methanol) for 10 minutes before the semi dry transfer.

Subsequently, the membrane was blocked with 4% skimmed milk in Tris-buffered saline (20 mM Tris 7.6 pH, 135 mM NaCl) 0.1% Tween-20 (TBS-T) for 1 hr at RT to reduce non-specific protein bindings. After that, the membrane was blotted with primary antibody specifically binding to the protein of interest overnight at 4°C, at the recommended concentration (Table 2-4). The next day, following washing of 3 times with TBS-T for 10 mins, the membrane was incubated with fluorescence secondary antibody (Table 2-4) for 1 hr at RT. Next, it was washed 3 times for 5 mins each with TBS-T. β-actin was used as a loading control in all experiments. The densitometry analysis was performed using LI-COR software (Biosciences) to compare the density of the apparent molecular mass of the proteins (bands). The bands were selected using the LI-COR software and a lane plot analysis was generated to analyse the selected bands. The selected areas were then quantified which represent the density of the bands. The relative band

intensity was performed by normalising the densitometry of the protein of interest to the densitometry of the loading control.

2.2.6.3 Immunofluorescence (IF) staining

Immunofluorescence analysis was done to study the expression pattern of a protein within the cell. For this, cells were first washed and resuspended in PBS. According to Shandon Single Cytofunnel kit protocol (Thermo scientific), 3 x10^4 cells were suspended in a volume of 100 µl and loaded into pre-labelled slides by centrifugation at 800 RPM for 3 mins. Slides were then allowed to air-dry overnight at RT. The day after, cells were fixed with 4% PFA for 30 mins at RT, followed by washing with PBS for 5 mins.

To permeabilize the cells, 100 µl of 0.1% TRITON X-100 permeabilizing solution (Sigma Aldrich, 93443) were added on each slide for 30 mins at RT. And in order to minimize the non-specific bindings of the secondary antibody, cells were blocked with 3% bovine serum albumin (BSA) for 1 hr at RT. After that, cells were probed with primary antibody (Table 2-4) overnight at 4°C. For negative control, cells were incubated with 3% BSA only without the primary antibody. The following day, slides were washed with 1% BSA 0.1% Tween 20 solution to remove the unbound antibodies 5 times for 10 mins. Then, Fluorochrome-conjugated secondary antibody was applied (including negative control) in the dark for 1 hr at RT (25°C) (Table 2-4). Finally, following 4 washings for 10 mins each, slides were mounted with Vectashield mounting medium with DAPI (Invitrogen, D1306). Slides were covered by coverslips, sealed with nail varnish and stored in the dark

overnight at 4°C. Images were taken with Leica DMI3000 B fluorescence microscope (Leica Microsystems) (Almars et al., 2019).

2.2.7 Giemsa staining

Giemsa staining for prepared air-dried AML cells and Lin-HSCs cytospin slides was preformed using modified giemsa stain (Sigma, GS10) following manufacturer procedure. For this, first the slides were fixed in methanol for 5 mins at RT. Followed by, immersing the slides in coplin jar filled with diluted 1:20 giemas stain for 15 mins. Finally, the slides were rinsed in dH2O, air-dried and microscopy evaluated. All slides were scanned using Reflecta DigitDia 7000 scanner and analysed using Image Viewer software.

2.2.8 DNA AND RNA ISOLATION AND ANALYSIS

2.2.8.1 Transforming Bacterial Competent Cells with Plasmid DNAs

Plasmid DNA were introduced into DH5α chemically competent *Escherichia coli* (*E. coli*) (Biolab, C2987H) by heat shock method. 100-500 ng of plasmid DNA was mixed with 50 µl of competent cells and incubated on ice for 30 mins. The mixture was exposed to a heat shock at 42°C for 1 min, followed by, chilling on ice for 10 mins and supplementing with 500 µl of Luria Broth medium (LB, Sigma Aldrich, L3022). Afterward, bacteria were incubated for 1 hr at 37°C while shaking. 10-15 µl of the transformed bacterial culture were spread on plates of LB agar (Sigma Aldrich, A5306) containing the suitable antibiotic for selection of positive clones and incubated at 37°C overnight. The day after, isolated colonies were grown into 5 ml and then further amplified into 100 ml of LB medium containing antibiotic, at 37°C in a

shaking incubator overnight. Finally, Midiprep kit was used to isolate plasmid DNA.

2.2.8.2 DNA Isolation Using Midiprep Kit

Plasmid DNA was isolated by Genopure Plasmid Midi Kit (Roche, 03143414001) following the manufacturer's instructions. Transformed *E. coli* bacteria were centrifuged for 10 min at 5000 g at 4°C. Then, they resuspended in 4 ml of chilled suspension Buffer/RNase and lysed with 4 ml lysis buffer. Then, Lysis buffer was deactivated by adding 4 ml of chilled Neutralization Buffer for 5 mins on ice. Cell debris were precipitated at 10,000 g for 40 mins at 4°C. A column was prepared by adding 2.5 ml of Equilibration Buffer and bacterial lysate was loaded. Next, the column was washed twice with 5 ml of wash buffer. DNA was eluted with 2.5 ml of Elution buffer, collected into a fresh tube and precipitated by adding 3.5 ml of isopropanol (Sigma Aldrich, I9516) at 10,000 g for 30 mins at 4°C. DNA pellet was washed with 2 ml of chilled 70% ethanol by centrifugation at 10,000 g for 10 mins at 4°C, air-dried and resuspended in 100 µl of DNase/RNase free water. DNA concentration was measured by Nanodrop 2000 spectrophotometer (Thermo Scientific) and stored at -20°C.

2.2.8.3 Restriction enzyme digestion

In order to validate the DNA plasmids, specific restriction enzymes were used according to the recognition sites. To, digest DNA plasmids, an enzymatic mixture containing (1 µg DNA, 10% 10X NEB buffer, 1 µl restriction enzyme, DNase free H_2O to the final volume of 20 µl). All restriction enzymes were purchased from New England Biolabs (NEB) and

were used according to the manufacturer's instructions with appropriate buffers and optimal temperatures. The digested DNA samples were run in ethidium-bromide (EtBr)-staining gel.

2.2.8.4 Agarose gel electrophoresis

To visualise the possible DNA bands, agsrose gel electrophoresis was used. Based on the product size, 1-2% [w/v] agarose gel was prepared by mixing 1-2g agarose powder (Eurogenetic, EP-0010-05) in 100 ml of 1X Tris Actate EDTA (TAE) buffer Sigma (T9650). The mixture was microwave-heated for 1-2 min and cooled down to 40-45°C. To detect DNA bands in the gel, about 10 µl EtBr (Sigma, E1385) (final concentration is 0.05 µg/µl) was added to the gel mixture. The gel was transferred into fixed gel casting tray with inserted appropriate comb and allowed to solidify at RT (Almars, Chondrou et al. 2019). DNA samples containing 1-2 µl of 10X gel loading buffer (final concentration is 1X) (30% glycerol and 0.25% bromophenol blue in dH2O) were loaded on the gel. DNA HyperLadderTM 1kb (BioLine, BIO-33025) was loaded alongside to estimate the DNA hands size. A Bio-Rad power supply (90-120 Volts for 50 min) was used for the electrophoresis with adding 1X TAE buffer as a running buffer. DNA bands were visualized and imaged using Ultraviolet Transilluminator Unit (UVidoc).

2.2.8.5 RNA Isolation

Total RNA was extracted from cells by using TRI Reagent (Sigma Aldrich, T9424) according to the manufacturer's instructions. First, cells were incubated with 1 ml of TRI reagent for 5 mins at RT. Subsequently, 200 µl of chloroform (Sigma Aldrich, 496189) per 1 ml of TRI reagent were added

to the samples, mixed vigorously and incubated for 3 mins at RT. Then, samples were centrifuged at 10,000 g at 4°C for 15 mins to separate RNA (aqueous phase), DNA (white interphase) and protein and lipids (organic phase). The aqueous phase containing RNA was transferred to a fresh tube and mixed with 500 µl of isopropanol and incubated for 10 mins at RT. RNA was precipitated at 10,000 g for 10 min at 4°C. Then, the pellets were washed twice with cold 75% ethanol by centrifugation at 7500 g for 5 mins at 4°C, air dried and resuspended with 50 µl of DNase/RNase free water (Figure 2-3). RNA concentration was measured by Nanodrop and stored at -80 °C.

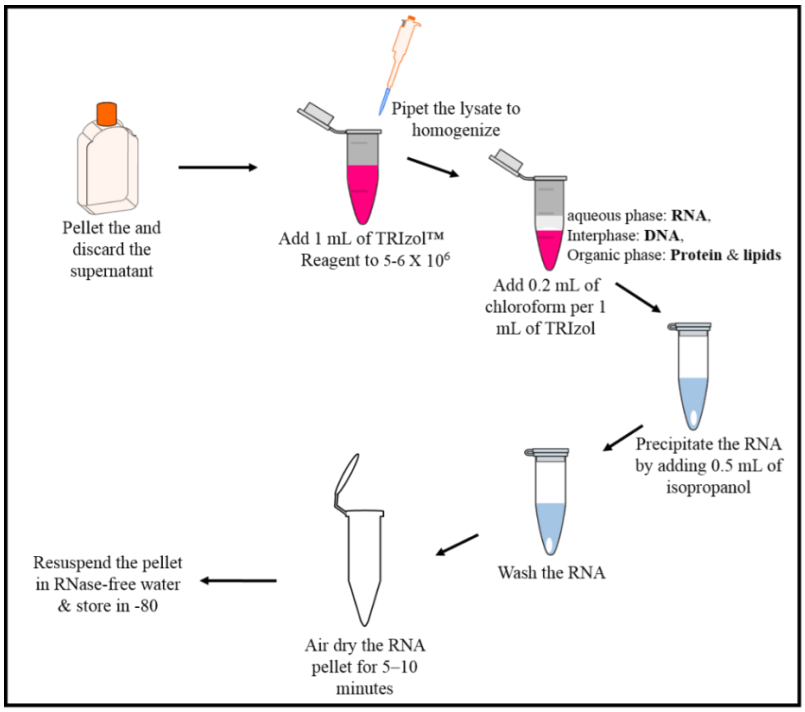


Figure 2-3: Schematic representation for the major step for Trizol RNA extraction.

2.2.8.6 RNA sequencing (RNA-seq) and small RNA-Seq (sRNA-seq)

RNA was isolated using PicoPure™ RNA Isolation Kit (Therofisher scientific, KIT0204), to ensure high-quality total RNA. Following manufacturer's instructions, cells were first incubated with the lysis buffer at 42°C for 20 mins. RNA purification columns were preconditioned by pipetting 250 µL of conditioning buffer onto the filter membrane of the columns. The columns were then incubated for 5 mins at RT, centrifuged at 16,000 g for 1 min and the liquid was discarded in the collection tubes. Next, 50 µL of 70% ethanol was added to the cell lysates, gently mixed by pipetting and transferred to the preconditioned columns. They were then centrifuged at 100 g for 2 mins to bind the RNA and then at 16,000 g for 30 secs to remove the flow through. After that, 100 µL of wash buffer 1 was added to each column, centrifuge at 8,000 g for 1 min and washed twice with 100 µL of wash buffer 2 and centrifuged at 8,000 g for 1 min. The columns were then transferred to fresh tubes and the RNA was eluted by adding 10-30 µL of elute buffer and centrifuged at 16,000 g for 1 min. RNA concentration was measured by Nanodrop and 4 µg of total RNA was shipped to Novogene (Cambridge, UK) for RNA sequencing analysis. The RNA quality was examined by testing RNA integrity number (RIN) and RNA with no degradation was processed for library preparation and RNA sequencing. RNA quantitation was performed using either NEBNext® Multiplex Small RNA Library Prep Set for Illumina for sRNA-seq or Illumina TruSeq RNA Library Prep kit for RNA-seq. Following RNA purification, the adaptors were ligated to cDNA during each library preparation. A minimum of 2 X 25

million reads were generated for each sample from each library. The raw data was then analysed by the bioinformatics facility at Novogene. The FastQ files were analysed using STAR software (Dobin et al., 2013). Gene expression was quantified using feature Counts software (Liao et al., 2014) and was then compared between different genes and between different samples, using DESeq2 software (Love et al., 2014). Finally, the normalised counts and DEseq2 files were exported to Excel.

2.2.8.7 Reverse transcription (RT)

Two micrograms of total RNA were used as template to synthesis cDNA using PrimeScript RT Reagent Kit (Perfect Real Time) (Takara-Clontech Laboratories, RR037A) following the manufacturer's instructions. RNA was supplemented with 1x Prime Script buffer, 25 pmol of oligo dT primers, 50 pmol of random six-mers primers, 0.5 µl of reverse transcription (RT) enzyme mix and RNase free distilled water to the final volume of the reaction (20 µl). The reaction mixture was incubated at 37°C for 15 mins for the cDNA synthesis and at 85°C for 5 sec to inactivate the reverse transcriptase. cDNA was stored at -20°C (Almars et al., 2019).

For miRNA quantification, cDNA synthesis was carried out using miScript® II RT kit (Qiagen, 218160) which utilizes miRNA as a starting material for reverse transcription. Following manufacturer's instructions, the reaction mixtur components per sample consisted of 4 µL 5x miScript HiSpec buffer, 2 µL 10x miScript Nucleics mix, 2 µL miScript reverse transcriptase mix (containing an optimized mixture of poly (A) polymerase and reverse transcriptase) and 12 µL of RNase free water. Samples were incubated for 60

mins at 37°C, followed by incubation for 5 mins at 95°C to inactivate the enzyme, and stored at -20°C.

2.2.8.8 Polymerase chain reaction (PCR)

Polymerase chain reaction (PCR) was done by preparing a reaction mixture composed of: 1 µl of genomic DNA, 0.25 µl of dNTPs (0.25 mM) (Qiagen, 201913), 5 µl 5x PCR buffer (Promega, M7805), 2 µl of MgCl2 (2 mM) (Promega, M7805), 0.125 µl Taq DNA polymerase (1.25 U) (Promega, M7805), 0.25 µl forward and reverse primers (1 pmol/µl) (primers used for genotyping are listed in Table 2-7), and nuclease-free water to reach a final volume of 25 µl. PCR reactions were carried out using a Veriti Thermal Cycler (Applied Biosystems) as follows: denaturation heating to 95°C for 5 mins; 37 cycles of 94°C for 40 sec (denaturation), 63°C for 40 sec (annealing of primers) and 72°C for 30-60sec (extension); subsequently, a final extension at 72°C for 10 mins. Annealing temperature was optimized and modified using a range of 55°C-65°C according to the length of the primers, whereas the extension time was set based on the length of the amplicon. PCR products were separated and visualized by agarose gel electrophoresis (Almars, Chondrou et al. 2019).

2.2.8.9 Quantitative real-time PCR (qRT-PCR)

Quantitative real-time PCR was done to evaluate the level of mRNA and measure the changes at gene expression. Primers (Sigma) listed in Table (2-5, 2-6) were designed to amplify a region of 100-200 bp of size and to target two consecutive exons within the gene of interest. Primers were resuspended in DNase/RNase free water to a final concentration of 100 Mmol/µl and

stored at -20°C. Both cDNA and primers were diluted (10x dilution) prior the experiment with nuclease-free water and final concentration of primers was 10 µM. qRT-PCR was performed in 20 µl reaction mixture that composed of: 2 µl of cDNA, 10 µl of 2x LightCycler 480 SYBR Green I Master Mix (Roche, 04707516001), 2 µl of primers and 6 µl of DNase/RNase free water. All reactions were loaded in triplicate into a 96-well plate and emitted fluorescence was evaluated by LightCycler 480 II instrument (Roche). Expression of housekeeping genes such as β-actin, glyceraldehyde 3-phosphate dehydrogenase (GAPDH) or *Homo sapiens* Hypoxanthine phosphoribosyltransferase 1 (HPRT1) was measured for data normalization. Threshold cycle (Ct) values were calculated by lightCycler 480 II software (Roche, https://www.roche-applied-science.com/sis/rtpcr/htc/index.jsp?id=htc_070400). The data were then exported to Microsoft Office Excel and analysed by the method described by (Livak and Schmittgen, 2001). In this method, relative gene expression was calculated using (ΔCT) and (2-ΔΔCT) and were finally presented as fold of changes over the control sample by dividing the values obtained from the 2-ΔΔCT to the corresponding values from the experimental control. A two-tailed Student T-test was carried out between control and the experimental sample using (Almars et al., 2019).

2.2.9 STATISTICAL ANALYSIS

Statistical analyses were obtained by using Microsoft Office Excel or GraphPad Prism 6 software. All experiments were performed in triplicate and repeated at least 2-3 times on independent occasions. P value < 0.05 was

considered statistically significant. Results are shown as mean ± standard deviation (STDEV), unless otherwise stated.

CHAPTER 3

Mechanisms, biological and clinical significance of HP1BP3 alteration in AML

3.1 **Brief introduction**

Acute myeloid leukaemia (AML) is a heterogeneous haematological malignancy that is characterized by aggressive proliferation of immature myeloid precursors (Goldman et al., 2019). Recently, numerous reports strongly point to mutations in epigenetic regulators as a leading cause of AML initiation and progression (Bullinger et al., 2010, Busque et al., 2012, Stasik et al., 2020). These mutations in epigenetic modifiers include a wide range of epigenetic writer, eraser and reader proteins (Sun-Chen et al., 2018). The epigenome is dynamically controlled by chemical alterations of DNA and RNA and the histone proteins that create an epigenetic mechanism for regulating a broad spectrum of normal and tumour-related processes (Cazaly et al., 2019). The coordinated response of epigenetic regulators is essential for controlling different cellular mechanisms, including DNA replication, transcription, cell cycle regulation and the DNA damage/repair process (Roberti et al., 2019). Histone post-translational modifications may impact the core histones in heterochromatin–euchromatin conversion; however, the identity of the heterochromatin-associated proteins and their binding proteins has remained largely unclear.

Heterochromatin protein 1 binding protein 3 (HP1BP3) was identified in our lab as a downstream target of FBXW7 for ubiquitin-mediated degradation [Sedaie-Bonab et al., in submission]. *FBXW7* is a tumour-suppressor gene that targets several proto-oncogenes and transcriptional modulators for degradation; hence, it plays a critical role in tumorigenesis (Davis et al., 2014, Heo et al., 2016). Moreover, HP1BP3 has been identified as a novel chromatin-related protein that directly binds to the chromoshadow domain of

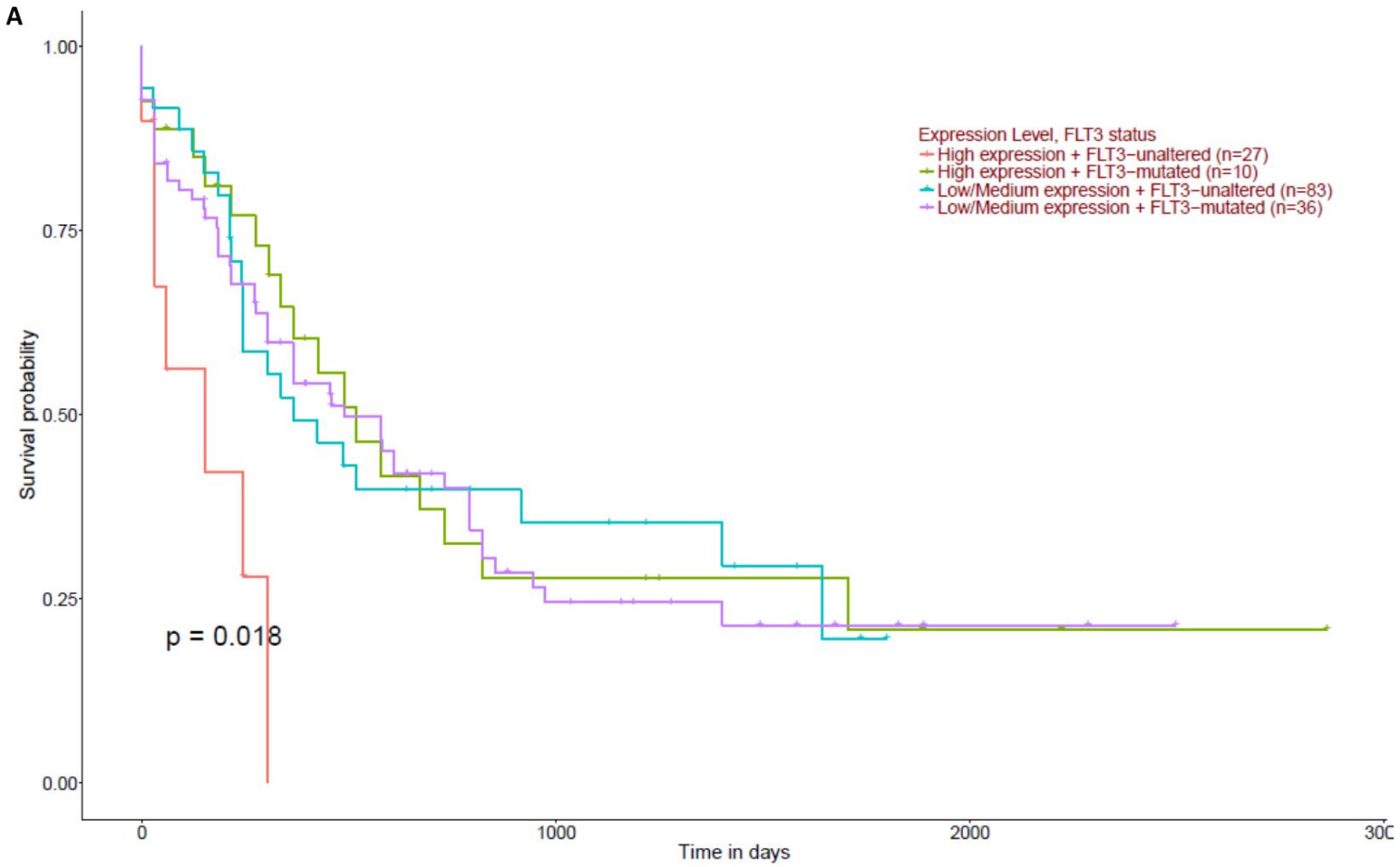
HP1α (Hayashihara et al., 2010, Garfinkel et al., 2015), where the histone methyltransferases SUV39H1/2 also bind to HP1α to mediate the formation of trimethylated histone H3 lysine 9 (H3K9me3) (Rea et al., 2000, Lachner-O'Carroll et al., 2001). Furthermore, the HP1α–H3K9me3 complex is enriched in the initiation of constitutive heterochromatin (Maison et al., 2002). Modulation of HP1α at chromatin conversion plays an important role in normal homeostasis and cancer (Maison et al., 2011, Vad-Nielsen and Nielsen, 2015). More importantly, HP1BP3–HP1α binding could be involved in chromatin integrity and higher-order chromatin structure. Considering that only a few articles have been published about HP1BP3, the role of HP1BP3 in leukemogenesis through epigenetic modification remains to be elucidated.

Herein, we show that the HP1BP3 protein is differentially expressed in AML cell lines. Our data indicate that the differential expression of HP1BP3 associated with the chromatin states alterations. To gain further insights into the molecular basis of HP1BP3 in AML progression, loss- and gain-of-function analyses of HP1BP3 were carried out in AML cell lines. High levels of HP1BP3 downregulated the triple-methylation of the lysine 9 residue in histone H3 (H3K9me3) and upregulated the acetylation of the same site (H3K9ac), which might lead to the formation of euchromatin. The downregulation of HP1BP3 reversed the result by inducing H3K9me3 and reducing H3K9ac. We also found that HP1BP3 regulated AML proliferation, clonogenic potential and cell cycle progression. Furthermore, our transcriptomic analysis revealed that HP1BP3 inhibition altered the expression of a number of proto-oncogenes and genes involved in cell cycle regulation which could be due to the induction of tumour-suppressor genes.

3.2 **Results**

3.2.1 *HP1BP3* as a potential prognostic marker in AML

UALCAN database TCGA and Kaplan–Meier analysis (http://ualcan.path.uab.edu/cgi-bin/TCGA-survival1.pl?genenam=HP1BP3&ctype=LAML) showed high *HP1BP3* expression level is correlated with poor overall survival among patients with AML (P = 0.018, n=156) and was not associated with *FLT3* status (Figure 3-1 A). Moreover, the cBioPortal database revealed that *HP1BP3* mutations are common in cancer, including myeloid neoplasms (n=1027, ~4.5% of samples) and it exhibits gain-of-function mutations that convert a proto-oncogene into an oncogene (https://www.cbioportal.org/patient/clinicalData?caseId=TCGA-AB-2820&studyId=laml_tcga_pub) (Figure 3-1 B)


A
1.00
0.75
0.50
0.25
0.00
Survival probability
p = 0.018
0
1000
2000
Time in days
Expression Level, FLT3 status
High expression + FLT3−unaltered (n=27)
High expression + FLT3−mutated (n=10)
Low/Medium expression + FLT3−unaltered (n=83)
Low/Medium expression + FLT3−mutated (n=36)

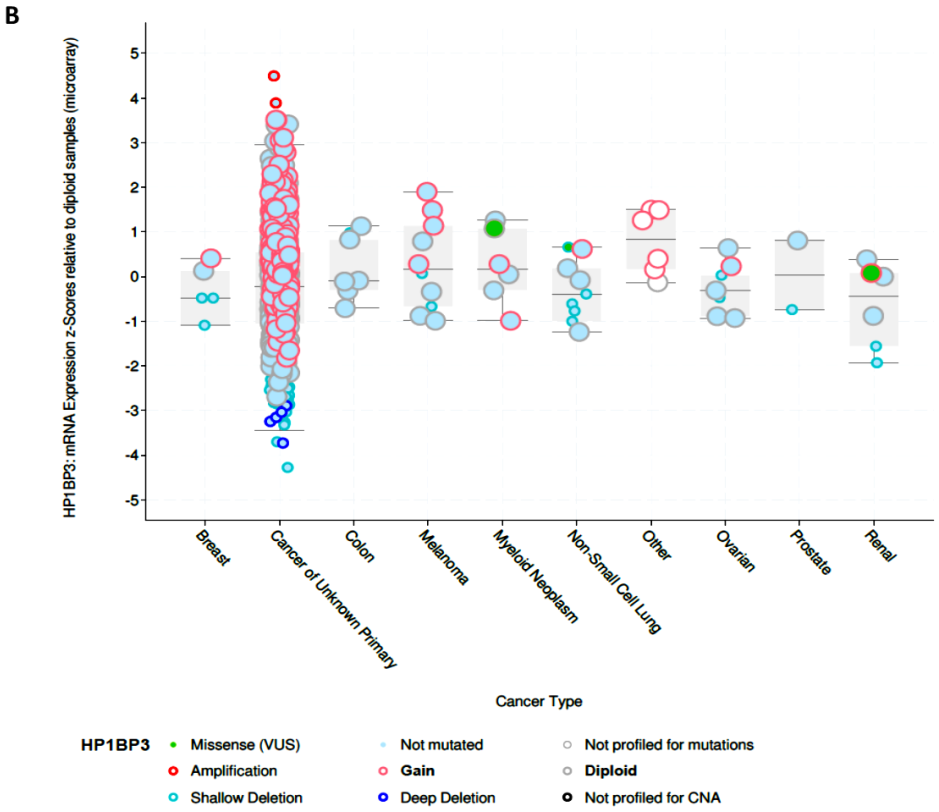


Figure 3-1: HP1BP3 as a potential prognostic marker in patients with AML. **(A)** Kaplan-Meier plots indicates the *HP1BP3* expression is negatively associated with overall survival in patients with AML and not associated with *FLT3* mutations. **(B)** cBioPortal analysis showed that *HP1BP3* mutations are common in cancer, including myeloid neoplasms (n=1027, ~4.5% of samples).

3.2.2 Differential expression of HP1BP3 and epigenetic markers associated with transcriptional activity among AML cell lines

To understand the role of HP1BP3 in AML, the endogenous expression of HP1BP3 was initially investigated using western blotting (WB) in nine AML cell lines: M091, U937, Mo7e, MOLM13, OCI-AML3, KG1a, MV4-11, TF-1a and HL-60. To achieve that, the protein was extracted from cultured cells in log phase using protein lysis buffer (*Chapter 2*). The cell lysates were quantified using Bradford assay and were then immunoblotted for HP1BP3 and the loading control β-actin. Interestingly, the WB results showed differential expression of HP1BP3 among these nine cell lines. Some cell lines such as MO91, Mo7e, OCI-AML3, KG-1a, MV4-11, TF1a and HL-60 expressed both isoforms of HP1BP3 at different levels (Figure 3-2 A). The long isoform was around 75 KDa and the short isoform was around 45 KDa. However, the U937 cells expressed only the short isoform while the MOLM13 cells showed no expression of HP1BP3 (Figure 3-2 A).

Next, we measure the *HP1BP3* transcripts in these cells, the mRNA expression level of long-isoform HP1BP3 was examined by designing primers that target the first two exons in qRT-PCR. Total RNA was isolated, and cDNA was synthesized as described earlier (*Chapter 2*). The qRT-PCR data showed differential mRNA expression level of *HP1BP3* in the AML cell samples (Figure 3-3 A). The highest expression was however in the Mo7e, TF1a, MO91 and MV4-11 cells, while the lowest expression was in the

MOLM13, U937, KG1a and HL-60 cells, which support the data obtained from WB analysis (Figure 3-2 A). The MOLM13 and U937 cells showed low

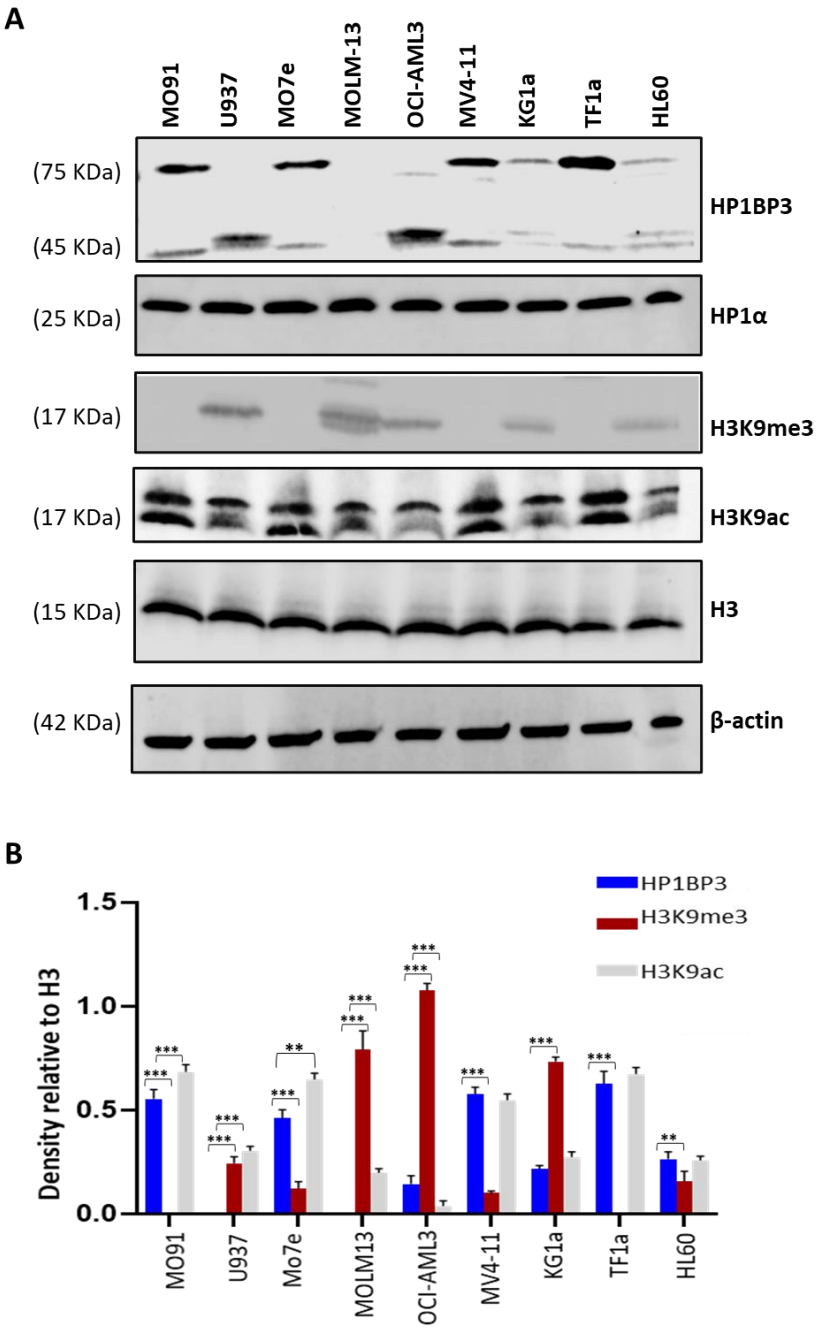


Figure 3-2: Differential expression of HP1BP3 among 9 different AML cell lines. (A) Western blotting analysis for endogenous HP1BP3, HP1 α, H3K9me3 and H3K9ac expression level in MO91, U937, M07e, MOLM13, OCI-AML3, MV4-11, KG1a, TF1a and HL-60 cell lines. 100 µg of total protein was loaded on 10% for (anti-HP1BP3) or 15% for (anti- HP1, -H3K9me3 and -H3K9ac) SDS-PAGE and transferred to PVDF membranes. Anti-HP1BP3, -HP1α, - H3K9me3 and -H3K9ac, have been used to detect the expression

level of HP1BP3, HP1α, H3K9me3 and H3K9ac. AML cell lines expressed HP1BP3 in different levels, M091, M07e, OCI-AML3, KG1a, MV4-11, TF1a and HL-60 expressed both long and short isoforms. Chromatin markers; H3k9me3 and H3K9ac were irreversibly correlated with the expression of long isoform of HP1BP3. β-actin and H3 are used as loading controls. WB experiments were repeated in three different occasions (N=3 independent experiments). **(B)** Histogram represents relative density value of HP1BP3/H3, H3K9me/H3 and H3K9ac/H3 from three biological repeats (± SD) (*P= 0.01 to 0.05, **p= 0.001 to 0.01, ***p<0.001).

mRNA expression of *HP1BP3* but no protein expression, which could be due to post-transcriptional/translational modifications. As HP1BP3 binds directly to HP1α, the expression of HP1α was also examined at both mRNA and protein level. The qRT-PCR (Figure 3-3 B) and WB (Figure 3-2 A) data showed that the expression of *HP1α* remained unchanged in all cell lines regardless of the expression of HP1BP3. Moreover, the endogenous expression patterns and the co-localization of HP1BP3 and HP1α were examined by immunofluorescence (IF). The MO91, U937 and MOLM13 cells were selected according to their expression of HP1BP3 protein obtained by WB (Figure 3-2 A). The cells were cytospun and stained with anti-HP1BP3 and anti-HP1α. The fluorescence images show the foci nuclear patterns of both HP1BP3 and HP1α while their differential expression and co-localization (Figure 3-4), may suggest that modulation of HP1BP3 expression or function might be located in both the euchromatic and heterochromatic activities.

To charcterise the differential expression HP1BP3 associated with the euchromatic and heterochromatic activities, we examined the expression levels of both H3K9me3 and H3K9ac, as markers of heterochromatin

(inactive chromatin) and euchromatin (active chromatin), respectively, using WB analysis. Interestingly, H3K9me3 and H3K9ac levels inversely correlated with the long HP1BP3 isoforms in most of the above AML cells (Figure 3-2 A). Therefore, these findings led us to hypothesise that the high level of HP1BP3 downregulated H3K9me3 and upregulated H3K9ac and was eventually associated with chromatin transition (Figure 3-2 A). These data prompted us to study the gain and loss of function further to understand the novel role of HP1BP3 in AML.

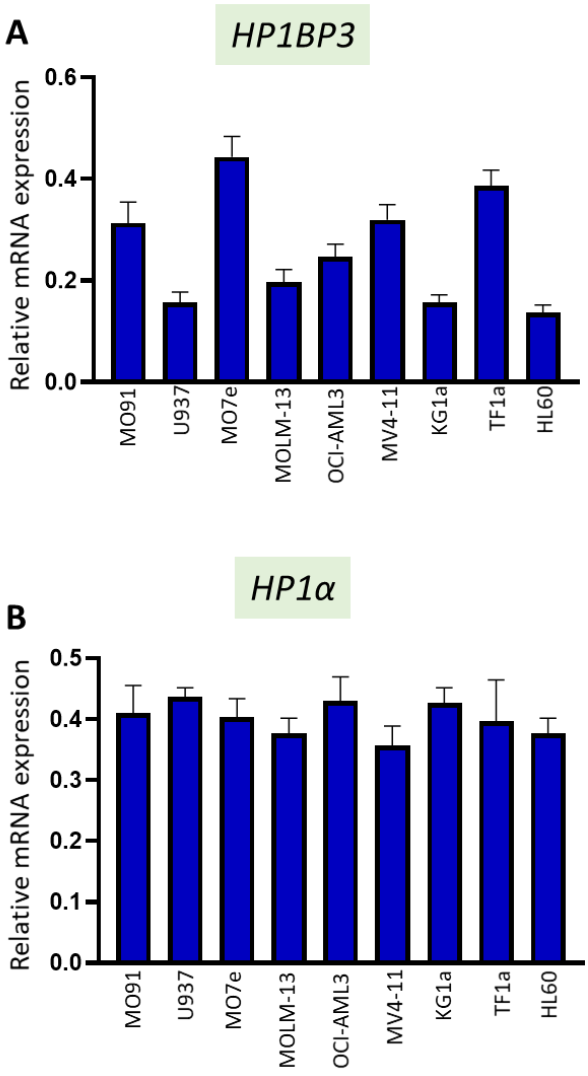


Figure 3-3: mRNA expression of *HP1BP3* and *HP1α* in AML cell lines. (A) Data indicates the differential expression of long *HP1BP3* in AML cells, the highest expression level was in Mo7e, TF1a, MO91 and MV4-11 and the lowest expression was in U937, MOLM13, KG1a and HL60. **(B)** Data demonstrates no change in the mRNA expression of *HP1α* among AML cells. The expression level was analysed by qRT-PCR, data was normalized to β-actin. The error bars show the SD of three biological repeats. This experiment was repeated in three different occasions (N=3 independent experiments).

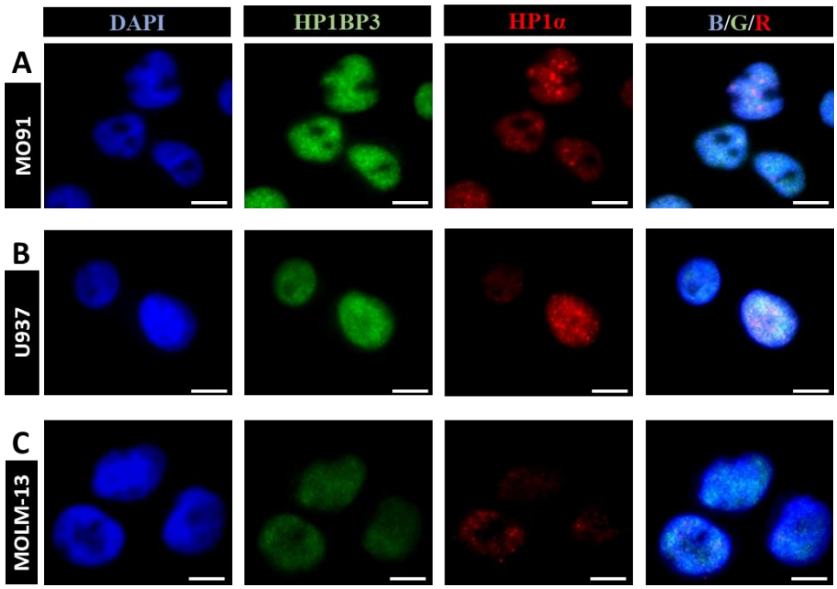


Figure 3-4: Fluorescence nuclear foci co-localization and expression patterns of HP1BP3 and HP1α in AML cell lines. HP1BP3 (green) and HP1α (red) endogenous proteins expression in **(A)** MO91, **(B)** U937 and **(C)** MOLM13 cells. Fluorescence images show the foci expression and co-localization of HP1BP3-HP1α examined by immunofluorescence technique. Scale bars, 25µm.

3.2.3 Generation of AML cells stably over-expressing HP1BP3 long and short isoforms

To address the biological function of HP1BP3 and its contribution to heterochromatin remodelling in AML cell lines, we generated cell lines stably overexpressing HP1BP3 using lentiviral (LV) infection. The MOLM13 cell line was selected for gene overexpression according to the expression of HP1BP3 (Figure 3-1 A). The MOLM13 cell line that showed no expression of HP1BP3 were transduced with pLVX-eGFP-HP1BP3“L” and pLVX-eGFP-HP1BP3“S” plasmids to overexpress long and short HP1BP3 isoforms, respectively, and with pLVX-eGFP plasmid as a control. Both pLVX-eGFP-HP1BP3“L” and pLVX-eGFP-HP1BP3“S” carried HP1BP3 as a downstream of the constitutive CMV promoter and carried puromycin resistance and GFP genes (selectable markers) (Figure 3-5 A-C). According to the restriction site in their multiple cloning site (MCS), all plasmids were validated using restriction digestion. Digested DNAs were run on 1% agarose gel; the digestion confirmed the presence of the expected DNA fragments (Figure 3-5 D-F). Following LV production and transduction (*Chapter 2*), cells stably expressing HP1BP3 were selected with puromycin (1.5 μg/ml) and then amplified prior to the validation assay. The cells were seeded and lysed using protein lysis buffer for immunoblotting analysis (Figure 3-6 A). The expression of *EGFP* (the reporter gene) further confirmed the stable expression of either HP1BP3-GFP or scrambled shRNA-GFP in the AML cells (Figure 3-6 B). Collectively, these data confirm the successful genome integration of EGFP-HP1BP3 in the stably transduced MOLM13 cell lines (Figure 3-6).

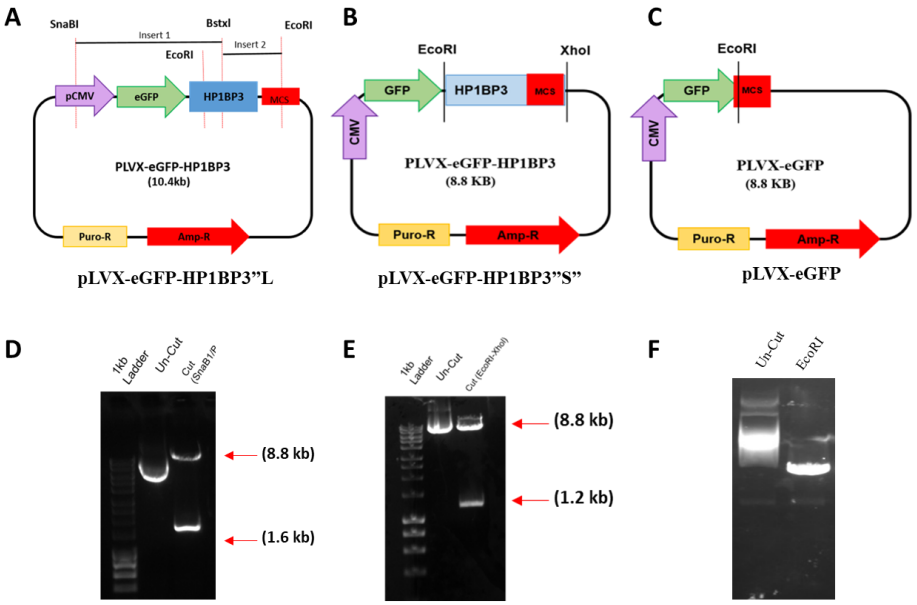


Figure 3-5: The pLVX-eGFP-HP1BP3"L", pLVX-eGFP-HP1BP3"S" and pLVX-eGFP plasmid maps and validation analysis by restriction enzyme digestion. (A-C) Schematic presentation showing the backbone vector pLVX-eGFP-HP1BP3"L" pLVX-eGFP-HP1BP3"S" and pLVX-eGFP plasmids respectively, with restriction enzymes sites. **(D-F)**, the digested DNAs (pLVX-eGFP-HP1BP3"L", pLVX-eGFP-HP1BP3"S" and pLVX-eGFP) were run on 1% agarose gel to confirm the release of the two expected DNA fragments.

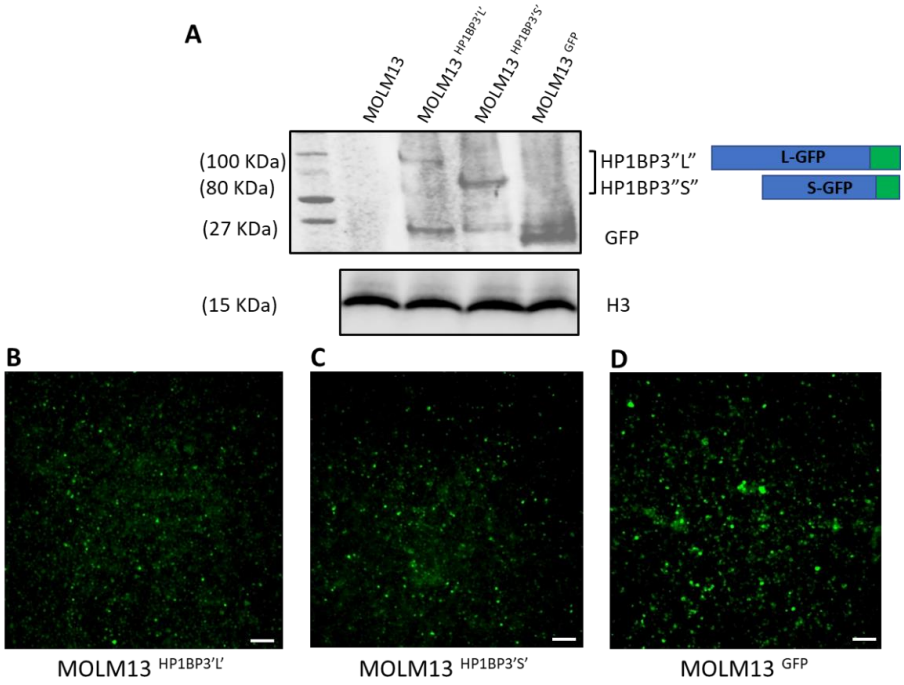


Figure 3-6: Expression of GFP-HP1BP3 protein in MOLM13 stable cell lines. **(A)** Western blotting analysis confirms GFP-HP1BP3 expression in MOLM13 stable cell lines. 100 µg of total protein was run on gradient 4-20% SDS-PAGE and transferred into PVDF membrane. Anti-GFP antibody was used to detect the exogenous expression of both GFP-HP1BP3 and GFP proteins in the generated cells, anti-H3 was used as a loading control. **(B-D)** Fluorescence microscopy of transduced MOLM13 stable cell lines overexpressing MLOM13^{HP1BP3L}, MOLM13^{HP1BP3S} and MOLM13^{GFP} respectively. Scale bare is 75 µm.

3.2.4 Generation of AML cells over-expressing HP1BP3-shRNA

Next, to identify whether the inactivation of HP1BP3 plays a role in AML progression, loss-of-function analyses were carried out. Clustered regularly interspaced short palindromic repeats (CRISPR) was initially used to generate knockout cells. For this, AML cell lines that highly expressed HP1BP3, i.e. MO91, U937, TF1a, MV4-11 and OCI-AML3, were transfected with PX459-Puro plasmids that were generated in our lab using electroporation. The transfection efficiency was less than 10–15% using this non-viral method. Additionally, the viability of the transfected cells decreased rapidly within 2–3 weeks which led us to use an LV method. Downregulated expression of HP1BP3 was ultimately achieved by small hairpin RNA (shRNA) using LV transduction. AML cell lines were transduced with either HP1BP3 shRNA-GFP or scrambled shRNA-GFP (control) (Figure 3-7 A). Plasmids were validated using restriction digestion according to the restriction site in their MCS. Digested DNA were run on 1% agarose gel (*Chapter 2*); the digestion confirmed the presence of the expected DNA fragment (Figure 3-7 B). Both the pLVX-shHP1BP3 and piLenti-shRNA-GFP vectors carry the puromycin resistance gene (Figure 3-7). Therefore, the cells were washed and incubated with fresh medium containing puromycin to select positively transduced cells 48 hrs post-transduction. Resistant cells were amplified and processed for validation. To confirm the shRNA-mediated downregulation of HP1BP3 in the transduced AML cells, WB analyses were carried out. All HP1BP3 shRNA-expressing AML cell lines showed reduced expression levels of HP1BP3 (Figure 3-8 A).

Moreover, the stable expression of either HP1BP3 shRNA-GFP or scrambled shRNA-GFP in the transduced AML cells was further confirmed by assessing EGFP expression using a fluorescence microscope (Figure 3-8 B).

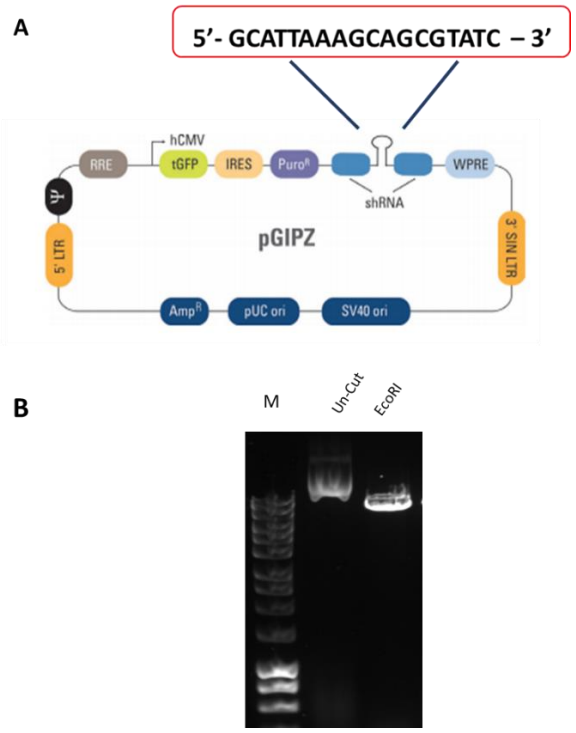


Figure 3-7: Schematic presentation of inserted HP1BP3-shRNA into pGIPZ plasmid and validation analysis by restriction enzyme digestion. (A) pGIPZ plasmid map showing the target sequence of HP1BP3 encompassed in red box. **(B)** The digested DNA was run on 1% agarose gel to confirm the DNA cut.

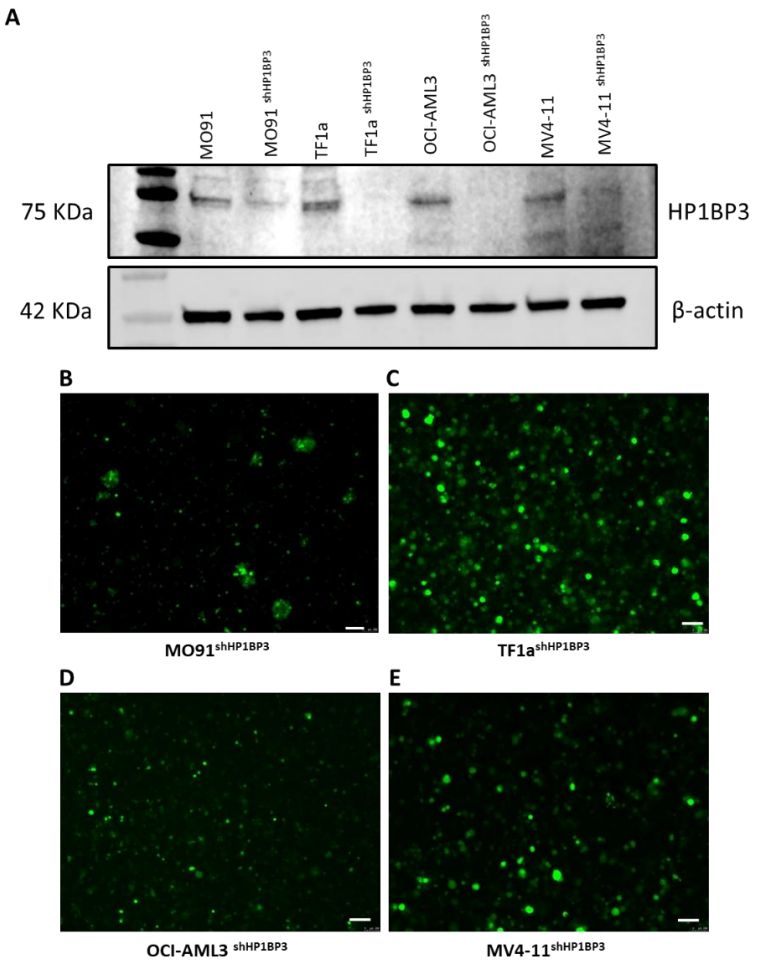


Figure 3-8: shRNA-mediated knockdown of HP1BP3 in AML cell lines. (A) Immunoblot result for endogenous expression of HP1BP3 knockdown in AML cells indicates reduction of HP1BP3 expression compared to parental cells. Cells were transduced with LV-sh*HP1BP3* particles, selected cells were amplified and harvested for validation. 100 µg of protein extracts were run on 10% SDS-PAGE, transferred into PVDF membrane and blotted with anti-HP1BP3 antibody. Anti-β-actin antibody was used as a loading control. **(B-E)** Fluorescence microscopy images of stable HP1BP3 shRNA-GFP expressing AML cell lines MO91, TF1a, OCI-AML3 and MV4-11 respectively. Scale bare is 75 µm.

3.2.5 Chromatin marker expression profiling of stable AML cell lines overexpressing HP1BP3 and of Lin$^-$ HSCs and AML cells lacking HP1BP3

As outlined above, HP1BP3 binds directly via its globular domain to the chromoshadow domain of HP1α (Garfinkel, Melamed-Book et al. 2015), where SUV39H1 also binds to the same domain of HP1α. HP1α interaction with SUV39H1 is involved in the methylation of H3K9, heterochromatin formation and gene silencing (Bannister, Zegerman et al. 2001, Yamamoto and Sonoda 2003). On the other hand, a high level of HP1BP3 is negatively correlated with the expression of H3K9me3 (Figure 3-2). It is well established that H3K9me3 is an epigenetic marker enriched in the heterochromatin regions, and is known as a transcriptional repressive marker. However, H3K9ac is a well-known euchromatic marker associated with transcriptional activation (Bártová, Krejčí et al. 2008, Wang, Zang et al. 2008, Bannister and Kouzarides 2011). Therefore, we questioned whether the stably downregulated or overexpressed HP1BP3 would affect the expression of the H3K9ac/H3K9me3 markers in AML cells.

To investigate the possibility of the deregulated expression of HP1BP3 in altering the heterochromatin–euchromatin transition of AML, MOLM13 cell lines that stably overexpressed GFP-HP1BP3“L”, GFP-HP1BP3“S” and GFP proteins were used. Interestingly, western blotting indicated that ectopic HP1BP3 expression decreased the expression level of H3K9me3 while inducing H3K9ac expression in the MOLM13^{HP1BP3L} and MOLM13^{HP1BP3S} cells compared with the control of MOLM13^{GFP} cells (Figure 3-9). Moreover,

the level of HP1α remained unchanged, which is consistent with our initial finding (Figure 3-1), (Figure 3-9).

To further test the downregulation of HP1BP3 in changing chromatin states, AML stable HP1BP3 shRNA-expressing cell lines, i.e. MO91^{KD}, TF1a^{KD} and MV4-11^{KD}, were used. WB analysis indicated that the inhibition of HP1BP3 increased H3K9me3 and reduced the level of H3K9ac. However, following our earlier data, the level of HP1α remained unchanged in all cells (Figure 3-10).

Taken together, these findings confirm our initial hypothesis and indicate the specific role of HP1BP3 in chromatin remodelling regardless of the expression level of HP1α. Moreover, these data suggest that HP1BP3 might act as an important chromatin modifier that regulates the transcription of many genes by modifying the expression of two well-known heterochromatin/euchromatin markers: H3K9me3 and H3K9ac.

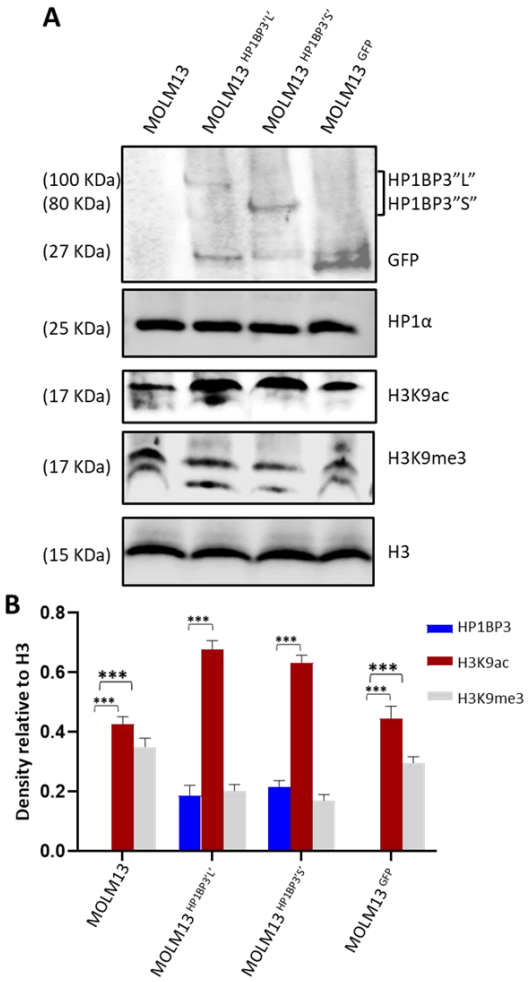


Figure 3-9: Ectopic expression of HP1PB3 decreases the expression of H3K9me3 while increases H3K9ac expression. (A) Western blot analysis was done in MOLM13^{WT} and MOLM13 stably expressing GFP-HP1BP3 or GFP. A 150 µg of total protein lysate (for anti-GFP) or 100 (for anti-HP1α, -H3K9me3, -H3K9ac, -H3) were run on 4-20 % SDS-PAGE, transferred to PVDF membranes and immunoprobed for (anti-GFP, -HP1α, -H3K9mac, -H3K9me3 and-H3) antibodies, H3 was used as loading control. WBs repeated in three independent times. **(B)** Histogram represents relative density value of HP1BP3/H3, H3K9ac/H3 and H3K9me/H3 in MOLM13 cells from three biological repeats (± SD). This experiment was repeated in three different occasions (N=3 independent experiments).

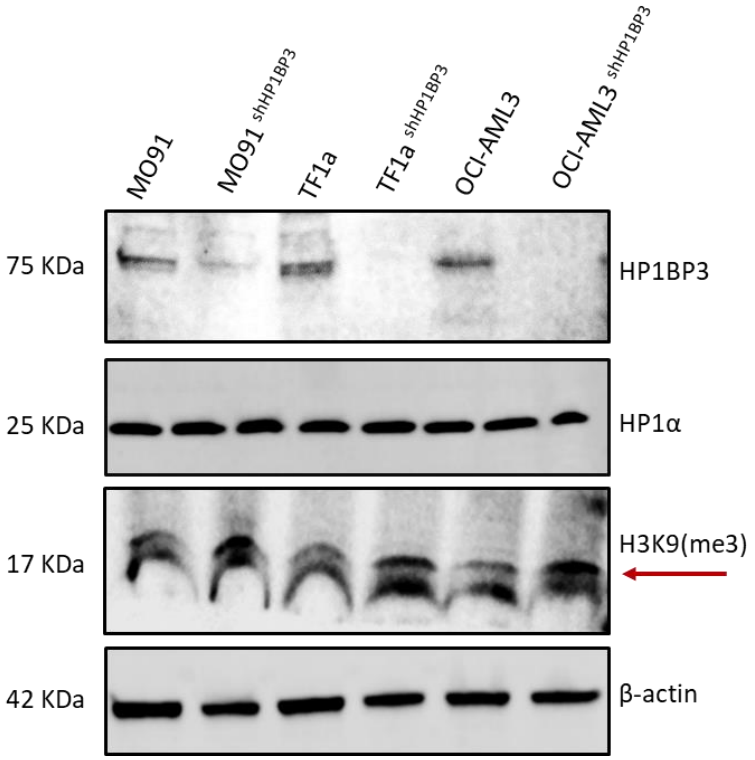


Figure 3-10: Loss of HP1BP3 induced the expression of H3K9me3 in AML cells. Western blotting analysis were performed in AML cell line stably expressing sh-*HP1BP3* or GFP. Total protein extracts, 100 µg of were run on 4-20 % SDS-PAGE, transferred to PVDF membranes and immunoblotted for (anti-HP1BP3, -HP1α, -H3K9me3 and-H3) antibodies, β-actin was used as loading control.

3.2.6 Overexpression/knockdown of *HP1BP3* alters the proliferation of AML cells

As the ectopic expression and downregulation of *HP1BP3* changed the expression of two well-known chromatin markers (H3K9me3 and H3K9ac), we therefore hypothesised that HP1BP3 could regulate chromatin compaction and eventually AML proliferation. *HP1BP3* overexpression downregulated H3K9me3 and upregulated H3K9ac (Figure 3-9), which could be involved in chromatin relaxation. However, *HP1BP3* knockdown (KD) upregulated H3K9me3, while H3K9ac was downregulated (Figure 3-10), which might be involved in chromatin organisation.

To test this, *HP1BP3*-overexpressing MOLM13^{HP1BP3L} and MOLM13^{HP1BP3S} cells and *HP1BP3* knockdown MV4-11^{KD} cells, as well as their corresponding control cells, were used in this experiment. The cells were seeded in 96-well plates and cell proliferation was examined using the colorimetric metabolic-based cell proliferation reagent WST-1. This assay is a metabolic based on the cleavage of tetrazolium salt by mitochondrial dehydrogenases to form formazan. The cells were incubated with the WST-1 reagent for 0.5–4 hrs; ultimately, the formed formazan dye was quantitated using a scanning multi-well spectrophotometer. Our data showed that the overexpression of *HP1BP3* significantly induced proliferation in the MOLM13 cell line compared with the control cells (Figure 3-11 A-B). However, the knockdown of *HP1BP3* reversed the result; the proliferation of MV4-11^{KD} cells was significantly reduced compared with their corresponding control MV4-11^{GFP} cells (Figure 3-11 C-D). These data suggest that HP1BP3 regulates proliferation in AML cells and could be

associated with the epigenetic mechanism of transcriptional modulation in AML cells.

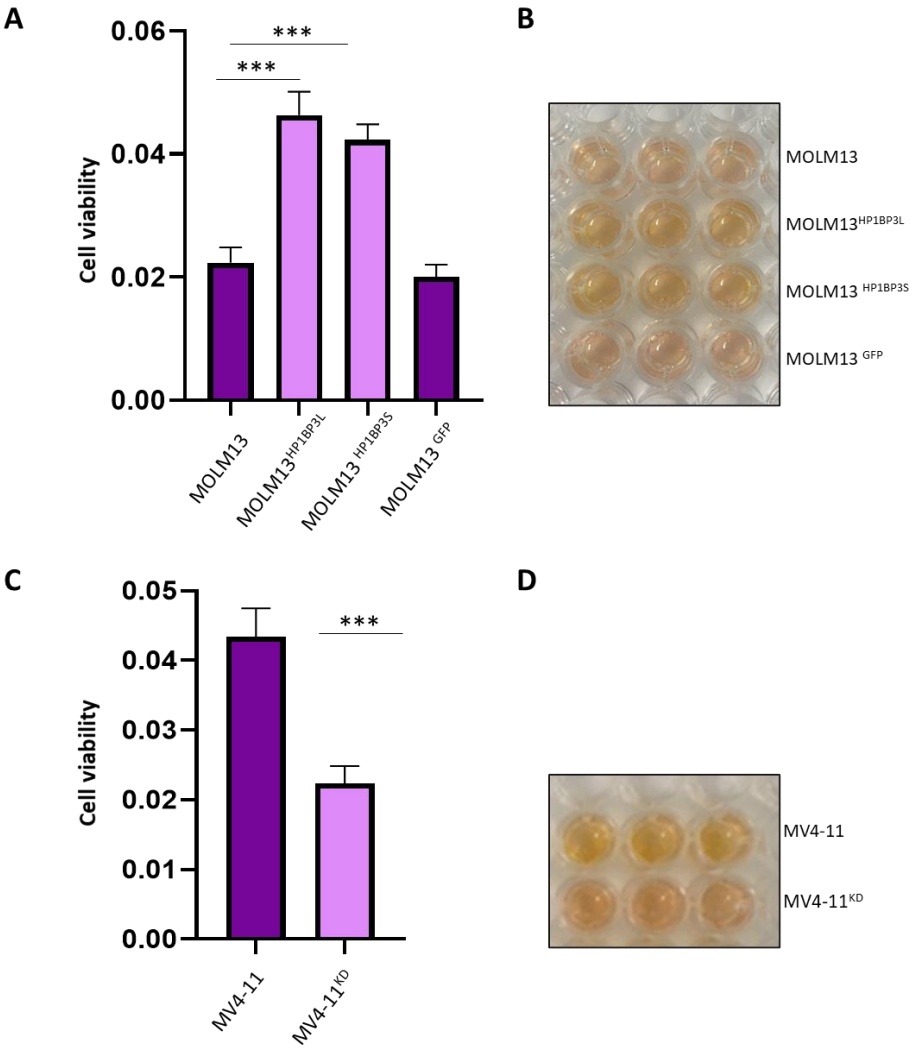


Figure 3-11: Expression of HP1BP3 changes AML cells proliferation. (A, C) Histograms show significant changes of cells proliferation in AML cells stably overexpressing HP1BP3 or shHP1BP3 respectively. **(B, D)** Representative images of WST-1 assay of MOLM13 cells overexpressing HP1BP3 or GFP control and MV4-11 cells lacking the expression of HP1BP3 respectively. Cells were seeded in 96 well plate and incubated with WST-1 reagent for 0.5- 4 hrs, the colour changes were measured using multi-well spectrophotometer. This experiment was performed in triplicate on at least three independent occasions. Statistical test: Two-tailed unpaired t-test (n=3; ***p<0.001). The error bars show the SD of three biological repeats.

3.2.7 Cell cycle progression in AML cells is highly regulated by the expression of HP1BP3

During cell division, the nuclear chromatin undergoes a number of changes that alter its shape and degree of condensation. Accurate genetic expression and genomic information transmission requires chromatin condensation to regulate the separation of two sister chromatin and to maintain genomic stability (Antonin and Neumann, 2016).

Throughout cell cycle progression, the chromatin is dynamically condensed and decondensed to enable cell biological processes. In the S-phase, chromatin is decondensed to facilitate DNA replication. DNA is wrapped around histone proteins, in which histone tails are subjected to a wide array of post-translational modifications. The landscape of histone modifications is altered during mitosis along with chromosome condensation (Piskadlo and Oliveira, 2016). Methylated H3K9, which is a marker of heterochromatin, is highly expressed in G2-to-M transition; however, acetylated H3K9, a marker of euchromatin, is highly expressed during S phase (Park et al., 2008). Therefore, deregulation of the chromatin remodelling machinery system may result in cell cycle deregulation. Deregulation of the cell cycle and uncontrolled proliferation are considered a hallmark of cancer cells (Malumbres and Carnero, 2003). In addition to histone post-translational modifications, the role of non-histone proteins during mitosis and cell cycle progression remains vague and poorly understood.

3.2.7.1 Constitutive overexpression of *HP1BP3* enhances cell cycle transition from G1 to S phase

To investigate the influence of *HP1BP3* overexpression on cell cycle progression, MOLM13 cells stably overexpressing *HP1BP3* were used in the experiment. The cells were fixed and stained with propidium iodide (PI) and analysed by fluorescence-activated cell sorting (FACS) to study the cell cycle distribution of the cells (*Chapter 2*). The cell cycle histogram and statistics were generated using Weasel software. Interestingly, forced expression of *HP1BP3* significantly reduced the percentage of cells in G0/G1 phase and increased the percentage of S- and G2/M cells as compared with the $MOLM13^{GFP}$ control cells expressing only GFP (Figure 3-12). The percentage of cells in G0/G1 phase in the *HP1BP3*-overexpressing cells was significantly lower, from 43.7% in $MOLM13^{HP1BP3S}$ cells and 41.12% in $MOLM13^{HP1BP3L}$ cells to 72% in $MOLM13^{GFP}$ cells. While there were significantly more $MOLM13^{HP1BP3S}$ and $MOLM13^{HP1BP3L}$ cells in S phase: 54.08% and 56.56%, respectively, and 25.96% in the control cells. These results suggest that ectopic expression of *HP1BP3* induces S phase entry and therefore induces cell division in AML cells.

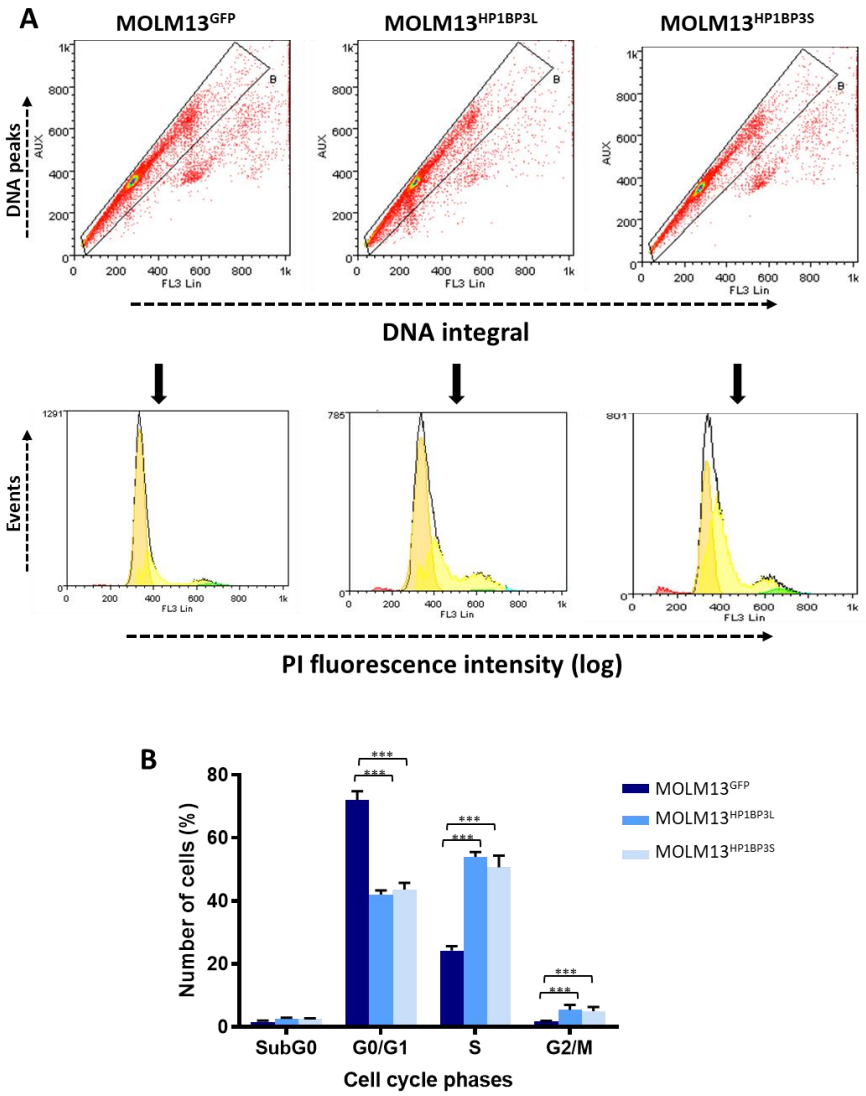


Figure 3-12: Overexpression of HP1BP3 induced MOLM13 cell cycle progression. (A) Histograms of cell cycle analysis were generated using Weasel software for MOLM13^{GFP}, MOLM13^{HP1BP3L} and MOLM13^{HP1BP3S}. Cells were fixed, PI stained and analysed by FACS. **(B)** Statistical analysis of cell cycle phases for MOLM13^{GFP}, MOLM13^{HP1BP3L} and MOLM13^{HP1BP3S} in which statistical differences in *HP1BP3*-overexpreesing cells are compared to *GFP*-expressing cells. Statistical test: Two-tailed unpaired t-test (n=3; ***p<0.001). The error bars show the SD of three biological repeats.

3.2.7.2 Knockdown of *HP1BP3* arrested the AML cells in G0/G1 phase

The ectopic expression of *HP1BP3* (gain-of-function) analysis indicated that the forced expression induced cell cycle progression of AML cells (Figure 3-12). This finding prompted us to investigate the growth activity regulated by *HP1BP3* deactivation (loss-of-function) in AML cells. This was accomplished by using *HP1BP3* knockdown MV4-11^{KD} cells versus control MV4-11^{GFP} cells. The cells were fixed, PI-stained and analysed by FACS. Interestingly, *HP1BP3* knockdown led to a considerable increase in the cell population in G0/G1 phase from 40.8% to 56.6% compared to the control, while cells in S- phase were decreased, from 39.9% to 26.4% (Figure 3-13). However, there was no change in the percentage of cell population in sub-G0 or G2/M between the KD and the control cells. These data suggest that *HP1BP3* downregulation delayed the S phase entry and eventually the cell cycle progression in AML cells.

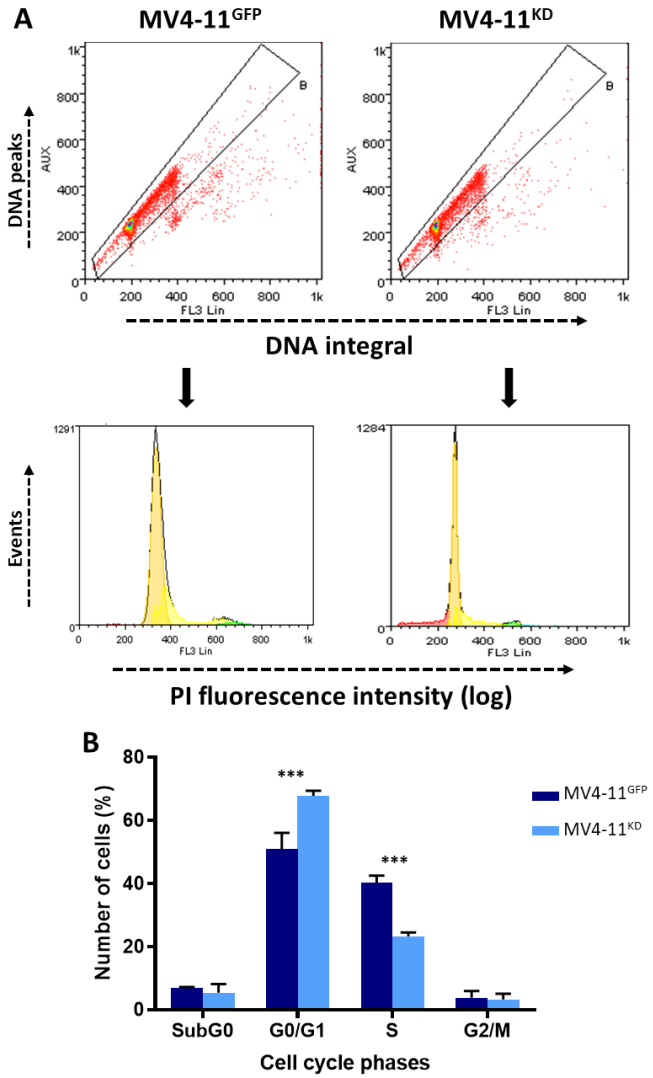


Figure 3-13: HP1BP3 inhibition induced G0/G1 phase arrest in MV4-11 cells. (A) Histograms of cell cycle analysis were generated using Weasel software for MV4-11^{GFP}and MV4-11^{KD}. Cells were fixed, PI stained and analysed by FACS. **(B)** Statistical analysis of cell cycle phases for MV4-11^{GFP}and MV4-11^{KD} in which statistical differences in *HP1BP3*-knockdown cells are compared to *GFP*-expressing cells. Statistical test: Two-tailed unpaired t-test (n=3; ***p<0.001). The error bars show the SD of three biological repeats.

3.2.8 Influence of HP1BP3 expression on the clonogenic potential in AML cell lines using colony-forming unit (CFU) assay

Leukemic stem-like cells (LSCs) are a sub-population of leukemic cells thought to favour self-renewal over differentiation. They have a number of features that allow them to become resistant to anti-cancer drugs and initiate cancer recurrence (Chan and Huntly, 2008, Hanekamp et al., 2017).

The low number of the seeded cells in the serum-free, cytokine-free stem cell medium allows a fraction of cells to undergo 'unlimited' division to form colonies. The colony-forming unit (CFU) assay is, therefore, useful for estimating the stemness activity *in vitro*, i.e. the presence of LSCs within a heterogeneous population of leukaemia cells (Franken et al., 2006). To examine whether the expression of HP1BP3 affects the CFU in AML cell lines, MO91, U937, MOLM13, OCI-AML3 and MV4-11 cells were selected according to HP1BP3 expression (Figure 3-2). Mo7e and KG1a cells were assumed to have stemness activity as they remain quiescent and need GM-CSF to grow, therefore they were also included in this assay. The cells were seeded at low density (1×10^3 cells/well) in 24-well plates in triplicate and cultured with semi-solid stem cell medium (*Chapter 2*). The data showed that the MOLM13, MV4-11 and Mo7e cells formed colonies, while the MO91, U937 and KG-1a cells formed scattered multicellular aggregates but did not organise in colony form (Figure 3-14). Therefore, the MOLM13 and MV4-11 cells were selected for gain- and loss-of-function analyses, respectively, using the generated gene-manipulated cells.

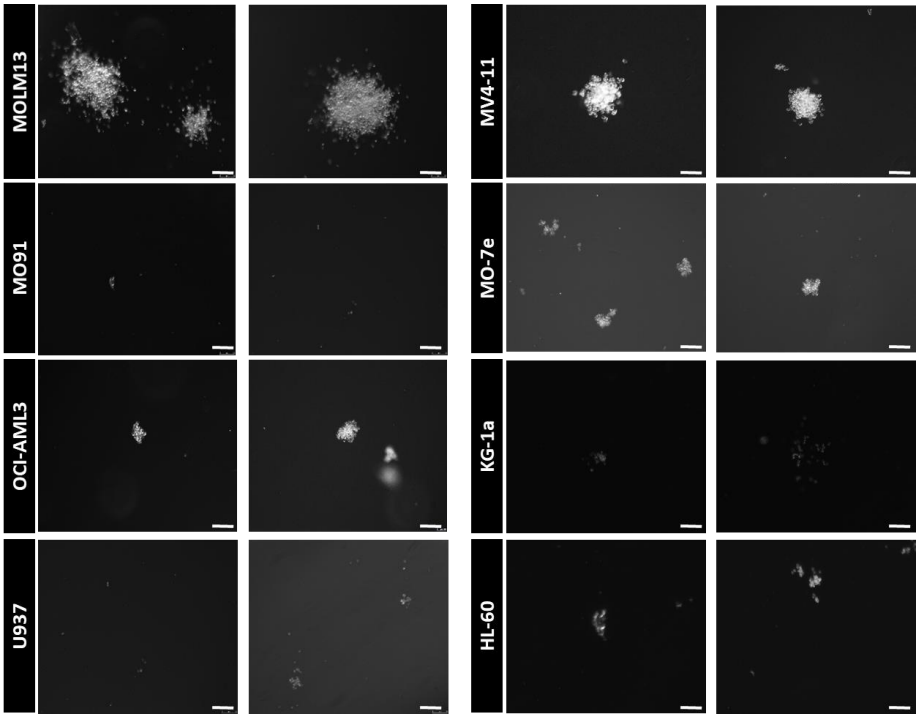


Figure 3-14: Representative images of CFUs formed by AML cell lines. $1X10^3$ of cells were seeded in triplicate and cultured in semi-solid serum free, cytokines free medium for 14 days. Data indicate that only MOLM13 and MV4-11 cells formed colonies. All experiments for all cell lines were performed in triplicates in three independent occasions. Scale bar= 75um.

3.2.8.1 Overexpression of *HP1BP3* increases the size but not the number of CFUs in AML cells

In order to investigate the property of *HP1BP3* overexpression in the stemness activity of AML, the CFU assay was performed. MOLM13 cells stably express the long and short HP1BP3 isoforms, i.e. MOLM13^{HP1BP3L} and MOLM13^{HP1BP3S} cells, as well as control cells expressing GFP, i.e. MOLM13^{GFP} cells, were used in this experiment. The cells were seeded in a low density in semi-solid methylcellulose-based medium (MethoCult™, STEMCELL Technologies) that permitted optimal growth of suspension cells in units. The cells were incubated to form colonies within 14 days, and ultimately, the colonies were imaged, counted and analysed. Both MOLM13^{HP1BP3L} and MOLM13^{HP1BP3S} cells exhibited larger CFU size compared to the corresponding control MOLM13^{GFP} cells (84 ± 3 µm vs 158.5 ± 8.5 µm, n =50) (Figure 4-15 A). However, the number of CFU was not significantly changed in the *HP1BP3*-overexpressing cells compared with the control cells (Figure 3-15 B).

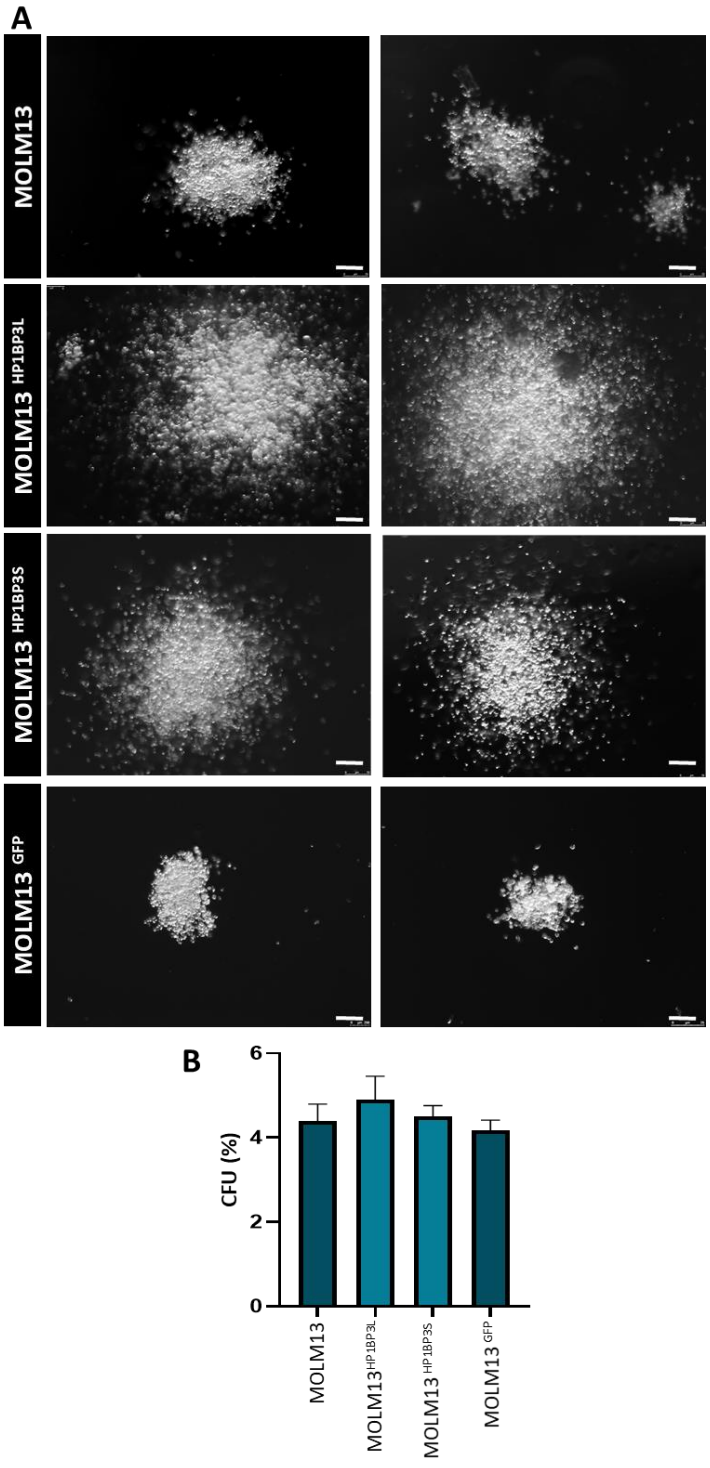


Figure 3-15: Ectopic expression of HP1BP3 increases the size of CFUs in MOLM13 cells. (A) Representative images of colonies formed by MOLM13^{WT} cell line and MOLM13 stably expressing HP1BPL, HP1BP3S and GPF (control); 1 x 10^3 of cells were seeded in semi-solid methylcellulose-based media in triplicate and incubated for 14 days. Scale bar= 75um. **(B)** Histogram shows percentages of CFUs formed by MOLM13 stably over-expressing HP1BP3s and GFP. All experiments were performed in triplicate for each cell line on at least three independent occasions.

3.2.8.2 Knockdown of *HP1BP3* reduces both number and colony size of MV4-11 cells

To examine the loss of *HP1BP3* on the stemness activity of AML cells, the CFU assay was further used in *HP1BP3* knockdown MV4-11^{KD} versus control MV4-11^{GFP} AML cells. A low number of cells (1×10^3 cells/well) were seeded in MethoCult medium in 24-well plates (*Chapter 2*). The cells were amplified to form colonies in 14 days, and eventually, the colonies were counted, imaged and analysed using a light microscope. Figure 3-16 A shows that the knockdown of *HP1BP3* significantly reduced the size (167 ± 4.5 µm vs. 79 ± 5 µm, n = 60) as well as the number of colonies of MV4-11^{KD} cells compared to the corresponding control MV4-11^{GFP} cells.

Taken together, this finding further confirms the direct influence of HP1BP3 on AML cell proliferation and is in line with the data outlined in this chapter.

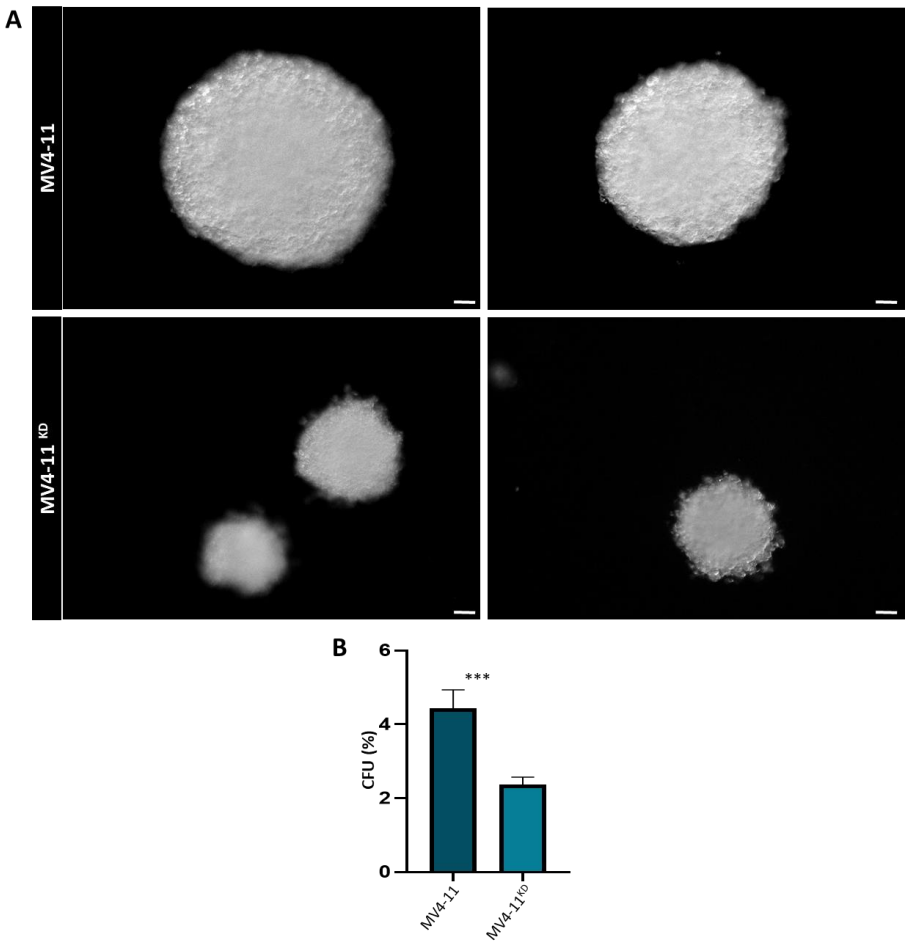


Figure 3-16: HP1BP3 downregulation reduces the number and the size of CFUs in MV4-11 cells. (A) Representative images (top) of colonies formed by MV4-11 cell line and MV4-11 stably expressing HP1BPL-shRNA. Cells (1 x 10^3) were seeded in semi-solid methylcellulose-based media in triplicate and amplified for 14 days. Scale bar= 75um. (B) Histogram (bottom) shows significant reduction in the percentages of CFUs formed by MV4-11 stably expressing *HP1BP3*-shRNA compared to control cells. All experiments were performed in triplicate for each cell line on at least three independent occasions. Statistical test: Two-tailed unpaired t-test (n=3; ***p<0.001). The error bars show the SD of three biological repeats.

3.2.9 RNA sequencing analysis to identify differential gene expression in *HP1BP3* knockdown cells

We used transcriptomics to understand the mechanisms that lead to the phenotypical changes observed in our *in vitro* analysis. In order to identify the HP1BP3 target genes associated with the KD phenotype, RNA-seq was performed using total adenylated RNA from $TF1a^{KD}$ and the corresponding control $TF1a^{GFP}$ cells. The TF1a cells were used in this experiment because they contain ($CD34^{+}/CD38^{-}$) subfraction (Chapter 4) and were also used for small RNA transcriptomic analysis (Chapter 4). Total RNA was extracted, and RNA purity was examined using a NanoPhotometer® spectrophotometer, and 4 µg/sample was shipped to Novogene (Cambridge, UK) for RNA-seq analysis. Prior to the library preparation, RNA degradation and contamination were examined on 1% agarose gels. RNA integrity and quantitation were assessed using an Agilent RNA 6000 Nano Kit for Agilent Bioanalyzer 2100 system (Agilent Technologies). A total of 21,397,478–24,326,176 raw reads were generated for each sample. Quality control was performed using TrimGalore software; this programme uses two tools (Cutadapt and FastQC) to retain high-quality reads. Clean reads were obtained by removing reads containing adapters, reads containing poly-N and low-quality reads from raw data, and the Q20, Q30 and GC content were calculated from the clean data. Our data show that the base composition of the raw sequence data was suitable, and the ratio of the low-quality base sequence reads (<20) was very small (Table 3-1). All the downstream analyses were based on the clean, high-quality reads.

Table 3-1: quality of RNA sequencing for TF1a AML cells.

Sample name	Raw reads	Clean reads	Raw bases	Clean bases	Error rate (%)	Q20 (%)	Q30 (%)	GC content (%)
$TF1a^{cont1}$	21399879	21040745	6.4G	6.3G	0.03	97.25	92.57	49.32
$TF1a^{cont2}$	24326176	21355630	7.3G	6.4G	0.03	97.91	94.17	49.65
$TF1a^{KD1}$	21397478	21054905	6.4G	6.3G	0.03	96.87	91.85	48.73
$TF1a^{KD2}$	21861849	21476902	6.6G	6.4G	0.03	96.91	91.92	49.24

The clean reads which reflect the abundance of transcripts (gene expression) were then mapped to the human genome using STAR software from Ensembl GTF genome annotation. STAR software alignment performs precisely and accurately, positioning junction reads for RNA-seq data analysis (Dobin et al., 2013). Gene expression was quantified using featureCounts software which counts the number of reads that are aligned to each gene (Liao et al., 2014). Gene expression levels were then estimated using the FPKM method (fragments per kilobase/millions), the most common method which takes into consideration the effects of both sequencing depth and gene length on fragment counting (Garber et al., 2011). The reads distribution was then compared between different genes and between different samples, and was calculated using DESeq2 software to identify the differential gene expression (Love et al., 2014). Significant genes were defined as having fold changes > 2 and adjusted P-value (padj) < 0.05. The FPKM distribution across the TF1a and $TF1a^{KD}$ samples is shown in Figure 3-17 to visually demonstrate the expression between the two groups.

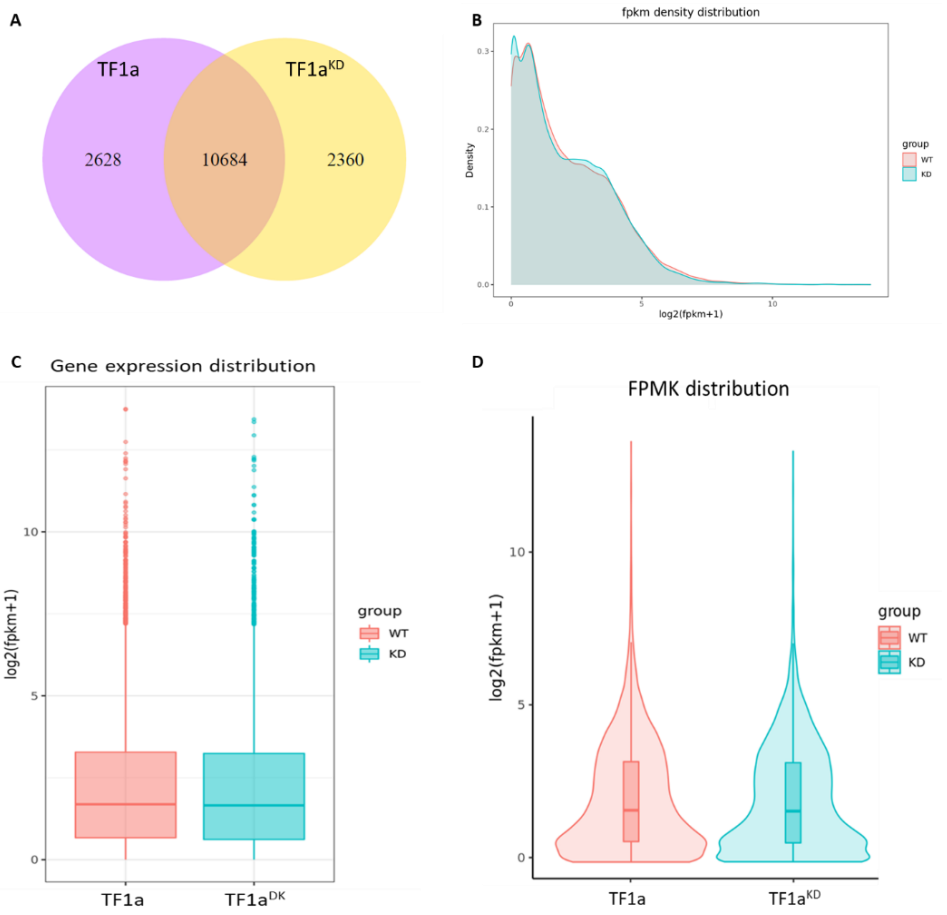


Figure 3-17: Overview of the RNA-seq data analysis in TF1a AML cells. (A) Venn diagram of the significantly differentially expressed genes in TF1^{KD} and control cells. **(B)** density distribution showing the distribution of RNA-seq read counts (FPKM) of TF1a^{GFP} (orange area) and TF1a^{KD} (blue area) samples. **(C)** Boxplot of log2 (FPKM) values within TF1a cells transcripts and **(D)** violin plots demonstrating the expression intensity distribution (FPKM) of the genes across TF1a cells transcriptome. The violin plots are coloured in orange (left) and green (right) for control cells and KD cells, respectively. FPKM indicates fragments per kilobase of transcript per million fragments mapped (Novogene analysis).

3.2.9.1 Genes differentially expressed between the TF1a and TF1a^{KD} groups

As mentioned above, DESeq2 software was used to calculate the differentially expressed genes (DEGs) between the groups. Interestingly, RNA-seq analysis indicated that 759 genes were upregulated, and 1238 genes were downregulated in the *HP1BP3* knockdown cells compared to their control cells, as shown in the volcano plot and the hierarchical clustering map (Figure 3-18). As the number of the upregulated genes is lower that the downregulated genes, might indicate the heterochromatin state in the *HP1BP3*-knockdown cells.

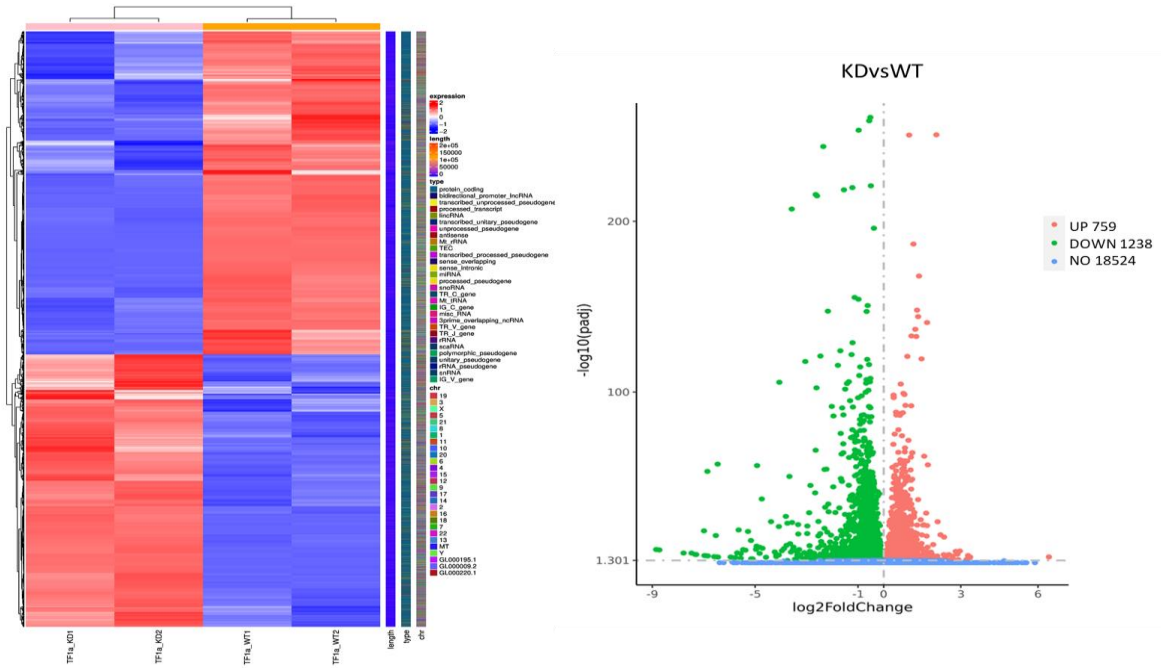


Figure 3-18: Visualization of DEGs between TF1a and TF1a^{KD} cells identified by RNA-seq analysis. Heatmap and hierarchical clustering analysis for significant changed genes **(left)**. Significant genes were selected with padj < 0.05 and fold change > 2.0. Colours on heatmap represent gene expression level, red indicates upregulation and blue denotes downregulation within the two groups. Areas of different colours represent different clusters of genes, and genes in each group share similar functions. Volcano plot **(right)**, red dots represent significant upregulated genes, green dots indicate significant downregulated genes and blue dots denote unchanged genes (Novogene analysis).

Interestingly, DEG analysis indicated that 401 genes involved in cancer were altered in the KD cells. Several important genes, including tumour-suppressor genes such as *TP53* and *FBXW7* were upregulated, while a number of proto-oncogenes, including *JUN*, *MYC*, *RAF1* and *KIT* and the cyclins and cyclin-dependent kinases were downregulated (Figure 3-19). Additionally, the HOX gene family as well as their upstream epigenetic regulators *NPM1* and *ASXL1* were also downregulated in the KD cells (Jung et al., 2015). Moreover, some chromatin modifiers were also altered in the KD cells (Figure 3-19).

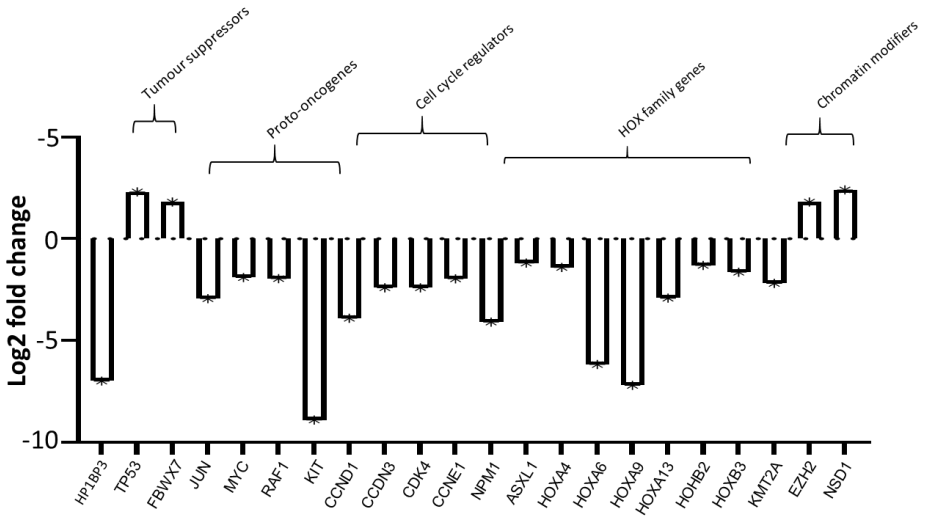


Figure 3-19: Expression patterns of twenty genes selected DEGs of TF1a^{KD} cells by RNA-Seq. The bar chart shows Log2 fold change of expression detected by RNA-Seq.

3.3 **Discussion**

Histones contain several amino acids that can be post-translationally modified; these modifications regulate the chromatin structure and therefore the cellular biological processes (Bowman and Poirier, 2015). Depending on their effect on gene expression, most post-translational modification markers are categorized as activating or repressing (Castillo et al., 2017). Histone methylation such as H3K9me is a conserved and prominent marker of heterochromatin and transcriptional repression (Saksouk et al., 2015, Monaghan et al., 2019). Meanwhile, histone acetylation is a marker of euchromatin and transcriptional activation (Eberharter and Becker, 2002). Disruption of epigenetic events such as chromatin modifiers and other non-histone cofactor molecules can lead to malignant cellular transformation by altering gene function (Baylin and Jones, 2016). In AML, several novel mutations involving genes associated with epigenetic regulation have been identified (Plass et al., 2008, Goldman et al., 2019). However, the role of non-histone proteins, which are implicated in histone regulation, is poorly understood and needs further investigation.

HP1BP3 was initially identified as a nuclear heterochromatin-associated protein that modulates the entry/exit of nucleosomal DNA via binding to HP1α (Hayashihara et al., 2010); the latter is a hallmark of heterochromatin formation and propagation (Machida et al., 2018). Here, we investigated whether the expression of HP1BP3 would impact the chromatin state through its binding to HP1α in nine AML cell lines. Initially, the expression of *HP1BP3* was examined in those cells using immunoblotting and IF. Consistent with previous reports (Hayashihara et al., 2010, Garfinkel et al.,

2015), the IF microscopy analysis showed the foci expression pattern of HP1BP3 and confirmed its nuclear expression in the AML cells (Figure 3-4). Intriguingly, the immunoblotting analysis showed differential expression levels of HP1BP3 in the AML cells. The high level of HP1BP3 was negatively correlated with the expression of H3K9me3 (heterochromatin marker) and positively correlated with the expression of H3K9ac (euchromatin marker) (Figure 3-2). This could be due to competition between HP1BP3 and the methyltransferase SUV39h for direct binding to the chromo-shadow domain of HP1α which will need further investigation.

Consequently, to gain more insight into the impact of HP1BP3 in chromatin state conversion in AML, HP1BP3 gain- and loss-of-function analyses were carried out. HP1BP3 gain-of-function confirmed that HP1BP3 is negatively correlated with the expression level of H3K9me3 and is positively correlated with the elevated H3K9ac in the MOLM13 cell line (Figure 3-9). Moreover, in line with our initial findings (Figure 3-2), the level of HP1α remained unchanged despite the forced upregulation of *HP1BP3* (Figure 3-9). However, in contrast to recent reports about HP1BP3–H3Kme3 negative correlation in alternative lengthening of telomeres (ALT) tumour cells (Shi et al., 2020), our loss-of-function analysis revealed a positive correlation between HP1BP3 and H3K9me3 (heterochromatin formation), which in turn negatively correlated with H3K9ac in the knockdown AML cells (Figure 3-10).

Moreover, *HP1BP3* expression on cell growth activity, clonogenic potential and cell cycle regulation in AML cells was evaluated using gain- and loss-of-function analysis. The CFU assay suggested that loss of *HP1BP3* impaired

clonogenicity by significantly decreasing both the size and colony numbers of MV4-11 cells (Figure 3-15); nevertheless, *HP1BP3* ectopic expression significantly induced colony size but not numbers in MOLM13 cells (Figure 4-16). Moreover, the data suggested that the accumulation of HP1BP3 mediates rapid proliferation through inducing transition from G1 to S phase (Figure 3-11 A-B & 3-12 A). However, *HP1BP3* downregulation decreased the growth activity by arresting the cells at G0 phase (Figure 3-11 C-D & 3-13 B). These findings confirm the regulation mediated by HP1BP3 as previously reported by Dutta *et al.*, that HP1BP3 regulates G1 duration (Dutta et al., 2014), and it possibly implicates chromosome organisation in mitosis (Hayashihara et al., 2010).

Furthermore, to identify the potential gene targets associated with the phenotype (stemness, proliferation and cell cycle regulation) we found in the KD cells, we carried out RNA-seq analysis. Interestingly, the RNA-seq analysis revealed that the inhibition of *HP1BP3* induced the expression of its own negative regulator *FBXW7*. Additionally, several proto-oncogenes, including *JUN* and *MYC*, and cyclins, which are substrates of FBXW7, were also downregulated (Figure 3-19). FBXW7 substrates have oncogenic function by regulating several pathways involved in cell proliferation, differentiation and apoptosis, and their accumulation leads to the acquisition of the hallmarks of cancer (Davis et al., 2014, Heo et al., 2016). *FBXW7* mutations are identified in many primary human tumours with an overall mutation frequency of around 6%. However, the mutation rate considerably differs among tumour types, from 35% in cholangiocarcinoma and 30% T-cell acute lymphoblastic leukaemia (T-ALL) to 15-20% in colorectal cancer

(Yeh et al., 2018). Intriguingly, the lack of *HP1BP3* upregulated the most studied tumour suppressor: *p53* (3-fold) (Rozan and El-Deiry, 2007, Olivier et al., 2010). Activation of TP53 supresses growth by inducing cell cycle arrest or apoptosis (Shaw, 1996, Fridman and Lowe, 2003). The tumour-suppressive activity of TP53 is through transcriptional regulation of the target genes that regulate many cellular processes, such as cell cycle progression and cell death (Rozan and El-Deiry, 2007, Fischer, 2017), which could explain the HP1BP3^{KD} phenotype. P53 mutation is frequently identified in patients with AML (Kindle et al., 2005), they have been reported in 7% of 500 cases with *de novo* AML and 58.8% of cases with complex karyotype (Hou et al., 2015). Moreover, p53 mutations are related to adverse effects to chemotherapy in patients with AML (Licht and Sternberg, 2005).

Although we did not complete the enrichment pathway analysis due to time limitations, the TP53 pathway was one of the pathways enriched as a consequence of *HP1BP3* downregulation. Moreover, the lack of *HP1BP3* drastically lowered the expression of *HOXA9,* a key oncogene involved in leukemogenesis (Abramovich and Humphries, 2005), and of other members of the HOX gene family with oncogenic activity, including *HOXB3–6* (Abramovich and Humphries, 2005, Fischbach et al., 2005, Harris Hazan-Haley et al., 2011) (Figure 3-19). The downregulation of the HOX genes could be due to the downregulation in their upstream epigenetic regulators *NPM1* and *ASXL1* (Abdel-Wahab et al., 2012, Jung et al., 2015) (Figure 3-19). However, further analysis such as chromatin immunoprecipitation sequencing (ChIP-seq) would be needed to evaluate the specificity of HP1BP3.

CHAPTER 4

HP1BP3 induction of AML activity, possibly mediated through miRNA regulation

4.1 **Brief introduction**

MicroRNAs (miRNAs) are a class of small conserved non-coding transcripts with an average length of 21–23 nucleotides and that are involved in the regulation of gene expression (Wahid et al., 2010). miRNAs are transcribed from DNA sequences by RNA polymerase II and III to generate primary miRNAs (pri-miRNAs) that undergo several cleavages to form precursor miRNAs (pre-miRNAs) and finally mature miRNAs (Borchert et al., 2006, MacFarlane and R Murphy, 2010, Wahid et al., 2010). Pri-miRNA is typically a large transcript that forms a stem-loop structure, also known as the hairpin structure. The hairpin is cleaved off by the microprocessor machinery, RNase III enzyme Drosha and DGCR8 (double-stranded RNA-binding protein) complex to form pre-miRNA containing ~60–100 nt (Beezhold, Castranova et al. 2010) (Figure 4-1). Pre-miRNA translocate

s from the nucleus to the cytoplasm in an exportin 5-dependent manner (Bartel, 2004) to be further processed by a second RNase III enzyme Dicer into ~22-nt miRNA (Bartel, 2004, Beezhold et al., 2010). Increasing evidence has suggested that miRNA biogenesis can occur co-transcriptionally (Kim and Kim, 2007, Morlando et al., 2008). Most pri-miRNAs are located in the intronic regions of other protein-coding transcripts and are processed as a part of their hosting gene before splicing (Kim and Kim, 2007). Intriguingly, cleavage of pri-miRNAs by the Drosha–DGCR8 complex during transcription occurs on both intronic and independently transcribed miRNAs (Morlando et al., 2008, Ballarino et al., 2009).

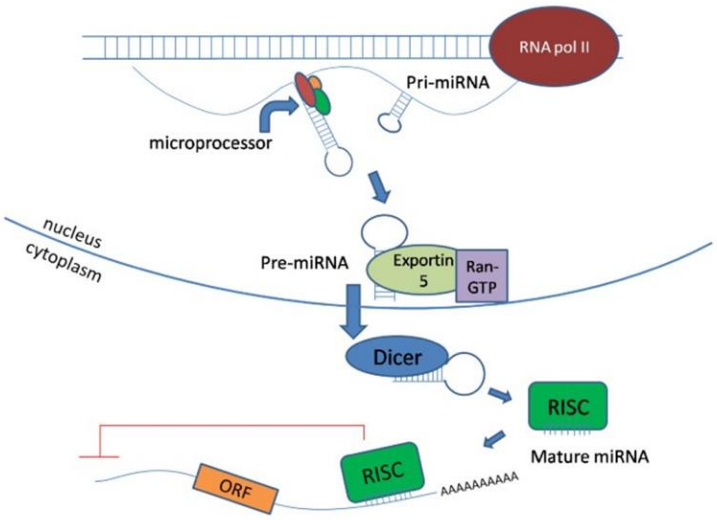


Figure 4-1: miRNA biogenesis. In the nucleus, the pri-miRNA transcript is transcribed by RNA polymerase II. The hairpin structure is cleaved by the microprocessor to generate pre-miRNA which then exported to the cytoplasm by exportin5 in a ran-GTP dependent manner. The pre-miRNA is processed in the cytoplasm by Dicer to generate mature miRNA. [Adapted from (Bartel, 2004)].

However, the molecular mechanisms of the co-transcription, intronic miRNA processing and the role of chromatin-binding protein regulation are poorly understood. Recently, a chromatin immunoprecipitation (ChIP) analysis revealed that HP1BP3 co-localizes with the microprocessor Drosha across the genome and facilitates miRNA biosynthesis (Liu et al., 2016). Moreover, it revealed that HP1BP3 enhances co-transcriptional miRNA processing through chromatin retention by binding to the nascent transcribed pri-miRNAs (Liu et al., 2016). Dysregulation of miRNA transcription due to genetic mutations or epigenetic alterations leads to dysregulated miRNA biogenesis machinery which affects the hallmarks of cancer (Peng and Croce, 2016).

miRNAs are strongly dysregulated in AML, they participate in AML pathogenesis through different mechanisms including copy number changes, proximity to oncogenes and epigenetic alterations (Wallace and O'Connell, 2017). It is well-established in AML that miRNAs can act as either onco-miRNAs or tumour suppressors by controlling a wide range of cellular processes including proliferation, survival, epigenetic changes and drug response. Moreover, distinctive miRNA profiles in AML highlighted the importance of miRNAs in the disease progression (Dixon-McIver et al., 2008, Li et al., 2008, De Leeuw et al., 2016) as well as leukemic stem cell (LSC) quiescence, self-renewal and chemotherapy response (Lechman et al., 2016). However, only ~100 miRNAs are differently expressed in AML compared to normal/background level (Starczynowski et al., 2011, Wallace and O'Connell, 2017), indicating that only a subset of miRNAs has a critical impact on AML pathogenesis and LSC properties. Therefore, understanding the role of HP1BP3 in miRNA expression regulation through chromatin remodelling could be a possible potential target for AML and LSCs.

In the previous chapter, we demonstrated that HP1BP3 modulates the heterochromatin/euchromatin state through altering the expression of H3K9me3/H3K9ac in AML cells. Our gain- and loss-of-function analysis revealed that HP1BP3 regulates proliferation and cell cycle progression. Moreover, our transcriptomic analysis showed that HP1BP3 is associated in regulating the expression of key oncogenes involved in leukemogenesis.

In this chapter, we examined the mechanism of HP1BP3 in miRNA regulation in AML using small RNA sequencing (sRNA-seq) analysis. Here,

we demonstrate that the loss of *HP1BP3* drastically downregulated miRNAs highly expressed in LSCs.

4.2 RESULTS

4.2.1 HP1BP3 may play a key role in AML-miRNA regulation

To understand the role of HP1BP3 in AML and to identify possible potential targeting of LSCs through miRNA regulation, we initially performed a small bioinformatic analysis using three published reports (Figure 4-2). To outline, Liu *et al.* have reported that HP1BP3 promotes miRNA biogenesis in HeLa cells (Liu, Liang et al. 2016). On the other hand, de Leeuw *et al*. have reported that miRNAs are differentially expressed in leukemic stem ($CD34^+/CD38^-$) cells and leukemic progenitor ($CD34^+/CD38^+$) cells (de Leeuw et al., 2014), and Lechman *et al*. showed that miRNAs are differentially expressed in LSCs and HSCs in patients with AML (Lechman et al., 2016). Hence, we compared the HP1BP3–miRNA data with miRNAs that are differentially expressed between LSCs, LPs and HSCs in patients with AML (Figure 4-2).

Interestingly, based on these data, around 60% of dysregulated LSC–miRNAs (Lechman et al., 2016) are associated with altered expression of HP1BP3 in human cells, as reported by Liu et al. (Liu et al., 2016). And 70.4% of the miRNAs that differentially expressed between LSCs and HSCs (de Leeuw et al., 2014) were also associated with the downregulation of HP1BP3 in HeLa cells (Liu et al., 2016). Excitingly, we have found three common miRNAs between these reports that are highly expressed in LSCs but not in HSCs. These three common miRNAs are human miR-126, miR-22 and miR-21. Both miR-22 and miR-21 are well studied and known as

onco-miRNAs in solid tumour and haematological malignancies (Feng and Tsao, 2016, Sekar et al., 2016, Jafarzadeh-Samani et al., 2017). miR-126 increases LSC and LP survival and self-renewal, and blocks differentiation (Lechman et al., 2016). The potential therapeutic value of these miRNAs is currently under investigation by several laboratories (Hanna et al., 2019, Zhang et al., 2019). Therefore, we initially aimed to investigate the expression of these three miRNAs as well as other miRNAs reported in the above three studies that we selected and compared (Figure 4-2).

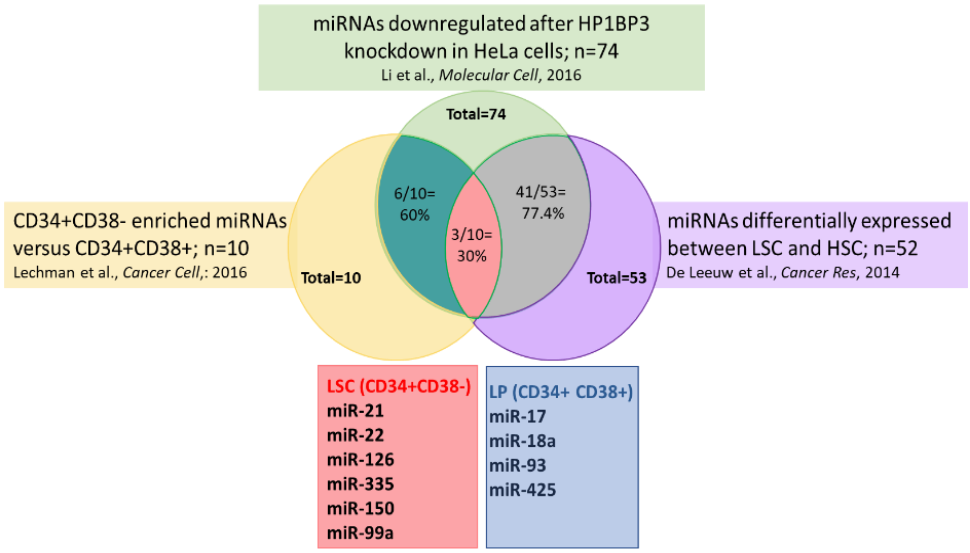


Figure 4-2: HP1BP3-mediated regulation of miRNAs might be linked to HSCs and LSCs. Venn Diagram represents a comparison analysis of three selected published reports (de Leeuw et al., 2014, Lechman et al., 2016, Liu et al., 2016). Around 60-77.4% of dysregulated LSC-miRNAs and not HSC-miRNAs are associated with altered expression of HP1BP3 in HeLa cells. Red and blue boxes show the selected miRNAs from the three compared reports.

4.2.2 Knockdown of HP1BP3 decreases the number of $CD34^+/CD38^-$ and $CD34^+/CD38^+$ cell populations in AML cell lines

LSCs are a low-frequency subpopulation of cells that have the ability to self-renewal, drug resistance and cancer recurrence (Hanekamp et al., 2017). In AML, the $CD34^+/CD38^-$ cell population represents the most relevant LSCs due to their ability to engraft and initiate AML when transplanted into immune-compromised mouse models (Lapidot et al., 1994, Bonnet and Dick, 1997). Moreover, other studies have suggested the complex heterogeneity of LSC phenotypes and other subpopulations, including $CD34^+/CD38^+$, $CD34^-$ and CD123+ cells, can also initiate AML (Taussig et al., 2008, Jin, Lee et al. 2009, Taussig et al., 2010, Eppert et al., 2011). However, the expression of cell surface markers is not enough to define the stem cell nature of sub populations of cells and a reconstitution method should be used to confirm that nature (Lapidot et al., 1994, Bonnet and Dick, 1997).

As outlined above, knockdown (KD) of *HP1BP3* changed the expression of miRNAs highly expressed in two of those subpopulations ($CD34^+/CD38^-$) and ($CD34^+/CD38^+$) (Figure 4-2). We, therefore, investigated whether knockdown of *HP1BP3* would affect the existence of the two fractions in our *HP1BP3* knockdown AML cell lines.

To test that, $TF1a^{KD}$ and $MV4\text{-}11^{KD}$ and their respective paired control cells $TF1a^{GFP}$ and $MV4\text{-}11^{GFP}$ were used in this experiment. Those two cell lines i.e., TF1a and MV4-11 were used in this experiment because they express CD34. The cells were fixed and stained with anti-CD34 and anti-CD38

antibodies and analysed with FACS. The CD34l/CD38 quadrant was set using conjugated isotype-matched controls (*Chapter 2*). Our data show that knockdown of *HP1BP3* significantly reduced the number of $CD34^{+}/CD38^{-}$ and $CD34^{+}/CD38^{+}$ subpopulations in the two AML cell lines (Figure 4-3 A-F). The percentage of $CD34^{+}/CD38^{-}$ cells was decreased from 0.43% to 0.002% in $MV4\text{-}11^{KD}$ cells compared to $MV4\text{-}11^{GFP}$ cells and from 23.2% to 11.8% in $TF1a^{KD}$ cells compared to $TF1a^{GFP}$ cells (Figure 4-3 B, E).

Moreover, the percentage of the $CD34^{+}/CD38^{+}$ fraction was reduced from 14.9% to 0.48% in $MV4\text{-}11^{KD}$ cells compared to $MV4\text{-}11^{GFP}$ cells and from 0.08% to 0.02% in $TF1a^{KD}$ cells compared to $TF1a^{GFP}$ cells (Figure 4-3 C, F). These data suggest that *HP1BP3* knockdown impacts negatively LSC frequency, possibly through miRNA regulation.

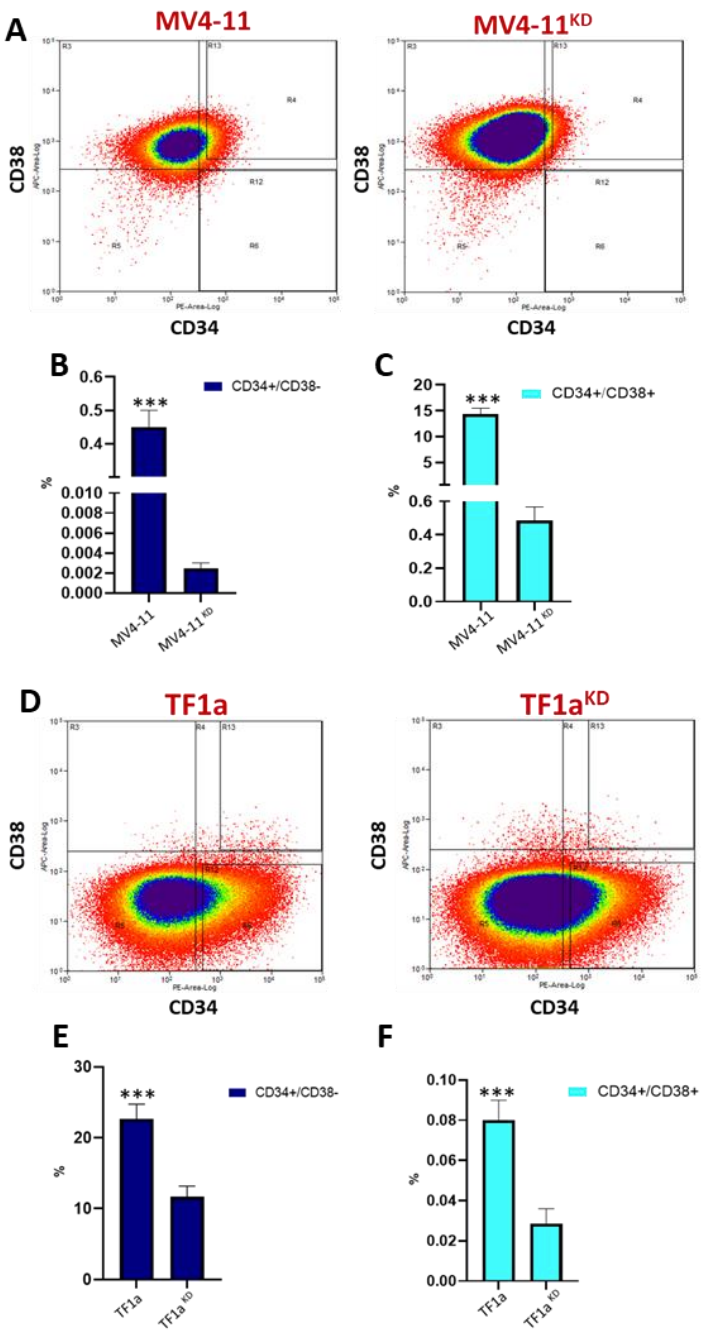


Figure 4-3: *HP1BP3*-knockdown reduces the number of (CD34$^+$/CD38$^-$) and (CD34$^+$/CD38$^+$) fractions in AML cell lines. FACS analysis for CD34 and CD38 expression in MV4-11^{KD}, MV4-11^{GFP} cells **(A)**, TF1a^{KD} and TF1a^{GFP} cells **(D)**. Statistical analysis **(B-C, E-F)**, histograms indicate a significant reduction in the number of (CD34$^+$/CD38$^-$) in MV4-11 **(B)** and TF1a **(E)** cells compared to their control cells and in (CD34$^+$/CD38$^+$) subpopulation **(C, F)** as a result of HP1BP3 downregulation. Statistical test: Two-tailed unpaired t-test (n=-3; ***p<0.001). The error bars show the SD of three biological repeats.

4.2.3 Inhibition of HP1BP3 expression changes the expression level of miRNAs in the TF1a AML cell line

As mentioned above, HP1BP3 is involved in miRNA biogenesis in human HeLa cells (Liu et al., 2016). Hence, we investigated whether the alteration of *HP1BP3* expression plays a role in the miRNA expression level in AML cells. To examine that, $TF1a^{KD}$ cells and $TF1a^{GFP}$ control cells were seeded, and total RNA was isolated using TRI Reagent (*Chapter 2*). Reverse transcription and cDNA synthesis were performed using miRNA-specific miScript II RT Kit (Qiagen), which utilizes miRNAs as starting material for the reverse transcription (*Chapter 2*). Next, the expression level of miR-21, miR-22, miR-126, miR-335, miR-18a and miR-425 was tested using a specific miScript SYBR® Green kit for qRT-PCR (Qiagen).

Our data show that *HP1BP3* knockdown significantly reduced the expression level of miR-21, miR-22, miR-335 and miR-425 (Figure 4-4); however, miR-18a was undetectable and the miR-126 level remained unchanged. These data suggest that *HP1BP3* is involved in the regulation of miRNA expression in AML. Additionally, it prompted us to explore more miRNAs regulated by *HP1BP3* using sRNA-seq analysis.

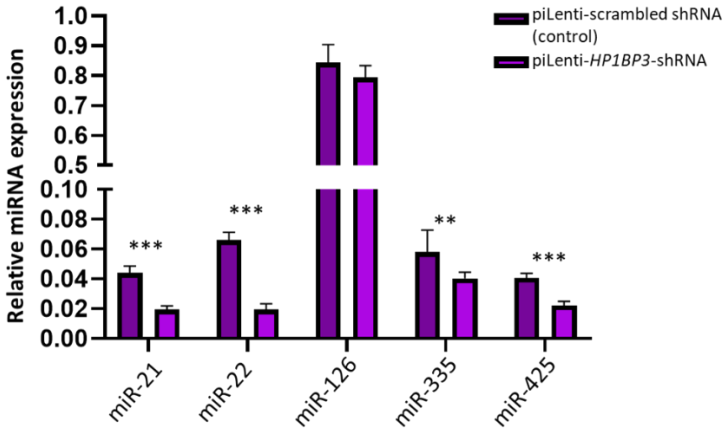


Figure 4-4: HP1BP3 downregulation alters the expression of miRNAs in TF1a AML cells. The expression level of miR-21, miR-22, miR-126, miR-335 and miR-425 was analysed by qRT-PCR. Data indicate a significant reduction in miR-21, miR-22, miR-335 and miR-425 after HP1BP3 knockdown while the expression level of miR-126 remained unchanged. The error bars show the SD of three biological repeats (*P= 0.01 to 0.05, **p= 0.001 to 0.01, ***p<0.001) (n=3).

4.2.4 sRNA sequencing analysis to identify differential miRNA expression in TF1a^{KD} AML cells

To gain further insight into the regulation of miRNA expression by HP1BP3 that led to the changes in the miRNA levels observed above, we carried out sRNA-seq. In order to identify the HP1BP3 miRNA targets, sRNA-seq was performed with total RNA from TF1a^{KD} cells and their control TF1a^{GFP} cells.

Total RNA was isolated and RNA purity was tested using a NanoPhotometer® spectrophotometer, and 4 µg/sample was shipped to Novogene (Cambridge, UK) for sRNA-seq analysis. Prior to the library preparation, RNA degradation and contamination were examined on 1% agarose gels. RNA integrity and quantitation were assessed using an Agilent

RNA 6000 Nano Kit for the Agilent Bioanalyzer 2100 system (Agilent Technologies). A total amount of 3 μg RNA/sample was used as input material for the sRNA library using NEBNext® Multiplex Small RNA Library Prep Set for Illumina®. Approximately 13,838,251–15,979,970 reads were generated from the Illumina sequencing for each sample. Raw reads in FASTQ format were first processed through custom Perl and Python scripts. Clean reads were produced by removing reads containing adapters, reads containing poly-N and low-quality reads from raw data, and the Q20, Q30 and GC content were calculated from the clean data. The analysed data showed that the base composition of the raw sequence data was suitable, and the ratio of the low-quality base sequence reads (<20) was very small. All downstream analyses were based on high-quality clean reads. The sRNA tags were mapped to reference sequences using Bowtie software (Langmead et al., 2009) to analyse their expression and distribution on the reference without any mismatch. Mapped sRNA tags were used to identify known miRNAs using miRBase 20.0 as the reference and modified miRDeep2 software (Friedländer et al., 2012). sRNAs, including small nuclear RNA (snRNA), transfer RNAs (tRNAs), ribosomal RNA (rRNA), small nucleolar RNA (snoRNA) and miRNA (Großhans and Filipowicz, 2008) tags, were then aligned to RepeatMasker and the Rfam database to remove tags originating from protein-coding genes.

The composition of the sRNAs in the TF1a^{GFP} and TF1a^{KD} cells was filtered according to their length (miRNA is 21–22 nt, small interfering RNA (siRNA) is 24 nt, and Piwi-associated RNA (piRNA) is 28–30 nt) (Figure 4-5).

Following miRNA alignment, miRNA expression levels were estimated by TPM (transcript per million) using a normalization formula (normalized expression = mapped read count/total reads × 1,000,000) (Zhou et al., 2010). Figure 4-6 shows the TPM distribution, and the TPM density distribution between all samples analysed.

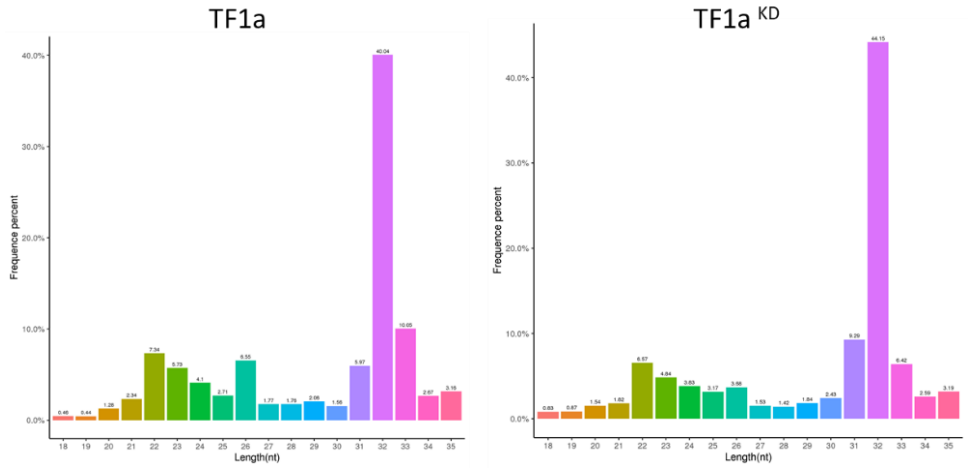


Figure 4-5: Sequence length distribution in TF1a and TF1^{KD} cells. sRNA-seq data shows that the small RNA (18nt- 30nt) composition was slightly changed in KD cells compared to control cells. The abscissa represents the length of the sRNA, and the ordinate shows the abundance of the sRNA (Novogene analysis).

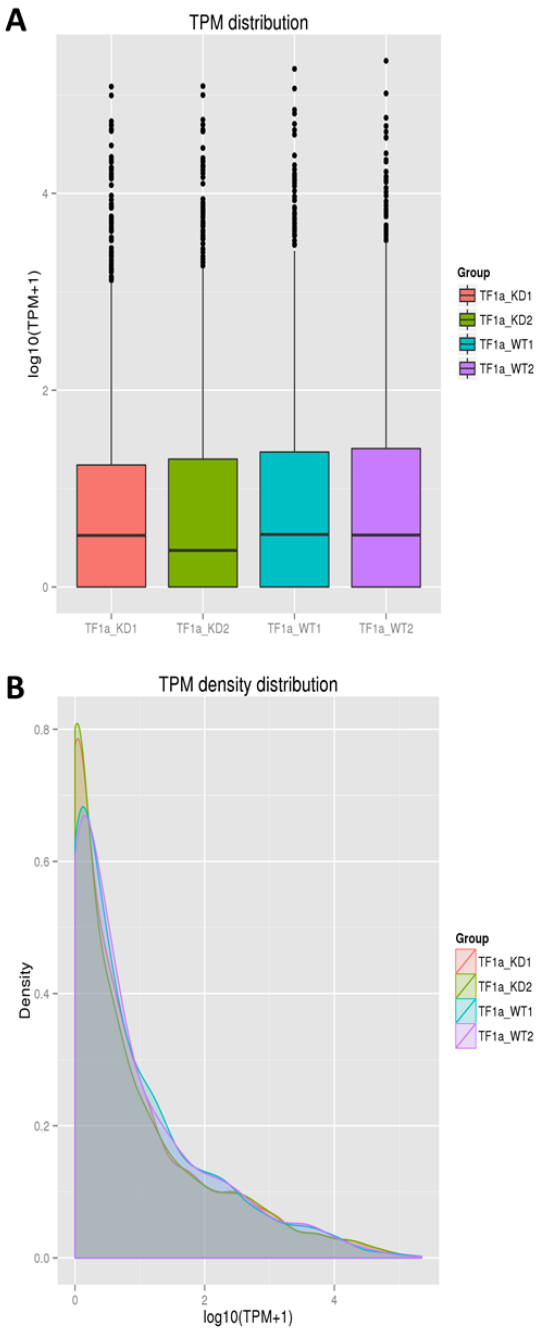


Figure 4-6: TPM distribution in TF1a cells. Boxplot of sRNAs expression amount transcript per million (TPM) **(A)** and density distribution map **(B)** in TF1a and TF1a^{KD} AML cells (Novogene analysis).

4.2.4.1 Differentially expressed miRNAs in TF1a^{KD} cells

Differential expression analysis was performed using DESeq2 (Varet et al., 2016) and a corrected P-value of 0.05 was set as the threshold for significantly differential expression (Storey, 2003). Interestingly, our data identified that 261 significant mature miRNAs, including known AML functionally essential miRNAs, were differentially expressed: 124 miRNAs were upregulated and 137 were downregulated, as shown in the volcano plot following *HP1BP3* knockdown in the TF1a cells (Figure 4-7 A) and as clustered into a heatmap (Figure 4-7 B).

For example, miR-21, miR-22, miR-27a, miR-99, miR-182-5p and miR-149-5p were downregulated, and miR-135a, Let-7c and miR-146a were upregulated in *HP1BP3*-knockdown compared to control TF1a AML cells (Table 4-1). Following miRNAs analysis, miR-150, miR-17, miR-18, miR-21, miR-93 and miR-99a were selected for validation (Figure 4-7 B). The qRT-PCR analysis shows the validity of the sRNA-seq analysis (Figure 4-7 A-B).

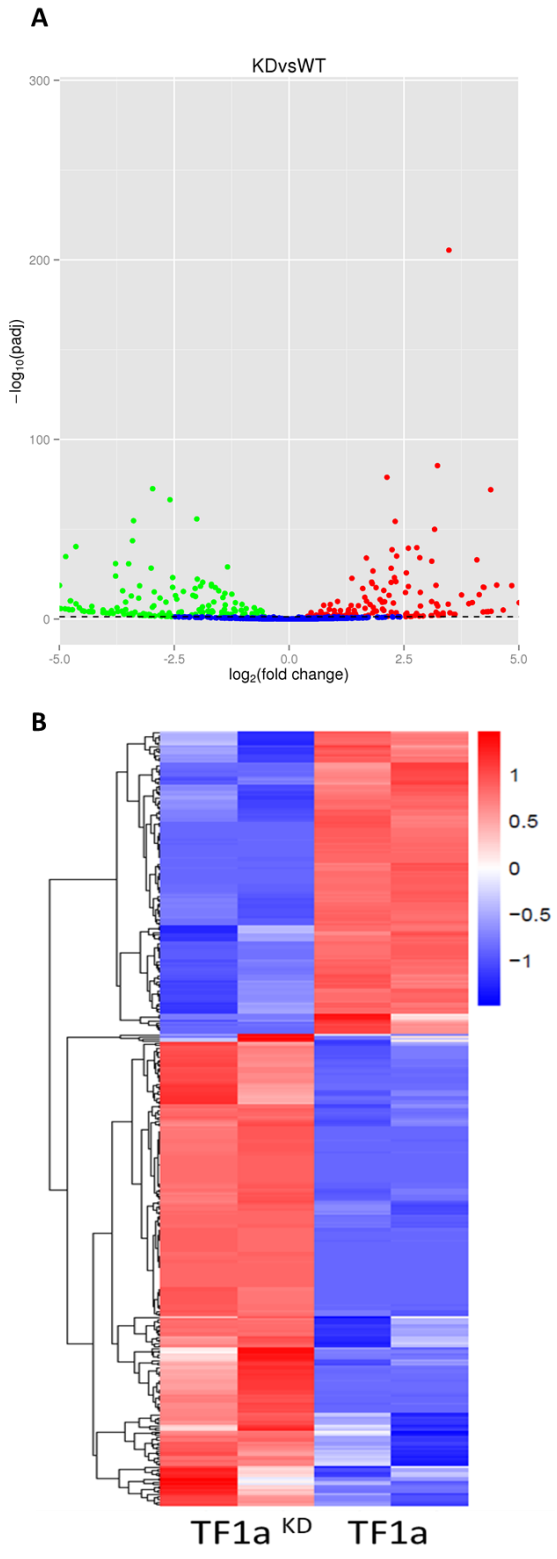


Figure 4-7: Analysis of differentially expressed miRNAs between TF1aKD and TF1a cells. Volcanic map of differentially expressed miRNAs **(A)**. The X-axis indicates the fold change in expression of miRNAs in TF1a and TF1a^{KD} and the Y-axis represents the statistically significant change in the expression (Blue dots represent no significant differences, red dots show significantly up-regulated and green dots for significant down-regulated

miRNAs). Hierarchical clustering analysis of differentially expressed miRNAs **(B)** red indicates high miRNA expression and blue indicates low miRNA expression (Novogene analysis).

Table 4-1: Differentially expressed miRNAs in TF1a^{KD} cells and their function in AML

miRNA	Function	Target	Ref.
Downregulated miRNAs			
miR-21	Onco-miRNA miR-21 downregulation inhibits AML proliferation and induces G1 arrest and apoptosis	*PTEN–AKT* Pathway	(Bai et al., 2011)
miR-22	Onco-miRNA Promotes HSC self-renewal and transformation	*TET2*	(Song et al., 2013)
miR-29b	Increases cell proliferation and AML progression Increases DNA methylation/hypermethylation	*AKT2* *CCND2* *DNMT3A, DNMT3B* *DNMT1*	(Blum et al., 2010) (Liu et al., 2010)
miR-125b	Onco-miRNA Uncontrolled formation of myeloid cells Induces tumorigenesis in myeloid progenitors leading to myeloid leukaemia	*LIN28A* *IRF4*	(Chaudhuri et al., 2012) (So-Sookram et al., 2014)
miR-126	Antiapoptotic Increases LSC and LP survival, self-renewal and maintenance	*PLK2* *ADAM9, ILK, GOLPH3, CDK3, TOM1*	(Dorrance et al., 2015) (Lechman et al., 2016)
miR-144-3p	Antiapoptotic	*NRF2*	(Sun et al., 2017)
miR-149-5p	Antiapoptotic	*FASLG*	(Tian and Yan, 2016)
miR-150	Onco-miRNA Increases proliferation and clonogenicity Exosomal miRNA in AML	*c-MYB* *NANOG*	(Hornick et al., 2016)
miR-17	Induces undifferentiated myeloid proliferation	*CBF*	(Fischer et al., 2015)
miR-182-5p	Stimulates cell proliferation and is related to drug resistance	*BCL2L12* *BCL2*	(Zhang et al., 2018)
miR-183	Upregulates *HIF1A* through *IDH2*	*HIF1A* *IDH2*	(Tanaka et al., 2013)
miR-9	Leukemic cells expressing miR-9 have more immature blasts	*RHOH* *RYBP*	(Senyuk et al., 2013)

	miR-9 knockdown suppresses AML proliferation by arresting cells at G0	*Hes1*	(Fu et al., 2017)
miR-99a	High expression of miR-99a is more dangerous than the known mutations and could predict worse outcome in patients with AML Blocks differentiation, increases cell proliferation and colony formation	*SMARCA5* *HS2ST3* *HOXA1*	(Si et al., 2016) (Khalaj et al., 2017)
miR-486	Promotes proliferation and suppresses apoptosis	*JAK–STAT*	(Sha et al., 2020)
Upregulated miRNAs			
miR-135a	Overexpression inhibits: proliferation and cell cycle and increases apoptosis	*HOXA10*	(Xu and Wen, 2018)
miR-146a	Knockout leads to myeloid and lymphoid malignancies in mice Deletion leads to myeloproliferation in mice	*IRAK1*	(Magilnick et al., 2017)
miR-27	Increases sensitivity to chemotherapy in AML cells	NA	(Feng et al., 2011)
miR-339-5p	Upregulation inhibits proliferation of AML cells	*SOX4*	(Sun et al., 2018)
Let-7c	Increases granulocytic differentiation	*PBX2*	(Pelosi et al., 2013)
Let-7b	Tumour-suppressive activity	*LIN28*	(Roos et al., 2018)
miR-497	Inhibits proliferation by targeting the MAPK–ERK pathway and eventually RAF1	*MAPK/ERK*	(Zheng Radziszewska et al., 2012)
miR-193b	Inhibits growth	*c-KIT* *CCND1*	(Bhayadia et al., 2018)
miR-34	Tumour suppressor	*MYC* Other oncogenes	(Yang et al., 2017)

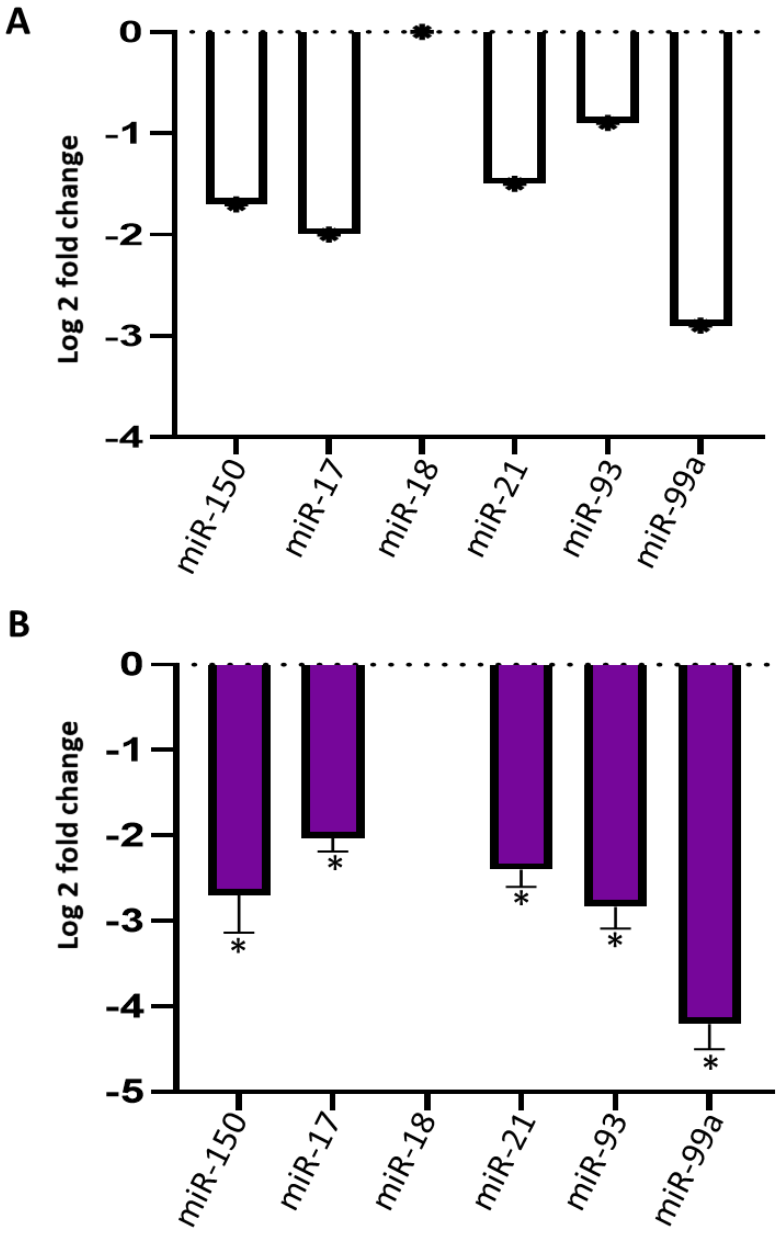
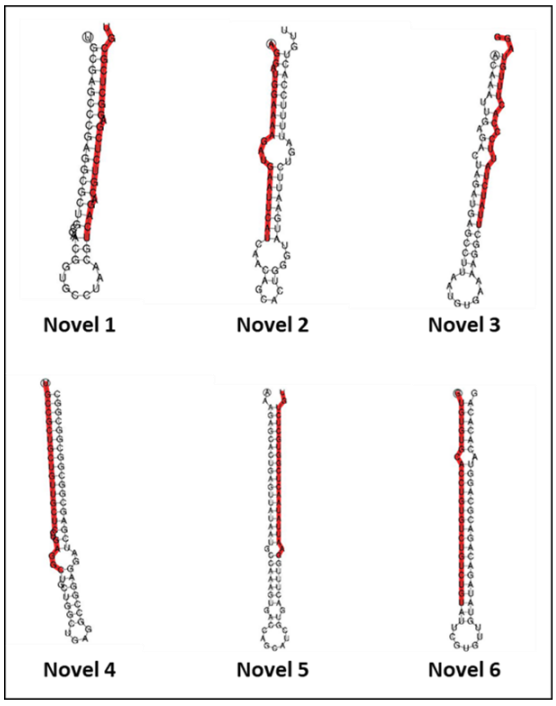


Figure 4-8: Expression patterns and qRT-PCR validation analysis of miRNAs differentially expressed in TF1a^{KD} cells by sRNA-Seq. The bar chart shows Log2 fold change of miR-150, miR-17, miR-18, miR-21, miR-93 and miR-99a expression detected by sRNA-Seq analysis (n=2; *q<0.05). **(B)** qRT-PCR showing the mRNA expression of miR-150, miR-17, miR-18, miR-21, miR-93 and miR-99a in TF1^{KD} and their paired control cells. Statistical test: Two-tailed unpaired t-test (n=3; * p<0.05). The error bars indicate the SD of three biological repeats.

4.2.4.2 Predicted novel uncharacterised miRNAs in TF1a cells

Our sRNA-seq analysis detected 31 functionally uncharacterized novel miRNAs among the known differentiated miRNAs using two software: miREvo (Wen et al., 2012) and miRDeep2 (Friedländer et al., 2012). They were predicted based on the characteristics of the hairpin structure of pre-miRNA and quantified using custom scripts. Figure 4-9 shows structural plot examples of the novel miRNAs and the altered expression.



>novel_1	ucagacgucucgaggcucgcgu
>novel_10	cacaccaccguguccaccauua
>novel_11	ucccuguccuccaggagcucacc
>novel_12	acaugcgcccucggcuucuggc
>novel_14	uguggcaccgaggcagcucucugc
>novel_15	ggaauaacggggugcuguaggcuuu
>novel_16	uggaggguguuucugagacagugu
>novel_17	gcaugcacgaggcccugggu
>novel_2	aggauggaaaagaugaauucau
>novel_20	gcuuguugugauuccuccauuuu
>novel_22	ucggucccuaaccccccuccgga
>novel_23	ccgcucucagccucucaucugug
>novel_24	ccccacugcuaaauuugacuggcuu
>novel_25	uccccaguacccccacca
>novel_26	uagacuuggcugugucu
>novel_27	uggcuucuuuagcacggacauggu
>novel_28	aacaggccuugcucugcucacaga
>novel_29	ucccagcugcucgaccucuugcgua
>novel_3	uuaucuauucccacuuuguagg
>novel_30	ucuauuucuuguguucccugc
>novel_31	uccgcgcugcgugggcugag
>novel_4	ugccgcugcuguugcuccugaggc
>novel_5	gaauuauaacucggugcucugu
>novel_6	gugugugcaccugugucugucugu
>novel_7	ucacccggggugugcucgacu
>novel_8	ccuccugcccuccuugcuguaga

Figure 4-9: Predicted novel miRNAs structures and sequence in TF1a cells. Predicted novel pre-miRNAs structures **(left)**, red coloured sequences represent mature miRNAs on the precursor arm. Predicted novel miRNA sequence **(right)**, green sequences represent downregulated miRNAs, black indicate unchanged expression and red represent upregulated miRNAs in KD cells compared to control cells (Novogene analysis).

4.2.5 *HP1BP3* downregulation does not change the expression of Drosha

As mentioned above, using a combination of ChIP-seq and ChIP analyses, Liu et al. reported co-localization between HP1BP3 and Drosha (Liu et al., 2016). Therefore, to identify whether HP1BP3 is involved in miRNA processing through regulation of the microprocessor machinery (Drosha in the nucleus and Dicer in the cytoplasm), we examined the expression of both enzymes, i.e. Drosha and Dicer, in *HP1BP3* knockdown AML cells. To test that, $TF1a^{KD}$ and MV4-11^{KD} cells and their respective paired controls $TF1a^{GFP}$ and MV4-11^{GFP} cells were used in this experiment. Total protein and total RNA were extracted using protein lysis buffer and TRI Reagent respectively (*Chapter 2*). The protein lysates were assayed for the expression of Drosha, and β-actin was used as a loading control. The data showed that the expression of Drosha did not change in the KD cells (Figure 4-10).

Moreover, the mRNA expression of both Drosha and Dicer was tested using qRT-PCR. The mRNA levels of both enzymes were unchanged in the *HP1BP3* knockdown cells. These data suggest the specific and selective role of HP1BP3 in miRNA expression regulation and that it was not due to altered expression in the microprocessor machinery enzymes.

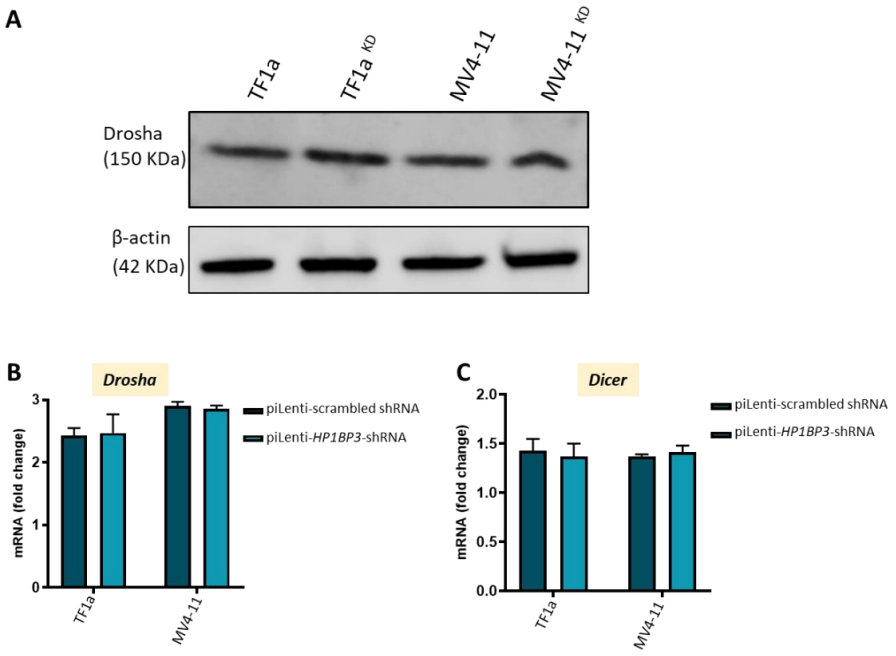


Figure 4-10: HP1BP3 inhibition doesn't change the expression of microprocessors. **(A)** Western blotting analysis were performed in TF1a and MV4-11 AML cell lines stably expressing sh*HP1BP3* or GFP. 100 µg of total protein extracts were run on 4-20 % SDS-PAGE, transferred to PVDF membranes and immunoblotted for anti-Drosha and anti-β-actin as a loading control. Data indicate no change in the expression of Drosha level in the KD cells compared to control cells. **(B-C)** mRNA expression level of Drosha and Dicer in AML cell lines. Data demonstrate no change in the mRNA expression level of microprocessor Drosha and Dicer. mRNA expression was analysed by qRT-PCR; data were normalized to β-actin. The error bars show the SD of three biological repeats.

4.3 **Discussion**

The discovery of miRNAs has increased our knowledge about many human diseases, including cancer. Many laboratories around the world have shown the implication of miRNAs in different types of cancer since the discovery of genetic mutations in miR-15a and miR-16-1 in chronic lymphocytic leukaemia (CLL) (Calin et al., 2002). miRNAs are strongly dysregulated in solid tumour and haematological malignancies, including AML (Peng and Croce, 2016). miRNAs are now broadly considered as having a crucial role in the pathogenesis of AML (Wallace and O'Connell, 2017). Such dysregulation could happen due to various causes, including mutations in the miRNA genes, aberrant transcription of the miRNA genes, dysregulation in the miRNA biogenesis machinery and disordered epigenetic changes (Wallace and O'Connell, 2017).

Abnormal expression of miRNAs in cancer cells allows the cells to sustain growth and proliferation, resist chemotherapy and escape apoptosis (Peng and Croce, 2016). Although miRNAs have several targets, their role in cancer could be due to the regulation of a few specific targets (Si et al., 2019). However, various mechanisms and complexities in miRNA biology remain unclear; therefore, understanding the regulation of their expression will substantially improve our understanding of how miRNAs function and identify critical targeting in cancer. Here, we demonstrate a new aspect of miRNA regulation through the chromatin-binding protein HP1BP3 to shed additional light on how AML cells and LSCs are epigenetically regulated.

We demonstrated in *Chapter 3* how the expression of HP1BP3 alters the chromatin state by diminishing the methylation of H3K9 and increasing the

acetylation of the same lysine site. Moreover, our RNA-seq data showed that several DEGs associated with leukemogenesis were downregulated in the KD cells compared to control cells. Additionally, another study conducted on HP1BP3 revealed that HP1BP3 binds to nascent pri-miRNA transcripts and the microprocessor Drosha–DGCR8 complex in human cells (Liu et al., 2016). Taking these findings together, we hypothesized that HP1BP3 could regulate miRNA expression in AML cells.

To test that, we initially performed a small-scale bioinformatic analysis based on available reports. We compared the miRNAs altered after *HP1BP3* inhibition with two more studies that compared a subset of miRNAs differentially expressed in HSCs and LSCs in patients with AML (Figure 4-2). Our qRT-PCR analysis showed that knockdown of *HP1BP3* downregulated two well-studied onco-miRNAs: miR-21 (Feng and Tsao, 2016) and miR-22 (Jafarzadeh-Samani et al., 2017). Furthermore, it significantly decreased the expression of two miRNAs involved in chemo-response in patients with AML, miR-335 and miR-425 (Yingchun et al., 2015) (Figure 4-3).

The alteration in the expression of the selected miRNAs in the KD cells prompted us to further identify the differentially expressed miRNAs using sRNA-seq analysis. The sRNA-seq data revealed that several miRNAs involved in leukemogenesis or highly expressed in LSCs were downregulated in the KD cells compared to their paired control cells, and included onco-miRNAs, and miRNAs associated with cell proliferation and cell cycle regulation (Table 4-1). Moreover, many miRNAs with tumour-suppressive function such as the let-7 family and miR-34 family were

upregulated. The expression of six miRNAs: miR-150, miR-17, miR-18, miR-21, miR-93 and miR-99a confirms the data obtained from the sRNA-seq analysis (Figure 4-8). miR-150 is one of the exosomal miRNA with oncogenic activity that suppresses haematopoiesis in AML by targeting *c-MYB* (Hornick et al., 2016), which was downregulated in the RNA-seq analysis. Fischer et al., reported that miR-17 upregulation induced proliferation of undifferentiated myeloid cells in both human U937 and mouse 32D myeloid clonal lines (Fischer et al., 2015). The oncogenic activity of miR-21 has been studied by different researchers and reported in different types of cancer including AML (Feng and Tsao, 2016). Upregulation of miR-21 induce the proliferation in AML while its downregulation induces G1 arrest and apoptosis (Bai et al., 2011) by targeting PTEN-AKT pathway. High expression of miR-99a blocks differentiation, increases cell proliferation and colony formation in AML by targeting several pathways including oncogenomic HOXA family (Khalaj et al., 2017). Indeed, high expression of miR-99a is more dangerous than the known mutations and could predict worse outcome in patients with AML (Si et al., 2016). Interestingly, our RNA-seq data revealed downregulation in most of HOXA gene family (Figure 3-19). Therefore, downregulation of those miRNAs in the *HP1BP3*-inhibition cells, could explain the significant reduction in the frequency of two subpopulations representing the LSCs ($CD34^+/CD34^-$ as well as $CD34^+/CD34^+$) in two AML cell lines (Figure 4-3).

Taken together, the data in this chapter demonstrate a novel aspect of HP1BP3/miRNA axis regulation in AML and LSCs and could also explain the phenotype in the KD cells (*Chapter 3*) through miRNA regulation.

Additional experiments required to explore the specificity of binding of HP1BP3 to the candidate miRNAs chromatin via ChIP-qPCR analysis in the future. The novel predicted miRNAs will be characterised by designing primers to investigate their expression in AML cells as well as human samples. Moreover, the potential effect of those miRNAs i.e. miR-21 and miR-99a on AML will be investigated in the future using miRNAs inhibitors.

CHAPTER 5

Hypoxia-induced HP1BP3 modulates AML cell survival

5.1 **Brief introduction**

Hematopoietic stem cells (HSCs) are physiologically located in stem cell niches in the bone marrow (BM) that are characterized by very low oxygen tension, and where AML cell initiation and progression also occur (Figure 5-1) (Parmar et al., 2007, Eliasson and Jönsson, 2010, Konopleva and Jordan, 2011). Reduced oxygen partial pressure (pO2, hypoxia, Hx) is a vital element of the BM microenvironment and HSC survival (Eliasson and Jönsson, 2010). Several studies have shown that the low level of oxygen retains the stemness potential of the HSCs favouring self-renewal over differentiation (Cipolleschi-Dello Sbarba et al., 1993, Ivanovic et al., 2002, Eliasson et al., 2010). Leukemic cells are in dynamic interaction with the BM microenvironment. Increasing evidence suggest that BM microenvironment protects the leukemic cells from chemotherapy (Chen et al., 2015, Kamga et al., 2016), apoptosis (Carter et al., 2016) and maintain their undifferentiated status (Ito et al., 2015). In solid tumour, it is well-proven that excessive proliferation of tumour cells will lead to hypoxia that enhances tumour progression (Hockel and Vaupel, 2001, Muz de la Puente et al., 2015). Similarly, in haematological malignancies, the concept of excessive proliferation and accumulation of blast cells will affect the BM microenvironment and blood, eventually causing hypoxia (Fiegl et al., 2009, Semenza 2013, Jabari et al., 2019). Hx stimulates several cell signalling pathways including the key HIF pathway (Maxwell et al., 2001) and other Hx-associated intracellular pathways such as; NFκB (Van Uden et al., 2008), PI3K/AKT/mTOR (Agani and Jiang, 2013), and MAPK/ERK (Agani and Jiang, 2013) pathways.

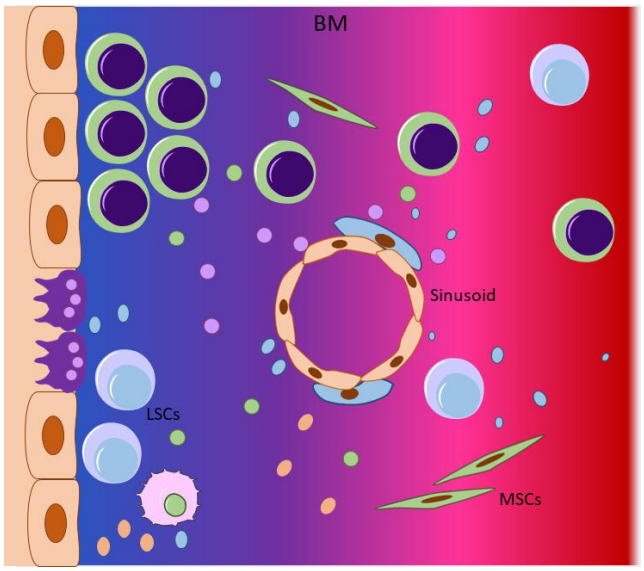


Figure 5-1: Cross-talk between LSCs and their niche. *In vivo* measurements in BM show a reduction in the O2 levels from the endosteum into the sinusoids. The colour gradient indicates the distribution of the O2 levels in the BM cavity from very hypoxic (blue) to less hypoxic (red). LSCs (grey-coloured nucleus) are scattered within the BM cavity. Abbreviations: BM; bone marrow, LSCs; leukemic stem cells, MSCs; mesenchymal stem cells. Modified from (Schito et al., 2017).

In both normal and malignant cells, cellular adaptation to low oxygen levels is mainly triggered by hypoxia-inducible factor 1 alpha HIF1α (Kaelin Jr and Ratcliffe, 2008). Moreover, stimulation of the three Hx-associated pathways under low oxygen tension, eventually activate HIF1 pathway (Muz de la Puente et al., 2015). HIF1 is a transcription factor that is rapidly degraded at normal oxygen tension (normoxia, Nx); however, under low oxygen tension (Hx), hypoxia protects HIF1 from O_2-mediated degradation in the cytoplasm and allowing transfer to the nucleus (Keith et al., 2012). HIF1 is a heterodimer protein that consists of an alpha subunit (HIF1α) and a beta subunit (HIF1β). In the nucleus under hypoxia, HIF1 regulates the expression of numerous downstream target genes, known as hypoxia response elements (HREs), by binding to DNA sequences (Keith et al., 2012, Paolillo et al.,

2015). HREs are involved in regulating various biological processes, including haematopoiesis, angiogenesis, cell proliferation, the cell cycle and apoptosis in response to low oxygen levels (Nicholas and Sumbayev, 2009, He et al., 2013). Studies have shown that angiogenesis is involved in AML progression by providing essential factors for blast proliferation and angiogenic factors (Albitar, 2001).

Chromatin remodelling such as chromatin condensation and decondensation takes place constantly under hypoxia, even though the detailed alterations in chromatin structure remain mainly undiscovered (Johnson and Barton, 2007). As mentioned above, the adaptive cellular mechanism in response to hypoxia is achieved by HIF1 binding to HREs, triggering transcriptional regulation. Hence, chromatin accessibility is one of the major cellular response elements to low oxygen availability (Kasper et al., 2005). Hypoxia induces novel changes in chromatin structure, mainly in histone methylation and acetylation, and DNA methylation. Hypoxia alters the expression level of some chromatin markers, including H3K4me3, H3K9me3 and H3K27me3 (Johnson et al., 2008).

As outlined in the previous chapters, HP1BP3 binds directly to HP1α, and modulates the expression of H3K9me3 and H3K9ac. Moreover, HP1BP3 regulates the expression of miRNAs in AML. Inhibition of HP1BP3 downregulated the expression of miR-21 and miR-17, both involved in HIF1α signalling pathway activation through deactivation of a tumour suppressor PTEN activity (Bai et al., 2011, Gao et al., 2014). PTEN regulates one of the hypoxia-associated pathway, the PIK3, and its deactivation enhances HIF-1-mediated gene expression (Stiehl et al., 2002). Moreover,

miR-143 which targets NF-κB and MAPK signalling pathways (He et al., 2020) was also upregulated in the knockdown cells. Further, a proteomics study reported that HP1BP3 was a key chromatin organizer in A431 cells that had been treated with 1% pO2 (Dutta et al., 2014). This study also showed that HP1BP3 was involved in the transformation of the A431 cancer cells into an aggressive phenotype (Dutta et al., 2014). Therefore, we aimed to investigate the possible epigenetic programming role of HP1BP3 in response to hypoxia in AML cells using loss-of-function analysis.

Herein, Western blotting (WB) and qRT-PCR were carried out to investigate the expression of HP1BP3 and HIF1α, and CA9 (carbonic anhydrase 9) and VEGFA (vascular endothelial growth factor A) as hypoxic markers. The cell proliferation in normoxia and hypoxia was studied using the WST-1 assay. Moreover, the expression level of several chromatin modifiers, including TET2 (tet methylcytosine dioxygenase 2), DNA methyltransferase 3 alpha (DNMT3A), KMT2A (lysine (K)-specific methyltransferase 2A), NSD1 (nuclear receptor binding SET domain protein 1, which is a histone-lysine *N*-methyltransferase) and EZH2, was tested in cells treated with 1% pO2 and 20% pO2. Consistent with the recent report (Dutta et al., 2014), HP1BP3 was induced in response to hypoxia. Interestingly, our loss-of-function analysis revealed that the downregulation of HP1BP3 led to a significant reduction in the expression level of HIF1α and consequently the hypoxic markers.

5.2 RESULTS

5.2.1 HP1BP3 expression is induced in hypoxia

Considering that, chromatin alteration is induced by extracellular stimuli, a former colleague at our lab showed that HP1BP3 is involved in chromatin modifications in response to UV-mediated DNA damage activated by the ATM–ATR axis [Normatova M. et al., in submission]. To investigate how HP1BP3 mediates chromatin modifications in response to hypoxia, MO91 cells highly expressing HP1BP3 were initially incubated in hypoxic as well as normoxic conditions for 24 hrs. Following the incubation period, the expression level of HP1BP3 was assessed at both protein and mRNA level. Moreover, the hypoxic status of the incubated cells was confirmed using qRT-PCR analysis of the relevant markers, including *CA9* and *VEGFA*. Total RNA was isolated using TRI Reagent, and cDNA was synthesised using the PrimeScript cDNA Synthesis Kit (*Chapter 2*).

The initial qRT-PCR results indicated significantly high *CA9* and *VEGFA* mRNA expression levels in the 1% pO2-treated cells, confirming the hypoxic state of the cells (Figure 5-2, C-D). Next, the cells were lysed using protein extraction buffer, and the protein level was quantified using colorimetric protein determination reagent (*Chapter 2*). The cell lysates were assayed for expression of HP1BP3, HP1α as well as the two heterochromatin/euchromatin markers H3K9me3 and H3K9ac using immunoblotting. Excitingly, our data showed that the expression of HP1BP3 was induced in hypoxia as compared with the normoxic condition at both protein and mRNA level (Figure 5-2, A & E).

Furthermore, the expression of H3K9me3, the heterochromatin marker, was reduced due to the hypoxia; however, the expression of the euchromatin marker, H3K9ac, was induced (Figure 5-2, E). These data suggest that HP1BP3 could be involved in chromatin alteration in hypoxia. Additionally, it confirms our hypothesis that the high level of HP1BP3 reduces the expression of H3K9me3, especially where in this case it is an endogenous induction of HP1BP3 and without any forced expression or gene manipulation. Moreover, the expression of HP1α remained unchanged (*Chapter 3*).

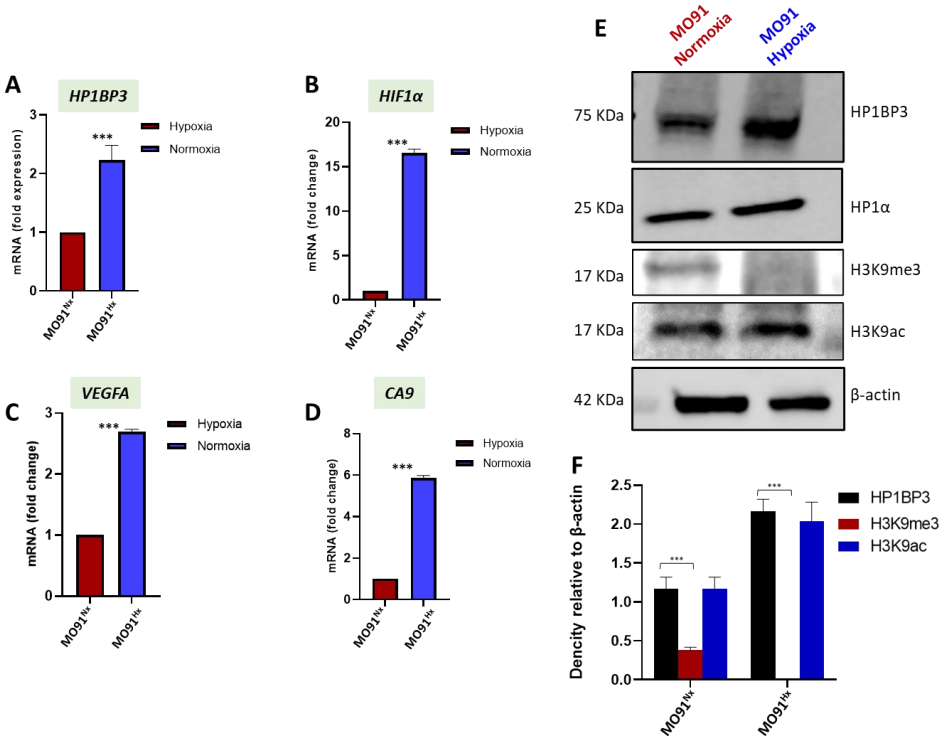


Figure 5-2: Expression of HP1BP3 is induced in hypoxia in MO91 AML cells. Data indicate significant induction in both mRNA **(A)** and protein level **(E)** of HP1BP3 in MO91 cell line treated with 1% pO2 (Hx) compared with cells treated with (Nx). mRNA expression level of hypoxic markers *CA9* **(C)** and *VEGFA* **(D)** and hypoxia inducible factor-1α; *HIF1α* **(B)** was significantly high in cells incubated in Hypoxia chamber confirming the hypoxic status of the cells. mRNA expression level was analysed by qRT-PCR and data was normalized to *β-actin*. The error bars show the SD of three biological

repeats, (***p<0.001). **(E)** Western blotting analysis for endogenous HP1BP3, HP1 α, H3K9me3 and H3K9ac expression level in M091 cell line. 100 µg of total protein was loaded on 10% for (anti-HP1BP3) or 15% for (anti- HP1, -H3K9me3 and -H3K9ac) SDS-PAGE and transferred to PVDF membranes. Anti-HP1BP3, -HP1α, -H3K9me3 and -H3K9ac, have been used to detect the expression level of HP1BP3, HP1α, H3K9me3 and H3K9ac. Chromatin markers; H3k9me3 was completely depleted due to the endogenous induction of HP1BP3 level and H3K9ac was induced. β-actin was used as a loading control. **(F)** Histogram represents relative density value of HP1BP3/ β-actin, H3K9ac/ β-actin and H3K9me/ β-actin in MO91 cells from three biological repeats (± SD).

5.2.2 HP1BP3 could be involved in the regulation of genes associated with hypoxia

To further assess the role of HP1BP3 on AML cells under hypoxia, loss-of-function analysis was carried out using the generated *HP1BP3* gene-manipulated AML cells. To determine whether the loss of HP1BP3 confers a hypoxic state through modulating HIF1α, *HP1BP3* knockdown AML cells $MO91^{KD}$ and $TF1a^{KD}$ versus control cells $MO91^{GFP}$ and $TF1a^{GFP}$, respectively, were subjected to 1% pO2 (Hx). The cells were seeded and incubated in hypoxic conditions by placing them in a sealed hypoxia chamber, and under normoxic conditions, for 24 hrs. Next, the expression level of *HP1BP3*, as well as the hypoxic markers (*CA9* and *VEGFA*), was tested using qRT-PCR to confirm the hypoxic condition. For this, the total RNA of the seeded cells in both conditions was isolated using TRI Reagent, and cDNA was synthesised as described in *Chapter 2.* Interestingly, the mRNA levels of the hypoxic markers were significantly decreased in the knockdown cell lines compared to the corresponding control cell lines (Figure 5-4).

Downregulation of the hypoxic markers upon *HP1BP3* knockdown raised the question of whether *HIF1a*, a transcriptional activator of those markers, is also regulated by HP1BP3. To examine this, the expression level of *HIF1a* was tested using qRT-PCR. Interestingly, the mRNA expression level of *HIF1a* was considerably reduced in the *HP1BP3* knockdown cells compared with the control cells (Figure 5-5). These data suggest that HP1BP3 could be involved in chromatin modification in response to hypoxia. This modification could be through regulating the expression of HIF1α. These data spurred us to look for a possible mechanism of how HP1BP3 would regulate the expression of HIF1α, which will be discussed in the following section.

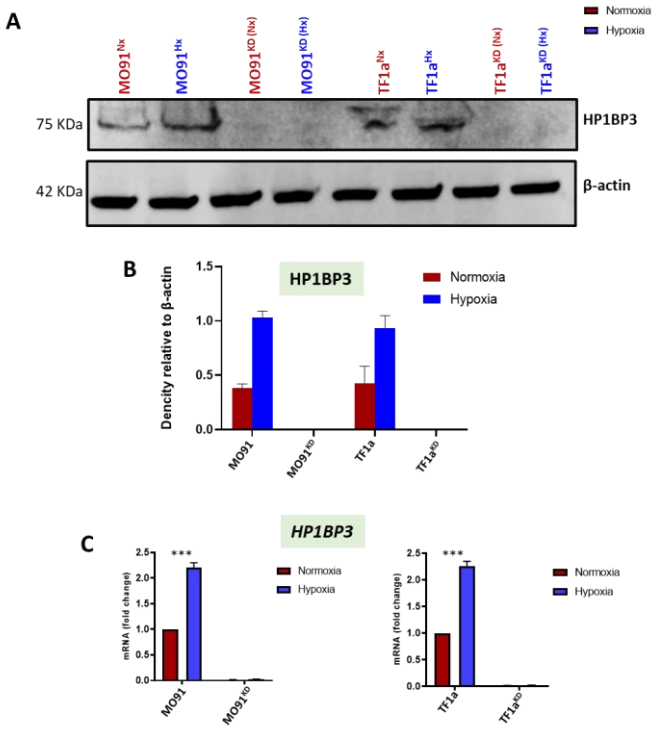


Figure 5-3: HP1BP3 is induced in AML cells in response to hypoxia (Hx). Data indicates that Hx induced the expression level of HP1BP3 in AML cells. **(A)** Immunoblot of MO91, MO91^{KD}, TF1a and TF1a^{KD} cell lysates treated with 20% pO2 (Nx) or 1% pO2 (Hx) for HP1BP3 and β-actin. A 100 µg of total protein extract was loaded on 10% SDS-PAGE, transferred to a PVDF membrane and blotted for anti-HP1BP3. β-actin was used as a loading

control. **(B)** Histogram represents relative density value of HP1BP3^{Nx}/ β-actin and HP1BP3^{Hx}/ in MO91, MO91^{KD}, TF1a and TF1a^{KD} cells from three independent experiments (± SD). **(C)** mRNA expression level of *HP1BP3* was analysed by qRT-PCR and data was normalized to *β-actin*. The error bars show the SD of three biological repeats (***p<0.001).

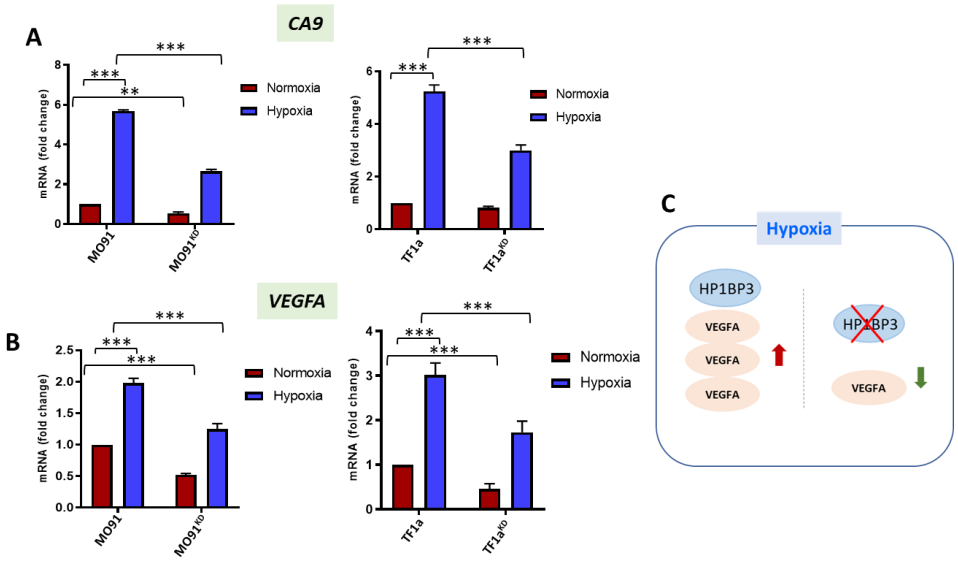


Figure 5-4: *HP1BP3*-knockdown reduced the expression of hypoxia-related genes in AML cells. (A) Data demonstrate loss of HP1BP3 induced a significant reduction in hypoxia-associated *CA9* in MO91 cells treated with hypoxia and normoxia and TF1a cells treated with 1% pO2 (Hx). **(B)** Data indicate a significant reduction in *VEGFA* level in MO91 and TF1a cells treated with Nx and Hx. mRNA expression level was analysed by qRT-PCR and data was normalized to *β-actin*. The error bars show the SD of three biological repeats (*P= 0.01 to 0.05, **p= 0.001 to 0.01, ***p<0.001). This experiment was performed in triplicate on at least three independent occasions. **(C)** Schematic representation shows the reduction in the expression of hypoxic marker; *VEGFA* after HP1BP3 knockdown.

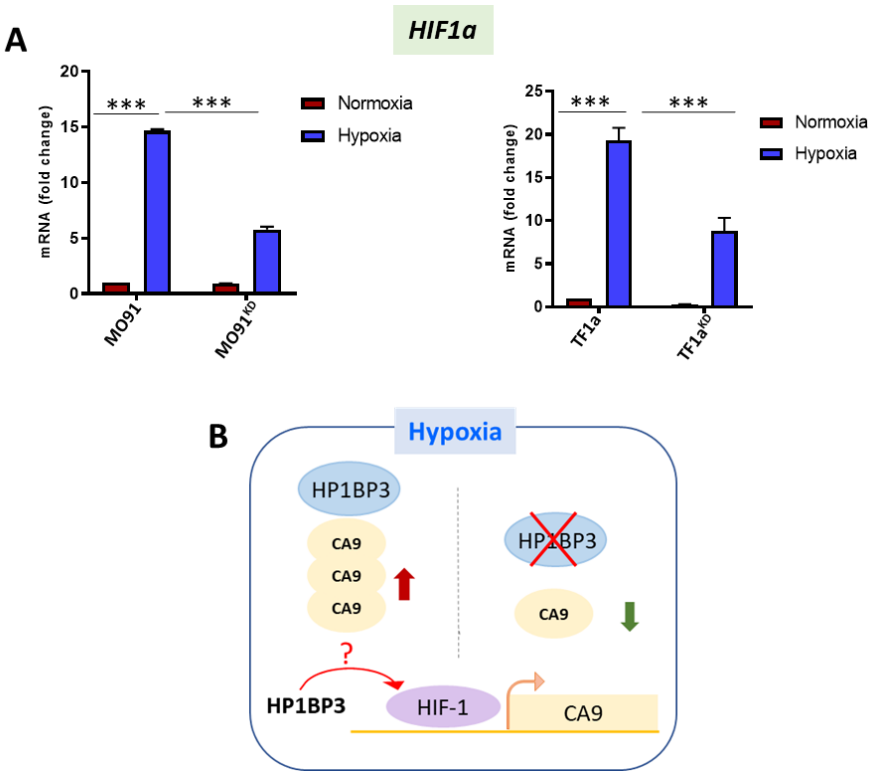


Figure 5-5: knockdown of *HP1BP3* decreased the expression level of Hypoxia-inducible factor 1-α in AML cells. (A) Data reveal a significant decrease in *HIF-1α* expression in *HP1BP3*-knocdown AML cell lines. mRNA expression was analysed by qRT-PCR and data was normalized to *β-actin*. The error bars show the SD of three biological repeats (***p<0.001). This experiment was performed in triplicate on at least three independent occasions. **(B)** Schematic representation shows that inhibition of HP1BP3 reduced the expression of hypoxic markers.

5.2.3 Knockdown of *HP1BP3* induced the expression of *FBXW7* in AML cell lines

As outlined above, the expression of *HIF1α* as well as the hypoxic markers was downregulated in *HP1BP3* knockdown AML cells. These data prompted us to investigate a potential mechanism of HIF1α regulation through HP1BP3. As described earlier, HP1BP3 was discovered in our lab as a downstream target of FBXW7 for degradation. On the other hand, in the literature, under hypoxia, FBXW7 also negatively regulates HIF1α through

UPS for degradation (Cassavaugh et al., 2011). Therefore, we speculated that this regulation by HP1BP3 could be in an indirect manner through FBXW7. Accordingly, we examined the expression level of *FBXW7* in *HP1BP3* knockdown AML cell lines in both hypoxia and normoxia.

To this, MO91^{KD} and TF1a^{KD} cells as well as their respective control cells MO91^{GFP} and TF1a^{GFP} were seeded and incubated in a hypoxia chamber and in normoxia for 24 hrs. Next, total RNA was isolated from the incubated cells, and cDNA was synthesised as outlined in *Chapter 2*. The mRNA expression level was tested using qRT-PCR. Our data shows that the mRNA expression of *FBXW7* was significantly increased in the *HP1BP3* knockdown AML cell lines treated with 1% pO2 (Hx) as well as ˜20% pO2 (Nx) (Figure 5-6).

These data may suggest that HP1BP3 negatively regulates its negative regulator, FBXW7. Excitingly, the induction of *FBXW7* after *HP1BP3* knockdown was also confirmed by RNA-seq analysis (*Chapter 3*). We found that FBXW7 is negatively regulated by HP1BP3, suggesting that FBXW7 is downregulated by HP1BP3 in hypoxia, and would lead to the upregulation of HIF1α, and finally CA9 and VEGFA. These data may explain the downregulation of *CA9* and *VEGFA* in the knockdown AML cell lines. Moreover, it may also describe the possible regulation of HIF1α by HP1BP3. However, further experiments will be required to determine the molecular mechanisms mediated by HP1BP3-HIF and HP1BP3-FBXW7 and their interconnected biological significances.

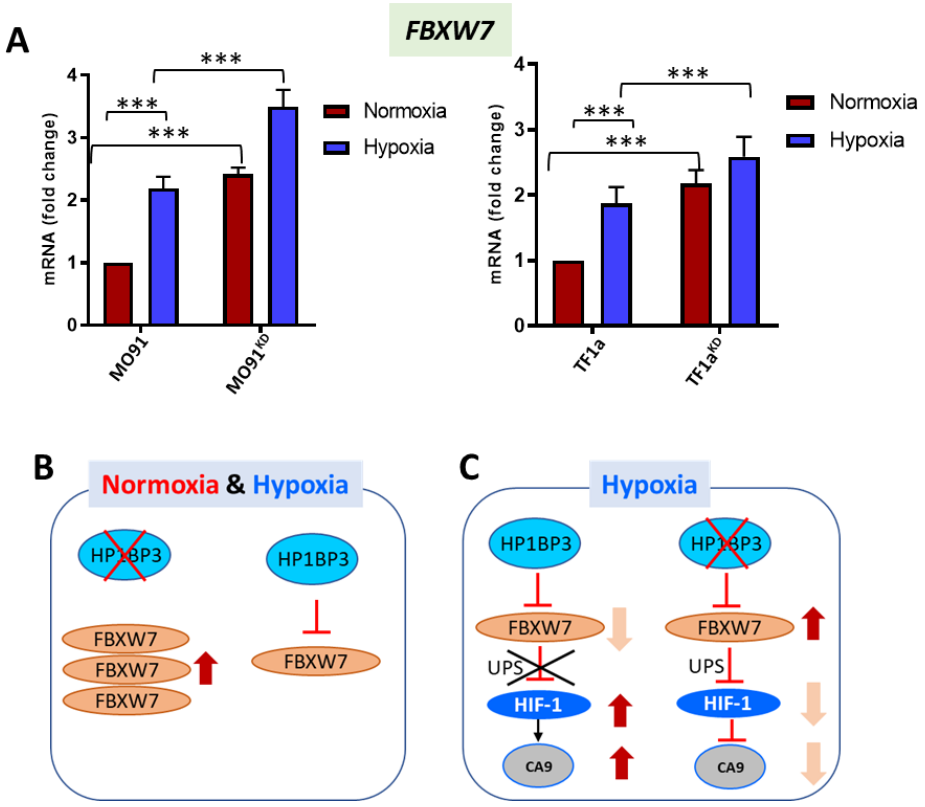


Figure 5-6: knockdown of HP1BP3 increased the expression level of *FBXW7* in AML cell lines. **(A)** Data demonstrate a significant induction in *FBXW7* expression level in *HP1BP3*-knockdown AML cell lines treated with 20% pO2 (Nx) or 1% pO2 (Hx). mRNA expression level was analysed by qRT-PCR and data was normalized to β-actin. The error bars show the SD of three biological repeats (***p<0.001). This experiment was performed in triplicate on at least three independent occasions. **(B)** Schematic representation of FBXW7 elevation after HP1BP3 knockdown in both normoxia and hypoxia conditions. **(C)** Schematic representation of a possible indirect regulation of *HIF1α* and eventually hypoxia-related markers through FBXW7 and not directly by HP1BP3.

5.2.4 Loss of HP1BP3 reduces the growth rate of AML cell lines

As the expression of HP1BP3 changed the proliferation and growth rate in AML cells and Lin^- cells (*Chapter 4*), here we aimed to test the loss of HP1BP3 on the growth rate in response to low oxygen availability. For that, *HP1BP3* knockdown cells $MO91^{KD}$ and $TF1a^{KD}$ and their corresponding control cells $MO91^{GFP}$ and $TF1a^{GFP}$, respectively, were used in this experiment. The cells were seeded in two 96-well plates, incubated under hypoxia and normoxia, and cell proliferation was examined using the spectrophotometric metabolic-based quantification reagent WST-1.

The cells were incubated in hypoxic or normoxic conditions for 24 hrs. The cells were then incubated with the WST-1 reagent for 0.5–4 hrs; finally, the formed formazan dye was measured using a scanning multi-well spectrophotometer. Figure 5-7 shows that the hypoxia induced HP1BP3 significantly induced proliferation in the MO91 and TF1a cells. However, in line with the data obtained in *Chapter 4*, the knockdown of *HP1BP3* significantly reduced the growth rate in both conditions regardless of the oxygen availability. These data further confirm that HP1BP3 regulates the growth rate in AML cells.

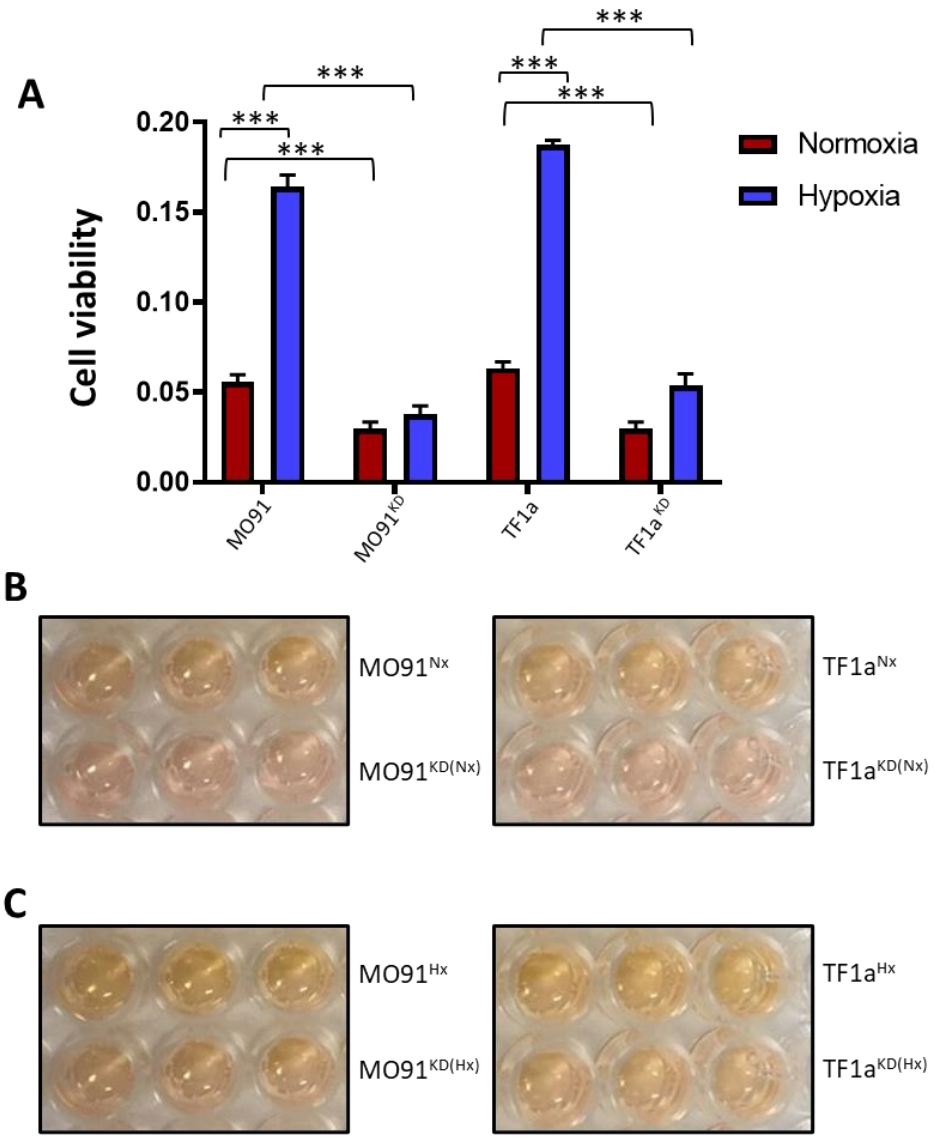


Figure 5-7: HP1BP3-knockdown reduced the proliferation in AML cells treated with Nx and Hx. (A) The histogram shows the significant reduction of cells proliferation in HP1BP3-knockdown AML cells treated with both Nx and Hx conditions. Statistical test: Two-tailed unpaired T-test (n=3; ***p<0.001). The error bars show the SD of three biological repeats. **(B, C)** Representative images of WST-1 quantification assay of MO91 and TF1a cells lacking the expression of HP1BP3 and their corresponding GFP control cells. Cells were seeded in two 96 well plate and incubated with WST-1 reagent for 0.5- 4 hrs in Nx and Hx, the colour changes was measured using multi-well spectrophotometer. This experiment was performed in triplicate on at least three independent occasions (N=3).

5.2.5 HP1BP3 can mediate chromatin modification by regulating different chromatin modifiers

Evolutionarily and structurally, HP1BP3 belongs to the linker histone H1 family (Garfinkel et al., 2015), and H1 regulates chromatin structure and function (Woodcock et al., 2006, Fyodorov et al., 2018). Moreover, HP1BP3 potentially regulates chromatin transition by binding to HP1α, and its loss/overexpression confers changes in AML cell proliferation, cell cycle progression and stemness potential (*Chapter 3*). Here, we investigated, using qRT-PCR, whether the expression level of HP1BP3 would affect the expression levels of other chromatin modifiers in an O_2-dependent manner, including SUV39H, DNMT3A, NSD1, TET2 and KMT2A. For that, $MO91^{KD}$ and $TF1a^{KD}$ cells and their control cells $MO91^{GFP}$ and $TF1a^{GFP}$, respectively, were seeded and incubated in hypoxia and normoxia conditions for 24 hrs. Total RNA was extracted from the cells in both conditions, and cDNA was synthesised as described in *Chapter 2*.

The expression of two of the chromatin modifiers, i.e. NSD1 and KMT2A, was significantly downregulated in the *HP1BP3* knockdown cell lines (Figure 5-8), which may have led to the formation of heterochromatin and the deactivation of gene expression. However, the expression levels of TET2, SUV39H and DNMT3A remained unchanged (Figure 5-8). These data may suggest that HP1BP3 acts as a global chromatin modifier and furthermore regulates gene expression.

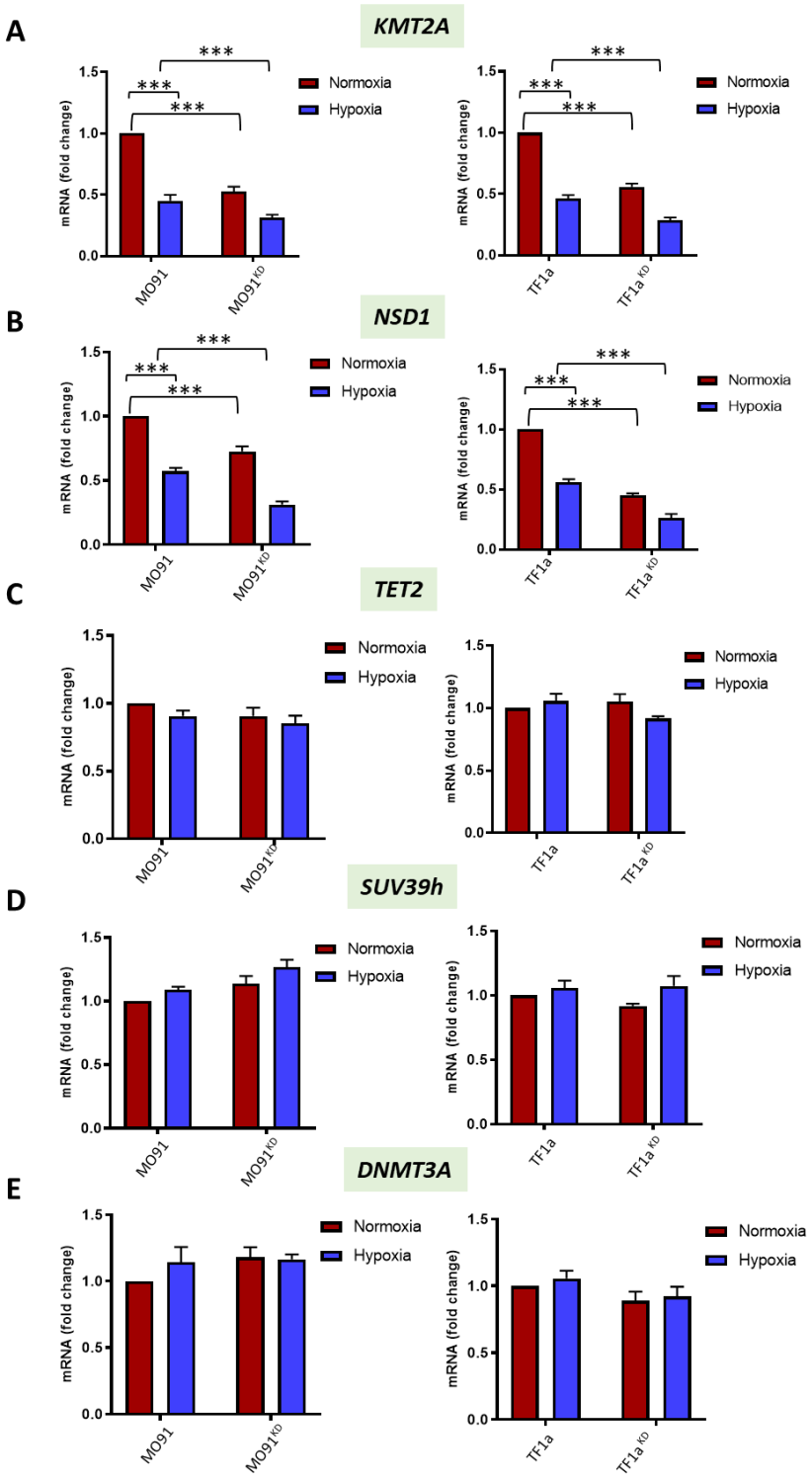


Figure 5-8: knockdown of *HP1BP3* changes the expression of some chromatin modifiers in AML cell lines. (A-B) Data demonstrate a significant reduction in *KMT2A* and *NSD1* expression levels in *HP1BP3*-knocdown AML cell lines treated with 20% pO2 (Nx) or 1% pO2 (Hx). **(C-E)** unchanged mRNA expression level of *TET2*, *SUV39h* and *DNMT3A* in AML cells. mRNA analysed by qRT-PCR and data was normalized to *β-actin*. The error bars show the SD

of three biological repeats (***p<0.001). This experiment was performed in triplicate on at least three independent occasions.

5.3 **Discussion**

Understanding the crosstalk between chromatin architecture and transcription is important for understanding the cellular response to hypoxia (Batie et al., 2018). Chromatin condensation and decondensation are rapidly reversible in response to extracellular stimuli, including oxygen levels and metabolic changes (Kirmes et al., 2015). In mammalian cells, chromatin is a key regulator of all cellular mechanisms such as; DNA replication, DNA repair and transcription. Alteration of gene transcription is the main factor in low oxygen stress response (Batie et al., 2018). Therefore, exploring the role of chromatin-associated proteins can provide better knowledge about chromatin biology, genetic expression and epigenomic regulation during hypoxia.

In the previous chapter, we demonstrated that HP1BP3 regulates miRNA expression in AML. The sRNA-seq analysis showed that HP1BP3 regulates miRNAs involved in regulation of hypoxia-associated pathways. Furthermore, a proteomics-based analysis further found that the chromatin-associated protein HP1BP3 is one of the proteins that induces cancer progression in hypoxia (Dutta et al., 2014). On the other hand, the BM microenvironment is one of the key elements in AML initiation, progression, resistance to therapy and recurrence (Meads et al., 2008, Ayala et al., 2009, Karantanou et al., 2018). The BM micro-niche which nurtures and determines HSC/LSC (leukaemia stem cell) fate is characterized by low oxygen availability (Ayala et al., 2009). Moreover, using a rat model, Jensen *et al.* reported that the BM microenvironment was more hypoxic during the development of leukaemia (Jensen et al., 2000). Hence, in this chapter, we

used loss-of-function analysis to investigate the role of HP1BP3 in response to hypoxia in AML cells.

Using western blotting and qRT-PCR assays, we found that the expression of HP1BP3 was considerably increased in response to hypoxia in MO91 AML cells (Figure 5-2). Moreover, the expression of *HIF1α*, which is the most important molecule that responds to hypoxia (Harrison et al., 2002), and the two hypoxia markers *CA9* and *VEGFA*, was also examined. The mRNA expression of the hypoxic markers confirmed the hypoxic state of the cells treated with 1% pO2 (Figure 5-2). Additionally, the expression of the two chromatin markers H3K9me3 and H3K9ac was tested using immunoblotting (Figure 5-2, E). Consistent with our finding in *Chapter 3*, the expression of H3K9me3 was completely depleted, while the expression H3K9ac was induced as a consequence of the upregulation of endogenous HP1BP3 expression level, confirming our initial hypothesis (Figure 3-1). These data prompted us to test the effect of the lack of HP1BP3 expression on chromatin regulation of AML in response to hypoxia using *HP1BP3* knockdown AML cells.

Interestingly, our loss-of-function analysis showed that HP1BP3 could be involved in the regulation of some hypoxia-associated genes through the regulation of HIF1α (Figure 5-3). mRNA expression of the hypoxia markers *VEGFA* and *CA9* was significantly downregulated in *HP1BP3* knockdown AML cells. VEGFA is one of the most important angiogenic factors involved in AML progression. Binding of VEGFA to its receptors on the leukemic cells, stimulates cell proliferation and survivability by inhibiting apoptosis (Song et al., 2012, Goulard et al., 2018). Moreover, the VEGFA binding to

its receptors on the epithelial cells in BM, stimulate the secretion of some important growth factors as G-CSF, GM-CSF and IL-6 which are involved in leukemic cells proliferation (Song et al., 2012). In solid tumour, the high level of HIF1α was a poor prognostic factor that leads to recurrence and drug resistance (Birner et al., 2000, Chi et al., 2006, Bangoura et al., 2007). Likewise, in leukaemia, many studies have reported that HIF1α levels are higher in patients with AML compared with control groups, suggesting an induction of pO2 and hypoxia in those patients (Deeb et al., 2011, Jabari et al., 2019). These findings could also explain the recurrence and the resistance to treatment in patients with AML.

To further investigate the effect of the hypoxia-induced HP1BP3on the growth rate of AML cells, we performed a metabolic-based quantification test. Interestingly, our data showed that the upregulation of endogenous HP1BP3 significantly induced the proliferation of AML cells (Figure 5-6); however, more excitingly, the loss of HP1BP3 reduced the growth rate considerably in both hypoxia and normoxia conditions. These data are in line with our finding on HP1BP3 in the regulation of AML cell proliferation (*Chapter 3*), and could be due to the downregulation of *VEGFA* expression in the knockdown cells.

Downregulation of HIF1α after *HP1BP3* knockdown led us to seek a possible mechanism of how HP1BP3 could regulate the expression of HIF1α. FBXW7 regulates HIF1α during hypoxia (Cassavaugh et al., 2011, Flügel et al., 2012), a HP1BP3 negative regulator. We, therefore, speculated that this regulation could be through FBXW7 and not directly by HP1BP3. Excitingly, our data show that *FBXW7* was significantly upregulated in

HP1BP3 knockdown AML cells in both hypoxia and normoxia conditions (Figure 5-6), suggesting that HP1BP3 could also regulate its negative regulator FBXW7. The upregulation of FBXW7 could explain the significant downregulation of HIF1α and consequently, the hypoxia markers VEGFA and CA9. These data were confirmed by RNA-seq analysis, which revealed elevated FBXW7 in the knockdown cells (*Chapter 3*); however, the negative regulation of FBXW7 through HP1BP3 could be through miRNA regulation (*Chapter 4*). Our sRNA-seq analysis revealed that the expression of miR-25, miR-27a, miR-92a, miR-182 and miR-223, which negatively regulate FBXW7 (Kumar et al., 2014, Wu et al., 2015, Zhou et al., 2015, Caiazza and Mallardo, 2016) were downregulated in the knockdown cells.

Moreover, considering that HP1BP3 potentially regulates the chromatin state by binding to HP1α (*Chapter 3*) and that it belongs to the linker histone H1 family (Garfinkel et al., 2015), we investigated whether the expression level of HP1BP3 would affect the expression of other chromatin modifiers during hypoxia. Our data show that the downregulation of HP1BP3 induced a significant reduction of *KMT2A* and *NSD1* expression and induced the expression of *EZH2* in both hypoxia and normoxia (Figure 5-8). KMT2A and NSD1 are methyltransferases that methylate H3K4 and H3K36, respectively (Lucio-Eterovic et al., 2010, Bochyńska et al., 2018). Methylation of H3K4 and H3K36 is associated with transcription activation (Zhang and Reinberg, 2001). EZH2 is a methyltransferase that methylates H3K27 and is associated with transcription repression (Gan et al., 2018). This finding was confirmed by RNA-seq analysis (Chapter 3). Moreover, the expression of *TET2*, *DNMT3A* and *SUV39H* remained unchanged. These findings suggest that

HP1BP3 could function as a global chromatin modulator similarly to the linker histone H1 that regulates chromatin structure and function (Woodcock et al., 2006, Fyodorov et al., 2018). Further ChIP analysis is required to investigate the specificity of HP1BP3 in regulating the expression of the tested genes in Nx and Hx.

CHAPTER 6

In vivo loss-of-function analyses of *Hp1bp3* and *Hp1bp3* knockout mouse haematopoietic stem cells

6.1 Brief introduction

Haematopoiesis is a process in which the whole range of mature blood lineages is manufactured. All blood cell types arise from a single progenitor cell known as the hematopoietic stem cell (HSC), which has the ability to self-renew and multilineage potential (Arai and Suda, 2007). HSCs reside in the bone marrow (BM) and they are in a relatively quiescent state of the cell cycle (Passegué and Wagers, 2006). Long-term HSCs (LT-HSCs) proliferate infrequently to generate more proliferative short-term HSCs (ST-HSCs) as well as to sustain a small pool of undifferentiated HSCs to maintain haematopoiesis homeostasis throughout the life of an organism (Boulais and Frenette, 2015, Grinenko et al., 2018). Extensive efforts have been made to understand the nature of the mechanism that controls the balance between the self-renewal and differentiation of HSCs, including *in vivo* knockout models (Thompson et al., 2008, Reavie et al., 2010, Iriuchishima et al., 2011). Accumulating evidence suggests the critical roles of epigenetics in maintaining both self-renewal and differentiation mechanisms in HSCs (Challen et al., 2012, Cabezas-Wallscheid et al., 2014, Cullen et al., 2014, Farlik et al., 2016, Luo et al., 2018). Most of these reports investigated the role of epigenetic post-translational histone modifications, including methylation, acetylation, sumoylation and phosphorylation, and their epigenetic mechanisms in regulating hematopoietic homeostasis (Katsumoto et al., 2008, Loizou et al., 2009, Hidalgo et al., 2012, Shide et al., 2012, Challen et al., 2014). These modifications mainly affect the transition of euchromatin/heterochromatin in core histones; however, there is little insight

into the mechanism of the heterochromatin proteins and their binding proteins in the regulation of haematopoiesis.

Heterochromatin protein 1 binding protein 3 (HP1BP3), previously known as HP1-BP74, is a nuclear heterochromatin-associated protein that binds directly to heterochromatin protein 1α (HP1α) (Hayashihara et al., 2010). HP1α is enriched at the pericentric heterochromatin regions and plays a critical role in regulating heterochromatin-mediated silencing in normal homeostasis and malignancy. There is a 93% similarity of HP1BP3 between humans and murine, and it is ubiquitously expressed in most tissues (Garfinkel et al., 2015). Moreover, HP1BP3 evolutionarily and structurally belongs to the linker histone H1 family. Like H1 subtypes, HP1BP3 contains several important domains, including three globular domains, HP1α binding motif (PxVxL), nuclear localisation signal (NLS), glutamine-rich N terminal (NTD) and a common C terminal region (CTD) (Garfinkel et al., 2015). Therefore, HP1BP3 can interact with the DNA nucleosome at the entry/exit points, which might implicate the higher order of chromatin architecture (Hayashihara et al., 2010). However, nothing is known about HP1BP3, particularly the chromatin regulatory machinery and the function of *HP1BP3* in normal haematopoiesis and haematological malignancies, including leukaemia; hence, its function remains to be explored.

In the previous chapters, our in vitro gain- and loss-of-function analysis provided convincing evidence that HP1BP3 influences leukemogenesis. In this chapter, we examined the regulation of murine haematopoiesis by HP1BP3 using *Hp1bp3* knockout mouse model. The use of the transgenic mouse model provides an excellent understanding of the biological function

of a normal gene (Cano et al., 2014). Currently, the Cre-loxP strategy is extensively used both *in vitro* and *in vivo* in many laboratories, including our lab, due to its efficiency and high-specificity DNA recombination in different cell types (Branda and Dymecki, 2004, Eisener-Dorman Lawrence et al., 2009, Babaei-Jadidi et al., 2011). As conventional knockout of *Hp1bp3* gave rise to dead embryos in utero (Hayashihara et al., 2010), it was necessary to us to generate a conditional transgenic mouse. The *Hp1bp3* mouse model was generated at Harwell Institute and shipped to us at the University of Nottingham in a heterozygous genotype. Hence, we started by generating a homozygous mouse model to explore the role of HP1BP3 in haematopoiesis. Different approaches, such as flow cytometry analysis of surface markers and histological staining assays, were employed. HP1BP3 controls HSC self-renewal and differentiation, as its deletion leads to impaired self-renewal and induces differentiation in all assays.

6.2 RESULTS:

6.2.1 Generation of the homozygous floxed *Hp1bp3* allele (*Hp1bp3*$^{fl/fl}$) mouse

The high similarity between mouse genes and human orthologs (80%) makes the mouse a useful experimental model system for studying basic normal molecular mechanisms and cancer development (Zerbino and Birney, 2008, Ogilvie et al., 2017). The transgenic mouse model refers to the presence or absence of mouse DNA or the gene of another species in all cells of the mouse model genome, and includes overexpression, knocking-in and knocking-out. They are also known as germline genetically engineered mouse models (GEMM) (Cano et al., 2014). The knockout mouse model is a transgenic mouse that enables the loss of gene function study via the deletion or silencing of a certain gene. This model provides an excellent understanding of the biological function of a normal gene (Cano et al., 2014). There are two types of knockout mouse model: conventional knockout, in which the targeted gene is permanently inactivated or depleted in all and every cell of the organism, and conditional knockout, where the expression of the targeted gene can be affected in a tissue/cell-specific manner (Kersten et al., 2017). The constitutive knockout model is mainly used for studying gene function and for the general characterization of a mouse phenotype such as behavioural changes and anatomical and physiological alterations when the whole animal lacks the expression of that given gene (Jiang, 2013). This type of knockout has been considered a powerful model in cancer research for the determination and validation of novel cancer genes (Polato et al.,

2014). However, one of the major disadvantages of using a conventional knockout model is that the loss of gene function in germlines causes developmental malformations and presents a challenge to reporting conclusive findings about genes (Eisener-Dorman et al., 2009). Therefore, this drawback of the conventional knockout model led to the development of the conditional knockout model to overcome its limitations (Branda and Dymecki, 2004).

In 2015, Garfinkel *et al*. reported that conventional knockout of *Hp1bp3* (*Hp1bp3*$^{-/-}$), led to significant embryonic and post-natal lethality in mice (Hayashihara et al., 2010, Garfinkel et al., 2015). Moreover, less than 40% of *Hp1bp3*$^{-/-}$ mice that survived showed growth retardation at weaning age and weighed 50% less than their control littermates (Garfinkel et al., 2015). More importantly, the work that has been carried out by the two groups did not provide any information about the role of HP1BP3 in haematopoiesis and was more focused about HP1BP3 binding, localisation, growth and viability (Hayashihara et al., 2010, Garfinkel et al., 2015). Hence, the use of a conditional knockout mouse model in the present study was necessary for us. As outlined earlier in *Chapter 2*, the *Hp1bp3*$^{fl/fl}$ mouse model was generated at Harwell Institute. This was accomplished by using the Cre-loxP recombination strategy. Two site-specific recombinases: bacterial Cre and yeast Flippase (FLP) recombinase enzymes, are the key actors in this technology, catalysing the recombination between specific 34-bp *lox*P and *FRT* sites, respectively (Branda and Dymecki, 2004). The *lox*P and *FRT* sites are oriented in the same direction, which leads to the deletion of the flanked gene of interest after recombination (Branda and Dymecki, 2004). The

expression of the two recombinase enzymes induces homologous recombination between these sites and can be controlled, which allowed us to study our gene of interest in a specific manner.

The *lox*P sites were introduced at the beginning and at the end of *exon 8* of *Hp1bp3* (Figure 6-1 A). The genetically heterozygous mice ($Hp1bp3^{fl/+}$) model was shipped to University of Nottingham, at the Transgenic Unit, as a heterozygous genotype. In order to generate a homozygous $Hp1bp3^{fl/fl}$ mouse model, we crossed and inbred mice that are genetically heterozygous at all loci ($Hp1bp3^{fl/+}$) (Figure 6-1 B). All offspring were genotyped using genomic DNAs and PCR analysis (Figure 6-1 C), and finally a homozygous $Hp1bp3^{fl/fl}$ male and female mouse were used as a breeding pair to maintain the colony and experimental plans. Some of previus studies have shown that bone marrow cell-targeted transgenic Cre-deletion lines in vivo are not specific and the recombination is incomplete or leaky, and every model has its own limitations (Kuhn et al., 1995, de Boer et al., 2003, De Lange et al., 2008, Park et al., 2012). Therefore, to delete *Hp1bp3* exclusively in the BM, cells were isolated and transduced *in vitro* with lentiviral (LV) particles expressing Cre, according to previously stablished mythologies using Lentiviral vector overexpressing Cre-recombinase (Alva et al., 2006).

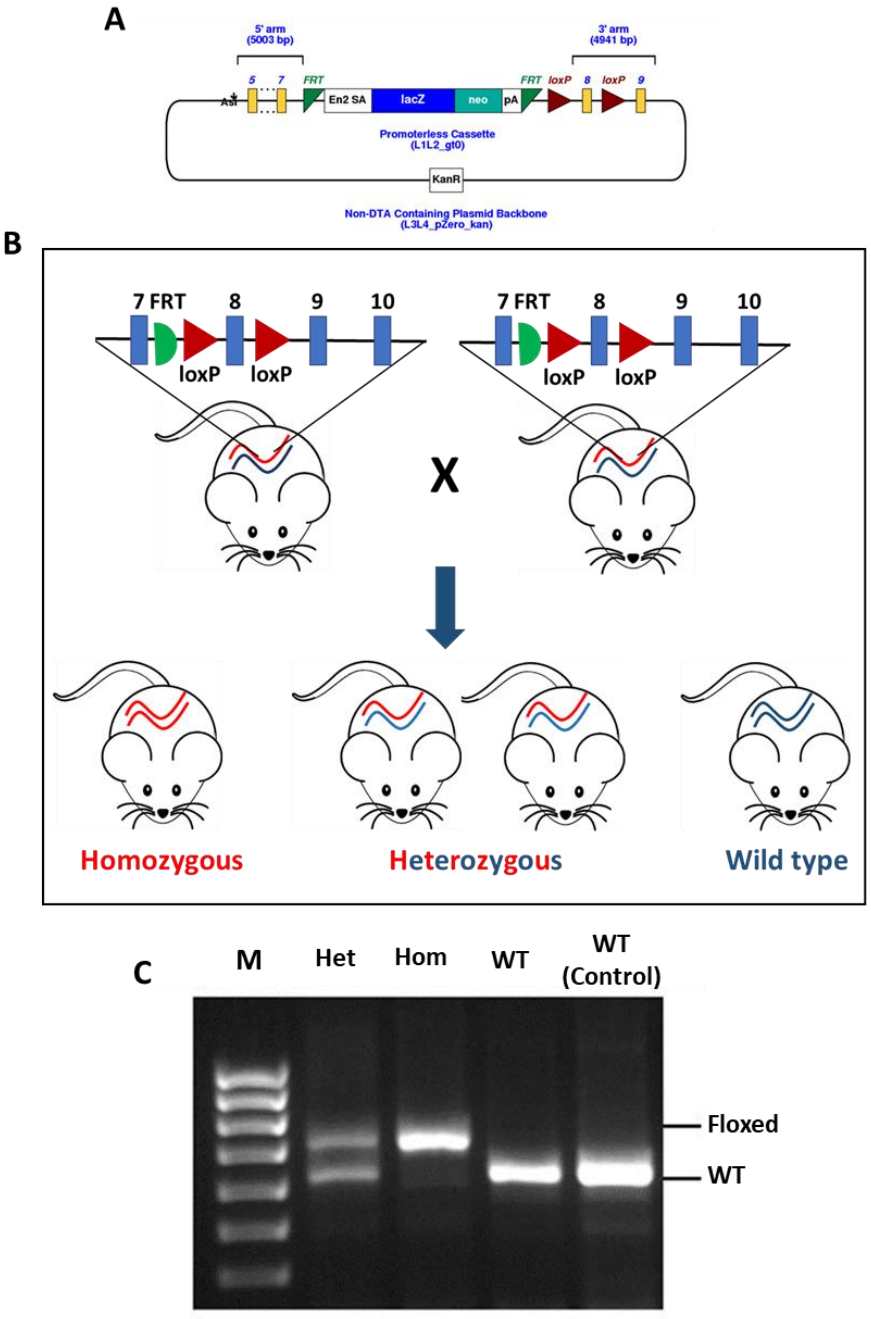


Figure 6-1: Generation of *Hp1bp3*$^{fl/fl}$ homozygous mouse model. (A) Genomic DNA plasmid used to generate *Hp1bp3*$^{fl/+}$ mouse model. **(B)** Schematics- The heterozygous mice were crossed to generate homozygous mice. **(C)** PCR analysis of genomic DNA of the offspring demonstrating heterozygous, homozygous and wild type genotypes.

6.2.2 Optimization of a lentivirus Cre-mediated DNA recombination system for *in vitro* knockout of murine *Hp1bp3* in lineage-negative (Lin^-) HSCs

HSCs are a cell fraction that has the ability to self-renew and replenish the entire blood system. Extensive studies have suggested that HSCs in the BM are in the quiescent state of the cell cycle (Arai and Suda, 2007, Orford and Scadden, 2008). Quiescence has been suggested to protect stem cells from exhaustion (Orford and Scadden, 2008) as well as prevent them from developing mutations and malignant transformation that lead to cancer stem cells (Park and Gerson, 2005, Lobo et al., 2007). However, this quiescence makes integration of the viral genome very challenging despite the capability of lentivirus for transfecting dormant cells (Naldini et al., 1996, Kafri-Blömer et al., 1997). Therefore, optimizing a lentivirus transduction protocol was a critical step for deciphering the role of HP1BP3 in haematopoiesis using a conditional *Hp1bp3* knockout mouse model.

In order to generate lentivirus particles expressing Cre recombinase enzyme fused GFP (CRE-GFP) and GFP (control), HEK293T cells were initially transfected with third-generation LV-expressing vectors as described in *Chapter 2*. Following the virus harvesting, validation was performed to evaluate the titration efficacy of the LV particles produced. The validation was achieved by transfecting HEK293T cells with virus supernatant (Figure 6-2 A). Around 5×10^4 cells/ml HEK293T cells were cultured in a 6-well plate with the addition of 100 µl unconcentrated LV-Cre-EGFP particles generated 48 hrs, 72 hrs and 96 hrs post-transfection (Figure 6-2 B–D).

The *Hp1bp3*$^{fl/fl}$ mouse model harbours a floxed *Hp1bp3* allele in which exon 2 of the *Hp1bp3* gene is flanked between two loxP sites (Section 6-2). Isolating the Lin$^-$ fraction from the BM of these mice and transducing them with LV-Cre-EGFP particles would lead to *Hp1bp3* deletion. Consequently, the biological effects of *Hp1bp3* knockout in these cells could be further explored *in vitro.*

The Lin$^-$ fraction of the BM contains the LT- and ST-HSCs as well as the multipotent hematopoietic progenitor cells (MPPs). This fraction lacks mature blood cells such as T-cells, B-cells, monocytes, macrophages, granulocytes, erythrocytes and their committed precursors (Adams and Scadden, 2006). Murine BM cells can be isolated from the tibia and femur and the Lin$^-$ fraction can be then purified. The Lin$^-$ fraction can be purified using either fluorescence-activated cell sorting (FACS) or magnetic-activated cell sorting (MACS) cell separation. Here, we used a commercially available MACS separation magnetic bead lineage depletion kit from Miltenyi Biotec (*Chapter 2*).

Previous studies have suggested the use of cytokine 'pre-stimulation' to enable virus transduction. Cytokine pre-stimulation is a method developed for inducing the proliferation of stem cell populations to facilitate virus integration (Peters et al., 1996, Yonemura et al., 1996, Mostoslavsky et al., 2005). This method involves using a cocktail of cytokines, including IL-3, IL-6 and stem cell factor (SCF) (Barrette et al., 2000). Here, we developed and optimized a strategy for isolating and purifying the Lin$^-$ as well as transducing HSCs in the Lin$^-$ fraction of mouse BM, which are mostly in a quiescent G0 state. Several factors, including cell fraction purity, cytokine

stimulation period and functional titre or MOI needed to achieve the maximum transduction of the HSCs, were tested and optimized. Briefly, the femurs and tibias were isolated, and the BM cells were then extracted.

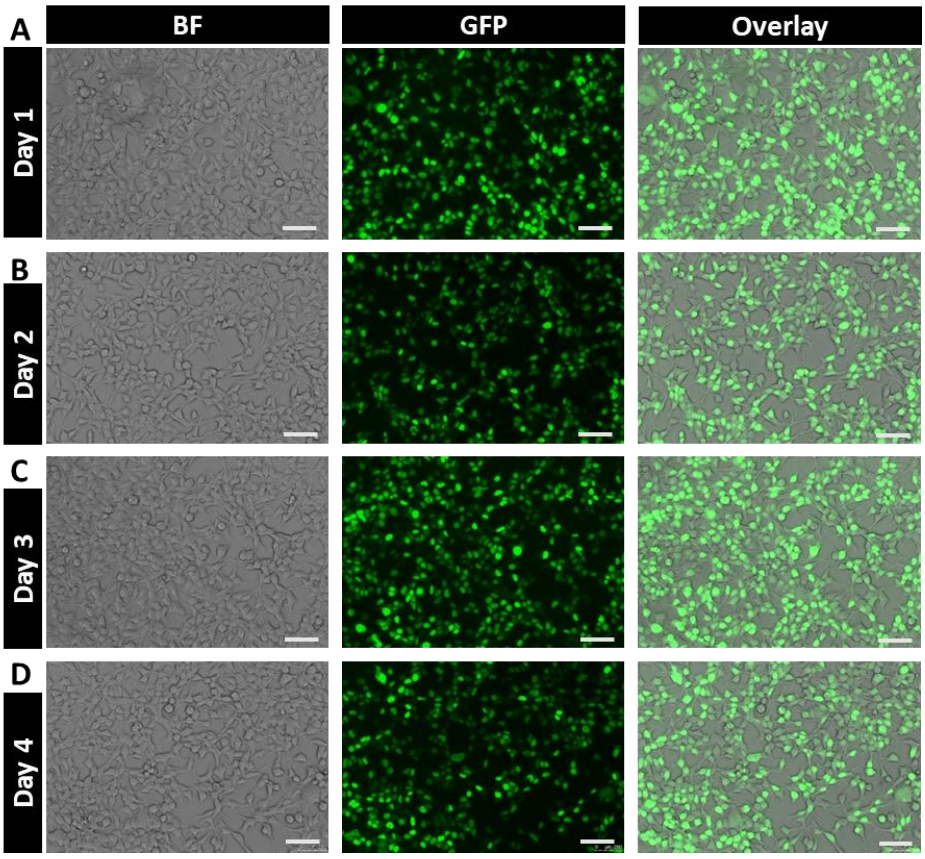


Figure 6-2: Cre-recombinase lentivirus generation and validation. (A) Representative image demonstrating the lentivirus production, human HEK 293T cells were transfected with Cre-recombinase mix. **(B-D)** The validity of the produced LV carried out by transduction of HEK 293T cells using 100µl of the collected LV supernatant after 24, 48 and 72 hrs post-transfection indicate the integration of the virus into the cell. Scale bar: 75µm

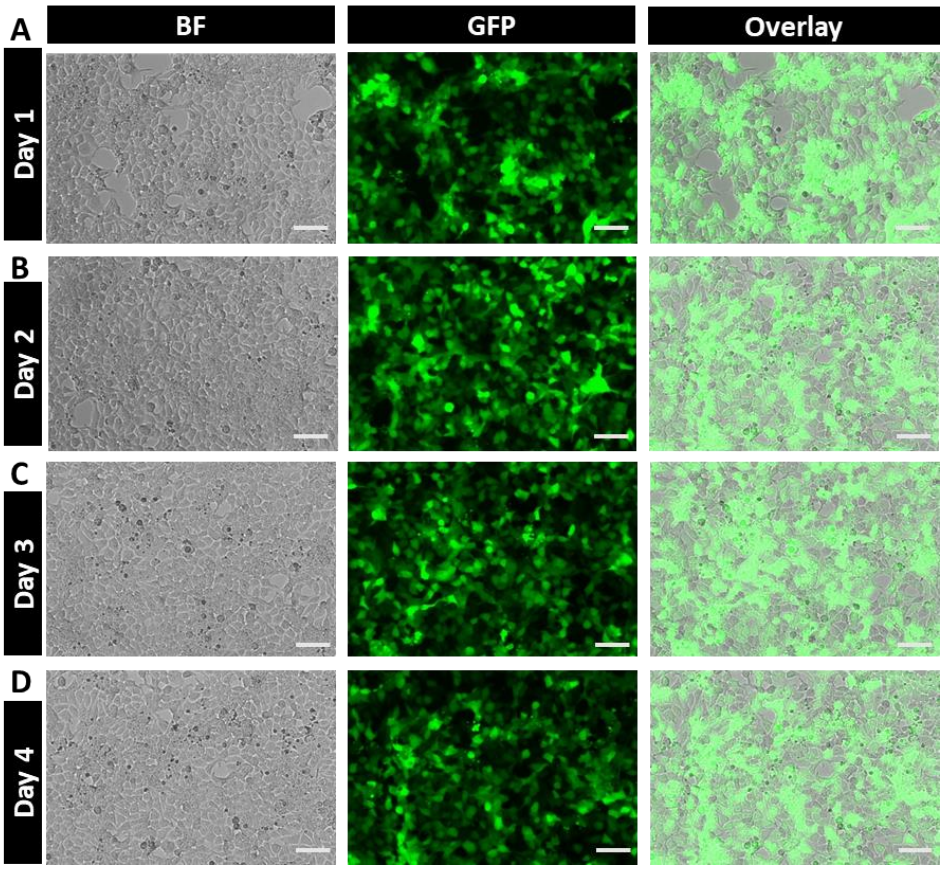


Figure 6-3: Control lentivirus production and validation. (A) Representative image demonstrating the lentivirus production, human HEK 293T cells were transfected with a control mix. **(B-D)** The validity of the produced LV carried out by transduction of HEK 293T cells using 100µl of the collected LV supernatant after 24, 48 and 72 hrs post-transfection indicate the integration of the virus into the cell. Scale bar: 75µm

The Lin^- fraction was purified using the MACS separation kit, which is capable of depleting mature hematopoietic cells. This procedure involved using a cocktail of biotin-conjugated antibodies against a panel of lineage antigens such as CD5, BB20, CD11b and anti-biotin microbeads to label and deplete all mature blood cells such as T-cells, B-cells, monocytes, macrophages, granulocytes and erythrocytes from the BM (*Chapter 2*). The purity of the isolated cells was then examined by staining a fraction of the cells with either florescent anti-biotin or FACS Lin^- cocktail. The HSCs were cultured with StemSpan medium and pre-stimulated with 100 ng SCF, 10 ng IL-6 and 100 ng IL-3 to enhance the transduction efficacy for 3 days. The cells were then transduced with different MOIs of lentivirus particles depending on the total plated cell number (Figure 6-4).

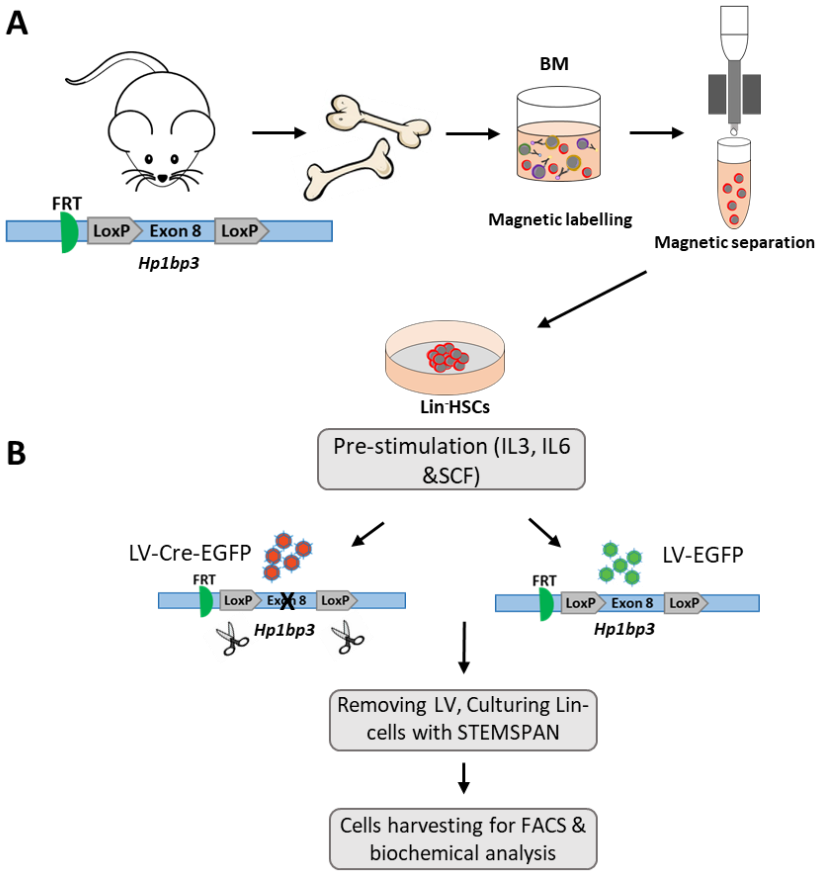


Figure 6-4: Schematic demonstration of murine Lin$^-$ HSCs isolation and *in-vitro* knock-out of *Hp1bp3*. (A) Schematic representation of Lin$^-$HSCs isolation and purification. Bone marrow total cells were isolated and Lin$^-$ fraction was purified using magnetic labelling (MACS separation). **(B)** HSCs were cultured in STEMSAPN and pre-stimulated using cytokines cocktail including IL3, IL6 and SCF around 16 hrs prior to transduction. Cells were transduced with Cre-LV particles to mediate recombination in *Hp1bp3*$^{fl/fl}$ mouse leading to *Hp1bp3* deletion *in-vitro* or with EGFP-LV as a control. Around 72 hrs post-transduction, the cells were washed and cultured in STEMSPAN medium.

The production of a high-titre virus was crucial for achieving the highest transduction efficiency of Lin$^-$ HSCs, due to the inactive nature of the cells. This facilitates the acquisition of robust HSC knockouts by Cre recombinase within a short period. The cells were transduced with different multiplicity of infection (MOIs) of lentivirus particles, and incubated for 16 hrs. The virus was then removed, and the cells were incubated with fresh StemSpan medium for 72 hrs (Figure 6-4). EGFP expression was examined using a fluorescence microscope (Figure 6-5). Genotyping PCR analysis was accomplished to examine the integration of Cre recombinase and *Hp1bp3* deletion (Figure 6-5).

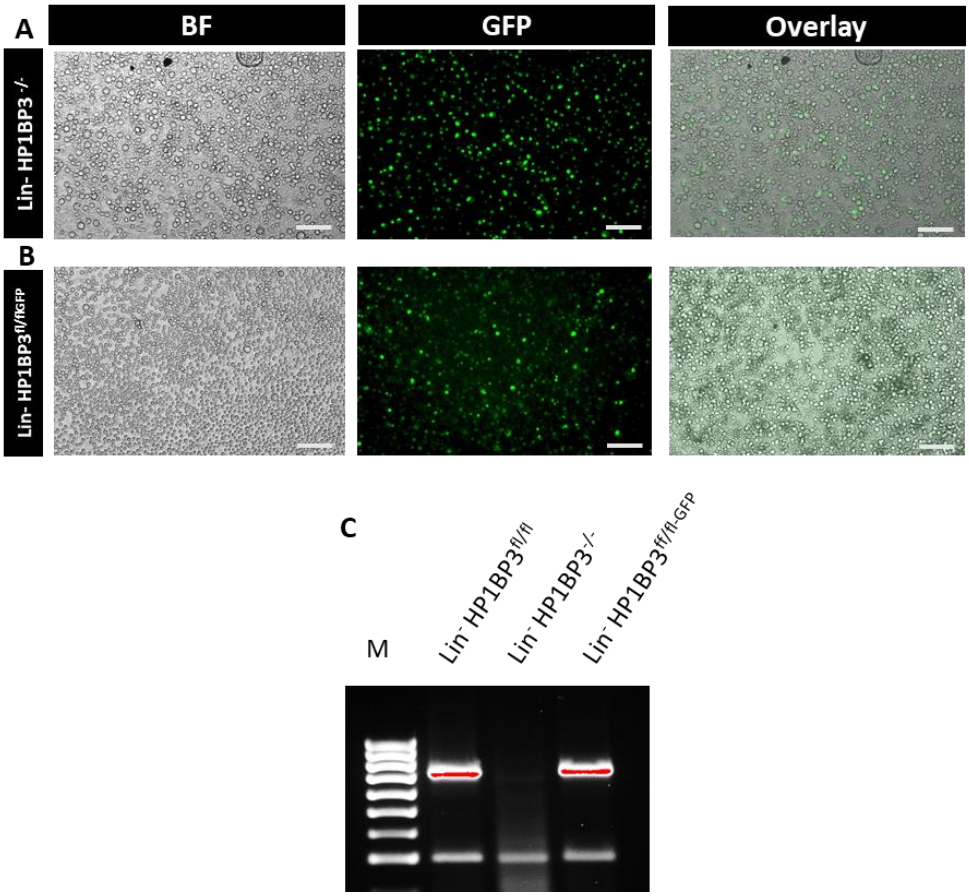


Figure 6-5: Efficient Cre-LV mediated *Hp1bp3* in-vitro knock-out in mouse Lin$^-$ HSCs. (A-B) representative image demonstrating of EGFP expression in murine HSCs transduced with Cre-recombinase (CRE-GFP) LV and GFP control LV particles indicate a high transduction efficiency. Scale bar:

75µm. **(C)** Genomic DNA PCR genotyping analysis for the floxed region of exon 8 of *Hp1bp3* confirming the Cre-loxP mediated recombination of *Hp1bp3* in the transduced cells.

6.2.3 Deletion of *Hp1bP3* induced H3K9me3 in murine Lin$^-$ HSCs

As mentioned above, expression of HP1BP3 alters the expression of two heterochromatin and euchromatin markers: H3K9me3 and H3K9ac respectively in AML cell lines (*Chapter 3*). Therefore, we intended to investigate their expression in the Lin$^-$HSCs after *Hp1bp3* deletion using immunoblotting analysis. For this, the protein extracts from the control cells were isolated from cells transduced with lentivirus expressing an empty vector, pLVX-EGFP control backbone vector. Protein extracts from the *Hp1bp3* knockout cells were taken from the cells infected with lentivirus expressing Cre recombinase. Our data here firstly, confirmed the expression of HP1BP3 in the Lin$^-$ cells (Figure 6-6). Interestingly, the knockout of HP1BP3 induced the level of H3K9me and reduced H3K9ac level (Figure 6-6), which is in line with the previous findings in AML cells (Chapter 3). Moreover, it shows the efficient depletion of HP1BP3 levels in the transduced cells (Figure 6-6).

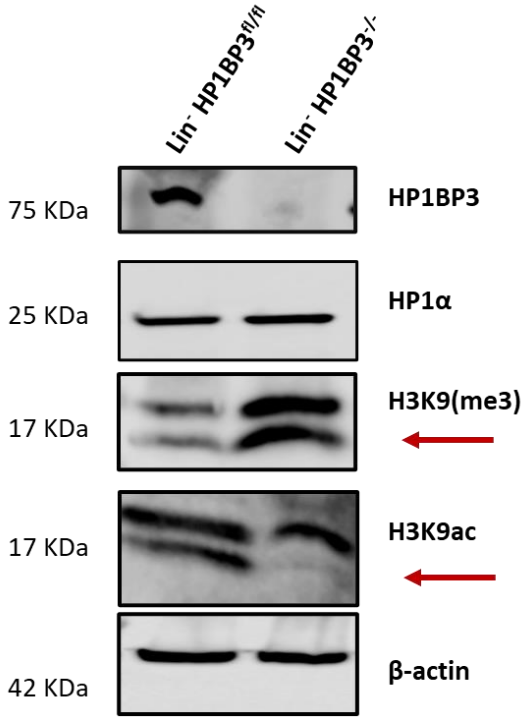


Figure 6-6: Loss of Hp1bp3 induced the expression of H3K9me3 in the Lin- HSCs. Western blotting analysis of HP1BP3 and chromatin markers in Lin- HSCs. Total protein extracts, 100 µg of were run on 4-20 % SDS-PAGE, transferred to PVDF membranes and immunoblotted for (anti-HP1BP3, -HP1α, -H3K9me3, -H3K9ac and-H3) antibodies, β-actin was used as loading control.

6.2.4 Loss of *Hp1bp3* induces early differentiation in murine Lin- HSCs

HSCs are the best phenotypically/functionally characterized adult somatic stem cell population. This facilitates the study of HSCs and their progenitors via investigation of the expression of their specific phenotypical surface markers using FACS-based analysis. Murine LT-HSCs lack the expression of CD34, are negative for lineage markers and express high levels of both c-Kit and Sca-1 (Takano et al., 2004). An LT-HSC can asymmetrically divide into another LT-HSC and a MPP cell with limited self-renewal capacity

(Takano et al., 2004). However, ST-HSCs express high levels of the surface marker CD34 and have a similar immunophenotype expression of Lin^-, c-Kit and Sca-1 compared to LT-HSCs (Wilson et al., 2008). The ST-HSC can differentiate into more differentiated progenitor cells (Cabezas-Wallscheid et al., 2014). The main objective of the present experiment was to investigate whether knocking out *Hp1bp3* in Lin^- HSCs would influence early stem cell differentiation. To achieve that, the Lin^- HSCs were stained for the surface marker CD34 that can distinguish between LT-HSCs, which are $CD34^-$, and ST-HSCs, which are $CD34^+$ (Cabezas-Wallscheid et al., 2014). Around 2.5 × 10^5 Lin^- HSCs were transduced with lentivirus expressing EGFP only or Cre-EGFP to achieve Lin^- *Hp1bp3*$^{fl/fl}$ control and Lin^- *Hp1bp3*$^{-/-}$ knockout, respectively, as described earlier (*Chapter 2*). The cells were then fixed and stained for surface markers at day 3 post-transduction, followed by FACS analysis as outlined in *Chapter 2*. Previous work by our group showed that the overexpression of HP1BP3 in murine Lin^- HSCs significantly increased the LT-HSCs and reduced the ST-HSCs (unpublished). Interestingly, we found that the percentage of LT-HSCs was significantly decreased from 37.5% to 25% in *Hp1bp3*-deleted Lin^- HSCs compared to the control cells. However, the percentage of the ST-HSCs was significantly increased from 62.5% to 75% as a consequence of *Hp1bp3* depletion (Figure 6-7 A-B). FACS analysis of surface marker expression in the murine Lin^- HSCs was carried out by first gating on the Lin^- HSC population, followed by gating on the HSC-EGFP–expressing population. All FACS experiments were carried out and analysed using the Astrios cell sorter with the help of Dr David Onion at the flow cytometry unit, University of Nottingham.

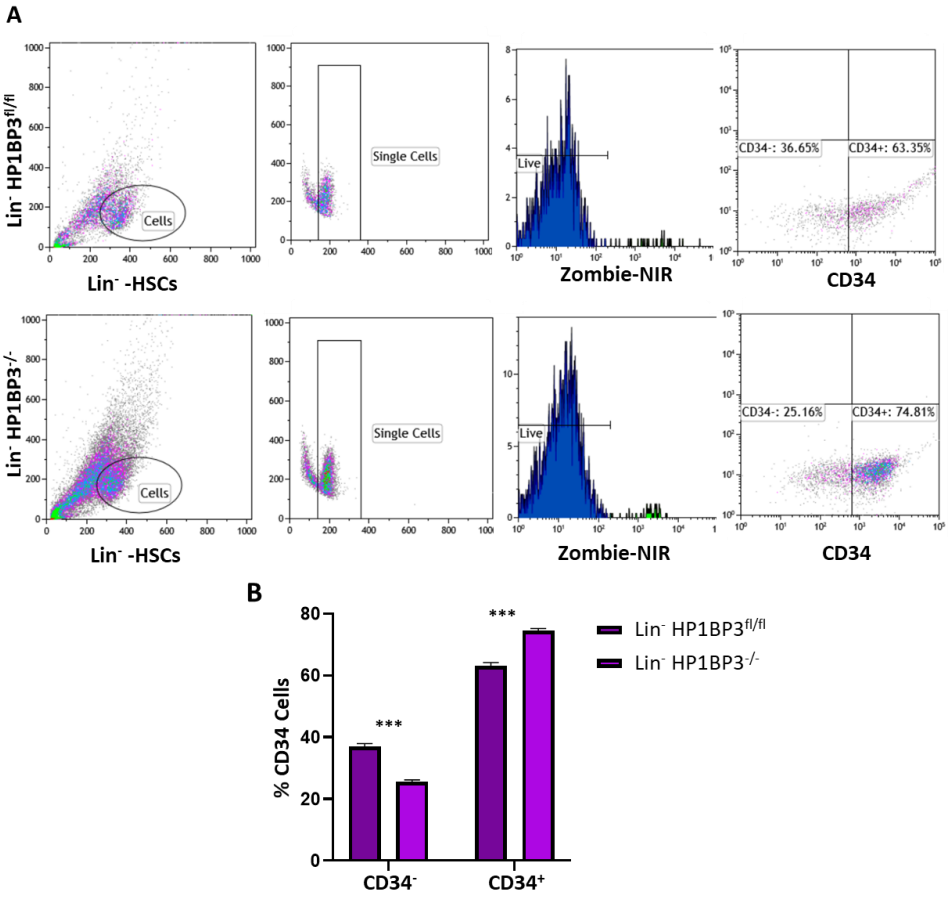


Figure 6-7: Deletion of Hp1bp3 leads to early haematopoiesis imbalance. **(A)** FACS analysis for CD34 expression in Lin$^-$ *Hp1bp3*$^{fl/fl}$ and Lin$^-$ *Hp1bp3*$^{-/-}$ HSCs. FACS data indicates a significant change in the percentages of CD34$^-$ HSCs (LT-HSCs) CD34$^+$ HSCs (ST-HSCs) due to *Hp1bp3* depletion. **(B)** Statistical analysis indicates a significant decrease in the percentage of LT-HSCs from 37.5% to 25% in *Hp1bp3*-deleted Lin$^-$ HSCs compared to the control cells and a significant increase in the ST-HSCs from 62.5% to 75% due to HP1BP3 deletion. The error bars show the SD of three biological repeats (***p<0.001). This experiment was performed in triplicate on at least three independent occasions.

6.2.5 *Hp1bp3* knockout impaired HSCs while inducing MMP3 population, a subset known for its myeloid potential

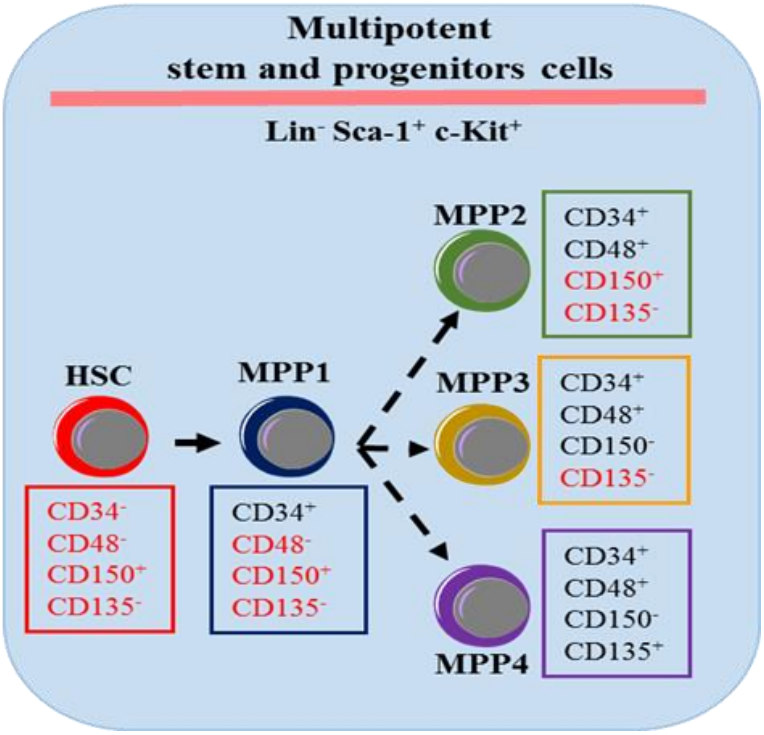
The LT-HSC ($CD34^-$ in mice) exists at the top of the hematopoietic hierarchy. LT-HSCs can self-renew and generate multipotent progenitor (MPP) cells to maintain homeostasis throughout the lifetime of the organism (Osawa et al., 1996). The transition from LT-HSCs to multipotent cells occurs by the acquisition and loss of expression' of a number of immunophenotype surface markers (Figure 6-8A). MPPs have been immunophenotypically divided into four populations known as MPP1, MPP2, MPP3 and MPP4 through the gain of expression of CD34, CD48 and CD135 and loss of the expression of CD150, respectively (Osawa et al., 1996, Ema et al., 2006). There have been extensive attempts to identify the gene expression and epigenome modification that regulate self-renewal and differentiation during haematopoiesis.

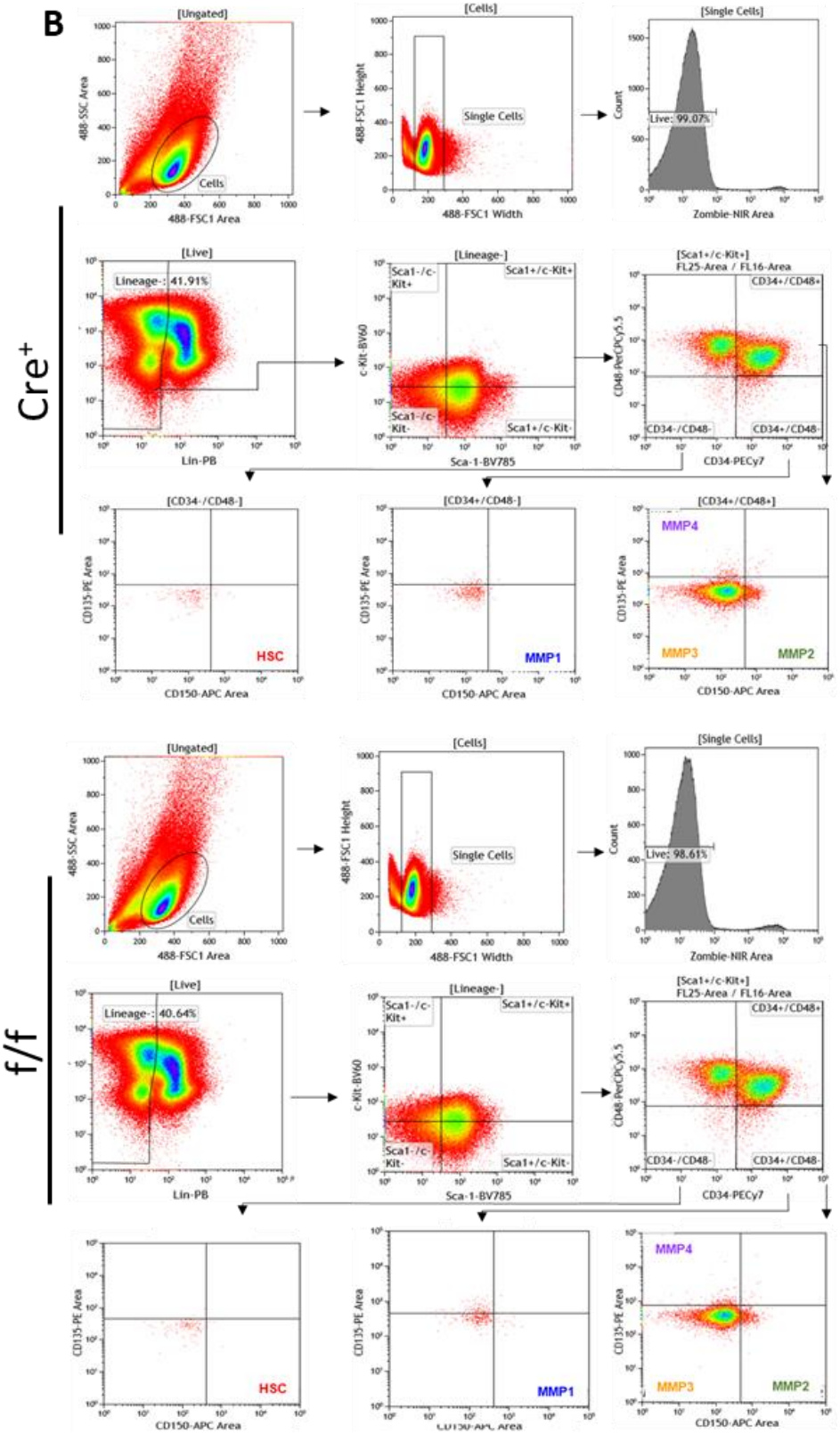
To further investigate the *in vitro* differentiation of HSCs in our *Hp1bp3* knockout models, we cultured Lin^- HSCs for 3 days in lentivirus transduction conditions described above to achieve the highest *Hp1bp3* knockout percentage HSCs. This was followed by cytokine pre-stimulation with SCF, IL-6 and IL-3 in a serum-free medium. The cells were then fixed and stained for a panel of seven different surface markers (Figure 6-8B). This included Lin^-, Sca1, c-Kit, CD34, CD48, CD150 and CD135. The percentage of the five stem/progenitor populations related to HSC and MPP1–MPP4 in the Lin^- *Hp1bp3* knockout and Lin^- *Hp1bp3* $^{fl/fl}$ mice were examined by FACS. The

use of Lin^- antibody enabled us to gate the Lin^- from the mature cells (Lin^+ cells) (Figure 6-8), and each quadrant was set up according to the isotype controls for each antibody used. Interestingly, our data show that the depletion of HP1BP3 decreased the expression of the LT-HSCs; the percentage of LT-HSCs (LSK, $CD34^-$, $CD48^-$, $CD135^+$ and $CD150^-$) was reduced from 5% to 2.5% in the knockout cells as compared with the control cells (Figure 6-8C). The MPP1 (LSK, $CD34^+$, $CD48^-$, $CD135^+$ and $CD150^-$) population is very similar to the LT-HSC population, with short-term self-renewal (Osawa et al., 1996, Ema et al., 2006, Cabezas-Wallscheid et al., 2014). Here, we found that the deletion of *Hp1bp3* in murine Lin^- cells increased the percentage of MPP1 cells (Figure 6-8). A comprehensive work carried out by Cabezas-Wallscheid *et al*. showed that MPP2 generates long-term myeloid, B-cell and T-cell progeny upon transplantation (Cabezas-Wallscheid et al., 2014). In contrast, MPP3 and MPP4 show myeloid bias and lymphoid bias, respectively (Cabezas-Wallscheid et al., 2014). Our study shows that the depletion of HP1BP3 significantly induced the percentage of the main myeloid progenitor MPP3 (LSK, $CD34^+$, $CD48^+$, $CD135^-$ and $CD150^-$); however, the percentage of MPP2 (LSK, $CD34^+$, $CD48^+$, $CD135^+$ and $CD150^-$) and MPP4 (LSK, $CD34^+$, $CD48^+$, $CD135^-$ and $CD150^+$) populations remained unchanged (Figure 6-8). Collectively, these data suggest that HP1BP3 is essential for maintaining the LT-HSC population and may also regulate haematopoiesis. However, as 50% of the cells were Lin^+ which could be due to the cytokine stimulation for virus transduction, this experiment will be repeated in the future using different concentration of the cytokines cocktail (IL3- IL6 and SCF). Moreover, it suggests that the use of

LV transduction is not ideal for the maintenance of HSCs and inevitably leads to differentiation which is one of the limitations of this project. Additionally, the data obtained from this experiment at this stage is only indicative of the Lin^- subpopulation and we will need to perform a competitive repopulation assay (CRP) *in vivo* to examine HSC function after *HP1BP3* deletion. For this, Lin^- *Hp1bp3*$^{-/-}$ and Lin^- *Hp1bp3*$^{fl/fl}$ will be transplanted into lethally irradiated mice; eventually, the relative reconstitution of the two populations in the transplanted mice will be measured in the peripheral blood.

A


Multipotent
stem and progenitors cells
Lin- Sca-1+ c-Kit+
HSC
CD34-
CD48-
CD150+
CD135-
MPP1
CD34+
CD48-
CD150+
CD135-
MPP2
CD34+
CD48+
CD150+
CD135-
MPP3
CD34+
CD48+
CD150-
CD135-
MPP4
CD34+
CD48+
CD150-
CD135+


B
Cre+
f/f
[Ungated]
488-SSC Area
488-FSC1 Area
Cells
[Cells]
488-FSC1 Height
488-FSC1 Width
Single Cells
[Single Cells]
Count
Zombie-NIR Area
Live: 99.07%
Live: 98.61%
[Live]
Lineage-: 41.91%
Lineage-: 40.64%
Lin-PB
[Lineage-]
Sca1-/c-Kit+
Sca1+/c-Kit+
Sca1-/c-Kit-
Sca1+/c-Kit-
c-Kit-BV60
Sca-1-BV785
[Sca1+/c-Kit+] FL25-Area / FL16-Area
CD34+/CD48+
CD34-/CD48-
CD48-PerCPCy5.5
CD34-PECy7
[CD34-/CD48-]
[CD34+/CD48-]
[CD34+/CD48+]
CD135-PE Area
CD150-APC Area
HSC
MMP1
MMP2
MMP3
MMP4

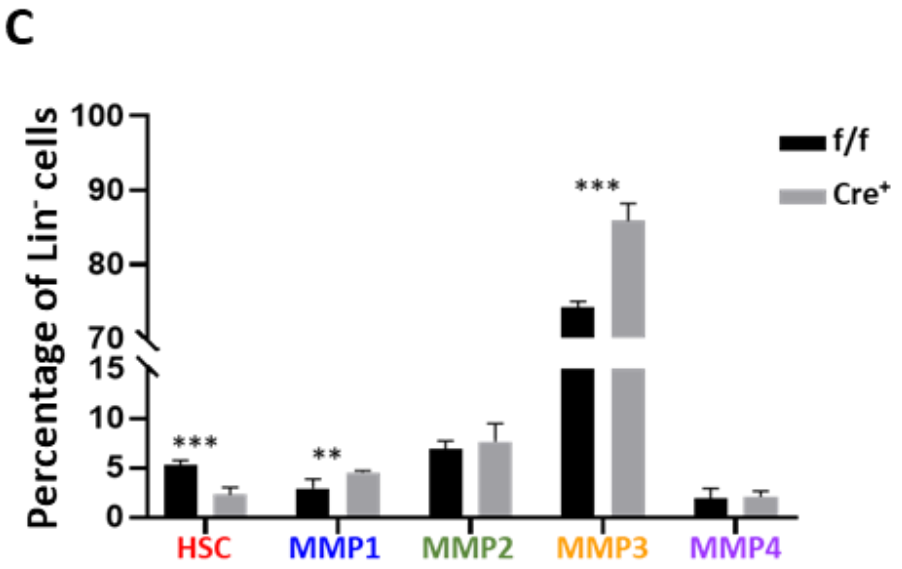


Figure 6-8: *Hp1bp3* inactivation reduced HSCs but increased the main myeloid multipotent progenitor MPP3. **(A)** Mouse haematopoiesis. HSCs give rise to four multipotent progenitors MPP1-4 by acquiring and losing the expression of cell surface markers: CD34, CD48, CD135 and CD150. **(B)** FACS analysis for HSCs and MPPs in Lin$^-$*Hp1bp3*$^{-/-}$ and Lin$^-$*Hp1bp3*$^{fl/fl}$ control cells. **(C)** Statistical analysis suggests considerable reduction in the percentage of HSCs (LSK, CD34$^-$, CD48$^-$, CD135$^+$ and CD150$^-$) and significant increase in the MPP1 (LSK, CD34$^+$, CD48$^-$, CD135$^+$ and CD150$^-$) and MPP3 (LSK, CD34$^+$, CD48$^+$, CD135$^-$ and CD150$^-$) progenitor due to *Hp1bp3*-knockout. The error bars show the SD of three biological repeats (***p<0.001). This experiment was performed in triplicate on at least three independent occasions.

6.2.6 Hp1bp3 depletion leads to differentiation towards mature cell lineages in murine Lin$^-$ HSCs

HSCs are distinctive in their ability to self-renew and reconstitute all blood lineages (Orkin and Zon, 2008). This population can be considered a morphologically homogenous population of cells; however, it appears to be heterogeneous based on its potential for differentiation and proliferation (Adolfsson-Månsson et al., 2005, Forsberg et al., 2006). Mature HSCs lack

self-renewal activity; however, when stimulated with cytokines such as IL-3, IL-6 and SCF, they form blast progenitor colonies committed to differentiation to mature blood cells (Metcalf, 1991, Metcalf and Nicola, 1991). Culturing HSCs in a serum-free medium and stimulating them with cytokines has been reported to be the best approach for their survival and expansion (Poloni et al., 1997).

Our data above show that the deletion of *Hp1bp3* promotes differentiation. These data prompted us to further stain and investigate the mature cells *in vitro* in our *Hp1bp3* knockout models. For this, Lin^- HSCs were cultured for 3 days, as described earlier, using our optimized lentivirus transduction strategy to achieve the highest HP1BP3 depletion. This was followed by pre-stimulation with cytokine cocktail containing IL-3, IL-6 and SCF in StemSpan medium every 2–3 days up to 14 days. The cells were then fixed and cytospun onto glass slides, followed by Giemsa staining, a widely used stain for examining the nuclear and cytoplasmic morphology of the various blood cells (Figure 6-9 A). The slides were then scanned, and 1000 cells were quantified in each view in triplicates. Different blood cell lineages were classified according to their morphology (Figure 6-9 D). Interestingly, the percentage of LT-HSCs was significantly decreased in the *Hp1bp3* knockout cells compared to control cells. This reduction was from 57% to 28.11% due to HP1BP3 depletion. Moreover, the percentages of the mature cells were increased in the knockout cells (Figure 6-9 B). These findings suggest that HP1BP3 could regulate ST-HSC haematopoiesis. However, further studies for myeloid differentiated cells would be needed using FACS analysis.

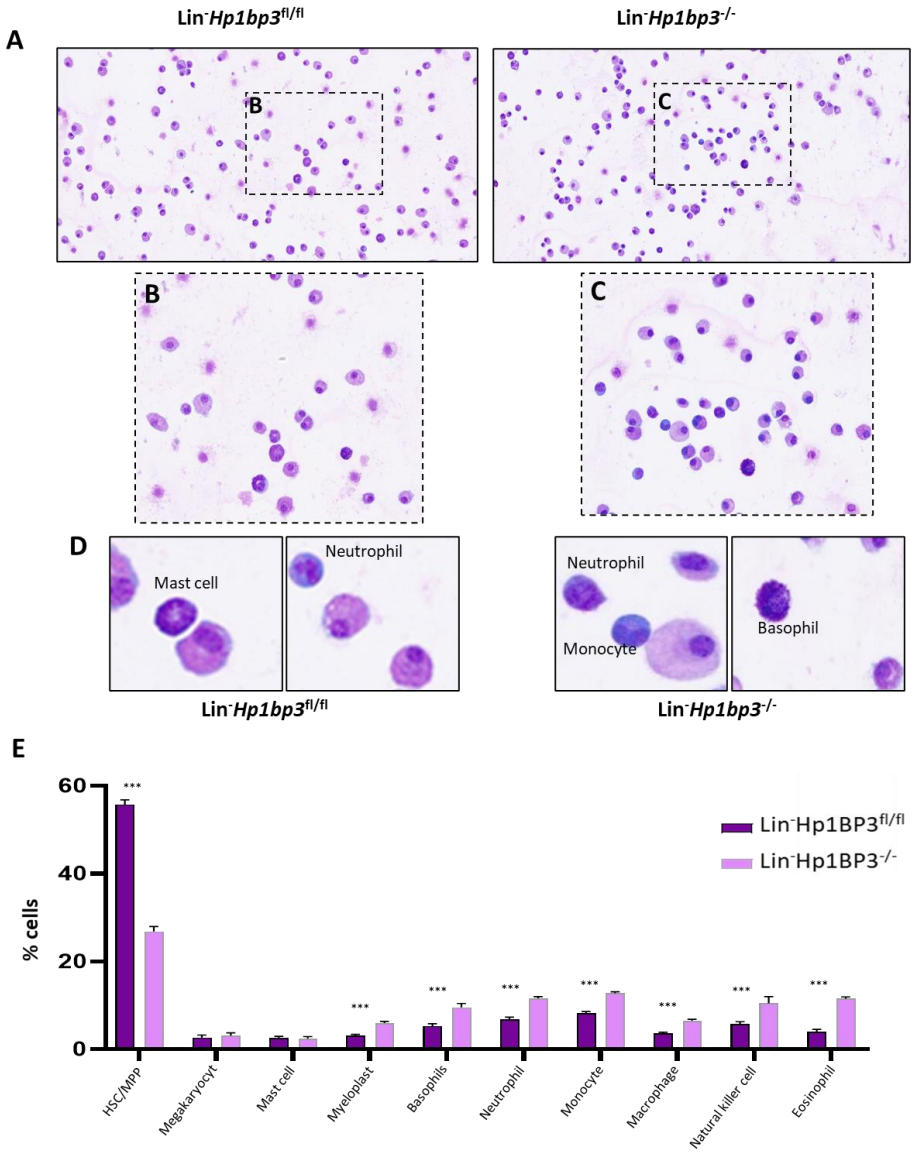


Figure 6-9: Knockout of *Hp1bp3* impaired HSCs and increased cells differentiation. (A) Representative images of Giemsa stain in Lin^{-}*Hp1bp3*$^{-/-}$ and Lin^{-}*Hp1bp3*$^{fl/fl}$ control cells. **(B-C)** Magnified images. **(D)** Examples of mature blood lineages in Lin^{-}*Hp1bp3*$^{-/-}$ and Lin^{-}*Hp1bp3*$^{fl/fl}$ control cells. **(E)** Statistical analysis suggests significant reduction in the number of HSCs and significant increase in differentiated cells due to *Hp1bp3*-knockout. The error bars show the SD of three biological repeats (***p<0.001). This experiment was performed in triplicate on at least three independent occasions.

6.3 Discussion

HP1BP3 is a novel chromatin modulator involved in the regulation of gene expression. In this chapter, we demonstrate that HP1BP3 may regulate murine HSC differentiation and haematopoiesis, using an *in vivo* transgenic mouse model.

The development of HSC-specific Cre lines has remained challenging for many researchers over the last three decades (Kuhn et al., 1995, Georgiades et al., 2002, Croker et al., 2004, Lazer and Katzav, 2011). All generated HSC-Cre lines such as Myxovirus resistance 1 (*Mx1*-Cre), *Vav*-Cre, *Tie2*-Cre and *Tie2*- are expressed in other cells/tissues, and they have several other limitations (Kuhn, Schwenk et al. 1995, de Boer et al., 2003, De Lange et al., 2008, Park et al., 2012). Hence, Cre-mediated *Hp1bp3* knockout in floxed Lin^- HSCs was induced *ex vivo* using LV particles expressing Cre enzyme. Therefore, developing and optimising a lentivirus transduction technique that is capable of delivering the Cre recombinase into Lin^- HSCs was a vital stage in this study. For this, we initially optimized a high-transfection efficiency system to transfect more than 95% of HEK293T cells. The cells were transfected with a mixture of constructs containing Cre-EGFP vector and two packaging plasmids using PEI transfection reagent. The capability of this generated virus for transduction was tested continuously throughout virus harvesting by infecting plated HEK293T cells with unconcentrated virus. Our data show the high transduction efficiency of the generated virus (Figure 6-2). However, research has shown that the ability to efficiently transduce non-dividing and quiescent cells such as HSCs requires very high virus titre (Ide et al., 2008, Thomas and Mostoslavsky, 2014, Jang et al., 2020).

Therefore, following lentivirus supernatant harvesting, the collected lentivirus was concentrated using ultracentrifugation.

Moreover, the purification and transduction of murine Lin^- HSCs from total BM is another crucial step in obtaining optimal delivery and expression of the transgenic Cre recombinase (Thomas and Mostoslavsky, 2014). To achieve that, the Lin^- fraction was isolated and purified using MACS separation methodology. Pre-stimulating Lin- HSCs facilitates their transduction (Miyoshi, 2004, Mostoslavsky et al., 2005, Morgan et al., 2017). Therefore, we pre-stimulated the purified murine Lin^- cells with a cocktail of cytokines containing IL-3, IL-6 and SCF for 16 hrs prior to transduction with LV Cre-EGFP (Figure 6-4). The integration of Cre recombinase was then tested by examining the GFP expression and Cre-mediated DNA recombination, and *Hp1bp3* deletion was investigated using genomic PCR and immunoblotting (Figure 6-5).

Optimizing a robust lentivirus system as well as the best conditions for Lin^- HSC culture/transduction to induce Cre recombinase *in vitro* allowed us to look at the consequences of *Hp1bp3* inactivation and to further explore the role of HP1BP3 in haematopoiesis through modulating the chromatin state at H3K9 residue. We initially investigated the effect of Hp1bp3 deletion on the expression of the chromatin markers H3K9me3 and H3K9ac. Interestingly, in line with the initial findings, our data here showed that the knockout of HP1BP3 induced the expression of H3K9me3 and reduced the level of H3K9ac (Figure 6-6).

Moreover, the effect of the loss of HP1BP3 on the expression of cell surface markers and morphology was analysed. The use of immunophenotypic cell surface markers has proven useful for studying HSCs. As murine LT-HSCs are $CD34^-$ (Park et al., 2002); we therefore stained the Lin^- cells with CD34 and analysed them with FACS. Our data show that the loss of HP1BP3 significantly reduced the number of LT-HSCs and increased the number of ST-HSCs as compared to the control cells (Figure 6-6). Moreover, based on the classification of the LT-HSCs and the four MPPs (MPP1–4) according to the expression of cell surface markers (Ema et al., 2006, Cabezas-Wallscheid et al., 2014), the Lin^- *Hp1bp3*$^{-/-}$ cells and Lin^- *Hp1bp3*$^{fl/fl}$ control cells were analysed with FACS. The cells were stained for a panel of surface markers, i.e. Lin^{neg}, Sca-1, c-Kit, CD34, CD135, CD150 and CD48 (Figure 6-8). Our data show that the knockout of *Hp1bp3* significantly reduced the number of HSCs and increased the number of MPP3 cells in Lin^- *Hp1bp3*$^{-/-}$ cells as compared to the control cells (Figure 6-8). Cabezas-Wallscheid *et al*. have reported that upon transplantation, MPP2 cells generate LT-myeloid and lymphoid progenies; however, MPP3 and MPP4 populations were biased towards generating myeloid or lymphoid cells, respectively (Cabezas-Wallscheid et al., 2014). Accordingly, our data suggest that the loss of HP1BP3 induces the main myeloid progenitor MPP3 in murine Lin^- fractions. This could be further studied in the future using animal reconstitution assays.

Furthermore, the morphology of the HSCs was examined after *Hp1bp3* inactivation using Giemsa staining. Consistent with the data in this chapter, we found that the *Hp1bp3* knockout considerably lowered the HSC and MPP

population numbers and significantly increased the number of differentiated cells (Figure 6-9). Collectively, these data suggest that HP1BP3 may regulate murine haematopoiesis. This regulation could be through regulating gene expression involved in self-renewal and differentiation, however further transcriptomic analysis is needed to investigate this regulation.

CHAPTER 7

General Discussion

7.1 Overview

7.1.1 HP1BP3-knockdown/ knockouts promotes the myeloid progenitor cells differentiation and apoptosis of AML cells

Hematopoietic Stem Cell (HSC) homeostasis has been extensively studied by many researchers for decades since the discovery of this cell population by Siminovitch et al. in 1963 (Siminovitch et al., 1963). Their revolutionary effort led to the 'HSC theory', which states that HSC self-renewal and differentiation need to be precisely balanced (Smith et al., 1991, McCulloch and Till, 2005, Jiang et al., 2019). HSC homeostasis can be regulated by genetic factors or epigenetic factors as well as the hematopoietic microenvironment. Dysregulated homeostasis can lead to the formation of serious hematopoietic malignancies, for example excessive HSC self-renewal or differentiation blockage may lead to leukaemia. Recently, most studies are focusing on the epigenetic modifications that alter the phenotype without any genotype alterations and implicate HSC fate and hematopoietic diseases including AML. Numerous reports strongly point to mutations in epigenetic regulators as a leading cause of AML initiation and progression (Bullinger et al., 2010, Busque et al., 2012, Stasik et al., 2020). These mutations in epigenetic modifiers include a wide range of epigenetic writer, eraser and reader proteins (Sun et al., 2018). Histone post-translational modifications may impact the core histones in heterochromatin–euchromatin conversion; however, the identity of the heterochromatin-associated proteins and their binding proteins has remained largely unclear.

Despite all the advances in proteomic and transcriptomic technologies, which have deepened our knowledge of the epigenetic regulations associated with haematopoiesis, it is still difficult to accurately identify the exact role of each protein/gene involved in this regulation. Therefore, the role of many epigenetic events, particularly chromatin-associated proteins, remains unclear. Here, the role of the chromatin-binding protein HP1BP3 in haematopoiesis was investigated using a conditional knockout mouse model. In this model, exon 8 of *Hp1bp3* is flanked between two *loxP* sites, which allowed us to study its role in a tissue/cell-specific manner. As far as we know, this is the first study using a conditional *in vitro* knockout model, as it has been reported previously that conventional knockout of *Hp1bp3* was lethal (Garfinkel et al., 2015). Therefore, these *in vitro* experiments may enable better understanding of the role of HP1BP3 in haematopoiesis.

In this study, we demonstrate that HP1BP3 may regulate murine haematopoiesis. Using FACS analysis for immunophenotypic cell surface markers, we were able to investigate the percentage of long term-hematopoietic stem cells (LT-HSCs) and multipotent progenitors; MPP1, MPP2, MPP3 and MPP4 (MPP1–4) (Figure 6-8). Our data show that the loss of HP1BP3 drastically decreased the number of HSCs in Lin^- *Hp1bp3*$^{-/-}$ cells as compared to the control cells (Figure 6-7). Moreover, it induced the number of MPP3 (Figure 6-7), a subpopulation known for its myeloid potential (Cabezas-Wallscheid et al., 2014). Although we showed an induction in the H3K9me3 level as a result of *Hp1bp3* depletion in the murine Lin^- cells, another study found no significant differences in the overall level of H3K9me3 among HSC-MPPs and fully mature cells (Ugarte et al., 2015).

Given that histone modifications are reversable and the bulk of the Lin^- fraction has different cells with specific molecular markers, it is difficult to conclude the precise mechanism of HP1BP3 at this stage. Further investigations are needed, such as transcriptomic analysis, for each sorted population, i.e. LT-HSCs and MPP1–4, to identify the genes differentially expressed in those populations.

Moreover, loss of *HP1BP3* expression on cell growth activity, clonogenic potential and cell cycle regulation in AML cells was evaluated using loss-of-function analysis. The colony forming unit (CFU) assay suggested that loss of *HP1BP3* impaired clonogenicity by drastically decreasing both the size and colony numbers of MV4-11 cells (Figure 3-15). Moreover, *HP1BP3* downregulation decreased the growth activity by arresting the cells at G0 phase (Figure 3-13 B). These findings confirm the regulation mediated by HP1BP3 as previously reported by Dutta *et al.*, that HP1BP3 regulates G1 duration (Dutta et al., 2014), and it possibly implicates chromosome organisation in mitosis (Hayashihara et al., 2010).

7.1.2 HP1BP3 modulates the chromatin state at the H3K9 residue in HSC and AML cells

Chromatin is a complex of double-stranded DNA wrapped around proteins called histones to form nucleosomes, which further assemble into a complex chromosome architecture (Comings, 1972, Fyodorov et al., 2018). Histones, a fundamental unit of nucleosomes, undergo various covalent post-translational modifications (PTMs) that take place on the histone tails

(Bowman and Poirier, 2015). PTMs could involve methylation of lysine or arginine residues, serine or threonine phosphorylation, lysine acetylation/deacetylation and lysine sumoylation or ubiquitylation (Bowman and Poirier, 2015).

Histone PTMs impact the dynamic of the nucleosome through wrapping/unwrapping, assembly/disassembly to form or disrupt the interactions between the DNA and the core histones. Histone–DNA interaction mainly determines the chromatin states and the dynamic conversion from heterochromatin to euchromatin and thereby DNA accessibility, and ultimately regulates cellular processes (Fyodorov et al., 2018). Extensive efforts have been made to investigate the role of histone PTM regulation in normal homeostasis and cancer-related processes through chromatin state modulation.

Our lab identified several proteins that are targeted by the tumour suppressor gene *FBXW7* for ubiquitin-mediated degradation (Babaei-Jadidi et al., 2011) (Babaei-Jadidi et al., 2019). Heterochromatin-associated protein HP1BP3 is one of those proteins that are targeted by FBXW7. HP1BP3 modulates the entry/exit point of nucleosomal DNA by binding to HP1α (Hayashihara et al., 2010) and maintains chromatin integrity during G1–S phase transition (Dutta et al., 2014). However, the mechanism of HP1BP3 in haematopoiesis and acute myeloid leukaemia (AML) is unclear.

HP1α interacts with H3K9me3 via its chromo-domain, while the methyl-transferases SUV39H1/2 bind to the chromo-shadow domain of HP1α (Peters-O'Carroll et al., 2001, Peng and Karpen, 2009). This complex, i.e.

HP1α–SUV39H is involved in heterochromatin formation and gene silencing (Peters-O'Carroll et al., 2001, Peng and Karpen, 2009). However, modulation of HP1α at chromatin conversion is critical in normal homeostasis and cancer (De Koning et al., 2009). In contrast to the methylation of H3K9, the acetylation of the same lysine residue, which is regulated by histone acetyltransferase, is a well-known euchromatin marker and is enriched at the region of activated genes (Vaute et al., 2002). Dysregulation of histone PTMs due to deregulation of chromatin modifier activity leads to cancer (Hayami et al., 2011, Hamamoto et al., 2015). Consequently, deregulation of H3K9me3 or H3K9ac levels has been considered a hallmark of many cancers, including AML (Müller-Tidow et al., 2010, Chopra and Bohlander, 2015, Monaghan et al., 2019, Dong et al., 2020). Therefore, the main objective of this study is to decipher the role of HP1BP3 underlying the epigenetic reprogramming mechanisms in normal haematopoiesis and leukemogenesis.

Here, we demonstrate that HP1BP3 modulates chromatin conversion, i.e. heterochromatin–euchromatin, by interacting with an evolutionarily conserved heterochromatin protein, HP1α, a hallmark of heterochromatin (Nielsen et al., 2001). The middle region of HP1BP3 binds to the chromoshadow domain of HP1α through a novel PxVxL binding motif at proline 255–leucine 259 (Hayashihara et al., 2010).

We showed that HP1BP3 expression alters the expression of H3K9me3 and H3K9ac, two well-known heterochromatin and euchromatin markers, respectively. We initially found that the high level of HP1BP3 is negatively correlated with H3K9me3 and positively correlated with H3K9ac in nine

AML cell lines (Figure 3-2). Further, using gain- and loss-of-function analysis, we showed that the accumulation of HP1BP3 in MOLM13 cells did not change the expression of HP1α, while it induced the acetylation of H3K9 and reduced the global methylation of the same lysine residue (Figure 3-9). In contrast, the loss of HP1BP3 in MO91, TF-1a and OCI-AML3 cells upregulated H3K9me3 9, while the expression of HP1α remained unchanged (Figure 3-10).

The aberrant methylation status of H3K9 has been reported in haematological malignancies, including AML (Müller-Tidow et al., 2010, Chopra and Bohlander, 2015, Monaghan et al., 2019, Dong et al., 2020). H3K9me3 levels are generally reduced at core promoter regions in patients with AML (Dong et al., 2020). More than 2000 genomic loci at 453 core promoters are differentially expressed due to alteration of H3K9me3 levels (Müller-Tidow et al., 2010). Promoter H3K9me3 levels were correlated with >70% of the disease outcome in AML compared to the normal white blood cells independent of age and genetic mutations (Monaghan et al., 2019). Here, we showed that HP1BP3 expression alters H3K9me3 levels (Figure 3-2, 3-9, 3-10).

Moreover, The Cancer Genome Atlas (TCGA) and Kaplan–Meier analysis revealed that high *HP1BP3* expression is correlated with poor overall survival among patients with AML and was not associated with FLT3 status (Figure 3-1). This highlights the important role of HP1BP3 in AML through the modulation of histone methylation and further suggests that the expression patterns of HP1BP3 can predict the outcome in patients with AML. However, further analysis such as chromatin immunoprecipitation

(ChIP) hybridization on microarray (ChIP-chip) is needed to identify the global changes of the epigenome in *HP1BP3* knockdown (KD) AML cells.

Modulation of H3K9, i.e. conversion between methylation and acetylation, has an important role not only in malignancy but in normal cellular development. In haematopoiesis, histone modifications maintain cell integrity and genome stability by regulating gene expression (Ugarte et al., 2015). In this study, we investigated the levels of H3K9me3 and H3K9ac in Lin$^-$ *Hp1bp3*$^{-/-}$ HSCs. In line with our findings in the AML cells, our data revealed induced H3K9me3 and a decrease in the acetylated form of H3K9 in the Lin$^-$ *Hp1bp3*$^{-/-}$ cells compared to Lin$^-$ *Hp1bp3*$^{fl/fl}$ cells (Figure 6-6).

The effect of HP1BP3 on chromatin compaction has been studied and reported by three research groups (Dutta et al., 2014, Garfinkel et al., 2015, Shi et al., 2020). Loss of HP1BP3 diminished H3K9me3 and chromatin condensation at the telomeres in alternative lengthening of telomeres (ALT) tumour cells (Shi et al., 2020). Moreover, *HP1BP3* null HEK293T cells showed less compact chromatin compared with control cells (Dutta et al., 2014). However, the loss of HP1BP3 had no impact on chromatin compaction in HeLa cells (Garfinkel et al., 2015). Here, we showed that loss of HP1BP3 induced H3K9me3 in both AML and Lin$^-$ HSCs. We additionally reported that the level of HP1α and SUV39H did not change in *HP1BP3*-downregulated AML cells. A recent finding suggested that HP1BP3 homodimerizes to multiple copies of histone proteins independent of HP1α (Shi, Hu et al. 2020). This suggests that a possible mechanism of HP1BP3 in modulating H3K9 could be through facilitating crosstalk between different

chromatin modifiers, i.e. methyltransferases, demethylases, acetylases or deacetylases and the histone residues, which needs further investigations.

7.1.3 HP1BP3 regulates gene and miRNA expression in AML

Histone modifications are a small part of a greater picture of regulation. A wide range of regulatory factors and chromatin modifiers act together to impact chromatin structure and function. some histone modifications can influence the chromatin architecture without any direct changes to chromatin accessibility (Henikoff and Shilatifard, 2011). To test whether HP1BP3 influences direct access to the chromatin and eventually regulates gene expression and cellular events, we carried out transcriptomic and miRNA transcriptomic analysis. Here, we demonstrated that HP1BP3 regulates both gene and miRNA transcription in AML. Our transcriptomic analysis revealed that HP1BP3 regulates several key genes involved in proliferation, the cell cycle, proto-oncogenes, tumour suppressor genes and chromatin modifiers.

We demonstrated that HP1BP3 regulates cell cycle progression in AML cells. Using gain- and loss-of-function analysis, we found that HP1BP3 overexpression enhances the cell cycle by inducing early S phase entry in MOLM13 cells (Figure 3-12 B). However, the downregulation of HP1BP3 delayed S phase entry and eventually cell cycle progression in AML cells (Figure 3-13 B). Progression through cell cycle phases is regulated by checkpoint regulatory protein kinases known as cyclin-dependent kinases (CDKs) (Malumbres, 2014). They play critical functions in controlling cell division in response to different extra- and intracellular signals (Malumbres 2014). Our RNA sequencing (RNA-seq) analysis revealed that loss of

HP1BP3 downregulated the expression of the CDKs (Figure 3-22). Using proteomic analysis, Dutta et al. reported the association between HP1BP3 and chromatin remodelling during cell cycle phases (Dutta et al., 2014). HP1BP3 was increased during the transition from G1–S phase to maintain chromatin integrity and control cell proliferation (Dutta et al., 2014). These findings suggest that HP1BP3 can regulate cell cycle progression through CDK regulation. Moreover, our miRNA sequencing (miRNA-seq) revealed that *HP1BP3* knockdown decreased the expression of several miRNAs involved in proliferation and cell cycle progression regulation (Table 4-1, Figure 5-8). For example, miR-21 increases cell proliferation by targeting the *PTEN–AKT* pathway, and its downregulation inhibits AML proliferation and induces G1 arrest and apoptosis (Bai et al., 2011) that was downregulated in our KD AML cells (Figure 5-8). miR-29b increases cell proliferation and AML progression by targeting *AKT2* (Blum et al., 2010) and inducing DNA hypermethylation (Liu et al., 2010), which was also downregulated in the HP1BP3 knockdown cells. This suggests that HP1BP3 can regulate cell cycle progression by regulating CKDs and miRNAs.

Moreover, proliferation and cell cycle progression can also be regulated through activation of the tumour suppressor genes. Interestingly, our transcriptomic analysis revealed that the inhibition of HP1BP3 induced the expression of tumour suppressor genes and miRNAs with tumour-suppressive activity (Figure 3-22, Table 4-1). RNA-seq analysis revealed that the HP1BP3 downregulation induced the expression of its own negative regulator FBXW7 [Sedaie-Bonab et al., in submission]. Additionally, several proto-oncogenes, including *JUN* and *MYC*, and cyclins, which are substrates

of FBXW7, were also downregulated (Figure 3-22). FBXW7 substrates have oncogenic function by regulating several pathways involved in cell proliferation, differentiation and apoptosis, and their accumulation leads to the acquisition of the hallmarks of cancer (Davis et al., 2014, Heo et al., 2016). Moreover, as FBXW7 also negatively regulates HIF1α through UPS for degradation under hypoxia (Cassavaugh et al., 2011), the induction of FBXW7 could also explains the downregulation of HIF1α and consequently the hypoxic markers CA9 and VEGFA in the AML^{KD} cells (Chapter 5). Furthermore, the lack of HP1BP3 increased the expression of the most studied tumour suppressor: p53 (3-fold) (Figure 3-22) (Rozan and El-Deiry, 2007, Olivier et al., 2010). Activation of TP53 regulates many cellular processes, such as cell cycle progression and cell death (Shaw, 1996, Fridman and Lowe, 2003). Interestingly, the miR-34 family was also induced in the KD cells (Table 4-1). miR-34 has tumour-suppressive activity and is directly controlled by TP53 (Zhang et al., 2019), and low expression of miR-34 is associated with poor outcome in AML (Yang et al., 2017). Moreover, the lack of HP1BP3 drastically lowered the expression of *HOXA9*, a key oncogene involved in leukemogenesis (Abramovich and Humphries, 2005), and of other members of the HOX gene family with oncogenic activity, including *HOXB3–6* (Fischbach et al., 2005) (Figure 3-19). The downregulation of the HOX family could be due to the downregulation of miR-99a that targets several pathways in AML, including the oncogenomic HOX family (Khalaj et al., 2017) (Figure 4-8). All these features indicate the distinct regulatory roles of HP1BP3 in chromatin remodelling and in epigenetic gene regulation. Moreover, the induction observed for H3K9me3

and the reduction in H3K9ac in response to HP1BP3 downregulation might reflect a direct effect of transcriptional regulation, which could influence proliferation and cell cycle progression in AML (Figure 7-1).

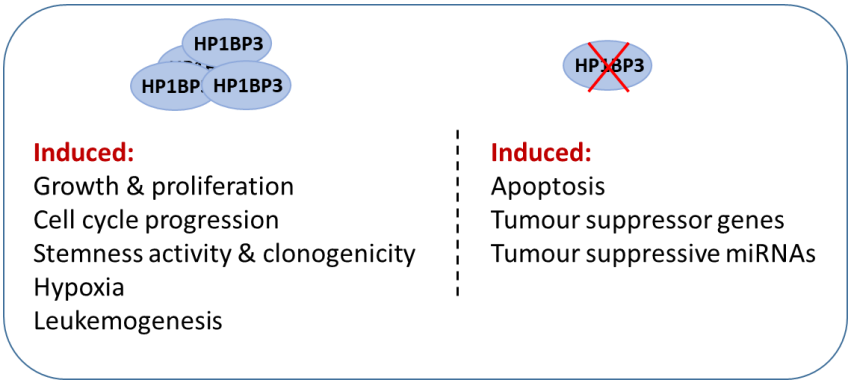


Figure 7-1: Schematic presentation of HP1BP3 role in AML. The diagram illustrates expression of HP1BP3 induced AML cell lines growth and proliferation, cell cycle progression, hypoxia and leukemogenesis. However, loss-of-function of HP1BP3 induces cell apoptosis and the expression of tumour suppressor genes and miRNAs in AML cells.

7.2 Experimental limitations and perspectives

To achieve the aim and objectives determined for the present research, a wide range of *in vitro* and *in vivo* analyses were carried out to decipher the role of HP1BP3 in haematopoiesis and leukemogenesis. However, several obstacles and experimental limitations were encountered.

For example:

- Generating *HP1BP3* knockout AML cells using CRISPR/Cas9 technology was not possible. The single guide RNAs (sgRNAs) of HP1BP3 was previously cloned into PX459-Puro plasmids in our lab. Physical and chemical transfection were carried out using electroporation and Lipofectamine 3000 (Invitrogen™), respectively. However, the transfection efficiency was very low, and the viability

of the transfected cells decreased rapidly within 2–3 weeks, which led us to use a lentivirus (LV) method.

- Due to time limitation, we could not complete the RNA-seq analysis, i.e. the gene ontology and the enrichment pathways. The national lockdown in response to the COVID-19 pandemic and the abrupt closure of the university has delayed shipping and later on processing of the RNA samples to and by Novogene, for RNA-seq analysis.
- Further analysis is required to explore how HP1BP3 modulates chromatin conversion through H3K9. This would shed light on the mechanism of HP1BP3 in the epigenome and therefore tumour biology.
- Additional investigation is required to discover the potential effect of the differentially expressed miRNAs in AML using miRNA inhibitors and to investigate their levels in patient samples.
- Additional experiments are required to explore the specificity of HP1BP3 binding to the candidate miRNA transcripts via ChIP-qPCR analysis.
- In future, we need to run a competitive repopulation assay (CRP) *in vivo* to examine HSC function after *HP1BP3* deletion. To outline, Lin^- $Hp1bp3^{-/-}$ and Lin^- $Hp1bp3^{fl/fl}$ cells can be transplanted into lethally irradiated mice; eventually, the relative reconstitution of the two populations in the transplanted mice will be measured in the peripheral blood.

7.3 Conclusions

Our findings unveiled a potential role of HP1BP3 in the regulation of haematopoiesis and AML through the modulation of chromatin conversion. We successfully identified HP1BP3 as a chromatin modifier that regulates cell cycle progression and proliferation in AML. Hence, the obtained data in this research provide valuable new evidence that HP1BP3 plays a significant role in AML by modulating the chromatin state and regulating gene/miRNA expression. The functions of HP1BP3 and the downstream miRNAs and their consequences in epigenetics-mediated regulation in the longer term, might represent a novel therapeutic target for drug discovery. That AML nowadays is considered a disease of chromatin has led to the development of several approved epigenetic therapies or clinical trials (Fennell et al., 2019). Moreover, identifying how epigenetic therapy can influence the sensitivity of cancer cells to chemotherapy is currently of great interest in this area of research.

Appendix

During my PhD, I have done a side project about the FLYWCH1/β-catenin pathway in AML cells, and I would like to thank all the co-authors.

International Journal of *Molecular Sciences*

MDPI

Article

Increased FLYWCH1 Expression is Negatively Correlated with Wnt/β-catenin Target Gene Expression in Acute Myeloid Leukemia Cells

Amany Almars [1], Panagiota S. Chondrou [1], Emenike K. Onyido [1], Sheema Almozyan [1], Claire Seedhouse [2], Roya Babaei-Jadidi [1,3] and Abdolrahman S. Nateri [1,*]

1 Cancer Genetics & Stem Cell Group, Cancer Biology, Division of Cancer and Stem Cells, School of Medicine, University of Nottingham, Nottingham NG7 2UH, UK; ttxaial@exmail.nottingham.ac.uk (A.A.); msxpc4@nottingham.ac.uk (P.S.C.); e.k.onyido@swansea.ac.uk (E.K.O.); ttxsa97@exmail.nottingham.ac.uk (S.A.); mszrb3@exmail.nottingham.ac.uk (R.B.-J.)
2 Haematology, Nottingham City Hospital, Division of Cancer and Stem Cells, School of Medicine, University of Nottingham, Nottingham NG5 1PB, UK; mrzcs@exmail.nottingham.ac.uk
3 Respiratory Medicine, School of Medicine, University of Nottingham, Nottingham NG7 2UH, UK
* Correspondence: a.nateri@nottingham.ac.uk; Tel.: +44-115-8231306; Fax: +44-115-8231137

Received: 28 March 2019; Accepted: 2 June 2019; Published: 4 June 2019

check for updates

Abstract: Acute myeloid leukaemia (AML) is a heterogeneous clonal malignancy of hematopoietic progenitor cells. The Wnt pathway and its downstream targets are tightly regulated by β-catenin. We recently discovered a new protein, FLYWCH1, which can directly bind nuclear β-catenin. Herein, we studied the FLYWCH1/β-catenin pathway in AML cells using qRT-PCR, Western blot, and immunofluorescence assays. In addition, the stemness activity and cell cycle were analysed by the colony-forming unit (CFU) using methylcellulose-based and Propidium iodide/flow cytometry assays. We found that FLYWCH1 mRNA and protein were differentially expressed in the AML cell lines. C-Myc, cyclin D1, and c-Jun expression decreased in the presence of higher FLYWCH1 expression, and vice versa. There appeared to be the loss of FLYWCH1 expression in dividing cells. The sub-G0 phase was prolonged and shortened in the low and high FLYWCH1 expression cell lines, respectively. The G0/G1 arrest correlated with FLYWCH1-expression, and these cell lines also formed colonies, whereas the low FLYWCH1 expression cell lines could not. Thus, FLYWCH1 functions as a negative regulator of the Wnt/β-catenin pathway in AML.

Keywords: acute myeloid leukaemia (AML); leukemic stem cell (LSC); FLYWCH1; WNT/β-catenin

References

Abbas, T., Keaton, M.A., and Dutta, A. (2013). Genomic instability in cancer. Cold Spring Harbor perspectives in biology *5*, a012914.

Abbasalipour, M., Khosravi, M.A., Zeinali, S., Khanahmad, H., Karimipoor, M., and Azadmanesh, K. (2019). Improvement of K562 cell line transduction by FBS mediated attachment to the cell culture plate. BioMed research international *2019*.

Abdel-Wahab, O., Adli, M., LaFave, L.M., Gao, J., Hricik, T., Shih, A.H., Pandey, S., Patel, J.P., Chung, Y.R., and Koche, R. (2012). ASXL1 mutations promote myeloid transformation through loss of PRC2-mediated gene repression. Cancer cell *22*, 180-193.

Abramovich, C., and Humphries, R.K. (2005). Hox regulation of normal and leukemic hematopoietic stem cells. Current opinion in hematology *12*, 210-216.

Adams, G.B., and Scadden, D.T. (2006). The hematopoietic stem cell in its place. Nature immunology *7*, 333-337.

Adolfsson, J., Månsson, R., Buza-Vidas, N., Hultquist, A., Liuba, K., Jensen, C.T., Bryder, D., Yang, L., Borge, O.-J., and Thoren, L.A. (2005). Identification of Flt3+ lympho-myeloid stem cells lacking erythro-megakaryocytic potential: a revised road map for adult blood lineage commitment. Cell *121*, 295-306.

Agani, F., and Jiang, B.-H. (2013). Oxygen-independent regulation of HIF-1: novel involvement of PI3K/AKT/mTOR pathway in cancer. Current cancer drug targets *13*, 245-251.

Albitar, M. (2001). Angiogenesis in acute myeloid leukemia and myelodysplastic syndrome. Acta haematologica *106*, 170-176.

Alcalay, M., Tiacci, E., Bergomas, R., Bigerna, B., Venturini, E., Minardi, S.P., Meani, N., Diverio, D., Bernard, L., and Tizzoni, L. (2005). Acute myeloid leukemia bearing cytoplasmic nucleophosmin (NPMc+ AML) shows a distinct gene expression profile characterized by up-regulation of genes involved in stem-cell maintenance. Blood *106*, 899-902.

Alexandrow, M.G., and Hamlin, J.L. (2005). Chromatin decondensation in S-phase involves recruitment of Cdk2 by Cdc45 and histone H1 phosphorylation. The Journal of cell biology *168*, 875-886.

Almars, A., Chondrou, P.S., Onyido, E.K., Almozyan, S., Seedhouse, C., Babaei-Jadidi, R., and Nateri, A.S. (2019). Increased FLYWCH1 Expression is Negatively Correlated with Wnt/β-catenin Target Gene Expression in Acute Myeloid Leukemia Cells. International journal of molecular sciences *20*, 2739.

Alva, J.A., Zovein, A.C., Monvoisin, A., Murphy, T., Salazar, A., Harvey, N.L., Carmeliet, P., and Iruela-Arispe, M.L. (2006). VE-Cadherin-Cre-recombinase transgenic mouse: a tool for lineage analysis and gene deletion in endothelial cells. Developmental dynamics: an official publication of the American Association of Anatomists *235*, 759-767.

Antonin, W., and Neumann, H. (2016). Chromosome condensation and decondensation during mitosis. Current opinion in cell biology *40*, 15-22.

Arai, F., and Suda, T. (2007). Maintenance of quiescent hematopoietic stem cells in the osteoblastic niche. Annals of the New York Academy of Sciences *1106*, 41-53.

Arents, G., and Moudrianakis, E.N. (1993). Topography of the histone octamer surface: repeating structural motifs utilized in the docking of

nucleosomal DNA. Proceedings of the National Academy of Sciences *90*, 10489-10493.

Ayala, F., Dewar, R., Kieran, M., and Kalluri, R. (2009). Contribution of bone microenvironment to leukemogenesis and leukemia progression. Leukemia *23*, 2233-2241.

Babaei-Jadidi, R., Li, N., Saadeddin, A., Spencer-Dene, B., Jandke, A., Muhammad, B., Ibrahim, E.E., Muraleedharan, R., Abuzinadah, M., and Davis, H. (2011). FBXW7 influences murine intestinal homeostasis and cancer, targeting Notch, Jun, and DEK for degradation. Journal of Experimental Medicine *208*, 295-312.

Bai, H., Xu, R., Cao, Z., Wei, D., and Wang, C. (2011). Involvement of miR-21 in resistance to daunorubicin by regulating PTEN expression in the leukaemia K562 cell line. FEBS letters *585*, 402-408.

Ballarino, M., Pagano, F., Girardi, E., Morlando, M., Cacchiarelli, D., Marchioni, M., Proudfoot, N.J., and Bozzoni, I. (2009). Coupled RNA processing and transcription of intergenic primary microRNAs. Molecular and cellular biology *29*, 5632-5638.

Bangoura, G., Liu, Z.-S., Qian, Q., Jiang, C.-Q., Yang, G.-F., and Jing, S. (2007). Prognostic significance of HIF-2α/EPAS1 expression in hepatocellular carcinoma. World journal of gastroenterology: WJG *13*, 3176.

Bannister, A.J., and Kouzarides, T. (2005). Reversing histone methylation. Nature *436*, 1103-1106.

Bannister, A.J., and Kouzarides, T. (2011a). Regulation of chromatin by histone modifications. Cell research *21*, 381-395.

Bannister, A.J., and Kouzarides, T. (2011b). Regulation of chromatin by histone modifications. Cell Res *21*, 381-395.

Bannister, A.J., Schneider, R., and Kouzarides, T. (2002). Histone methylation: dynamic or static? Cell *109*, 801-806.

Bannister, A.J., Zegerman, P., Partridge, J.F., Miska, E.A., Thomas, J.O., Allshire, R.C., and Kouzarides, T. (2001). Selective recognition of methylated lysine 9 on histone H3 by the HP1 chromo domain. Nature *410*, 120-124.

Barrette, S., Douglas, J.L., Seidel, N.E., and Bodine, D.M. (2000). Lentivirus-based vectors transduce mouse hematopoietic stem cells with similar efficiency to Moloney murine leukemia virus–based vectors. Blood, The Journal of the American Society of Hematology *96*, 3385-3391.

Bartel, D.P. (2004). MicroRNAs: genomics, biogenesis, mechanism, and function. cell *116*, 281-297.

Bártová, E., Krejčí, J., Harničarová, A., Galiová, G., and Kozubek, S. (2008). Histone modifications and nuclear architecture: a review. Journal of Histochemistry & Cytochemistry *56*, 711-721.

Batie, M., Del Peso, L., and Rocha, S. (2018). Hypoxia and chromatin: a focus on transcriptional repression mechanisms. Biomedicines *6*, 47.

Baylin, S.B., and Jones, P.A. (2016). Epigenetic determinants of cancer. Cold Spring Harbor perspectives in biology *8*, a019505.

Beezhold, K.J., Castranova, V., and Chen, F. (2010). Microprocessor of microRNAs: regulation and potential for therapeutic intervention. Molecular cancer *9*, 1-9.

Benard, A., Goossens-Beumer, I.J., van Hoesel, A.Q., de Graaf, W., Horati, H., Putter, H., Zeestraten, E.C., van de Velde, C.J., and Kuppen, P.J. (2014). Histone trimethylation at H3K4, H3K9 and H4K20 correlates with patient

survival and tumor recurrence in early-stage colon cancer. BMC cancer *14*, 1.

Bertoli, C., Skotheim, J.M., and de Bruin, R.A. (2013). Control of cell cycle transcription during G1 and S phases. Nature reviews Molecular cell biology *14*, 518-528.

Bhaskara, S., Jacques, V., Rusche, J.R., Olson, E.N., Cairns, B.R., and Chandrasekharan, M.B. (2013). Histone deacetylases 1 and 2 maintain S-phase chromatin and DNA replication fork progression. Epigenetics & chromatin *6*, 1.

Bhayadia, R., Krowiorz, K., Haetscher, N., Jammal, R., Emmrich, S., Obulkasim, A., Fiedler, J., Schwarzer, A., Rouhi, A., and Heuser, M. (2018). Endogenous tumor suppressor microRNA-193b: therapeutic and prognostic value in acute myeloid leukemia. Journal of Clinical Oncology *36*, 1007-1016.

Birner, P., Schindl, M., Obermair, A., Plank, C., Breitenecker, G., and Oberhuber, G. (2000). Overexpression of hypoxia-inducible factor 1α is a marker for an unfavorable prognosis in early-stage invasive cervical cancer. Cancer research *60*, 4693-4696.

Blum, W., Garzon, R., Klisovic, R.B., Schwind, S., Walker, A., Geyer, S., Liu, S., Havelange, V., Becker, H., and Schaaf, L. (2010). Clinical response and miR-29b predictive significance in older AML patients treated with a 10-day schedule of decitabine. Proceedings of the National Academy of Sciences *107*, 7473-7478.

Bochyńska, A., Lüscher-Firzlaff, J., and Lüscher, B. (2018). Modes of interaction of KMT2 histone H3 lysine 4 methyltransferase/COMPASS complexes with chromatin. Cells *7*, 17.

Bonnet, D., and Dick, J.E. (1997). Human acute myeloid leukemia is organized as a hierarchy that originates from a primitive hematopoietic cell. Nature medicine *3*, 730-737.

Borchert, G.M., Lanier, W., and Davidson, B.L. (2006). RNA polymerase III transcribes human microRNAs. Nature structural & molecular biology *13*, 1097-1101.

Boulais, P.E., and Frenette, P.S. (2015). Making sense of hematopoietic stem cell niches. Blood *125*, 2621-2629.

Bowman, G.D., and Poirier, M.G. (2015). Post-translational modifications of histones that influence nucleosome dynamics. Chemical reviews *115*, 2274-2295.

Branda, C.S., and Dymecki, S.M. (2004). Talking about a revolution: The impact of site-specific recombinases on genetic analyses in mice. Developmental cell *6*, 7-28.

Bröske, A.-M., Vockentanz, L., Kharazi, S., Huska, M.R., Mancini, E., Scheller, M., Kuhl, C., Enns, A., Prinz, M., and Jaenisch, R. (2009). DNA methylation protects hematopoietic stem cell multipotency from myeloerythroid restriction. Nature genetics *41*, 1207-1215.

Bullinger, L., Ehrich, M., Döhner, K., Schlenk, R.F., Döhner, H., Nelson, M.R., and van den Boom, D. (2010). Quantitative DNA methylation predicts survival in adult acute myeloid leukemia. Blood, The Journal of the American Society of Hematology *115*, 636-642.

Busque, L., Patel, J.P., Figueroa, M.E., Vasanthakumar, A., Provost, S., Hamilou, Z., Mollica, L., Li, J., Viale, A., and Heguy, A. (2012). Recurrent somatic TET2 mutations in normal elderly individuals with clonal hematopoiesis. Nature genetics *44*, 1179-1181.

Cabezas-Wallscheid, N., Klimmeck, D., Hansson, J., Lipka, D.B., Reyes, A., Wang, Q., Weichenhan, D., Lier, A., Von Paleske, L., and Renders, S. (2014). Identification of regulatory networks in HSCs and their immediate progeny via integrated proteome, transcriptome, and DNA methylome analysis. Cell stem cell *15*, 507-522.

Caiazza, C., and Mallardo, M. (2016). The roles of miR-25 and its targeted genes in development of human cancer. Microrna *5*, 113-119.

Calin, G.A., Dumitru, C.D., Shimizu, M., Bichi, R., Zupo, S., Noch, E., Aldler, H., Rattan, S., Keating, M., and Rai, K. (2002). Frequent deletions and down-regulation of micro-RNA genes miR15 and miR16 at 13q14 in chronic lymphocytic leukemia. Proceedings of the national academy of sciences *99*, 15524-15529.

Cano, D.A., Soto-Moreno, A., and Leal-Cerro, A. (2014). Genetically engineered mouse models of pituitary tumors. Frontiers in oncology *4*, 203.

Carter, B.Z., Mak, P.Y., Chen, Y., Mak, D.H., Mu, H., Jacamo, R., Ruvolo, V., Arold, S.T., Ladbury, J.E., and Burks, J.K. (2016). Anti-apoptotic ARC protein confers chemoresistance by controlling leukemia-microenvironment interactions through a NFκB/IL1β signaling network. Oncotarget *7*, 20054.

Cassavaugh, J.M., Hale, S.A., Wellman, T.L., Howe, A.K., Wong, C., and Lounsbury, K.M. (2011). Negative regulation of HIF-1α by an FBW7-mediated degradation pathway during hypoxia. Journal of cellular biochemistry *112*, 3882-3890.

Castillo, J., López-Rodas, G., and Franco, L. (2017). Histone post-translational modifications and nucleosome organisation in transcriptional regulation: some open questions. Protein Reviews, 65-92.

Cazaly, E., Saad, J., Wang, W., Heckman, C., Ollikainen, M., and Tang, J. (2019). Making sense of the epigenome using data integration approaches. Frontiers in pharmacology *10*, 126.

Challen, G.A., Sun, D., Jeong, M., Luo, M., Jelinek, J., Berg, J.S., Bock, C., Vasanthakumar, A., Gu, H., and Xi, Y. (2012). Dnmt3a is essential for hematopoietic stem cell differentiation. Nature genetics *44*, 23-31.

Challen, G.A., Sun, D., Mayle, A., Jeong, M., Luo, M., Rodriguez, B., Mallaney, C., Celik, H., Yang, L., and Xia, Z. (2014). Dnmt3a and Dnmt3b have overlapping and distinct functions in hematopoietic stem cells. Cell stem cell *15*, 350-364.

Chan, W.-I., and Huntly, B.J. (2008). Leukemia stem cells in acute myeloid leukemia. Paper presented at: Seminars in oncology (Elsevier).

Charames, G.S., and Bapat, B. (2003). Genomic instability and cancer. Current molecular medicine *3*, 589-596.

Chaudhuri, A.A., So, A.Y.-L., Mehta, A., Minisandram, A., Sinha, N., Jonsson, V.D., Rao, D.S., O'Connell, R.M., and Baltimore, D. (2012). Oncomir miR-125b regulates hematopoiesis by targeting the gene Lin28A. Proceedings of the National Academy of Sciences *109*, 4233-4238.

Chen, C.C., Gau, J.P., You, J.Y., Lee, K.D., Yu, Y.B., Lu, C.H., Lin, J.T., Lan, C., Lo, W.H., and Liu, J.M. (2009). Prognostic significance of β-catenin and topoisomerase IIα in de novo acute myeloid leukemia. American journal of hematology *84*, 87-92.

Chen, P., Huang, H., Wu, J., Lu, R., Wu, Y., Jiang, X., Yuan, Q., and Chen, Y. (2015). Bone marrow stromal cells protect acute myeloid leukemia cells from anti-CD44 therapy partly through regulating PI3K/Akt–p27Kip1 axis. Molecular carcinogenesis *54*, 1678-1685.

Cherukuri, S., Hock, R., Ueda, T., Catez, F., Rochman, M., and Bustin, M. (2008). Cell cycle-dependent binding of HMGN proteins to chromatin. Molecular biology of the cell *19*, 1816-1824.

Chevillard, C., Reik, W., McDermott, M., Fontes, M., Mattei, M.G., and Singh, P.B. (1993). CHROMOSOMAL LOCALIZATION OF HUMAN HOMOLOGS OF THE DROSOPHILA HETEROCHROMATIN PROTEIN-1 (HP1) GENE. Mammalian Genome *4*.

Chi, J.-T., Wang, Z., Nuyten, D.S., Rodriguez, E.H., Schaner, M.E., Salim, A., Wang, Y., Kristensen, G.B., Helland, Å., and Børresen-Dale, A.-L. (2006). Gene expression programs in response to hypoxia: cell type specificity and prognostic significance in human cancers. PLoS Med *3*, e47.

Chou, W.-C., Chou, S.-C., Liu, C.-Y., Chen, C.-Y., Hou, H.-A., Kuo, Y.-Y., Lee, M.-C., Ko, B.-S., Tang, J.-L., and Yao, M. (2011). TET2 mutation is an unfavorable prognostic factor in acute myeloid leukemia patients with intermediate-risk cytogenetics. Blood *118*, 3803-3810.

Cipolleschi, M.G., Dello Sbarba, P., and Olivotto, M. (1993). The role of hypoxia in the maintenance of hematopoietic stem cells.
Cooper, G.M. (2000). The eukaryotic cell cycle.

Croker, B.A., Metcalf, D., Robb, L., Wei, W., Mifsud, S., DiRago, L., Cluse, L.A., Sutherland, K.D., Hartley, L., and Williams, E. (2004). SOCS3 is a critical physiological negative regulator of G-CSF signaling and emergency granulopoiesis. Immunity *20*, 153-165.

Cullen, S.M., Mayle, A., Rossi, L., and Goodell, M.A. (2014). Hematopoietic stem cell development: an epigenetic journey. In Current topics in developmental biology (Elsevier), pp. 39-75.

Czvitkovich, S., Sauer, S., Peters, A.H., Deiner, E., Wolf, A., Laible, G., Opravil, S., Beug, H., and Jenuwein, T. (2001). Over-expression of the

SUV39H1 histone methyltransferase induces altered proliferation and differentiation in transgenic mice. Mechanisms of development *107*, 141-153.

Davie, J.R., and Spencer, V.A. (1999). Control of histone modifications. J Cell Biochem, 141-148.

Davis, R.J., Welcker, M., and Clurman, B.E. (2014). Tumor suppression by the Fbw7 ubiquitin ligase: mechanisms and opportunities. Cancer cell *26*, 455-464.

Dawson, Mark A., and Kouzarides, T. (2012). Cancer epigenetics: from mechanism to therapy. Cell *150*, 12-27.

de Boer, J., Williams, A., Skavdis, G., Harker, N., Coles, M., Tolaini, M., Norton, T., Williams, K., Roderick, K., and Potocnik, A.J. (2003). Transgenic mice with hematopoietic and lymphoid specific expression of Cre. European journal of immunology *33*, 314-325.

De Braekeleer, E., Douet-Guilbert, N., Basinko, A., Le Bris, M.-J., Morel, F., and De Braekeleer, M. (2014). Hox gene dysregulation in acute myeloid leukemia. Future Oncology *10*, 475-495.

De Lange, W.J., Halabi, C.M., Beyer, A.M., and Sigmund, C.D. (2008). Germ line activation of the Tie2 and SMMHC promoters causes noncell-specific deletion of floxed alleles. Physiological genomics *35*, 1-4.

De Leeuw, D., Verhagen, H., Denkers, F., Kavelaars, F., Valk, P., Schuurhuis, G.J., Ossenkoppele, G., and Smit, L. (2016). MicroRNA-551b is highly expressed in hematopoietic stem cells and a biomarker for relapse and poor prognosis in acute myeloid leukemia. Leukemia *30*, 742-746.

de Leeuw, D.C., Denkers, F., Olthof, M.C., Rutten, A.P., Pouwels, W., Schuurhuis, G.J., Ossenkoppele, G.J., and Smit, L. (2014). Attenuation of

microRNA-126 expression that drives CD34+ 38− stem/progenitor cells in acute myeloid leukemia leads to tumor eradication. Cancer research *74*, 2094-2105.

Deeb, G., Vaughan, M.M., McInnis, I., Ford, L.A., Sait, S.N., Starostik, P., Wetzler, M., Mashtare, T., and Wang, E.S. (2011). Hypoxia-inducible factor-1α protein expression is associated with poor survival in normal karyotype adult acute myeloid leukemia. Leukemia research *35*, 579-584.

Di Paola, D., Rampakakis, E., Chan, M.K., and Zannis-Hadjopoulos, M. (2012). Differential chromatin structure encompassing replication origins in transformed and normal cells. Genes & cancer *3*, 152-176.

Dillon, N., and Festenstein, R. (2002). Unravelling heterochromatin: competition between positive and negative factors regulates accessibility. TRENDS in Genetics *18*, 252-258.

Dixon-McIver, A., East, P., Mein, C.A., Cazier, J.-B., Molloy, G., Chaplin, T., Lister, T.A., Young, B.D., and Debernardi, S. (2008). Distinctive patterns of microRNA expression associated with karyotype in acute myeloid leukaemia. PloS one *3*, e2141.

Dobin, A., Davis, C.A., Schlesinger, F., Drenkow, J., Zaleski, C., Jha, S., Batut, P., Chaisson, M., and Gingeras, T.R. (2013). STAR: ultrafast universal RNA-seq aligner. Bioinformatics *29*, 15-21.

Dohner, H., Weisdorf, D. J. & Bloomfield, C. D. 2015. Acute Myeloid Leukemia. N Engl J Med, 373, 1136-52.

Dong, X., and Weng, Z. (2013). The correlation between histone modifications and gene expression. Epigenomics *5*, 113-116.

Dorrance, A.M., Neviani, P., Ferenchak, G.J., Huang, X., Nicolet, D., Maharry, K.S., Ozer, H.G., Hoellarbauer, P., Khalife, J., and Hill, E.B. (2015). Targeting leukemia stem cells in vivo with antagomiR-126 nanoparticles in acute myeloid leukemia. Leukemia *29*, 2143-2153.

Dutta, B., Ren, Y., Hao, P., Sim, K.H., Cheow, E., Adav, S., Tam, J.P., and Sze, S.K. (2014a). Profiling of the chromatin-associated proteome identifies HP1BP3 as a novel regulator of cell cycle progression. Molecular & Cellular Proteomics *13*, 2183-2197.

Dutta, B., Yan, R., Lim, S.K., Tam, J.P., and Sze, S.K. (2014b). Quantitative profiling of chromatome dynamics reveals a novel role for HP1BP3 in hypoxia-induced oncogenesis. Molecular & Cellular Proteomics *13*, 3236-3249.

Eberharter, A., and Becker, P.B. (2002). Histone acetylation: a switch between repressive and permissive chromatin. EMBO reports *3*, 224-229.

Eisener-Dorman, A.F., Lawrence, D.A., and Bolivar, V.J. (2009). Cautionary insights on knockout mouse studies: the gene or not the gene? Brain, behavior, and immunity *23*, 318-324.

Eissenberg, J.C., and Elgin, S.C.R. (2000). The HP1 protein family: getting a grip on chromatin. Current Opinion in Genetics & Development *10*.

Eliasson, P., and Jönsson, J.I. (2010). The hematopoietic stem cell niche: low in oxygen but a nice place to be. Journal of cellular physiology *222*, 17-22.

Eliasson, P., Rehn, M., Hammar, P., Larsson, P., Sirenko, O., Flippin, L.A., Cammenga, J., and Jönsson, J.-I. (2010). Hypoxia mediates low cell-cycle activity and increases the proportion of long-term–reconstituting hematopoietic stem cells during in vitro culture. Experimental hematology *38*, 301-310. e302.

Ema, H., Morita, Y., Yamazaki, S., Matsubara, A., Seita, J., Tadokoro, Y., Kondo, H., Takano, H., and Nakauchi, H. (2006). Adult mouse hematopoietic stem cells: purification and single-cell assays. Nature protocols *1*, 2979-2987.

Eppert, K., Takenaka, K., Lechman, E.R., Waldron, L., Nilsson, B., Van Galen, P., Metzeler, K.H., Poeppl, A., Ling, V., and Beyene, J. (2011). Stem cell gene expression programs influence clinical outcome in human leukemia. Nature medicine *17*, 1086-1093.

Estey, E., and Döhner, H. (2006). Acute myeloid leukaemia. The Lancet *368*, 1894-1907.

Falini, B., Mecucci, C., Tiacci, E., Alcalay, M., Rosati, R., Pasqualucci, L., La Starza, R., Diverio, D., Colombo, E., and Santucci, A. (2005). Cytoplasmic nucleophosmin in acute myelogenous leukemia with a normal karyotype. New England Journal of Medicine *352*, 254-266.

Fan, Y., Nikitina, T., Morin-Kensicki, E.M., Zhao, J., Magnuson, T.R., Woodcock, C.L., and Skoultchi, A.I. (2003). H1 linker histones are essential for mouse development and affect nucleosome spacing in vivo. Molecular and cellular biology *23*, 4559-4572.

Fan, Y., Nikitina, T., Zhao, J., Fleury, T.J., Bhattacharyya, R., Bouhassira, E.E., Stein, A., Woodcock, C.L., and Skoultchi, A.I. (2005). Histone H1 depletion in mammals alters global chromatin structure but causes specific changes in gene regulation. Cell *123*, 1199-1212.

Fanti, L., Berloco, M., Piacentini, L., and Pimpinelli, S. (2003). Chromosomal distribution of Heterochromatin Protein 1 (HP1) in Drosophila: a cytological map of euchromatic HP1 binding sites. Genetica *117*.

Farlik, M., Halbritter, F., Müller, F., Choudry, F.A., Ebert, P., Klughammer, J., Farrow, S., Santoro, A., Ciaurro, V., and Mathur, A. (2016). DNA methylation dynamics of human hematopoietic stem cell differentiation. Cell stem cell *19*, 808-822.

Feng, D.D., Zhang, H., Zhang, P., Zheng, Y.S., Zhang, X.J., Han, B.W., Luo, X.Q., Xu, L., Zhou, H., and Qu, L.H. (2011). Down-regulated miR-331–5p and miR-27a are associated with chemotherapy resistance and relapse in leukaemia. Journal of cellular and molecular medicine *15*, 2164-2175.

Feng, Y.-H., and Tsao, C.-J. (2016). Emerging role of microRNA-21 in cancer. Biomedical reports *5*, 395-402.

Fiegl, M., Samudio, I., Clise-Dwyer, K., Burks, J.K., Mnjoyan, Z., and Andreeff, M. (2009). CXCR4 expression and biologic activity in acute myeloid leukemia are dependent on oxygen partial pressure. Blood, The Journal of the American Society of Hematology *113*, 1504-1512.

Figueroa, M.E., Abdel-Wahab, O., Lu, C., Ward, P.S., Patel, J., Shih, A., Li, Y., Bhagwat, N., Vasanthakumar, A., and Fernandez, H.F. (2010). Leukemic IDH1 and IDH2 mutations result in a hypermethylation phenotype, disrupt TET2 function, and impair hematopoietic differentiation. Cancer cell *18*, 553-567.

Fischbach, N.A., Rozenfeld, S., Shen, W., Fong, S., Chrobak, D., Ginzinger, D., Kogan, S.C., Radhakrishnan, A., Le Beau, M.M., and Largman, C. (2005). HOXB6 overexpression in murine bone marrow immortalizes a myelomonocytic precursor in vitro and causes hematopoietic stem cell expansion and acute myeloid leukemia in vivo. Blood *105*, 1456-1466.

Fischer, J.A., Rossetti, S., Datta, A., Eng, K.H., Beghini, A., and Sacchi, N. (2015). miR-17 deregulates a core RUNX1-miRNA mechanism of CBF acute myeloid leukemia. Molecular cancer *14*, 1-13.

Fischer, M. (2017). Census and evaluation of p53 target genes. Oncogene *36*, 3943-3956.

Fischle, W., Tseng, B.S., Dormann, H.L., Ueberheide, B.M., Garcia, B.A., Shabanowitz, J., Hunt, D.F., Funabiki, H., and Allis, C.D. (2005). Regulation of HP1–chromatin binding by histone H3 methylation and phosphorylation. Nature *438*, 1116-1122.

Flügel, D., Görlach, A., and Kietzmann, T. (2012). GSK-3β regulates cell growth, migration, and angiogenesis via Fbw7 and USP28-dependent degradation of HIF-1α. Blood *119*, 1292-1301.

Forsberg, E.C., Serwold, T., Kogan, S., Weissman, I.L., and Passegué, E. (2006). New evidence supporting megakaryocyte-erythrocyte potential of flk2/flt3+ multipotent hematopoietic progenitors. Cell *126*, 415-426.

Fouad, Y.A., and Aanei, C. (2017). Revisiting the hallmarks of cancer. American journal of cancer research *7*, 1016.

Franken, N.A., Rodermond, H.M., Stap, J., Haveman, J., and Van Bree, C. (2006). Clonogenic assay of cells in vitro. Nature protocols *1*, 2315-2319.

Franz, M., Rodriguez, H., Lopes, C., Zuberi, K., Montojo, J., Bader, G.D., and Morris, Q. (2018). GeneMANIA update 2018. Nucleic acids research *46*, W60-W64.

Fridman, J.S., and Lowe, S.W. (2003). Control of apoptosis by p53. Oncogene *22*, 9030-9040.

Friedländer, M.R., Mackowiak, S.D., Li, N., Chen, W., and Rajewsky, N. (2012). miRDeep2 accurately identifies known and hundreds of novel microRNA genes in seven animal clades. Nucleic acids research *40*, 37-52.

Fu, L., Shi, J., Liu, A., Zhou, L., Jiang, M., Fu, H., Xu, K., Li, D., Deng, A., and Zhang, Q. (2017). A minicircuitry of microRNA-9-1 and RUNX1-RUNX1T1 contributes to leukemogenesis in t (8; 21) acute myeloid leukemia. International journal of cancer *140*, 653-661.

Fyodorov, D.V., Zhou, B.-R., Skoultchi, A.I., and Bai, Y. (2018). Emerging roles of linker histones in regulating chromatin structure and function. Nature reviews Molecular cell biology *19*, 192.

Gan, L., Yang, Y., Li, Q., Feng, Y., Liu, T., and Guo, W. (2018). Epigenetic regulation of cancer progression by EZH2: from biological insights to therapeutic potential. Biomarker research *6*, 1-10.

Gao, Y., Luo, L.-h., Li, S., and Yang, C. (2014). miR-17 inhibitor suppressed osteosarcoma tumor growth and metastasis via increasing PTEN expression. Biochemical and biophysical research communications *444*, 230-234.

Garber, M., Grabherr, M.G., Guttman, M., and Trapnell, C. (2011). Computational methods for transcriptome annotation and quantification using RNA-seq. Nature methods *8*, 469-477.

García-Giménez, J.L. (2015). Epigenetic biomarkers and diagnostics (Elsevier Science).

Garfinkel, B.P., Arad, S., Le, P.T., Bustin, M., Rosen, C.J., Gabet, Y., and Orly, J. (2015a). Proportionate dwarfism in mice lacking Heterochromatin Protein 1 Binding Protein 3 (HP1BP3) is associated with alterations in the endocrine IGF-1 pathway. Endocrinology *156*, 4558-4570.

Garfinkel, B.P., Arad, S., Neuner, S., Netser, S., Wagner, S., Kaczorowski, C.C., Rosen, C.J., Gal, M., Soreq, H., and Orly, J. (2016). HP1BP3 expression determines maternal behavior and offspring survival. Genes, Brain and Behavior *15*, 678-688.

Garfinkel, B.P., Melamed-Book, N., Anuka, E., Bustin, M., and Orly, J. (2015b). HP1BP3 is a novel histone H1 related protein with essential roles in viability and growth. Nucleic acids research *43*, 2074-2090.

Gargalionis, A.N., Piperi, C., Adamopoulos, C., and Papavassiliou, A.G. (2012). Histone modifications as a pathogenic mechanism of colorectal tumorigenesis. The International Journal of Biochemistry & Cell Biology *44*, 1276-1289.

Georgiades, P., Ogilvy, S., Duval, H., Licence, D.R., Charnock-Jones, D.S., Smith, S.K., and Print, C.G. (2002). VavCre transgenic mice: a tool for mutagenesis in hematopoietic and endothelial lineages. genesis *34*, 251-256.

Ghattass, K., Assah, R., El-Sabban, M., and Gali-Muhtasib, H. (2013). Targeting hypoxia for sensitization of tumors to radio-and chemotherapy. Current cancer drug targets *13*, 670-685.

Goldman, S.L., Hassan, C., Khunte, M., Soldatenko, A., Jong, Y., Afshinnekoo, E., and Mason, C.E. (2019). Epigenetic modifications in acute myeloid leukemia: prognosis, treatment, and heterogeneity. Frontiers in genetics *10*, 133.

Goulard, M., Dosquet, C., and Bonnet, D. (2018). Role of the microenvironment in myeloid malignancies. Cellular and Molecular Life Sciences *75*, 1377-1391.

Grimwade, D., Hills, R.K., Moorman, A.V., Walker, H., Chatters, S., Goldstone, A.H., Wheatley, K., Harrison, C.J., and Burnett, A.K. (2010). Refinement of cytogenetic classification in acute myeloid leukemia: determination of prognostic significance of rare recurring chromosomal abnormalities amongst 5,876 younger adult patients treated in the UK Medical Research Council trials. Blood, blood-2009-2011-254441.

Grinenko, T., Eugster, A., Thielecke, L., Ramasz, B., Krüger, A., Dietz, S., Glauche, I., Gerbaulet, A., Von Bonin, M., and Basak, O. (2018). Hematopoietic stem cells can differentiate into restricted myeloid progenitors before cell division in mice. Nature communications *9*, 1-10.

Großhans, H., and Filipowicz, W. (2008). The expanding world of small RNAs. Nature *451*, 414-416.

Grunstein, M., Hecht, A., Fisher-Adams, G., Wan, J., Mann, R.K., Strahl-Bolsinger, S., Laroche, T., and Gasser, S. (1995). The regulation of euchromatin and heterochromatin by histones in yeast. Journal of cell science Supplement *19*, 29-36.

Hadac, J.N., Miller, D.D., Grimes, I.C., Clipson, L., Newton, M.A., Schelman, W.R., and Halberg, R.B. (2016). Heterochromatin Protein 1 Binding Protein 3 expression as a candidate marker of intrinsic 5-fluorouracil resistance. Anticancer research *36*, 845-852.

Hanahan, D., and Weinberg, R.A. (2000). The hallmarks of cancer. cell *100*, 57-70.

Hanekamp, D., Cloos, J., and Schuurhuis, G.J. (2017). Leukemic stem cells: identification and clinical application. International journal of hematology *105*, 549-557.

Hanna, J., Hossain, G.S., and Kocerha, J. (2019). The potential for microRNA therapeutics and clinical research. Frontiers in genetics *10*, 478.

Harris, D.M., Hazan-Haley, I., Coombes, K., Bueso-Ramos, C., Liu, J., Liu, Z., Li, P., Ravoori, M., Abruzzo, L., and Han, L. (2011). Transformation of human mesenchymal cells and skin fibroblasts into hematopoietic cells. PLoS One *6*, e21250.

Harrison, J.S., Rameshwar, P., Chang, V., and Bandari, P. (2002). Oxygen saturation in the bone marrow of healthy volunteers. Blood, The Journal of the American Society of Hematology *99*, 394-394.

Hayakawa, T., Haraguchi, T., Masumoto, H., and Hiraoka, Y. (2003). Cell cycle behavior of human HP1 subtypes: distinct molecular domains of HP1 are required for their centromeric localization during interphase and metaphase. Journal of Cell Science *116*, 3327-3338.

Hayashihara, K., Uchiyama, S., Shimamoto, S., Kobayashi, S., Tomschik, M., Wakamatsu, H., No, D., Sugahara, H., Hori, N., and Noda, M. (2010a). The middle region of an HP1-binding protein, HP1-BP74, associates with linker DNA at the entry/exit site of nucleosomal DNA. Journal of Biological Chemistry *285*, 6498-6507.

Hayashihara, K., Uchiyama, S., Shimamoto, S., Kobayashi, S., Tomschik, M., Wakamatsu, H., No, D., Sugahara, H., Hori, N., Noda, M., *et al.* (2010b). The Middle Region of an HP1-binding Protein, HP1-BP74, Associates with Linker DNA at the Entry/Exit Site of Nucleosomal DNA. Journal of Biological Chemistry *285*.

He, L., and Hannon, G.J. (2004). MicroRNAs: small RNAs with a big role in gene regulation. Nature Reviews Genetics *5*, 522-531.

He, M., Wang, Q., Yin, Q., Tang, J., Lu, Y., Zhou, C., Duan, C., Hong, D., Tanaka, T., and Chen, G. (2013). HIF-1 α downregulates miR-17/20a directly targeting p21 and STAT3: a role in myeloid leukemic cell differentiation. Cell Death & Differentiation *20*, 408-418.

He, Q., Kim, H., Huang, R., Lu, W., Tang, M., Shi, F., Yang, D., Zhang, X., Huang, J., and Liu, D. (2015). The Daxx/Atrx complex protects tandem repetitive elements during DNA hypomethylation by promoting H3K9 trimethylation. Cell stem cell *17*, 273-286.

He, X., Zhu, L., An, L., and Zhang, J. (2020). MiR-143 Inhibits Osteoclastogenesis by Targeting RANK and NF-KB and MAPK Signaling Pathways. Current molecular pharmacology *13*, 224-232.

Hebbes, T.R., Thorne, A.W., and Cranerobinson, C. (1988). A direct link between core histone acetylation and transcriptionally active chromatin. Embo Journal *7*, 1395-1402.

Heo, J., Eki, R., and Abbas, T. (2016). Deregulation of F-box proteins and its consequence on cancer development, progression and metastasis. Paper presented at: Seminars in cancer biology (Elsevier).

Hidalgo, I., Herrera-Merchan, A., Ligos, J.M., Carramolino, L., Nuñez, J., Martinez, F., Dominguez, O., Torres, M., and Gonzalez, S. (2012). Ezh1 is required for hematopoietic stem cell maintenance and prevents senescence-like cell cycle arrest. Cell stem cell *11*, 649-662.

Hockel, M., and Vaupel, P. (2001). Tumor hypoxia: definitions and current clinical, biologic, and molecular aspects. Journal of the National Cancer Institute *93*, 266-276.

Hoelper, D., Huang, H., Jain, A.Y., Patel, D.J., and Lewis, P.W. (2017). Structural and mechanistic insights into ATRX-dependent and-independent functions of the histone chaperone DAXX. Nature communications *8*, 1-13.

Hope, K.J., Jin, L., and Dick, J.E. (2004). Acute myeloid leukemia originates from a hierarchy of leukemic stem cell classes that differ in self-renewal capacity. Nature immunology *5*, 738.

Hornick, N.I., Doron, B., Abdelhamed, S., Huan, J., Harrington, C.A., Shen, R., Cambronne, X.A., Verghese, S.C., and Kurre, P. (2016). AML suppresses hematopoiesis by releasing exosomes that contain microRNAs targeting c-MYB. Science signaling *9*, ra88-ra88.

Horton, S.J., and Huntly, B.J. (2012). Recent advances in acute myeloid leukemia stem cell biology. Haematologica *97*, 966-974.

Hou, H., Chou, W., Kuo, Y., Liu, C., Lin, L., Tseng, M., Chiang, Y., Liu, M., Liu, C., and Tang, J. (2015). TP53 mutations in de novo acute myeloid leukemia patients: longitudinal follow-ups show the mutation is stable during disease evolution. Blood cancer journal *5*, e331.

Hübner, M.R., Eckersley-Maslin, M.A., and Spector, D.L. (2013). Chromatin organization and transcriptional regulation. Current opinion in genetics & development *23*, 89-95.

Ide, L.M., Javazon, E., and Spencer, H.T. (2008). Transduction of murine hematopoietic stem cells and in vivo selection of gene-modified cells. In Gene Therapy Protocols (Springer), pp. 213-228.

Iriuchishima, H., Takubo, K., Matsuoka, S., Onoyama, I., Nakayama, K.I., Nojima, Y., and Suda, T. (2011). Ex vivo maintenance of hematopoietic stem cells by quiescence induction through Fbxw7α overexpression. Blood, The Journal of the American Society of Hematology *117*, 2373-2377.

Ismail, T., Lee, H.-K., Kim, C., Kwon, T., Park, T.J., and Lee, H.-S. (2018). KDM1A microenvironment, its oncogenic potential, and therapeutic significance. Epigenetics & chromatin *11*, 1-15.

Ito, S., Barrett, A.J., Dutra, A., Pak, E., Miner, S., Keyvanfar, K., Hensel, N.F., Rezvani, K., Muranski, P., and Liu, P. (2015). Long term maintenance of myeloid leukemic stem cells cultured with unrelated human mesenchymal stromal cells. Stem cell research *14*, 95-104.

Ivanovic, Z., Belloc, F., Faucher, J.-L., Cipolleschi, M.-G., Praloran, V., and Sbarba, P.D. (2002). Hypoxia maintains and interleukin-3 reduces the pre–colony-forming cell potential of dividing CD34+ murine bone marrow cells. Experimental hematology *30*, 67-73.

Jabari, M., Farsani, M.A., Salari, S., Hamidpour, M., Amiri, V., and Mohammadi, M.H. (2019). Hypoxia-Inducible Factor 1-A (HIF1α) and Vascular Endothelial Growth Factor-A (VEGF-A) Expression in De Novo AML Patients. Asian Pacific Journal of Cancer Prevention: APJCP *20*, 705.

Jaenisch, R., and Bird, A. (2003). Epigenetic regulation of gene expression: how the genome integrates intrinsic and environmental signals. Nature genetics *33*, 245.

Jafarzadeh-Samani, Z., Sohrabi, S., Shirmohammadi, K., Effatpanah, H., Yadegarazari, R., and Saidijam, M. (2017). Evaluation of miR-22 and miR-20a as diagnostic biomarkers for gastric cancer. Chinese clinical oncology *6*, 16-16.

Jagannathan-Bogdan, M., and Zon, L.I. (2013). Hematopoiesis. Development *140*, 2463-2467.

James, T.C., Eissenberg, J.C., Craig, C., Dietrich, V., Hobson, A., and Elgin, S.C.R. (1989). DISTRIBUTION PATTERNS OF HP1, A HETEROCHROMATIN-ASSOCIATED NONHISTONE CHROMOSOMAL PROTEIN OF DROSOPHILA. European Journal of Cell Biology *50*.

Jang, Y., Kim, Y.-S., Wielgosz, M.M., Ferrara, F., Ma, Z., Condori, J., Palmer, L.E., Zhao, X., Kang, G., and Rawlings, D.J. (2020). Optimizing lentiviral vector transduction of hematopoietic stem cells for gene therapy. Gene Therapy, 1-12.

Jayani, R.S., Ramanujam, P.L., and Galande, S. (2010). Studying histone modifications and their genomic functions by employing chromatin immunoprecipitation and immunoblotting. Methods in cell biology *98*, 35-56.

Jensen, P., Mortensen, B., Hodgkiss, R., Iversen, P., Christensen, I., Helledie, N., and Larsen, J. (2000). Increased cellular hypoxia and reduced proliferation of both normal and leukaemic cells during progression of acute myeloid leukaemia in rats. Cell proliferation *33*, 381-395.

Jenuwein, T., and Allis, C.D. (2001). Translating the histone code. Science *293*, 1074-1080.

Ji, H., Ehrlich, L.I., Seita, J., Murakami, P., Doi, A., Lindau, P., Lee, H., Aryee, M.J., Irizarry, R.A., and Kim, K. (2010). A comprehensive methylome map of lineage commitment from hematopoietic progenitors. Nature *467*, 338.

Ji, M., Lee, E.J., Kim, K.B., Kim, Y., Sung, R., Lee, S.-J., Kim, D.S., and Park, S.M. (2015). HDAC inhibitors induce epithelial-mesenchymal transition in colon carcinoma cells. Oncology reports *33*, 2299-2308.

Jiang, W., Hua, R., Wei, M., Li, C., Qiu, Z., Yang, X., and Zhang, C. (2015). An optimized method for high-titer lentivirus preparations without ultracentrifugation. Scientific reports *5*, 13875.

Jiang, X.-C. (2013). Generation of general and tissue-specific gene knockout mouse models. In Lipoproteins and Cardiovascular Disease (Springer), pp. 253-271.

Jin, B., Li, Y., and Robertson, K.D. (2011). DNA methylation: superior or subordinate in the epigenetic hierarchy? Genes & cancer *2*, 607-617.

Jin, L., Lee, E.M., Ramshaw, H.S., Busfield, S.J., Peoppl, A.G., Wilkinson, L., Guthridge, M.A., Thomas, D., Barry, E.F., and Boyd, A. (2009). Monoclonal antibody-mediated targeting of CD123, IL-3 receptor α chain, eliminates human acute myeloid leukemic stem cells. Cell stem cell *5*, 31-42.

Johnson, A.B., and Barton, M.C. (2007). Hypoxia-induced and stress-specific changes in chromatin structure and function. Mutation Research/Fundamental and Molecular Mechanisms of Mutagenesis *618*, 149-162.

Johnson, A.B., Denko, N., and Barton, M.C. (2008). Hypoxia induces a novel signature of chromatin modifications and global repression of transcription. Mutation Research/Fundamental and Molecular Mechanisms of Mutagenesis *640*, 174-179.

Jordan, C.T. (2007). The leukemic stem cell. Best practice & research Clinical haematology *20*, 13-18.

Jung, N., Dai, B., Gentles, A.J., Majeti, R., and Feinberg, A.P. (2015). An LSC epigenetic signature is largely mutation independent and implicates the HOXA cluster in AML pathogenesis. Nature communications *6*, 1-12.

Kaelin Jr, W.G., and Ratcliffe, P.J. (2008). Oxygen sensing by metazoans: the central role of the HIF hydroxylase pathway. Molecular cell *30*, 393-402.

Kafri, T., Blömer, U., Peterson, D.A., Gage, F.H., and Verma, I.M. (1997). Sustained expression of genes delivered directly into liver and muscle by lentiviral vectors. Nature genetics *17*, 314-317.

Kamga, P.T., Bassi, G., Cassaro, A., Midolo, M., Di Trapani, M., Gatti, A., Carusone, R., Resci, F., Perbellini, O., and Gottardi, M. (2016). Notch signalling drives bone marrow stromal cell-mediated chemoresistance in acute myeloid leukemia. Oncotarget *7*, 21713.

Karantanou, C., Godavarthy, P.S., and Krause, D.S. (2018). Targeting the bone marrow microenvironment in acute leukemia. Leukemia & lymphoma *59*, 2535-2545.

Kasper, L.H., Boussouar, F., Boyd, K., Xu, W., Biesen, M., Rehg, J., Baudino, T.A., Cleveland, J.L., and Brindle, P.K. (2005). Two transactivation mechanisms cooperate for the bulk of HIF-1-responsive gene expression. The EMBO journal *24*, 3846-3858.

Katsumoto, T., Yoshida, N., and Kitabayashi, I. (2008). Roles of the histone acetyltransferase monocytic leukemia zinc finger protein in normal and malignant hematopoiesis. Cancer science *99*, 1523-1527.

Kaushansky, K. (2005). On the molecular origins of the chronic myeloproliferative disorders: it all makes sense. Blood *105*, 4187-4190.

Keith, B., Johnson, R.S., and Simon, M.C. (2012). HIF1α and HIF2α: sibling rivalry in hypoxic tumour growth and progression. Nature Reviews Cancer *12*, 9-22.

Kersten, K., de Visser, K.E., van Miltenburg, M.H., and Jonkers, J. (2017). Genetically engineered mouse models in oncology research and cancer medicine. EMBO molecular medicine *9*, 137-153.

Khalaj, M., Woolthuis, C.M., Hu, W., Durham, B.H., Chu, S.H., Qamar, S., Armstrong, S.A., and Park, C.Y. (2017). miR-99 regulates normal and malignant hematopoietic stem cell self-renewal. Journal of Experimental Medicine *214*, 2453-2470.

Kim, Y.K., and Kim, V.N. (2007). Processing of intronic microRNAs. The EMBO journal *26*, 775-783.

Kindle, K.B., Troke, P.J., Collins, H.M., Matsuda, S., Bossi, D., Bellodi, C., Kalkhoven, E., Salomoni, P., Pelicci, P.G., and Minucci, S. (2005). MOZ-TIF2 inhibits transcription by nuclear receptors and p53 by impairment of CBP function. Molecular and cellular biology *25*, 988-1002.

Kirmes, I., Szczurek, A., Prakash, K., Charapitsa, I., Heiser, C., Musheev, M., Schock, F., Fornalczyk, K., Ma, D., and Birk, U. (2015). A transient ischemic environment induces reversible compaction of chromatin. Genome biology *16*, 1-19.

Klein, G. (2004). Cancer, apoptosis, and nonimmune surveillance. Cell Death & Differentiation *11*, 13-17.

Kogure, M., Takawa, M., Cho, H.-S., Toyokawa, G., Hayashi, K., Tsunoda, T., Kobayashi, T., Daigo, Y., Sugiyama, M., and Atomi, Y. (2013). Deregulation of the histone demethylase JMJD2A is involved in human carcinogenesis through regulation of the G 1/S transition. Cancer letters *336*, 76-84.

Konopleva, M.Y., and Jordan, C.T. (2011). Leukemia stem cells and microenvironment: biology and therapeutic targeting. Journal of clinical oncology *29*, 591.

Kouzarides, T. (2007). Chromatin modifications and their function. Cell *128*, 693-705.

Kuhn, R., Schwenk, F., Aguet, M., and Rajewsky, K. (1995). Inducible gene targeting in mice. Science *269*, 1427-1429.

Kumar, V., Palermo, R., Talora, C., Campese, A., Checquolo, S., Bellavia, D., Tottone, L., Testa, G., Miele, E., and Indraccolo, S. (2014). Notch and NF-kB signaling pathways regulate miR-223/FBXW7 axis in T-cell acute lymphoblastic leukemia. Leukemia *28*, 2324-2335.

Kuo, M.H., and Allis, C.D. (1998). Roles of histone acetyltransferases and deacetylases in gene regulation. Bioessays *20*, 615-626.

Lachner, M., O'Carroll, D., Rea, S., Mechtler, K., and Jenuwein, T. (2001). Methylation of histone H3 lysine 9 creates a binding site for HP1 proteins. Nature *410*, 116-120.

Lane, S.W., Scadden, D.T., and Gilliland, D.G. (2009). The leukemic stem cell niche: current concepts and therapeutic opportunities. Blood *114*, 1150-1157.

Langmead, B., Trapnell, C., Pop, M., and Salzberg, S.L. (2009). Ultrafast and memory-efficient alignment of short DNA sequences to the human genome. Genome biology *10*, 1-10.

Lapidot, T., Sirard, C., Vormoor, J., Murdoch, B., Hoang, T., Caceres-Cortes, J., Minden, M., Paterson, B., Caligiuri, M.A., and Dick, J.E. (1994). A cell initiating human acute myeloid leukaemia after transplantation into SCID mice. Nature *367*, 645-648.

Laufer, B.I., and Singh, S.M. (2015). Strategies for precision modulation of gene expression by epigenome editing: an overview. Epigenetics & chromatin *8*, 34.

Lazer, G., and Katzav, S. (2011). Guanine nucleotide exchange factors for RhoGTPases: good therapeutic targets for cancer therapy? Cellular signalling *23*, 969-979.

Lechman, E.R., Gentner, B., Ng, S.W., Schoof, E.M., van Galen, P., Kennedy, J.A., Nucera, S., Ciceri, F., Kaufmann, K.B., and Takayama, N. (2016). miR-126 regulates distinct self-renewal outcomes in normal and malignant hematopoietic stem cells. Cancer cell *29*, 214-228.

Ley, T.J., Ding, L., Walter, M.J., McLellan, M.D., Lamprecht, T., Larson, D.E., Kandoth, C., Payton, J.E., Baty, J., and Welch, J. (2010). DNMT3A mutations in acute myeloid leukemia. New England Journal of Medicine *363*, 2424-2433.

Li, Z., Cai, X., Cai, C.-L., Wang, J., Zhang, W., Petersen, B.E., Yang, F.-C., and Xu, M. (2011). Deletion of Tet2 in mice leads to dysregulated hematopoietic stem cells and subsequent development of myeloid malignancies. Blood *118*, 4509-4518.

Li, Z., Lu, J., Sun, M., Mi, S., Zhang, H., Luo, R.T., Chen, P., Wang, Y., Yan, M., and Qian, Z. (2008). Distinct microRNA expression profiles in acute myeloid leukemia with common translocations. Proceedings of the National Academy of Sciences *105*, 15535-15540.

Liao, Y., Smyth, G.K., and Shi, W. (2014). featureCounts: an efficient general purpose program for assigning sequence reads to genomic features. Bioinformatics *30*, 923-930.

Licht, J.D., and Sternberg, D.W. (2005). The molecular pathology of acute myeloid leukemia. ASH Education Program Book *2005*, 137-142.

Liso, A., Bogliolo, A., Freschi, V., Martelli, M., Pileri, S., Santodirocco, M., Bolli, N., Martelli, M., and Falini, B. (2008). In human genome, generation of a nuclear export signal through duplication appears unique to nucleophosmin (NPM1) mutations and is restricted to AML. Leukemia *22*, 1285-1289.

Liu, H., Liang, C., Kollipara, R.K., Matsui, M., Ke, X., Jeong, B.-C., Wang, Z., Yoo, K.S., Yadav, G.P., and Kinch, L.N. (2016a). HP1BP3, a chromatin retention factor for co-transcriptional MicroRNA processing. Molecular Cell *63*, 420-432.

Liu, S., Wu, L.-C., Pang, J., Santhanam, R., Schwind, S., Wu, Y.-Z., Hickey, C.J., Yu, J., Becker, H., and Maharry, K. (2010). Sp1/NFκB/HDAC/miR-29b regulatory network in KIT-driven myeloid leukemia. Cancer cell *17*, 333-347.

Liu, X., Liao, W., Peng, H., Luo, X., Luo, Z., Jiang, H., and Xu, L. (2016b). miR-181a promotes G1/S transition and cell proliferation in pediatric acute myeloid leukemia by targeting ATM. Journal of cancer research and clinical oncology *142*, 77-87.

Livak, K.J., and Schmittgen, T.D. (2001). Analysis of relative gene expression data using real-time quantitative PCR and the 2(-Delta Delta C(T)) Method. Methods 25, 402-408.

Lobo, N.A., Shimono, Y., Qian, D., and Clarke, M.F. (2007). The biology of cancer stem cells. Annu Rev Cell Dev Biol *23*, 675-699.

Lockwood, W. (2015). Leukemia: AML, CML, ALL and CLL.

Loizou, J.I., Oser, G., Shukla, V., Sawan, C., Murr, R., Wang, Z.-Q., Trumpp, A., and Herceg, Z. (2009). Histone acetyltransferase cofactor Trrap is essential for maintaining the hematopoietic stem/progenitor cell pool. The Journal of Immunology *183*, 6422-6431.

Lomberk, G., Wallrath, L.L., and Urrutia, R. (2006). The Heterochromatin Protein 1 family. Genome Biology *7*.

Love, M.I., Huber, W., and Anders, S. (2014). Moderated estimation of fold change and dispersion for RNA-seq data with DESeq2. Genome biology *15*, 1-21.

Lucio-Eterovic, A.K., Singh, M.M., Gardner, J.E., Veerappan, C.S., Rice, J.C., and Carpenter, P.B. (2010). Role for the nuclear receptor-binding SET domain protein 1 (NSD1) methyltransferase in coordinating lysine 36 methylation at histone 3 with RNA polymerase II function. Proceedings of the National Academy of Sciences *107*, 16952-16957.

Luger, K., Mader, A.W., Richmond, R.K., Sargent, D.F., and Richmond, T.J. (1997). Crystal structure of the nucleosome core particle at 2.8 angstrom resolution. Nature *389*, 251.

Lund, K., Adams, P., and Copland, M. (2014). EZH2 in normal and malignant hematopoiesis. Leukemia *28*, 44.

Luo, C., Hajkova, P., and Ecker, J.R. (2018). Dynamic DNA methylation: In the right place at the right time. Science *361*, 1336-1340.

Ma, Y., Kanakousaki, K., and Buttitta, L. (2014). How the cell cycle impacts chromatin architecture and influences cell fate. Frontiers in genetics *6*, 19-19.

MacFarlane, L.-A., and R Murphy, P. (2010). MicroRNA: biogenesis, function and role in cancer. Current genomics *11*, 537-561.

Machida, S., Takizawa, Y., Ishimaru, M., Sugita, Y., Sekine, S., Nakayama, J.-i., Wolf, M., and Kurumizaka, H. (2018). Structural basis of heterochromatin formation by human HP1. Molecular cell *69*, 385-397. e388.

Magilnick, N., Reyes, E.Y., Wang, W.-L., Vonderfecht, S.L., Gohda, J., Inoue, J.-i., and Boldin, M.P. (2017). miR-146a–Traf6 regulatory axis controls autoimmunity and myelopoiesis, but is dispensable for hematopoietic stem cell homeostasis and tumor suppression. Proceedings of the National Academy of Sciences *114*, E7140-E7149.

Maison, C., and Almouzni, G. (2004). HP1 and the dynamics of heterochromatin maintenance. Nature reviews Molecular cell biology *5*, 296.

Maison, C., Bailly, D., Peters, A.H., Quivy, J.-P., Roche, D., Taddei, A., Lachner, M., Jenuwein, T., and Almouzni, G. (2002). Higher-order structure in pericentric heterochromatin involves a distinct pattern of histone modification and an RNA component. Nature genetics *30*, 329-334.

Maison, C., Bailly, D., Roche, D., de Oca, R.M., Probst, A.V., Vassias, I., Dingli, F., Lombard, B., Loew, D., and Quivy, J.-P. (2011). SUMOylation promotes de novo targeting of HP1α to pericentric heterochromatin. Nature genetics *43*, 220-227.

Malumbres, M., and Carnero, A. (2003). Cell cycle deregulation: a common motif in cancer. Progress in cell cycle research *5*, 5.

Maresca, T.J., Freedman, B.S., and Heald, R. (2005a). Histone H1 is essential for mitotic chromosome architecture and segregation in Xenopus laevis egg extracts. J Cell Biol *169*, 859-869.

Maresca, T.J., Freedman, B.S., and Heald, R. (2005b). Histone H1 is essential for mitotic chromosome architecture and segregation in Xenopus laevis egg extracts. The Journal of Cell Biology *169*, 859-869.

Marks, P.A. (2010). Histone deacetylase inhibitors: A chemical genetics approach to understanding cellular functions. Biochimica Et Biophysica Acta-Gene Regulatory Mechanisms *1799*, 717-725.

Mateescu, B., Bourachot, B., Rachez, C., Ogryzko, V., and Muchardt, C. (2008). Regulation of an inducible promoter by an HP1 beta-HP1 gamma switch. Embo Reports *9*.

Maxwell, P.H., Pugh, C.W., and Ratcliffe, P.J. (2001). Activation of the HIF pathway in cancer. Current opinion in genetics & development *11*, 293-299.

Meads, M.B., Hazlehurst, L.A., and Dalton, W.S. (2008). The bone marrow microenvironment as a tumor sanctuary and contributor to drug resistance. Clinical Cancer Research *14*, 2519-2526.

Mehdipour, P., Santoro, F., and Minucci, S. (2015). Epigenetic alterations in acute myeloid leukemias. The FEBS journal *282*, 1786-1800.

Metcalf, D. (1991). Lineage commitment of hemopoietic progenitor cells in developing blast cell colonies: influence of colony-stimulating factors. Proceedings of the National Academy of Sciences *88*, 11310-11314.

Metcalf, D., and Nicola, N. (1991). Direct proliferative actions of stem cell factor on murine bone marrow cells in vitro: effects of combination with colony-stimulating factors. Proceedings of the National Academy of Sciences *88*, 6239-6243.

Millington, M., Arndt, A., Boyd, M., Applegate, T., and Shen, S. (2009). Towards a clinically relevant lentiviral transduction protocol for primary human CD34+ hematopoietic stem/progenitor cells. PloS one *4*.

Miyoshi, H. (2004). Gene delivery to hematopoietic stem cells using lentiviral vectors. In Gene Delivery to Mammalian Cells (Springer), pp. 429-438.

Monaghan, L., Massett, M.E., Bunschoten, R.P., Hoose, A., Pirvan, P.-A., Liskamp, R.M., Jørgensen, H.G., and Huang, X. (2019). The emerging role of H3K9me3 as a potential therapeutic target in acute myeloid leukemia. Frontiers in oncology *9*, 705.

Morgan, M.A., and Shilatifard, A. (2015). Chromatin signatures of cancer. Genes & development *29*, 238-249.

Morgan, R.A., Gray, D., Lomova, A., and Kohn, D.B. (2017). Hematopoietic stem cell gene therapy: progress and lessons learned. Cell stem cell *21*, 574-590.

Morlando, M., Ballarino, M., Gromak, N., Pagano, F., Bozzoni, I., and Proudfoot, N.J. (2008). Primary microRNA transcripts are processed co-transcriptionally. Nature structural & molecular biology *15*, 902.

Mostoslavsky, G., Kotton, D.N., Fabian, A.J., Gray, J.T., Lee, J.-S., and Mulligan, R.C. (2005). Efficiency of transduction of highly purified murine hematopoietic stem cells by lentiviral and oncoretroviral vectors under conditions of minimal in vitro manipulation. Molecular Therapy *11*, 932-940.

Mrozek, K., Heerema, N.A., and Bloomfield, C.D. (2004). Cytogenetics in acute leukemia. Blood reviews *18*, 115-136.

Mrózek, K., Heinonen, K., and Bloomfield, C.D. (2001). Clinical importance of cytogenetics in acute myeloid leukaemia. Best Practice & Research Clinical Haematology *14*, 19-47.

Muchardt, C., Guilleme, M., Seeler, J.S., Trouche, D., Dejean, A., and Yaniv, M. (2002). Coordinated methyl and RNA binding is required for heterochromatin localization of mammalian HP1 alpha. Embo Reports *3*.

Müller-Tidow, C., Klein, H.-U., Hascher, A., Isken, F., Tickenbrock, L., Thoennissen, N., Agrawal-Singh, S., Tschanter, P., Disselhoff, C., and Wang, Y. (2010). Profiling of histone H3 lysine 9 trimethylation levels predicts transcription factor activity and survival in acute myeloid leukemia. Blood *116*, 3564-3571.

Muz, B., de la Puente, P., Azab, F., and Azab, A.K. (2015). The role of hypoxia in cancer progression, angiogenesis, metastasis, and resistance to therapy. Hypoxia *3*, 83.

Naldini, L., Blömer, U., Gallay, P., Ory, D., Mulligan, R., Gage, F.H., Verma, I.M., and Trono, D. (1996). In vivo gene delivery and stable transduction of nondividing cells by a lentiviral vector. Science *272*, 263-267.

Nateri, A.S., Riera-Sans, L., Da Costa, C., and Behrens, A. (2004). The ubiquitin ligase SCFFbw7 antagonizes apoptotic JNK signaling. Science *303*, 1374-1378.

Network, C.G.A.R. (2013). Genomic and epigenomic landscapes of adult de novo acute myeloid leukemia. N Engl j Med *2013*, 2059-2074.

Neuner, S.M., Garfinkel, B.P., Wilmott, L.A., Ignatowska-Jankowska, B.M., Citri, A., Orly, J., Lu, L., Overall, R.W., Mulligan, M.K., and Kempermann, G. (2016). Systems genetics identifies Hp1bp3 as a novel modulator of cognitive aging. Neurobiology of Aging *46*, 58-67.

Nicholas, S.A., and Sumbayev, V.V. (2009). The involvement of hypoxia-inducible factor 1 alpha in Toll-like receptor 7/8-mediated inflammatory response. Cell research *19*, 973-983.

Nielsen, N.H., Lodén, M., Cajander, J., Emdin, S.O., and Landberg, G. (1999). G1-S transition defects occur in most breast cancers and predict outcome. Breast cancer research and treatment *56*, 103-110.

Nimer, S.D. (2008). Is it important to decipher the heterogeneity of "normal karyotype AML"? Best Practice & Research Clinical Haematology *21*, 43-52.

Ogilvie, L.A., Kovachev, A., Wierling, C., Lange, B.M., and Lehrach, H. (2017). Models of models: a translational route for cancer treatment and drug development. Frontiers in Oncology *7*, 219.

Olivier, M., Hollstein, M., and Hainaut, P. (2010). TP53 mutations in human cancers: origins, consequences, and clinical use. Cold Spring Harbor perspectives in biology *2*, a001008.

Orford, K.W., and Scadden, D.T. (2008). Deconstructing stem cell self-renewal: genetic insights into cell-cycle regulation. Nature Reviews Genetics *9*, 115-128.

Orkin, S.H., and Zon, L.I. (2008). Hematopoiesis: an evolving paradigm for stem cell biology. Cell *132*, 631-644.

Osawa, M., Hanada, K.-i., Hamada, H., and Nakauchi, H. (1996). Long-term lymphohematopoietic reconstitution by a single CD34-low/negative hematopoietic stem cell. Science *273*, 242-245.

Pan, C., and Fan, Y. (2016). Role of H1 linker histones in mammalian development and stem cell differentiation. Biochimica et Biophysica Acta (BBA)-Gene Regulatory Mechanisms *1859*, 496-509.

Paolillo, R., Spinello, I., Quaranta, M.T., Pasquini, L., Pelosi, E., Lo Coco, F., Testa, U., and Labbaye, C. (2015). Human TM9SF4 is a new gene down-regulated by hypoxia and involved in cell adhesion of leukemic cells. PLoS One *10*, e0126968.

Park, D., Spencer, J.A., Koh, B.I., Kobayashi, T., Fujisaki, J., Clemens, T.L., Lin, C.P., Kronenberg, H.M., and Scadden, D.T. (2012). Endogenous bone marrow MSCs are dynamic, fate-restricted participants in bone maintenance and regeneration. Cell stem cell *10*, 259-272.

Park, I.-K., He, Y., Lin, F., Laerum, O.D., Tian, Q., Bumgarner, R., Klug, C.A., Li, K., Kuhr, C., and Doyle, M.J. (2002). Differential gene expression profiling of adult murine hematopoietic stem cells. Blood, The Journal of the American Society of Hematology *99*, 488-498.

Park, J.-A., Kim, A.-J., Kang, Y., Jung, Y.-J., Kim, H.K., and Kim, K.-C. (2011). Deacetylation and methylation at histone H3 lysine 9 (H3K9) coordinate chromosome condensation during cell cycle progression. Molecules and cells *31*, 343-349.

Park, S.H., Yu, S.E., Chai, Y.G., and Jang, Y.K. (2014). CDK2-dependent phosphorylation of Suv39H1 is involved in control of heterochromatin

replication during cell cycle progression. Nucleic Acids Research *42*, 6196-6207.

Park, Y., and Gerson, S.L. (2005). DNA repair defects in stem cell function and aging. Annu Rev Med *56*, 495-508.

Park, Y.S., Jin, M.Y., Kim, Y.J., Yook, J.H., Kim, B.S., and Jang, S.J. (2008). The global histone modification pattern correlates with cancer recurrence and overall survival in gastric adenocarcinoma. Annals of surgical oncology *15*, 1968.

Parmar, K., Mauch, P., Vergilio, J.-A., Sackstein, R., and Down, J.D. (2007). Distribution of hematopoietic stem cells in the bone marrow according to regional hypoxia. Proceedings of the National Academy of Sciences *104*, 5431-5436.

Passegué, E., and Wagers, A.J. (2006). Regulating quiescence: new insights into hematopoietic stem cell biology. Developmental cell *10*, 415-417.

Pelosi, A., Careccia, S., Lulli, V., Romania, P., Marziali, G., Testa, U., Lavorgna, S., Lo-Coco, F., Petti, M.C., and Calabretta, B. (2013). miRNA let-7c promotes granulocytic differentiation in acute myeloid leukemia. Oncogene *32*, 3648-3654.

Peng, Y., and Croce, C.M. (2016). The role of MicroRNAs in human cancer. Signal transduction and targeted therapy *1*, 1-9.

Peters, S.O., Kittler, E., Ramshaw, H.S., and Quesenberry, P.J. (1996). Ex vivo expansion of murine marrow cells with interleukin-3 (IL-3), IL-6, IL-11, and stem cell factor leads to impaired engraftment in irradiated hosts.

Petitjean, A., Achatz, M., Borresen-Dale, A., Hainaut, P., and Olivier, M. (2007). TP53 mutations in human cancers: functional selection and impact on cancer prognosis and outcomes. Oncogene *26*, 2157.

Petti, E., Jordi, F., Buemi, V., Dinami, R., Benetti, R., Blasco, M.A., and Schoeftner, S. (2015). Altered telomere homeostasis and resistance to skin carcinogenesis in Suv39h1 transgenic mice. Cell Cycle *14*, 1438-1446.

Piatti, P., Zeilner, A. and Lusser, A. (2011). ATP-Dependent Chromatin Remodeling Factors and Their Roles in Affecting Nucleosome Fiber Composition. Int J Mol Sci. 2011; 12(10): 6544–6565.

Piskadlo, E., and Oliveira, R.A. (2016). Novel insights into mitotic chromosome condensation. F1000Research *5*.

Plass, C., Oakes, C., Blum, W., and Marcucci, G. (2008). Epigenetics in acute myeloid leukemia. Paper presented at: Seminars in oncology (Elsevier).

Pogribny, I.P., Tryndyak, V.P., Muskhelishvili, L., Rusyn, I., and Ross, S.A. (2007). Methyl deficiency, alterations in global histone modifications, and carcinogenesis. The Journal of nutrition *137*, 216S-222S.

Polato, F., Rusconi, P., Zangrossi, S., Morelli, F., Boeri, M., Musi, A., Marchini, S., Castiglioni, V., Scanziani, E., and Torri, V. (2014). DRAGO (KIAA0247), a New DNA Damage–responsive, p53-inducible Gene that cooperates With p53 as Oncosuppressor. JNCI: Journal of the National Cancer Institute *106*.

Poloni, A., Douay, L., Giarratana, M., Kobari, L., Gorin, N., Olivieri, A., and Leoni, P. (1997). The potential role of FLT3 ligand in progenitor and primitive hematopoietic cell expansion. Bollettino della Societa italiana di biologia sperimentale *73*, 55-62.

Pratcorona, M., Abbas, S., Sanders, M.A., Koenders, J.E., Kavelaars, F.G., Erpelinck-Verschueren, C.A., Zeilemakers, A., Löwenberg, B., and Valk, P.J. (2012). Acquired mutations in ASXL1 in acute myeloid leukemia: prevalence and prognostic value. Haematologica *97*, 388-392.

Probst, A.V., and Almouzni, G. (2008). Pericentric heterochromatin: dynamic organization during early development in mammals. Differentiation *76*, 15-23.

Rakheja, D., Konoplev, S., Medeiros, L.J., and Chen, W. (2012). IDH mutations in acute myeloid leukemia. Human pathology *43*, 1541-1551.

Ramadoss, S., Chen, X., and Wang, C.-Y. (2012). Histone demethylase KDM6B promotes epithelial-mesenchymal transition. Journal of Biological Chemistry *287*, 44508-44517.

Rea, S., Eisenhaber, F., O'Carroll, D., Strahl, B.D., Sun, Z.-W., Schmid, M., Opravil, S., Mechtler, K., Ponting, C.P., and Allis, C.D. (2000). Regulation of chromatin structure by site-specific histone H3 methyltransferases. Nature *406*, 593-599.

Reavie, L., Della Gatta, G., Crusio, K., Aranda-Orgilles, B., Buckley, S.M., Thompson, B., Lee, E., Gao, J., Bredemeyer, A.L., and Helmink, B.A. (2010). Regulation of hematopoietic stem cell differentiation by a single ubiquitin ligase–substrate complex. Nature immunology *11*, 207-215.

Renneville, A., Roumier, C., Biggio, V., Nibourel, O., Boissel, N., Fenaux, P., and Preudhomme, C. (2008). Cooperating gene mutations in acute myeloid leukemia: a review of the literature. Leukemia *22*, 915.

Rice, J.C., and Allis, C.D. (2001). Histone methylation versus histone acetylation: new insights into epigenetic regulation. Current opinion in cell biology *13*, 263-273.

Rice, K., Hormaeche, I., and Licht, J. (2007). Epigenetic regulation of normal and malignant hematopoiesis. Oncogene *26*, 6697-6714.

Richards, E.J., and Elgin, S.C. (2002). Epigenetic codes for heterochromatin formation and silencing: rounding up the usual suspects. Cell *108*, 489-500.

Riether, C., Schürch, C., and Ochsenbein, A. (2015). Regulation of hematopoietic and leukemic stem cells by the immune system. Cell death and differentiation *22*, 187.

Roberti, A., Valdes, A.F., Torrecillas, R., Fraga, M.F., and Fernandez, A.F. (2019). Epigenetics in cancer therapy and nanomedicine. Clinical epigenetics *11*, 1-18.

Roos, M.M., Li, M., Amara, P., and Chute, J.P. (2018). Pharmacologic Targeting of LIN28/Let-7 in Acute Myeloid Leukemia. Blood *132*, 4072-4072.

Rozan, L., and El-Deiry, W. (2007). p53 downstream target genes and tumor suppression: a classical view in evolution. Cell death and differentiation *14*, 3.

Saksouk, N., Simboeck, E., and Déjardin, J. (2015). Constitutive heterochromatin formation and transcription in mammals. Epigenetics & chromatin *8*, 1-17.

Schäfer, S., and Jung, M. (2005). Chromatin modifications as targets for new anticancer drugs. Archiv der Pharmazie *338*, 347-357.

Schito, L., Rey, S., and Konopleva, M. (2017). Integration of hypoxic HIF-α signaling in blood cancers. Oncogene *36*, 5331-5340.

Sekar, D., Krishnan, R., Panagal, M., Sivakumar, P., Gopinath, V., and Basam, V. (2016). Deciphering the role of microRNA 21 in cancer stem cells (CSCs). Genes & diseases *3*, 277-281.

Semenza, G.L. (2013). HIF-1 mediates metabolic responses to intratumoral hypoxia and oncogenic mutations. The Journal of clinical investigation *123*, 3664-3671.

Senyuk, V., Zhang, Y., Liu, Y., Ming, M., Premanand, K., Zhou, L., Chen, P., Chen, J., Rowley, J.D., and Nucifora, G. (2013). Critical role of miR-9 in myelopoiesis and EVI1-induced leukemogenesis. Proceedings of the National Academy of Sciences *110*, 5594-5599.

Sha, C., Jia, G., Jingjing, Z., Yapeng, H., Zhi, L., and Guanghui, X. (2020). miR-486 is involved in the pathogenesis of acute myeloid leukemia by regulating JAK-STAT signaling. Naunyn-Schmiedeberg's Archives of Pharmacology, 1-11.

Sharma, S., and Gurudutta, G. (2016). Epigenetic regulation of hematopoietic stem cells. International journal of stem cells *9*, 36.

Shaw, P.H. (1996). The role of p53 in cell cycle regulation. Pathology-Research and Practice *192*, 669-675.

Shi, G., Hu, Y., Zhu, X., Jiang, Y., Pang, J., Wang, C., Huang, W., Zhao, Y., Ma, W., and Liu, D. (2020). A critical role of telomere chromatin compaction in ALT tumor cell growth. Nucleic acids research *48*, 6019-6031.

Shide, K., Kameda, T., Shimoda, H., Yamaji, T., Abe, H., Kamiunten, A., Sekine, M., Hidaka, T., Katayose, K., and Kubuki, Y. (2012). TET2 is essential for survival and hematopoietic stem cell homeostasis. Leukemia *26*, 2216-2223.

Si, W., Shen, J., Zheng, H., and Fan, W. (2019). The role and mechanisms of action of microRNAs in cancer drug resistance. Clinical epigenetics *11*, 1-24.

Si, X., Zhang, X., Hao, X., Li, Y., Chen, Z., Ding, Y., Shi, H., Bai, J., Gao, Y., and Cheng, T. (2016). Upregulation of miR-99a is associated with poor prognosis of acute myeloid leukemia and promotes myeloid leukemia cell expansion. Oncotarget *7*, 78095.

So, A.Y.-L., Sookram, R., Chaudhuri, A.A., Minisandram, A., Cheng, D., Xie, C., Lim, E.L., Flores, Y.G., Jiang, S., and Kim, J.T. (2014). Dual mechanisms by which miR-125b represses IRF4 to induce myeloid and B-cell leukemias. Blood, The Journal of the American Society of Hematology *124*, 1502-1512.

Song, G., Li, Y., and Jiang, G. (2012). Role of VEGF/VEGFR in the pathogenesis of leukemias and as treatment targets. Oncology reports *28*, 1935-1944.

Song, G., Wang, L., Bi, K., and Jiang, G. (2015). Regulation of the C/EBPα signaling pathway in acute myeloid leukemia. Oncology reports *33*, 2099-2106.

Song, S.J., Ito, K., Ala, U., Kats, L., Webster, K., Sun, S.M., Jongen-Lavrencic, M., Manova-Todorova, K., Teruya-Feldstein, J., and Avigan, D.E. (2013). The oncogenic microRNA miR-22 targets the TET2 tumor suppressor to promote hematopoietic stem cell self-renewal and transformation. Cell stem cell *13*, 87-101.

Soshnev, A.A., Josefowicz, S.Z., and Allis, C.D. (2016). Greater than the sum of parts: complexity of the dynamic epigenome. Molecular cell *62*, 681-694.

Starczynowski, D.T., Morin, R., McPherson, A., Lam, J., Chari, R., Wegrzyn, J., Kuchenbauer, F., Hirst, M., Tohyama, K., and Humphries, R.K. (2011). Genome-wide identification of human microRNAs located in leukemia-associated genomic alterations. Blood, The Journal of the American Society of Hematology *117*, 595-607.

Stasik, S., Middeke, J.M., Kramer, M., Röllig, C., Krämer, A., Scholl, S., Hochhaus, A., Crysandt, M., Brümmendorf, T.H., and Naumann, R. (2020). EZH2 mutations and impact on clinical outcome: an analysis in 1,604 patients with newly diagnosed acute myeloid leukemia. haematologica *105*, e228-e231.

Steffen, B., Müller-Tidow, C., Schwäble, J., Berdel, W.E., and Serve, H. (2005). The molecular pathogenesis of acute myeloid leukemia. Critical reviews in oncology/hematology *56*, 195-221.

Stiehl, D.P., Jelkmann, W., Wenger, R.H., and Hellwig-Bürgel, T. (2002). Normoxic induction of the hypoxia-inducible factor 1α by insulin and interleukin-1β involves the phosphatidylinositol 3-kinase pathway. FEBS letters *512*, 157-162.

Storey, J.D. (2003). The positive false discovery rate: a Bayesian interpretation and the q-value. The Annals of Statistics *31*, 2013-2035.

Strahl, B.D., and Allis, C.D. (2000). The language of covalent histone modifications. Nature *403*, 41.

Stypula-Cyrus, Y., Damania, D., Kunte, D.P., Cruz, M.D., Subramanian, H., Roy, H.K., and Backman, V. (2013). HDAC up-regulation in early colon field carcinogenesis is involved in cell tumorigenicity through regulation of chromatin structure. PLoS One *8*, e64600.

Sun, X., Liu, D., Xue, Y., and Hu, X. (2017). Enforced miR-144-3p Expression as a Non-Invasive Biomarker for the Acute Myeloid Leukemia Patients Mainly by Targeting NRF2. Clinical laboratory *63*, 679-687.

Sun, X., Liu, H., Li, T., and Qin, L. (2018a). MicroRNA-339-5p inhibits cell proliferation of acute myeloid leukaemia by directly targeting SOX4. Molecular medicine reports *18*, 5261-5269.

Sun, Y., Chen, B.-R., and Deshpande, A. (2018b). Epigenetic regulators in the development, maintenance, and therapeutic targeting of acute myeloid leukemia. Frontiers in oncology *8*, 41.

Szklarczyk, D., Gable, A.L., Nastou, K.C., Lyon, D., Kirsch, R., Pyysalo, S., Doncheva, N.T., Legeay, M., Fang, T., and Bork, P. (2021). The STRING database in 2021: customizable protein–protein networks, and functional characterization of user-uploaded gene/measurement sets. Nucleic Acids Research *49*, D605-D612.

Tadokoro, Y., Ema, H., Okano, M., Li, E., and Nakauchi, H. (2007). De novo DNA methyltransferase is essential for self-renewal, but not for differentiation, in hematopoietic stem cells. Journal of Experimental Medicine *204*, 715-722.

Takano, H., Ema, H., Sudo, K., and Nakauchi, H. (2004). Asymmetric division and lineage commitment at the level of hematopoietic stem cells: inference from differentiation in daughter cell and granddaughter cell pairs. The Journal of experimental medicine *199*, 295-302.

Tanaka, H., Sasayama, T., Tanaka, K., Nakamizo, S., Nishihara, M., Mizukawa, K., Kohta, M., Koyama, J., Miyake, S., and Taniguchi, M. (2013). MicroRNA-183 upregulates HIF-1α by targeting isocitrate dehydrogenase 2 (IDH2) in glioma cells. Journal of neuro-oncology *111*, 273-283.

Tang, M., Li, Y., Zhang, Y., Chen, Y., Huang, W., Wang, D., Zaug, A.J., Liu, D., Zhao, Y., and Cech, T.R. (2015). Disease mutant analysis identifies a new function of DAXX in telomerase regulation and telomere maintenance. Journal of cell science *128*, 331-341.

Taussig, D.C., Miraki-Moud, F., Anjos-Afonso, F., Pearce, D.J., Allen, K., Ridler, C., Lillington, D., Oakervee, H., Cavenagh, J., and Agrawal, S.G.

(2008). Anti-CD38 antibody–mediated clearance of human repopulating cells masks the heterogeneity of leukemia-initiating cells. Blood, The Journal of the American Society of Hematology *112*, 568-575.

Taussig, D.C., Vargaftig, J., Miraki-Moud, F., Griessinger, E., Sharrock, K., Luke, T., Lillington, D., Oakervee, H., Cavenagh, J., and Agrawal, S.G. (2010). Leukemia-initiating cells from some acute myeloid leukemia patients with mutated nucleophosmin reside in the CD34− fraction. Blood, The Journal of the American Society of Hematology *115*, 1976-1984.

Thomas, D., and Mostoslavsky, G. (2014). Efficient transduction of hematopoietic stem cells and its potential for gene correction of hematopoietic diseases. In Gene Correction (Springer), pp. 441-450.

Thompson, B.J., Jankovic, V., Gao, J., Buonamici, S., Vest, A., Lee, J.M., Zavadil, J., Nimer, S.D., and Aifantis, I. (2008). Control of hematopoietic stem cell quiescence by the E3 ubiquitin ligase Fbw7. The Journal of experimental medicine *205*, 1395-1408.

Tian, P., and Yan, L. (2016). Inhibition of MicroRNA-149-5p induces apoptosis of acute myeloid leukemia cell line THP-1 by targeting fas ligand (FASLG). Medical science monitor: international medical journal of experimental and clinical research *22*, 5116.

Tickenbrock, L., Klein, H.-U., Trento, C., Hascher, A., Göllner, S., Bäumer, N., Kuss, R., Agrawal, S., Bug, G., and Serve, H. (2011). Increased HDAC1 deposition at hematopoietic promoters in AML and its association with patient survival. Leukemia research *35*, 620-625.

Trowbridge, J.J., Snow, J.W., Kim, J., and Orkin, S.H. (2009). DNA methyltransferase 1 is essential for and uniquely regulates hematopoietic stem and progenitor cells. Cell stem cell *5*, 442-449.

Ulirsch, J.C., Lareau, C.A., Bao, E.L., Ludwig, L.S., Guo, M.H., Benner, C., Satpathy, A.T., Kartha, V.K., Salem, R.M., and Hirschhorn, J.N. (2019). Interrogation of human hematopoiesis at single-cell and single-variant resolution. Nature genetics *51*, 683-693.

Vad-Nielsen, J., and Nielsen, A.L. (2015). Beyond the histone tale: HP1α deregulation in breast cancer epigenetics. Cancer Biology & Therapy *16*, 189-200.

Vaiopoulos, A.G., Athanasoula, K.C., and Papavassiliou, A.G. (2014). Epigenetic modifications in colorectal cancer: molecular insights and therapeutic challenges. Biochimica et Biophysica Acta (BBA)-Molecular Basis of Disease *1842*, 971-980.

van Engeland, M., Derks, S., Smits, K.M., Meijer, G.A., and Herman, J.G. (2011). Colorectal cancer epigenetics: complex simplicity. Journal of Clinical Oncology *29*, 1382-1391.

Van Uden, P., Kenneth, N.S., and Rocha, S. (2008). Regulation of hypoxia-inducible factor-1α by NF-κB. Biochemical Journal *412*, 477-484.

Varet, H., Brillet-Guéguen, L., Coppée, J.-Y., and Dillies, M.-A. (2016). SARTools: a DESeq2-and EdgeR-based R pipeline for comprehensive differential analysis of RNA-Seq data. PloS one *11*, e0157022.

Vermaak, D., Henikoff, S., and Malik, H.S. (2005). Positive selection drives the evolution of rhino, a member of the heterochromatin protein 1 family in Drosophila. Plos Genetics *1*.

Wadleigh, M., DeAngelo, D.J., Griffin, J.D., and Stone, R.M. (2005). After chronic myelogenous leukemia: tyrosine kinase inhibitors in other hematologic malignancies. Blood *105*, 22-30.

Wagatsuma, V.M.D.D., Koury, L.C., Sánchez, S.E., Pontes, L.L.F., da Silva, F.B., Dore, A.I., de Lima, A.S.G., Lucena-Araujo, A.R., Almeida, L.Y., and Traina, F. (2016). Nuclear SET Domain (NSD) Protein Lysine Methyltransferases (KMT) Family Members Expression in Acute Myeloid Leukemia (Am Soc Hematology).

Wahid, F., Shehzad, A., Khan, T., and Kim, Y.Y. (2010). MicroRNAs: synthesis, mechanism, function, and recent clinical trials. Biochimica et Biophysica Acta (BBA)-Molecular Cell Research *1803*, 1231-1243.

Wakita, S., Yamaguchi, H., Miyake, K., Mitamura, Y., Kosaka, F., Dan, K., and Inokuchi, K. (2011). Importance of c-kit mutation detection method sensitivity in prognostic analyses of t (8; 21)(q22; q22) acute myeloid leukemia. Leukemia *25*, 1423.

Wallace, J.A., and O'Connell, R.M. (2017). MicroRNAs and acute myeloid leukemia: therapeutic implications and emerging concepts. Blood *130*, 1290-1301.

Wang, H., Huang, Z.-Q., Xia, L., Feng, Q., Erdjument-Bromage, H., Strahl, B.D., Briggs, S.D., Allis, C.D., Wong, J., and Tempst, P. (2001). Methylation of histone H4 at arginine 3 facilitating transcriptional activation by nuclear hormone receptor. Science *293*, 853-857.

Wang, Q., Zhai, Y.-Y., Dai, J.-H., Li, K.-Y., Deng, Q., and Han, Z.-G. (2014). SAMD9L inactivation promotes cell proliferation via facilitating G1-S transition in hepatitis B Virus-associated hepatocellular carcinoma. International journal of biological sciences *10*, 807.

Wang, X., Huang, S., and Chen, J.-L. (2017). Understanding of leukemic stem cells and their clinical implications. Molecular cancer *16*, 2.

Wang, Z., Zang, C., Rosenfeld, J.A., Schones, D.E., Barski, A., Cuddapah, S., Cui, K., Roh, T.-Y., Peng, W., and Zhang, M.Q. (2008). Combinatorial

patterns of histone acetylations and methylations in the human genome. Nature genetics *40*, 897-903.

Ward, A.F., Braun, B.S., and Shannon, K.M. (2012). Targeting oncogenic Ras signaling in hematologic malignancies. Blood *120*, 3397-3406.

Wen, M., Shen, Y., Shi, S., and Tang, T. (2012). miREvo: an integrative microRNA evolutionary analysis platform for next-generation sequencing experiments. BMC bioinformatics *13*, 1-10.

Wilson, A., Laurenti, E., Oser, G., van der Wath, R.C., Blanco-Bose, W., Jaworski, M., Offner, S., Dunant, C.F., Eshkind, L., and Bockamp, E. (2008). Hematopoietic stem cells reversibly switch from dormancy to self-renewal during homeostasis and repair. Cell *135*, 1118-1129.

Woodcock, C.L., Skoultchi, A.I., and Fan, Y. (2006). Role of linker histone in chromatin structure and function: H1 stoichiometry and nucleosome repeat length. Chromosome Research *14*, 17-25.

Wu, X.-Z., Wang, K.-P., Song, H.-J., Xia, J.-H., Jiang, Y., and Wang, Y.-L. (2015). MiR-27a-3p promotes esophageal cancer cell proliferation via F-box and WD repeat domain-containing 7 (FBXW7) suppression. International journal of clinical and experimental medicine *8*, 15556.

Wu, X., and Zhang, Y. (2017). TET-mediated active DNA demethylation: mechanism, function and beyond. Nature Reviews Genetics.

Xiao, L., Huang, Y., Zhen, R., Chiao, J., Liu, D., and Ma, X. (2010). Deficient histone acetylation in acute leukemia and the correction by an isothiocyanate. Acta haematologica *123*, 71-76.

Xu, H., and Wen, Q. (2018). Downregulation of miR-135a predicts poor prognosis in acute myeloid leukemia and regulates leukemia progression via

modulating HOXA10 expression. Molecular medicine reports *18*, 1134-1140.

Yamamoto, K., and Sonoda, M. (2003). Self-interaction of heterochromatin protein 1 is required for direct binding to histone methyltransferase, SUV39H1. Biochemical and biophysical research communications *301*, 287-292.

Yang, D.Q., Zhou, J.D., Wang, Y.X., Deng, Z.Q., Yang, J., Yao, D.M., Qian, Z., Yang, L., Lin, J., and Qian, J. (2017). Low miR-34c expression is associated with poor outcome in de novo acute myeloid leukemia. International journal of laboratory hematology *39*, 42-50.

Yeh, C.-H., Bellon, M., and Nicot, C. (2018). FBXW7: a critical tumor suppressor of human cancers. Molecular cancer *17*, 1-19.

Yingchun, L., Rong, Z., Kun, Y., Ying, Y., and Zhuogang, L. (2015). Bone marrow MicroRNA-335 level predicts the chemotherapy response and prognosis of adult acute myeloid leukemia. Medicine *94*.

Yonemura, Y., Ku, H., Hirayama, F., Souza, L.M., and Ogawa, M. (1996). Interleukin 3 or interleukin 1 abrogates the reconstituting ability of hematopoietic stem cells. Proceedings of the National Academy of Sciences *93*, 4040-4044.

Ysebaert, L., Chicanne, G., Demur, C., De Toni, F., Prade-Houdellier, N., Ruidavets, J., Mansat-De Mas, V., Rigal-Huguet, F., Laurent, G., and Payrastre, B. (2006). Expression of [beta]-catenin by acute myeloid leukemia cells predicts enhanced clonogenic capacities and poor prognosis. Leukemia *20*, 1211.

Zeng, W., Ball Jr, A.R., and Yokomori, K. (2010). HP1: heterochromatin binding proteins working the genome. Epigenetics *5*, 287-292.

Zerbino, D.R., and Birney, E. (2008). Velvet: algorithms for de novo short read assembly using de Bruijn graphs. Genome research *18*, 821-829.

Zhang, L., Nguyen, L.X.T., Wu, D., Brewer, C.J., He, X., Li, M., Zhao, D., Cook, G.J., Qi, J., and Wu, H. (2019). Anti-MiR-126 Therapy for Inv (16) Acute Myeloid Leukemia (American Society of Hematology Washington, DC).

Zhang, S., Zhang, Q., Shi, G., and Yin, J. (2018). MiR-182-5p regulates BCL2L12 and BCL2 expression in acute myeloid leukemia as a potential therapeutic target. Biomedicine & Pharmacotherapy *97*, 1189-1194.

Zhang, Y., Cooke, M., Panjwani, S., Cao, K., Krauth, B., Ho, P.-Y., Medrzycki, M., Berhe, D.T., Pan, C., and McDevitt, T.C. (2012). Histone h1 depletion impairs embryonic stem cell differentiation. PLoS Genet *8*, e1002691.

Zhang, Y., and Reinberg, D. (2001). Transcription regulation by histone methylation: interplay between different covalent modifications of the core histone tails. Genes & development *15*, 2343-2360.

Zheng, D., Radziszewska, A., and Woo, P. (2012). MicroRNA 497 modulates interleukin 1 signalling via the MAPK/ERK pathway. FEBS letters *586*, 4165-4172.

Zhou, C., Shen, L., Mao, L., Wang, B., Li, Y., and Yu, H. (2015). miR-92a is upregulated in cervical cancer and promotes cell proliferation and invasion by targeting FBXW7. Biochemical and biophysical research communications *458*, 63-69.

Zhou, L., Chen, J., Li, Z., Li, X., Hu, X., Huang, Y., Zhao, X., Liang, C., Wang, Y., and Sun, L. (2010). Integrated profiling of microRNAs and mRNAs: microRNAs located on Xq27. 3 associate with clear cell renal cell carcinoma. PloS one *5*, e15224.

Zhu, H., Guo, Z.-K., Jiang, X.-X., Li, H., Wang, X.-Y., Yao, H.-Y., Zhang, Y., and Mao, N. (2010). A protocol for isolation and culture of mesenchymal stem cells from mouse compact bone. Nature protocols *5*, 550.

Zon, L.I. (2008). Intrinsic and extrinsic control of haematopoietic stem-cell self-renewal. Nature *453*, 306-313.